New Reactivity of High Oxidation State Palladium Complexes

by

Joy Marie Racowski

A dissertation submitted in partial fulfillment
of the requirements for the degree of
Doctor of Philosophy
(Chemistry)
in The University of Michigan
2012

Doctoral Committee:

Professor Melanie S. Sanford, Chair
Professor Adam J. Matzger
Assistant Professor Kenichi Kuroda
Assistant Professor Anne J. McNeil

Acknowledgements

Ten years ago when I graduated high school I never imagined that I would pursue a Ph.D. in chemistry. Without the encouragement and support of some extraordinary mentors and the community at Bryn Mawr College, I am sure I would have taken a different path.

First, I would like to thank Professor Melanie Sanford for the opportunity to work on some really exciting projects. Her constant enthusiasm and work ethic that is focused on achieving groundbreaking chemistry is absolutely contagious. I appreciated the freedom to explore and take my project various directions, and know that I was always supported. I am thankful for the many times that I went into her office, exhaustively stuck, and she would have the most brilliant suggestions to help me move forward.

I would to thank Professors Sally and Frank Mallory. Professor Frank Mallory allowed me to do research in his laboratory after my junior year at Bryn Mawr College and this experience changed the direction of my educational path. I was immediately taken by the creativity and persistence that it took to be successful in the laboratory. His calm and patient encouragement was critical to my development as a scientist at this stage in my education. Professor Sally Mallory played a major role in honing my early research skills. Sally demanded technical mastery in the laboratory. Additionally, she mentored me when I was applying for graduate school and we also had lots of great conversations about women in chemistry and life in general. I am so very grateful to both of the Mallorys for their mentorship and friendship.

I owe my decision to major in chemistry to several members of the chemistry department at Bryn Mawr College: Professor White, Professor Burgmayer and Professor Lukacs-for their encouragement my freshman year and beyond to pursue chemistry; Professor Francl and Professor Nerz-Stormes-for their commitment to teaching and answering endless questions.

I am also indebted to the Bryn Mawr College community as a whole. Bryn Mawr College is a place filled with extraordinary women, who push their own bounds as well as others. Debates and discussions are encouraged not for the pursuit of ‘winning’ but for the sheer pursuit of learning. The community is filled with self-confident, intelligent and open-minded women, which propels a college life-style that allows for a significant amount of learning to take place outside of the classroom. I am sure that attending Bryn Mawr College was crucial to

emboldening me with the confidence to pursue a major and a career in the sciences.

Next, I would like to thank several people at the University of Michigan who have impacted my education and life. Thank you Professor Matzger for allowing me to rotate in your laboratory for two semesters. I really appreciate the time you took to mount crystals with me and set up calculations. I also respect your honesty whether it was on science, careers or restaurants.

Professors McNeil and Kuroda- thank you for your kind encouragement and for your smiles. Something as simple as a smile really makes an impact during the 'process' of graduate school.

Jeff Kampf, Jim Windak, Paul Lennon, Eugenio Alvarado and Chris Kojiro - my research certainly would not have been possible without the support that I received from your expertise. Thank you!

Thank you to Allison Dick for starting the exciting chemistry that I was able to pursue in my first project. Without your initial work in this area I could not have worked on such an exciting project.

I owe a lot of my initial successes in graduate school to the mentorship of Dipa Kalyani. Dipa was my 'assigned' mentor when I first rotated in the Sanford Laboratory. Her mentorship continued 'in an unassigned role' when I joined the group. Our discussions about chemistry really pushed me to critically evaluate reaction mechanisms and common assumptions. I am also grateful for the time she took to teach me new techniques or explain concepts. Lastly, I am thankful for the company she kept me on all of those nights when we would leave the Church St. parking lot and the console in the garage would read 'good morning'.

Kami Hull was also a big part of my education as a young graduate student. She always took the time to answer my questions and made me feel like I would eventually get to the point where I would feel ready to graduate.

Salena Whitfield, I would like to thank you for being an example of how to have school/life balance and still accomplish fantastic chemistry. I consider you the founding member of Club Palladium. You did discover our song!!

Deprez!! Thanks for all of the coffee trips and the constant entertainment of trying to put Dipa in the garbage can!!

Nick Ball, I appreciate all of our discussions about chemistry. Thank you for the random gifts of candy and cookies when you just sensed that I was having a bad day. You really set an example in the group with your positive attitude and willingness to discuss chemistry. Your persistence in discussing our chemistry together in Club Palladium led to a great paper! Thank you for the starting complex to try it out!!

Tom Lyons, without your friendship and our ‘couples pass’ at Planet Rock I’m not sure if I would have made it through the last few years of graduate school as easily. Our inaugural climbing expedition to the Red was epic! You have been an amazing friend and I’m so grateful.

Andrew Higgs if there is anyone whom I have met at Michigan that would drop anything to hang out when I really needed it, it was you.

Andy Satterfield, I appreciated all of the Eagles games that we watched together! It was nice to have another Philadelphia fan in Michigan!

Kara Stowers, we started this trip together and we are finishing together! Thank you for all of the gum and headphones over the years! I knew I could always stop by your desk and leave smiling! I wish you so much happiness in future!

Brannon Gary, thank you for all of your last minute ordering, chemistry discussions and stepping in to help with calculations!

Amanda Hickman, yes we did make it –together!! Our conversations about life helped me to keep some perspective during this journey and enabled me to remain centered around what really matters at the end of the day. I cannot say enough here to convey how much you have meant to me and how fantastic of a friend you are! I am so excited that we will be in Chicago together.

Asako Kubota and Sharon Neufeldt, thank you for all of your yummy baked goods and your willingness to let me stop by and just say, “Hi”, some days.

Yingda Ye, I appreciated all of the time you took to help me with my computer troubles. I appreciated all of your smiles and positive energy in the lab!

Kate McMurtry you have such a contagious, optimistic attitude! It has been such a pleasure to work with you in Club Palladium! From BMC to U of M (Sanford Lab) –we are continuing a very awesome trend!

Chelsea Huff, I had so much fun on all of our travels together! Your easy-going demeanor made it real pleasure to work with you!

Monica Lotz, it has been so nice to chat with you over the last few months. Have confidence and trust in yourself and I know you will do great!

Ansis Maleckis, thank you for teaching me 2D NMR spectroscopy over the summer. I appreciate all of our chemistry and life discussions and your humorous remarks! Cheers to Pd^{IV}!

Finally and most importantly, I would like to thank my family. Mom and Dad, you have instilled in me the values that have enabled me to be successful in life, from the first time I joined a team sport and you told me that I could not quit because I had a made a commitment to the team, to every night on the

phone when you tell me how proud you are of me for just being me. I am so blessed to have you as parents!

Mom- you gave me my first taste of feminism (I think even before I started kindergarten) when you told me how important it was as a woman to get an education and to be able to support yourself. I owe much of my blatant disregard for gender stereotypes to you. The love and trust that you give me allows me to explore life and know that no matter what you will still be there for me. Your unconditional selflessness, support, encouragement and hugs have kept me buoyant for 28 (almost 29 ☺) years!

Dad- all of my determination and work ethic has come from the example you set for me in your own life. You are the most resolute and hard working person I have ever met, from chopping wood every summer so that we could heat the house, to teaching yourself to be able to fix almost anything. Your determination to survive through difficult circumstances at so many stages in your life has truly been an inspiration to me. I love you so much and I am so thankful for every night that you tell me that you love me too!

Ken -When we were growing up I wished that I could be as smart as my older brother! Thank you for spending time with me when we were younger – playing Stratego, Chess, video games, sleigh riding, games in the pool or backyard. These are some of my favorite memories! Granted I never won very much, but it taught me to keep trying and work hard. I appreciate that you took me various museums, orchestras and plays while you were in college. You really enriched my life and taught me about the knowledge and beauty that comes from independent learning. Most importantly, I think all of these experiences enabled us to build a special bond. I really could not have asked for a more caring and loving brother! I'm so glad you placed the order for me! ;-)

Noni, when I describe you to people, I tend to refer to you as the matriarch of the family. Your fun loving attitude and generosity were so prevalent throughout my childhood. I am so grateful to have had such an amazing woman influencing me so early in my life. Thank you for all of my style!!

J, aka Honey, thank you so much for taking care of me, from packing my lunches throughout my pre-college education to picking me up from school and teaching me how to multiple and divide! I am so lucky that I have someone in my life who cares about me as much you do.

Leila, you are my sister for sure! Thank you for your unconditional love and support! I know that I can always count on you. Our ability to forgive and forget has allowed our friendship to grow incredibly strong. You will always be such an important part of my life. I'm excited to see where the future takes us!

Lastly, thank you to all of the many friends that I have met over the last few years through running and climbing in Ann Arbor. You have kept me

company and helped me to make it through graduate school while keeping balance in my life!

Table of Contents

List of Figures

List of Tables

List of Schemes

Abstract

New methodology involving Pd-mediated catalysis that proposes $Pd^{II/IV}$ mechanisms has exploded over the past decade. Despite the implication of Pd^{IV} intermediates prior to bond-forming C–X reductive elimination in these catalytic reactions, the reported organometallic Pd^{IV} complexes in the literature primarily underwent C–C bond-forming reductive elimination. The goal of this dissertation was to design systems to study C–X reductive elimination from observable Pd^{IV} complexes. In addition to reductive elimination reactions from Pd^{IV}, we sought to explore other organometallic reactions at Pd^{IV} centers such as C–H activation.

This thesis presents the design and synthesis of novel Pd^{IV} complexes that undergo clean sp^2- and sp^3-carbon-heteroatom coupling as well as C–H activation at a discrete Pd^{IV} center. Furthermore, mechanistic aspects of these reactions are discussed in detail.

Chapter 2 presents a detailed mechanistic study of C–O and C–C bond-formation from isolable Pd^{IV} complexes. A variety of complexes were synthesized to explore how electronic factors, activation parameters, solvent effects and additive effects are involved in/influence C–O reductive elimination from a Pd^{IV} center. Additionally, we identified a system that yielded competing C–O and C–C reductive elimination from Pd^{IV}. Therefore, we conducted mechanistic studies to probe C–C bond formation from Pd^{IV}; we were able to propose a mechanism for this transformation as well.

Chapter 3 investigates sp^2 versus sp^3-C–X bond formation from Pd^{IV} complexes. Interestingly, in all of the systems that were studied, sp^3-C–X bond formation out competes sp^2 reductive elimination. This chapter presents novel examples of sp^3-C–F, C–N and C–O reductive elimination from Pd^{IV} in addition to

sp^3-C–Cl bond-formation. These reactions represent the first examples of high yielding sp^3-C–X reductive elimination from Pd^{IV}. Furthermore, the mechanisms of these transformations were explored. Lastly, the mechanistic insights gained from these studies lead us to examine systems for sp^3-C–X bond-formation that do not use the oxidant to deliver the desired functionality.

Next, Chapter 4 of this thesis describes the development a ligand system to explore C–H activation directly at a Pd^{IV} center. We designed a complex where reductive elimination is slow and C–H activation is observed. This enabled us to compare the selectively of C–H activation at a Pd^{IV} center versus a Pd^{II} center.

Finally, the thesis concludes with a discussion of the future for the development of Pd^{IV} chemistry.

Chapter 1: Introduction

1.1 Introduction

Palladium represents an essential tool for organic synthesis due to its wide spread use in catalysis for the construction of challenging types of C–C and C–heteroatom bonds.[1] As a result, palladium-catalyzed reactions have found vast applications in the area of pharmaceutical, natural product, and commodity chemical synthesis. The development of novel methodologies, the invention of new catalysts, and the investigation of mechanism for insight into how these reactions proceed account for the continued advancement in the arena of Pd catalysis. Over the past 70 years, the vast majority of reported, well-developed catalytic reactions have involved $Pd^{0/II}$ catalysis. For instance, in 2010 the Nobel Prize was awarded to Heck, Negishi and Suzuki for the development of cross-coupling reactions, which utilize two different pre-functionalized starting materials to afford new C–C bonds through a $Pd^{0/II}$ catalytic cycle (Scheme 1.1). Only since 2004 has Pd^{IV} routinely emerged as a proposed intermediate in Pd-catalyzed reactions.[2]

Scheme 1.1. Suzuki Cross-Coupling Reaction

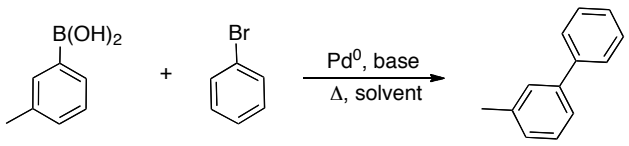

$Pd^{II/IV}$ catalysis has the potential to afford highly complementary and unique reactivity compared to $Pd^{0/II}$ catalysis. One key feature of organometallic Pd^{IV} intermediates is that they are generally moisture-stable due to the highly

polarized nature of the Pd^{IV}–C bond (Scheme 1.2). Additionally, Pd^{IV} complexes are typically octahedral and diamagnetic with a low spin t_{2g}^6 configuration, thus forming fully saturated complexes that are not prone to β-hydride elimination reactions (a common source of unwanted side products in $Pd^{0/II}$ catalytic reactions) (Scheme 1.3).[3] Pd^{IV} also has a unique advantage over Pd^{II} or Pt^{IV} because of its decreased stability, which contributes to the enhanced propensity of Pd^{IV} species towards reductive elimination to form challenging types of C–heteroatom bonds (Scheme 1.4).[4]

Scheme 1.2 Moisture Stable Alkyl/Aryl Ligands on Pd^{IV}

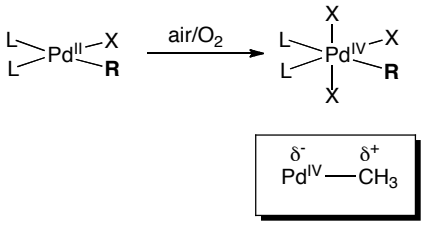

Scheme 1.3 Pd^{II} versus Coordinatively Saturated Pd^{IV}

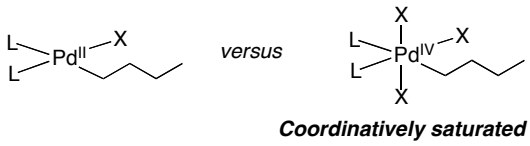

Scheme 1.4 Potential Driving Force for Ar–X Reductive Elimination from Pd^{IV}

As early as 1971, C–O bond-forming reductive elimination from a $Pd^{IV}(Ph)(OAc)$ species was implicated in the $Pd(OAc)_2$-catalyzed oxidation of benzene with $K_2Cr_2O_7$ by Henry (Scheme 1.5).[5] In 1974 Eberson proposed a similar mechanism for the acetoxylation of benzene with $K_2S_2O_8$ and $Pd(OAc)_2$.[6] Although these reactions were quite interesting because they directly converted

inert C–H bonds of benzene to C–O bonds, the reactions were not selective and resulted in mixtures of mono and diacetoxylated products. While Pd^{IV} complexes were alluded to as possible intermediates in these catalytic reactions, no examples of Pd^{IV} complexes containing a carbon ligand had been reported in the literature up to this point.

Scheme 1.5 Acetoxylation of Benzene with Proposed Pd^{IV} Intermediate

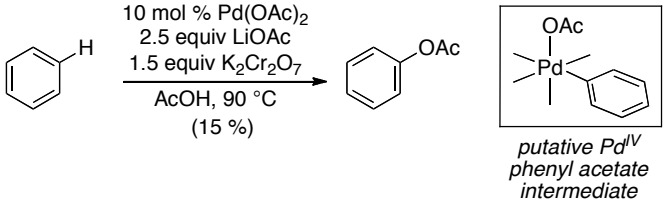

The first organometallic Pd^{IV} complex was synthesized in 1975 by Uson via the oxidation of $Pd^{II}(C_6F_5)_2$(tmeda) with Cl_2 to afford $Pd^{IV}(Cl)_2(C_6F_5)_2$(tmeda).[7] In 1986, another seminal milestone for Pd^{IV} came in the realm of stoichiometric chemistry, when Canty reported the first example of a crystallographically characterized organometallic Pd^{IV} complex, *fac*-[(bpy)$Pd^{IV}(CH_3)_3(I)$] (bpy = 2,2'-bipyridine) (**1**). In addition, his group demonstrated that this species undergoes facile C–C bond-forming reductive elimination to release ethane (Scheme 1.6).[8] This report supported the hypothesis that an organometallic Pd^{IV} complex could undergo clean reductive elimination to generate organic products.

Scheme 1.6 C–C Bond-Forming Reductive Eliminaton from the First Crystallographically Characterized Pd^{IV} Complex (1)

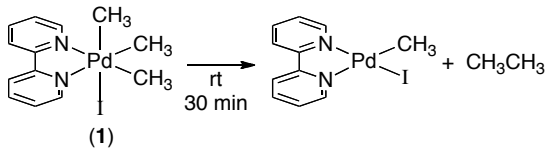

However, even though Pd^{IV} intermediates have been implicated since the 1970's it was not until mid-2000 that the field of $Pd^{II/IV}$ catalysis exploded. Over the past decade, carbon-heteroatom bond-forming reductive elimination from

transient Pd^{IV} intermediates has been proposed as the product-release step of a variety of important Pd-catalyzed transformations, including arene and alkane C–H bond functionalization[9,10,11] allylic acetoxylation,[12] alkene borylation[13], and olefin difunctionalization.[14] Examples of C–C bond forming reactions from proposed Pd^{IV} intermediates have also emerged;[15] however, this thesis will focus predominantly on carbon-heteroatom bond forming reactions from Pd^{IV}.

The rapid expansion in the area of $Pd^{II/IV}$ catalysis was initially due to the merger of ligand directed C–H activation and functionalization. One of the pivotal reports emerged from our group in 2004.[16] In this communication, we demonstrated the conversion of C–H bonds to C–OAc bonds using $Pd(OAc)_2$ and $PhI(OAc)_2$ affording products selectively and in high yields (Scheme 1.6).

Scheme 1.6 Ligand Directed C–H Activation/Acetoxylation Reaction

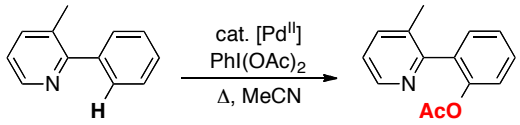

This methodology was in contrast to the reactions developed by Henry, Eberson and later by Crabtree.[17] The incorporation of a ligand for directed C–H activation was a key development for limiting the formation of over functionalized side products. The following mechanism was proposed for this transformation: (1) rate limiting ligand directed C–H activation to afford a palladacycle, (2) oxidation with $PhI(OAc)_2$ to yield a Pd^{IV} intermediate, and (3) product forming reductive elimination and regeneration of the Pd^{II} catalyst (Scheme 1.7).[16]

Scheme 1.7 Proposed Mechanism for Directed C–H Activation/Acetoxylation Reaction

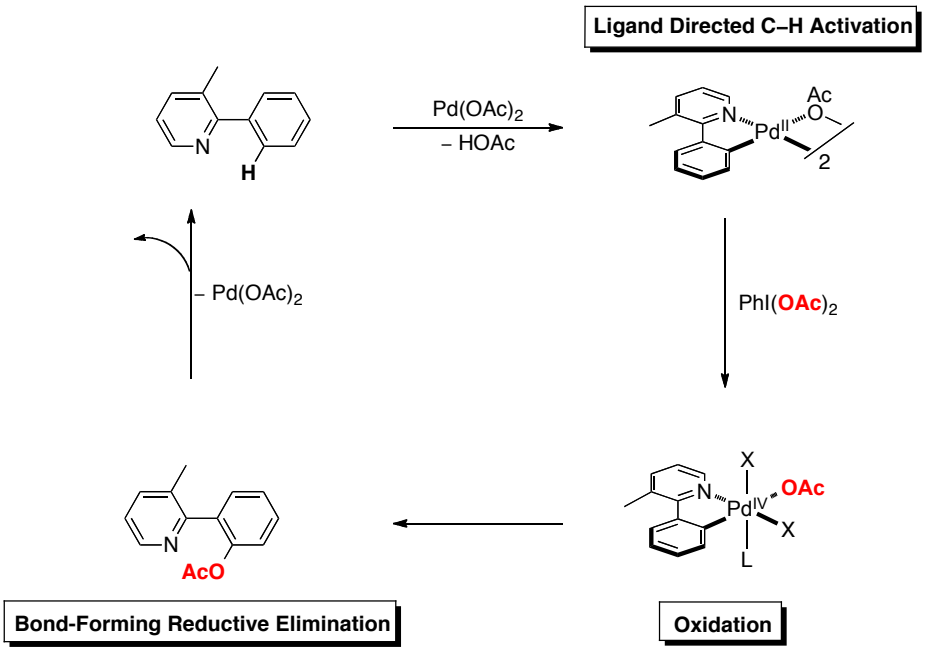

Since then, ligand-directed oxygenation of sp^2 and sp^3 C–H bonds with $PhI(OAc)_2$[18,19], Oxone[20,21], $K_2S_2O_8$[20], IOAc[21], $CH_3CO_2O^tBu$[22], lauroyl peroxide[23], and O_2[24] have all been suggested to proceed via $Pd^{II/IV}$ pathways in which C–O bond-forming reductive elimination serves as the product-forming step of the catalytic cycle.

Numerous Pd-catalyzed olefin difunctionalization reactions are also hypothesized to involve C–O bond-forming reductive elimination from Pd^{IV} as a key step. For example, diverse α-olefins have been shown to undergo Pd-catalyzed dioxygenation with oxidants including $PhI(OAc)_2$[24,25], O_2[26,27], and peracetic acid[28] via a putative $Pd^{II/IV}$ pathway (Scheme 1.8). In addition, the Pd-catalyzed aminooxygenation of olefins with $PhI(OAc)_2$ is thought to involve C–OAc bond formation at Pd^{IV} as the product release step (Scheme 1.9)[29,30,31].

Scheme 1.8 Olefin Difunctionalization Reactions

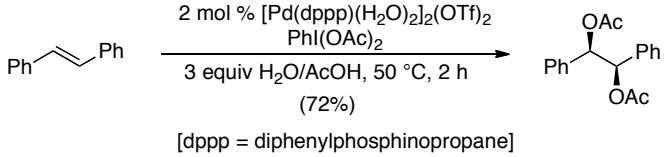

Scheme 1.9 Pd-Catalyzed Aminooxygenation of Olefins

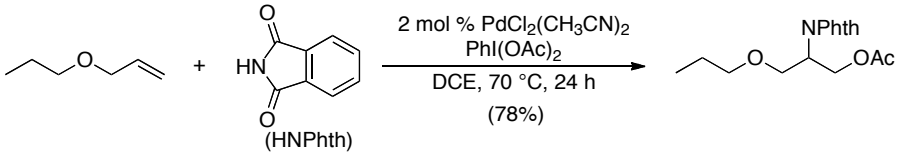

A wide variety of Pd-catalyzed ligand-directed C–H halogenation reactions have also been reported. For example C–H iodination with *N*-iodosuccinimide (NIS)[32], $IOAc/Bu_4NI$[33], and $I_2/PhI(OAc)_2$[34], C–H bromination with *N*-bromosuccinimide (NBS)[35], $Cu(OAc)_2/CuBr_2$[36], $BrOAc/Bu_4NBr$[37], and $CuBr_2/LiBr$[38,39], C–H chlorination with Cl_2[40], *N*-chlorosuccinimide (NCS)[32], $PhICl_2$[32], and $Cu(OAc)_2/CuCl_2$[36,39], and C–H fluorination with *N*-fluoropyridinium reagents[41,42] have all been applied to both arene and alkane substrates (Scheme 1.10-1.12). The structures of reactive Pd intermediates in these transformations have not been definitively elucidated. However, $Pd^{II/IV}$ mechanisms that involve carbon-halogen bond formation from transient Pd^{IV} intermediates have been proposed in many of these systems.

Scheme 1.10 C–H Iodination

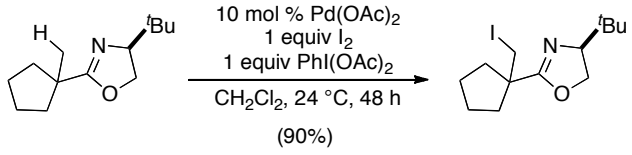

Scheme 1.11 C–H Bromination with NBS

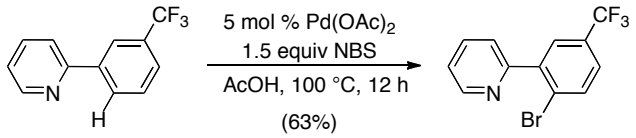

Scheme 1.12 C–H Fluorination with *N*-Fluoropyridinium Reagents

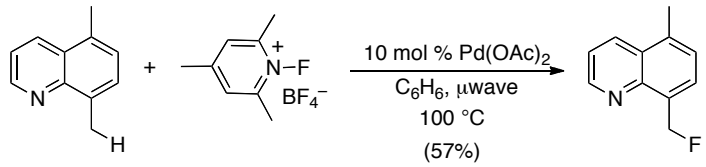

Several Pd-catalyzed olefin difunctionalization reactions have also been terminated by oxidative carbon–halogen bond formation. For example, both intra- and intermolecular aminohalogenations with NCS[43], NIS[44], $CuCl_2$[45,46], $CuBr_2/O_2$[47], and $AgF/PhI(O_2C^tBu)_2$ [48] have been achieved (Scheme 1.13). Henry has reported a related synthesis of halohydrins via oxypalladation/C–X coupling (Scheme 1.14) [48]. In addition, the arylhalogenation of diverse α-olefins with $PhICl_2$, $CuCl_2$, and $CuBr_2$ was recently disclosed (Scheme 1.15)[49,50]. While the reactive intermediates in these transformations have not been characterized, C–halogen bond-formation from Pd^{IV} intermediates has been suggested in many cases.

Scheme 1.13 Intermolecular Aminohalogenations

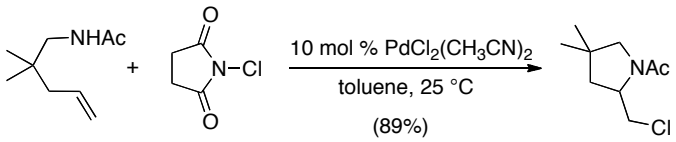

Scheme 1.14 Oxypalladation/C–X coupling

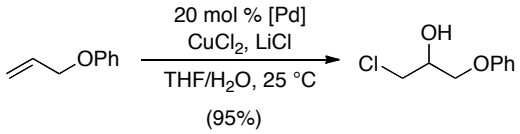

Scheme 1.15 Arylhalogenation of α-Olefins

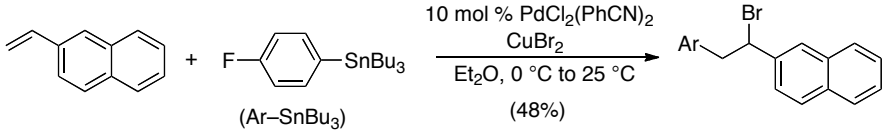

Although examples of C–S bond formation from proposed Pd^{IV} intermediates are rare, a recent report by Dong and coworkers demonstrated the Pd-catalyzed ligand-directed sulfonylation of arylpyridine, arylpyrazole, and aryloxime ether derivatives with $ArSO_2Cl$ (Scheme 1.16)[51a]. The authors speculated that a $Pd^{II/IV}$ mechanism (involving oxidative addition into the S–Cl bond and subsequent C–S bond-forming reductive elimination from Pd^{IV}) was potentially operative. Recently, the authors have isolated Pd^{IV} sulfinate complexes and studied C–S bond formation directly from the metal center. [51b]

Scheme 1.16 Directed Sulfonylation

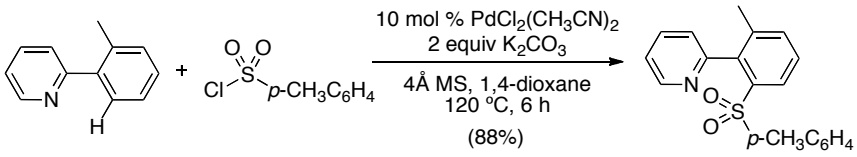

Since the rate determining step of the above mentioned catalytic reactions usually precedes the product determining reductive elimination step from the

proposed Pd^{IV} intermediate, it is challenging to identify how these transformations occur by directly studying the catalytic reactions. Therefore, a variety of Pd^{IV} model complexes have been synthesized to study reductive elimination reactions at Pd^{IV} centers. Since the report of the first characterized organometallic Pd^{IV} complex by Canty[8], numerous examples of C–C bond-forming reductive elimination from Pd^{IV} complexes have been demonstrated[51,52,53,54,55,56]. In contrast, C–heteroatom bond-forming reactions from Pd^{IV} species remain much rarer. This thesis presents the design and synthesis of novel Pd^{IV} complexes that undergo clean sp^2- and sp^3-carbon-heteroatom coupling as well as C–H activation at a discrete Pd^{IV} center. Furthermore, mechanistic aspects of these reactions are discussed in detail.

Chapter 2 presents a detailed mechanistic study of C–O and C–C bond-formation from isolable Pd^{IV} complexes. A variety of complexes were synthesized to explore how electronic factors, activation parameters, solvent effects and additive effects are involved in/influence C–O reductive elimination from a Pd^{IV} center. Additionally, we identified a system that yielded competing C–O and C–C reductive elimination from Pd^{IV}. Therefore, we conducted mechanistic studies to probe C–C bond formation from Pd^{IV}; we were able to propose a mechanism for this transformation as well. The work in this Chapter on C–O reductive elimination from Pd^{IV} lends support for the proposed mechanism for the Pd-catalyzed acetoxylation reaction represented in Scheme 1.7.

Chapter 3 investigates sp^2 versus sp^3-C–X bond formation from Pd^{IV} complexes. Interestingly, in all of the systems that were studied, sp^3-C–X bond formation out competes sp^2 reductive elimination. This chapter presents novel examples of sp^3-C–F, C–N and C–O reductive elimination from Pd^{IV} in addition to sp^3-C–Cl bond-formation. These reactions represent the first examples of high yielding sp^3-C–X reductive elimination from Pd^{IV}. Furthermore, the mechanisms of these transformations were explored. Lastly, the mechanistic insights gained from these studies lead us to examine systems for sp^3-C–X bond-formation that do not use the oxidant to deliver the desired functionality.

As mentioned above, most of the catalytic reactions that propose $Pd^{II/IV}$ mechanisms suggest C–H activation at a Pd^{II} center, followed by oxidation, then reductive elimination. The next goal of my thesis was to explore organometallic transformations other than reductive elimination at a Pd^{IV} complex. Until very recently, no organometallic transformation (either catalytically or stoichiometrically) besides reductive elimination had been proposed at Pd^{IV}. Since there is a large driving force for Pd^{IV} to undergo reductive elimination, it was typically assumed that this reaction would always out compete any other type of organometallic transformation at Pd^{IV}. Then in 2006 our group disclosed a mechanism for the oxidative dimerization of 2-arylpyridine derivatives, in which a second C–H activation event takes place at a Pd^{IV} center.[57] Following this initial publication, there emerged four other reports in the literature of catalytic reactions that are believed to involve C–H activation at Pd^{IV}.[58] Chapter 4 of this thesis describes the development a ligand system to explore C–H activation directly at a Pd^{IV} center. We designed a complex where reductive elimination is slow and C–H activation is observed. This enabled us to compare the selectively of C–H activation at a Pd^{IV} center versus a Pd^{II} center.

Finally, Chapter 5 concludes this thesis and also presents an outlook for Pd^{IV} chemistry.

1.2 References

1. Negishi E (ed), Handbook of organopalladium chemistry for organic synthesis. **2002**, Wiley, New York

2. Lyons T.W.; Sanford, M. S. *Chem. Rev.*, **2010**, *110*, 1147.

3. (a) Miessler, G. L.; Tarr, D. A. Inorganic chemistry. Pearson education, **2004**, Upper Saddle River, New Jersey. (b) Albright, T. A. *Tetrahedron*, **1982**, *38*, 1339.

4. Sehnal, P.; Taylor, R. J. K.; Fairlamb, I. J. S. *Chem. Rev.*, **2010**, *110*, 824.

5. Henry, P. M. *J. Or.g Chem.* **1971**, *36*, 1886.

6. Eberson, L.; Jonsson, L. *J. Chem. Soc. Chem. Commun.,* **1974**, 885.

7. Uson, R.; Fornies, J.; Navarro, R. *J. Organomet. Chem.* **1975**, *96*, 307.

8. Byers, P. K.; Canty, A. J.; Skelton, B. W.; White, A. H. *J. Chem. Soc. Chem. Commun.,* **1986**, 1722.

9. Lyons T.W.; Sanford, M. S. *Chem. Rev.*, **2010**, *110*, 1147.

10. Dick, A. R.; Sanford, M. S. *Tetrahedron*, 2006, *62*, 2439-2463.

11. Aydin, J.; Larsson, J. M.; Selander, N.; Szabo, K. J. *Org. Lett.*, **2009,** *11*, 2852-2854.

12. Selander, N.; Willy, B.; Szabo, K. J. *Angew. Chem. Int. Ed.,* **2010**, *49*, 4051-4053.

13. Muniz, K. *Angew. Chem. Int. Ed.,* **2009**, *48*, 9412-9423.

14. (a) Kalyani, D.; Deprez, N. R.; Desai, L. V.; Sanford, M. S. *J. Am. Chem. Soc.* **2005**, *127*, 7330. (b) Deprez, N. R.; Sanford, M. S. *Inorg. Chem.* **2007**, *46*, 1924. (72) Daugulis, O.; Zaitsev, V. G. *Angew. Chem., Int. Ed.* **2005**, *44*, 4046. (73) Spencer, J.; Chowdhry, B. Z.; Mallet, A. I.; Rathnam, R. P.; Adatia, T.; Bashall, A.; Rominger, F. *Tetrahedron* **2008**, *64*, 6082. (75) Yang, F.; Wu, Y.; Li, Y.; Wang, B.; Zhang, J. *Tetrahedron* **2009**, *65*, 914. (76) Shabashov, D.; Daugulis, O. *Org. Lett.* **2005**, *7*, 3657. (77) Zaitsev, V. G.; Shabashov, D.; Daugulis, O. *J. Am. Chem. Soc.* **2005**, *127*, 13154. (78) Yang, F.; Wu, Y.; Zhu, Z.; Zhang, J.; Li, Y. *Tetrahedron* **2008**, *64*, 6782. Tobisu, M.; Ano, Y.; Chatani, N. *Org. Lett.* **2009**, *11*, 3250.

15. Dick, A. R.; Hull, K. L.; Sanford, M. S. *J. Am. Chem. Soc.*, **2004**, *126*, 2300-2301.

16. Yoneyama, T.; Crabtree, R. H. *J. Mol. Catal. A,* **1996**, *108*, 35-40.

17. Dick, A. R.; Hull, K. L.; Sanford, M. S. *J. Am. Chem. Soc.* **2004**, *126*, 2300-2301.

18. Desai, L. V.; Hull, K. L.; Sanford, M. S. *J. Am. Chem. Soc.* **2004**, *126*, 9542-9543.

19. Desai, L.V.; Malik, H. A.; Sanford, M. S. *Org. Lett.* **2006**, *8*, 1141-1144.

20. Reddy, B. V. S.; Reddy, L. R.; Corey, E. J. *Org. Lett.* **2006**, *8*, 3391-3394.

21. Wang, D. H.; Hao, X. S.; Wu, D.F.; Yu, J. Q. *Org. Lett.* **2006**, *8*, 3387-3390.

22. Giri, R.; Liang, J.; Lei, J. Q.; Li, J. J.; Wang, D. H.; Chen, X.; Naggar, I. C.; Guo, C.; Foxman, B. M.; Yu, J. Q. *Angew. Chem. Int. Ed.* **2005**, *44*, 7420-7424.

23. Zhang, J.; Khaskin, E.; Anderson, N. P.; Zavalij, P. Y.; Vedernikov, A. N. *Chem. Commun.* **2008**, *31*, 3625-3627.

24. Li, Y.; Song, D.; Dong, V. M. *J. Am. Chem. Soc*. **2008**, *130*, 2962-2964.

25. Wang, W. F.; Wang, F.J.; Shi, M. *Organometallics* **2010**, *29*, 928-933.

26. Zhu, M. K.; Zhao, J. F.; Loh, T. P. *J. Am. Chem. Soc.* 2010, *132*, 6284-6285.

27. Wang, A. Z.; Jiang, H. F.; Chen, H. J *J. Am. Chem. Soc*. **2009**, *131*, 3846-3847.

28. Park, C. P.; Lee, J. H.; Yoo, K. S.; Jung, K. W. *Org. Lett.* **2010**, *12*, 2450-2452.

29. Alexanian, E. J.; Lee, C.; Sorensen, E. J. *J. Am. Chem. Soc.* **2005**, *127*, 7690-7691.

30. Liu, G. S.; Stahl, S. S. *J. Am. Chem. Soc.* **2006**, *128*, 7179-7181.

31. Desai, L. V.; Sanford, M. S. *Angew. Chem. Int. Ed.* **2007**, *46*, 5737-5740.

32. Kalyani, D.; Dick, A. R.; Anani, W. Q.; Sanford, M. S. *Tetrahedron* **2006**, *62*, 11483-11498.

33. Giri, R.; Chen, X.; Yu, J. Q. *Angew. Chem. Int. Ed.* **2005**, *44*, 2112-2115.

34. Giri, R.; Chen, X.; Hao, X. S.; Li, J. J.; Liang, J.; Fan, P.; Yu, J. Q. *Tetrahedron: Asymmetry* **2005**, *16*, 3502-3505.

35. Wan, X.; Ma, Z.; Li, B.; Zhang, K.; Cao, S.; Zhang, S.; Shi, Z. *J. Am. Chem. Soc.* **2006**, *128*, 7416-7417.

36. Mei, T. S.; Giri, R.; Maugel, N.; Yu, J. Q. *Angew. Chem. Int. Ed.* **2008**, *47*, 5215-5212.

37. Savitha, G.; Felix, K.; Perumal, P. T. *Synlett* **2009**, 2079-2082.

38. Bedford, R. B.; Mitchell, C. J.; Webster, R. L. *Chem. Commun.* **2010**, *46*, 3095-3097

39. Fahey, D. R. *J. Chem. Soc. Chem. Commun.* **1970**, 417.

40. Hull, K. L.; Anani, W. Q.; Sanford, M. S. *J. Am. Chem. Soc.* **2006**, *128*, 7134-7135.

41. Wang, X.; Mei, T. S.; Yu, J. Q. *J. Am. Chem. Soc.* **2009**, *131*, 7520-7521.

42. Michael, F. E.; Sibbald, P. A.; Cochran, B. M. *Org. Lett.* **2008**, *10*, 793-796.

43. Doroski, T. A.; Cox, M. R.; Morgan, J. B. *Tetrahedron Lett.* **2009**, *50*, 5162-5164.

44. Lei, A.; Lu, X.; Liu, G. *Tetrahedron Lett.* **2004**, *45*, 1785-1788.

45. Christie, S. D. R.; Warrington, A. D.; Lunniss, C. J. *Synthesis* **2009**, 148-154.

46. Manzoni, M. R.; Zabawa, T. P.; Kasi, D.; Chemler, S. R. *Organometallics* **2004**, *23*, 5618-5621.

47. Wu, T.; Yin, G.; Lui, G. *J. Am. Chem. Soc.* **2009**, *131*, 16354-16255.

48. El-Qisairi, A. K.; Henry, P. M. *J. Organomet. Chem.* **2000**, *603*, 50-60.

49. Kalyani, D.; Satterfield, A. D.; Sanford, M. S. *J. Am. Chem. Soc.* **2010**, *138*, 8419-8427.

50. Kalyani, D.; Sanford, M. S. *J. Am. Chem. Soc.* **2008**, *130*, 2150-2151.

51. (a) Zhao, X.; Dimitrijevic, E.; Dong, V. M. *J. Am. Chem. Soc.* **2009**, *131*, 3466-3467. (b) Zhao, X.; Dong, V. M. *Angew. Chem. Int. Ed.* **2011**, *123*, 962-964.

52. Canty, A. J. *Acc. Chem. Res.* **1992**, *25*, 83-90.

53. Canty, A. J.; van Koten, G. *Acc. Chem. Res.* **1995***, 28*, 406-413.

54. Canty, A. J. *Dalton. Trans.* **2009** *47*, 10409-10417.

55. Xu, L. M.; Li, B. J.; Yang, Z.; Shi, Z. J. *Chem. Soc. Rev.* **2010**, *39*, 712-733.

56. Sehnal, P.; Taylor, R. J. K.; Fairlamb, I. J. S. *Chem. Rev.* **2010**, *110*, 824-889.

57. Hull, K. L.; Lanni, E. L.; Sanford, M. S. *J. Am. Chem. Soc.* **2006**, *128*, 14047.

58. Sibbald, P. A.; Rosewall, C. F.; Swartz, R. D.; Michael, F. E. *J. Am. Chem. Soc.* **2009**, *131*, 15945. Pilarski, L. T.; Selander, N.; Bose, D.; Szabo, K. J. *Org. Lett.* **2009**, *11*, 5518. Hickman, A. J.; Sanford, M. S. *ACS Catal.* **2011**, *1*, 170. Kawai, H.; Kobayshi, Y.; Oi, S.; Inoue, Y. *Chem. Commun*. **2008**, 1464.

Chapter 2: Detailed Study of C–O and C–C Bond-Forming Reductive Elimination from Stable C2N2O2–Ligated Palladium(IV) Complexes

2.1 Introduction

Our group has recently reported a Pd-catalyzed reaction for the ligand-directed acetoxylation of carbon-hydrogen bonds using $PhI(OAc)_2$ as the terminal oxidant (Scheme 2.1.1).[1,2,3] The key carbon-oxygen coupling step of this transformation was proposed to involve C–O bond-forming reductive elimination from a rare, high oxidation state Pd^{IV} species of general structure **A**.[1,4] While analogous C–O bond-forming reductive elimination reactions from Ni^{III},[5] Pd^{II},[6] and Pt^{IV} [7] centers have been studied extensively, detailed investigation of such reactions at Pd^{IV} complexes has thus far remained elusive.[8,9]

Scheme 2.1.1 Proposed Mechanism for Pd-Catalyzed Acetoxylation of 2-Phenylpyridine

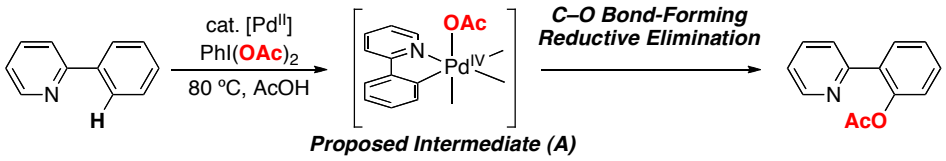

Studies of C–O bond formation at Pd^{IV} have proven challenging for two major reasons. First, there are relatively few examples of isolable Pd^{IV} complexes containing oxygen donor ligands.[8,9] Second, the available complexes are typically stabilized by the presence of multiple σ-alkyl and/or aryl ligands. As a

result, investigations of C–O bond-forming reductive elimination have been hampered by competing C–C coupling processes.[8,9] Hence, we sought to design a new model system that would allow for systematic mechanistic investigations of C–O bond-forming reductive elimination from Pd^{IV} centers.

We reasoned that Pd^{IV} complexes of general structure $(N\sim C)_2Pd^{IV}(O_2CR)_2$ (**B**) (N~C = a rigid cyclometalated ligand) might serve as attractive models for **A** on the basis of several key design features (Scheme 2.1.2). First, the N~C ligands were selected to stabilize the desired Pd^{IV} species, due to their rigid, bidentate structures[8-10] and the fact that they contribute two electron-donating σ-aryl ligands to the high oxidation state Pd complex.[8-11] Additionally, we hypothesized that the rigid and chelating nature of the two N~C ligands would limit competing C–C bond-forming processes relative to the desired C–O coupling. Finally, we reasoned that the two carboxylates could be incorporated by oxidation of $(N\sim C)_2Pd^{II}$ with $PhI(O_2CR)_2$, which is the same terminal oxidant used for the catalytic reactions in Scheme 2.1.1.

Scheme 2.1.2. Design of Complex B **for Study of C–O Bond-Forming Reductive Elimination at Pd^{IV}**

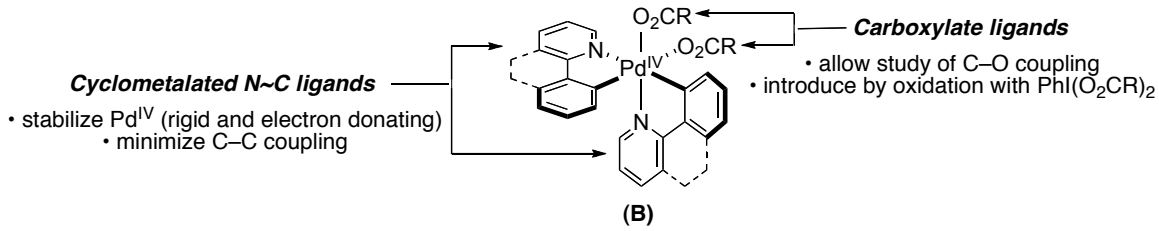

(**B**)

Herein, we report detailed studies on the synthesis and reactivity of Pd^{IV} complexes of general structure **B**. These complexes are readily prepared by the oxidation of $(N\sim C)_2Pd^{II}$ with $PhI(O_2CR)_2$ and are remarkably stable at room

temperature.[12,13] However, at elevated temperatures, most undergo clean C–O bond-forming reductive elimination to afford ester products. This chapter describes full mechanistic investigations of this C–O bond-forming process and also provides mechanistic insights into competing C–C coupling reactions.

2.2 Results and Discussion for C–O Bond-Formation from Pd(IV)

The following work was done in collaboration with Dr. Allison Dick and Professor Melanie Sanford. Where Dr. Allison Dick carried out the experiments I have denoted them specifically in this chapter.

Initial Investigations. 2-Phenylpyridine (Phpy) was selected as the N~C chelating ligand due to its high reactivity in Pd-catalyzed C–H activation/acetoxylation reactions[1] and the availability of the starting material $(Phpy)_2Pd^{II}$ (**1**).[14] Gratifyingly, treatment of **1** with $PhI(OAc)_2$ in CH_2Cl_2 at 25 ºC for 30 min produced a single inorganic product (**2**) (Scheme 2.2.1). Complex **2** was isolated in 93% yield as a pale yellow solid by precipitation with diethyl ether. This species was remarkably stable in the solid state and could be stored for 12 months at –35 ºC without significant decomposition.

Scheme 2.2.1 Oxidation of $(Phpy)_2Pd^{II}$ (1) with $PhI(OAc)_2$

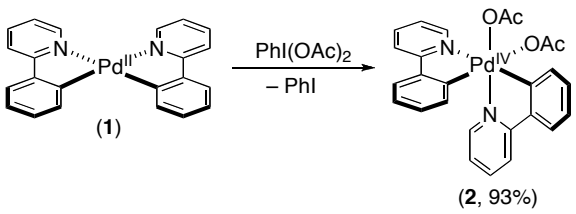

The ^{1}H NMR spectrum of **2** in acetone-d_6 shows 16 distinct aromatic signals between 6.29 and 9.46 ppm and two different acetate resonances at 1.63 and 1.74 ppm. These spectroscopic data are indicative of an unsymmetrical octahedral Pd^{IV} species with two different Phpy and acetate ligand environments. Further characterization of **2** by X-ray crystallography confirmed that this complex has an octahedral geometry with *cis*-phenylpyridine and acetate ligands (Figure 2.2.1). *Importantly, this is a highly unusual example of a room temperature stable Pd^{IV} complex containing a $C_2N_2O_2$ coordination environment.*

Figure 2.2.1 ORTEP of $(Phpy)_2Pd^{IV}(OAc)_2$ (2)

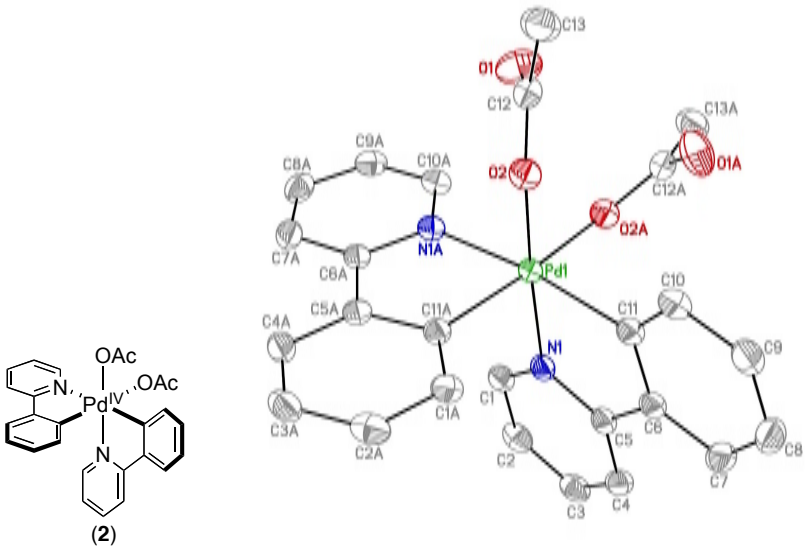

Next, we examined the reactivity of Pd^{IV} complex **2** towards thermally-induced reductive elimination. Two possible reductive elimination reactions are possible from **2** – carbon–oxygen bond-forming reductive elimination to generate 2-(2-acetoxyphenyl)pyridine (**3**) and/or C–C bond-forming reductive elimination to afford 2,2'-di(pyridin-2-yl)biphenyl (**4**) (Scheme 2.2.2). Literature reports have

shown that related Pd^{IV} species [for example, (bipy)$Pd^{IV}(Me)_3(O_2CPh)$ (bipy = 2,2'-bipyridine)] undergo C–C bond formation at comparable or faster rates than the desired C–O coupling reaction.[8,9]

Scheme 2.2.2 Possible Organic Products of Reductive Elimination from 2

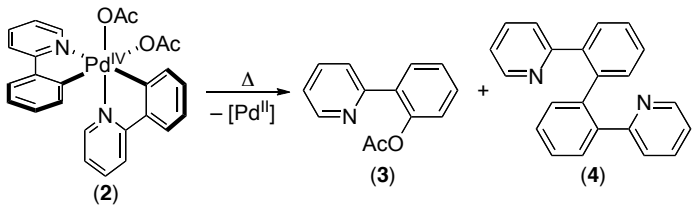

We were pleased to find that heating a solution of **2** in CH_3CN for 30 min at 80 ºC resulted in the formation of **3** as the sole organic product in nearly quantitative yield (95%) as determined by ^1H NMR spectroscopy. The inorganic product of this reaction was the cyclometalated Pd^{II} dimer **5**, which was obtained in 98% yield (Scheme 2.2.3). *This is the first direct observation of sp^2 C–O bond-forming reductive elimination from an isolated Pd^{IV} center.* As a result, this system presented a unique opportunity for mechanistic studies relevant to the proposed product-forming step in Pd-catalyzed C–H bond acetoxylation reactions.[1-3]

Scheme 2.2.3 Reductive Elimination from $(Phpy)_2Pd^{IV}(OAc)_2$ (2)

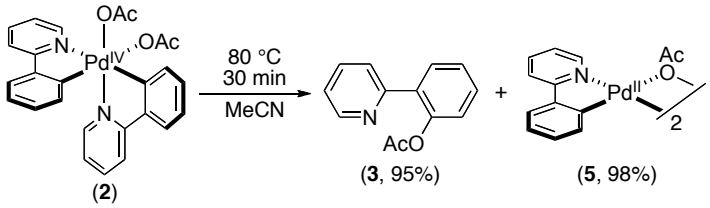

Mechanistic Considerations. We considered three mechanisms for C–O bond-forming reductive elimination from complexes of general structure **I** (Scheme 2.2.4). The first possibility was an ionic mechanism (**A**), which would proceed via carboxylate dissociation from **I** to form five-coordinate intermediate **II**, followed by reductive elimination from this cationic species. Mechanism **B**, concerted bond formation, would involve direct C–O reductive elimination from the coordinatively saturated octahedral Pd^{IV} complex **I**. Finally, Mechanism **C**, chelate dissociation, would involve dissociation of an N-donor ligand to generate the neutral 5-coordinate species **III**, followed by reductive elimination. Notably, within all three mechanisms, there are two distinct carboxylates that could participate in C–O bond-forming reductive elimination. In mechanism **A**, C–O coupling from intermediate **II** could occur via nucleophilic attack by the dissociated carboxylate or by direct reaction of the coordinated carboxylate. In mechanisms **B** and **C**, reductive elimination could involve C–O coupling with the carboxylate *trans* to the pyridine nitrogen or with the carboxylate *trans* to the σ-Ar ligand.

Scheme 2.2.4 Possible Mechanisms for C–O Bond-Forming Reductive Elimination

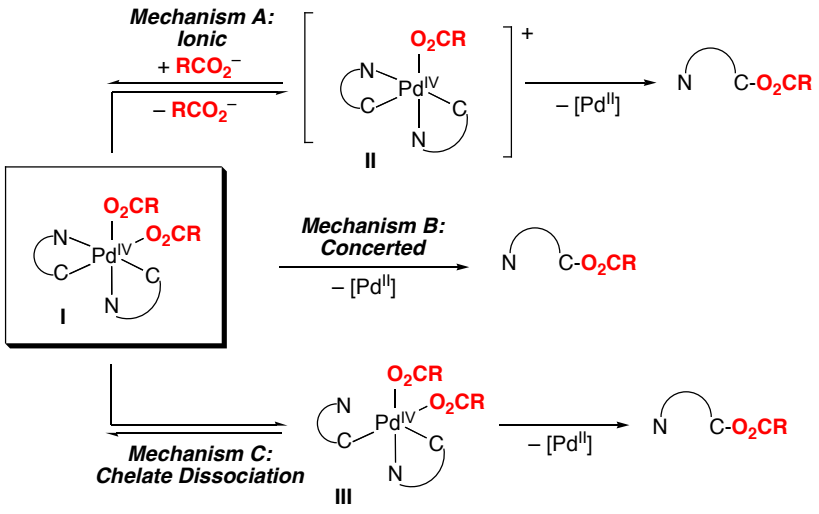

There is literature precedent for each of these mechanisms in reductive elimination reactions at group 10 metal centers. For example, mechanism **A** has been implicated for sp^3 C–O,[7] sp^3 C–halogen,[15] sp^3 C–N,[16] and sp^2 C–halogen[17] bond-forming reductive elimination from Pt^{IV}. A concerted mechanism has been proposed for sp^2 C–O,[5] sp^2 C–N,[18] and sp^2 C–S[19] bond-forming reductive elimination from Pd^{II} centers. Finally, mechanism **C** has been reported for some C–C bond-forming reactions from Pt^{IV}.[20]

We aimed to distinguish among these mechanistic possibilities by systematically studying C–O bond-forming reductive elimination from $(Arpy)_2Pd^{IV}(O_2CR)_2$ (Arpy = substituted arylpyridine, O_2CR = substituted carboxylate). These complexes were synthesized by the reaction of **1** with $PhI(O_2CR)_2$ (Scheme 2.2.5).[21]

Scheme 2.2.5 General Synthetic Route to $(Arpy)_2Pd^{IV}(O_2CR)_2$

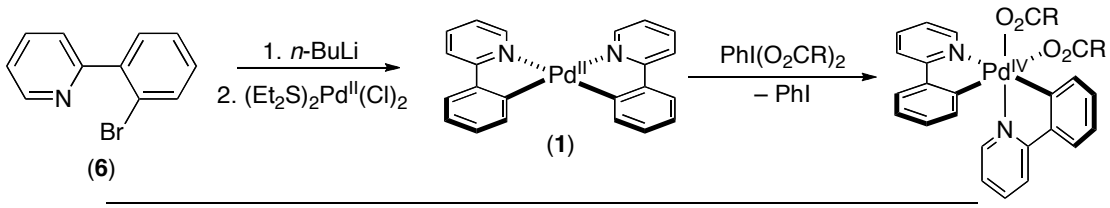

(**6**) (**1**)

R	complex	yield	R	complex	yield
C_9H_{19}	**7**	78%	*p*-ClC_6H_4	**13**	78%
p-$MeOC_6H_4$	**8**	83%	*p*-BrC_6H_4	**14**	82%
p-MeC_6H_4	**9**	88%	*p*-AcC_6H_4	**15**	80%
C_6H_5	**10**	90%	*p*-$CF_3C_6H_4$	**16**	74%
p-$PhOC_6H_4$	**11**	83%	*p*-CNC_6H_4	**17**	94%
p-FC_6H_4	**12**	93%	*p*-$NO_2C_6H_4$	**18**	85%

Initial investigations in this area provided preliminary evidence in support of mechanism **C**.[12] More recently, a computational study by Liu and coworkers has suggested that mechanism **B** is operating in these systems.[22] To gain further insights into this transformation, I carried out numerous additional experiments to probe both C–O and related C–C bond-forming reductive elimination processes from $(Arpy)_2Pd^{IV}(O_2CR)_2$. As detailed below, these new investigations, as well as reevaluation/reinterpretation of the previous data, lead me to conclude that mechanism **A** is, in fact, most likely operating in this system.

Mechanism of C–O Bond-Forming Reductive Elimination: Carboxylate Exchange. Initial mechanistic studies probed the viability of mechanism **A** by investigating whether complex **2** undergoes exchange between free and bound carboxylates at temperatures below those required for reductive elimination (Scheme 2.2.6). Because **2** is coordinatively saturated, carboxylate exchange would require dissociation of an acetate ligand via a process analogous to the first step of mechanism **A**. Notably, Goldberg and coworkers have shown that such exchange reactions occur rapidly at the Pt^{IV} complex *fac*-(dppbz)$PtMe_3$(OAr) (dppbz = bis(diphenylphosphino)benzene), which undergoes C–O bond-forming reductive elimination via mechanism **A**.[7b]

Scheme 2.2.6 Potential Products of Carboxylate Exchange Reaction

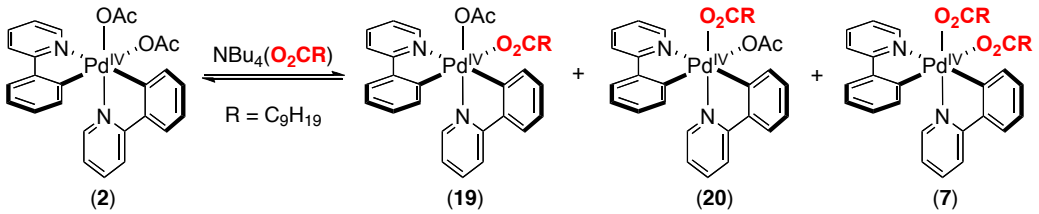

Carboxylate exchange was first studied by treating complex **2** with 1 equiv of $NBu_4(O_2CC_9H_{19})$ at 25 ºC in acetone-d_6. Importantly, these conditions are far milder than those required to induce C–O bond-forming reductive elimination from **2**. Analysis of the reaction by ^{1}H NMR spectroscopy after 5 min showed formation of one major new Pd^{IV} species with characteristic upfield and downfield ^{1}H NMR resonances at 6.31 and 9.49 ppm. These are slightly shifted relative to the starting material, which has signals at 6.29 and 9.44 ppm. We hypothesized that this new complex was the mono-acetate adduct **19** where the acetate ligand *trans* to C was replaced with $O_2CC_9H_{19}$. The selective replacement of this OAc can be rationalized on the basis of the larger *trans* influence of the σ-aryl ligand versus the pyridine nitrogen.[23]

The isolation of **19** from the reaction mixture was challenging because this species was not readily separable from tetrabutylammonium-containing by-products. Thus, an authentic sample of **19** was synthesized independently by reaction of $(Phpy)_2Pd^{IV}(Cl)(OAc)$[24] (**21**) with 1 equiv of $AgO_2CC_9H_{19}$ (Scheme 9). This product showed identical ^{1}H NMR resonances to those observed in the exchange reaction. In addition, its structure was unambiguously established by X-ray crystallography (Scheme 2.2.7).

Scheme 2.2.7 Independent Synthesis of Complex 19 and ORTEP of 19

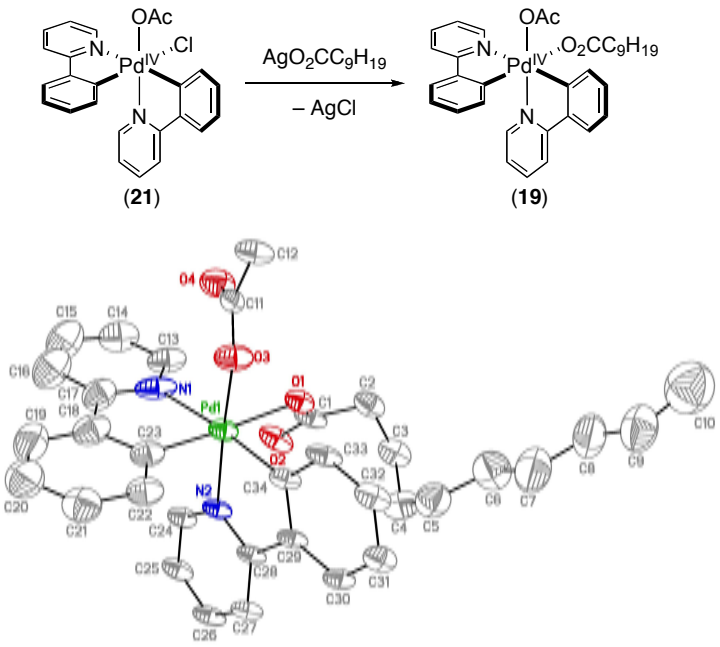

While ^{1}H NMR spectroscopic analysis was consistent with **19** as the major product of the exchange process, we were unable to definitively establish whether small quantities of **20** and **7** were also formed, since these have closely overlapping ^{1}H NMR resonances. As such, electrospray mass spectrometry was used to analyze the products of a closely related reaction – the thermoneutral exchange between $(Phpy)_2Pd^{IV}(OAc)_2$ and $NBu_4(OAc\text{-}d_3)$ (Scheme 2.2.8). Electrospray MS of all of the possible products (which were each synthesized independently)[25] showed major peaks consistent with loss of the acetate ligand *trans* to the σ-aryl group. For example, the peak for $(Phpy)_2Pd^{IV}(OAc\text{-}d_3)(OAc)$ (**2a-*d*$_3$**) was $[(Phpy)_2Pd^{IV}(OAc)]^+$ (MW = 473.0) while that for $(Phpy)_2Pd^{IV}(OAc)(OAc\text{-}d_3)$ (**2b-*d*$_3$**) was $[(Phpy)_2Pd^{IV}(O_2CCD_3)]^+$ (MW = 476.0). Furthermore, co-injection of a 1 : 1 mixture of **2** : **2-*d*$_6$** showed peaks of equal intensity, demonstrating that peak intensities can be used to determine the relative concentrations of these species.

Scheme 2.2.8 Electrospray MS Data for Reaction between 2 and $NBu_4(OAc\text{-}d_3)$

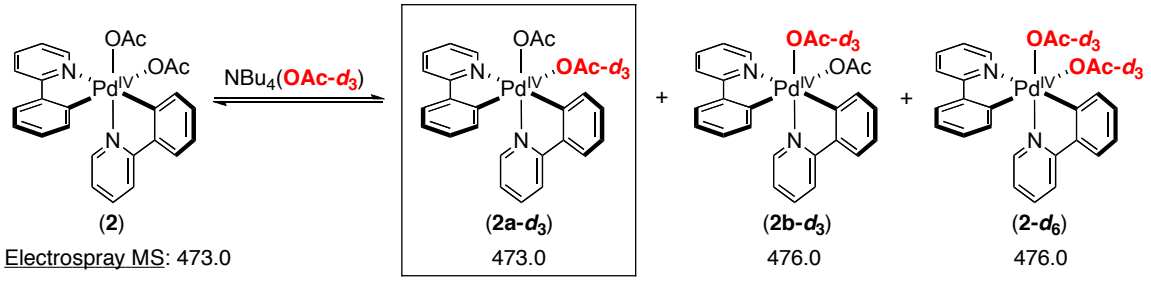

When a 1 : 1 mixture of $(Phpy)_2Pd^{IV}(OAc)_2$ and $NBu_4(OAc\text{-}d_3)$ was combined in CH_2Cl_2, stirred for 20 min, and then analyzed by electrospray MS, a single peak for $[(Phpy)_2Pd^{IV}(OAc)]^+$ (MW = 473.0) was observed (Scheme 2.2.8). This result indicates that neither **2b-*d*$_3$** nor **2-*d*$_6$** is formed, thereby providing further evidence that carboxylate exchange occurs solely at the site *trans* to the σ-aryl ligand.

As discussed above, carboxylate exchange cannot occur by an associative mechanism, since the starting complex is coordinatively saturated. Thus, the observation of rapid exchange suggests strongly that carboxylate dissociation (the first step of mechanism **A**) can occur at temperatures below those required for reductive elimination. However, more experiments were required to determine whether this exchange was mechanistically relevant to C–O bond-forming reductive elimination.

Mechanism of C–O Bond-Forming Reductive Elimination: Cross-Over Studies. Next, Dr. Allison Dick investigated whether cross-over between free and bound carboxylate occurred during the course of the reductive elimination reaction. A first cross-over study involved thermolysis of the bis-benzoate complex **8** in the presence of 5 equiv of NBu_4OAc in either $CDCl_3$ or DMSO.[12]

Analysis of the reaction mixture by GC and GCMS showed that the predominant organic product was **22**, and that <5% of the cross-over product **3** was formed.

Scheme 2.2.9 Initial Cross-Over Experiment

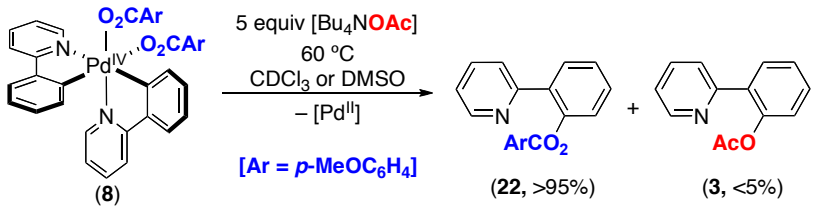

We reasoned that the absence of cross-over might be due to an electronic bias for reductive elimination of the benzoate in preference to the acetate ligand. As such, we designed a system to eliminate this electronic bias and differentiate the bound and free carboxylates solely based on isotopic labeling. However, thermolysis of $(Phpy)_2Pd^{IV}(OAc\text{-}d_3)_2$ (**2-*d*$_6$**) in the presence of 5 equiv of NBu_4OAc under otherwise identical conditions to Scheme 2.2.9 still afforded <6% of cross-over product **3** (Scheme 2.2.10).

Scheme 2.2.10 AcO/AcO-*d*$_3$ Cross-over Experiment

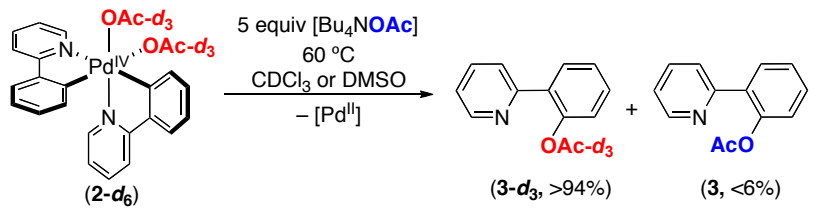

These results indicate that the non-exchangeable carboxylate ligand participates selectively in the C–O bond-forming reaction. This was confirmed by subjecting complex **2b-*d*$_3$**,[25] which contains two different carboxylate ligands, to the standard reductive elimination conditions. The major product (>95% yield)

was **3-d_3** and <5% of **3** was observed as determined by ^{1}H and ^{2}H NMR spectroscopy (Scheme 2.2.11).

Scheme 2.2.11 Selectivity of C–O Bond-Formation from 2b-d_3

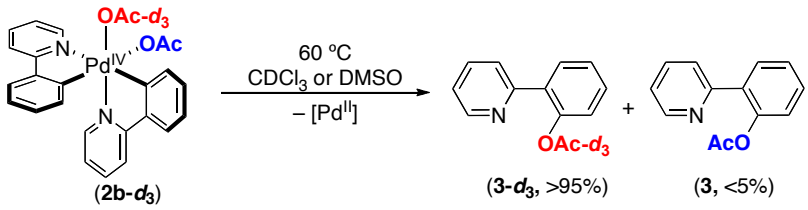

Mechanism of C–O Bond-Forming Reductive Elimination: Solvent Effects. Polar solvents often accelerate reductive elimination and ligand exchange reactions that proceed via ionic mechanisms.[7,26,27] Thus, we next investigated the effect of solvent on the rates of both C–O bond-forming reductive elimination and carboxylate exchange in a series of solvents with diverse polarities. The bis-decanoate complex $(Phpy)_2Pd^{IV}(O_2CC_9H_{19})_2$ (**7**) was used for these studies due to its high solubility in many different solvents.

The rate of C–O bond-forming reductive elimination from **7** was examined as a function of solvent under standard conditions (55 ºC, 15.2 mM in solvent with 5% v/v pyridine) by Dr. Allison Dick.[28] The disappearance of starting material **7** and concomitant formation of **23** and **24** were monitored by ^{1}H NMR spectroscopy. Interestingly, changing the solvent had very little influence on the reaction rate, and k_{obs} varied by only ~3-fold over a wide array of solvents (Table 2.2.1). In addition, there was no clear correlation between k_{obs} and the solvent polarity. For example, nearly identical rates were observed in benzene and acetone (k_{rel} = 1), despite a large difference in dielectric constant (e = 2 and 21, respectively). Furthermore, comparable and relatively fast rates were observed in non-polar $CDCl_3$ (e = 4.8, k_{rel} = 2.3) and polar CH_3CN (e = 38, k_{rel} = 2.4).

Table 2.2.1 Effect of Solvent on the Rate of Reductive Elimination from 7

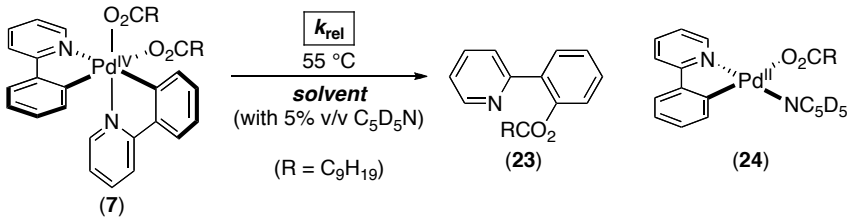

Entry	Solvent	ε	k_{rel}
1	acetone-d_6	21	1.0 ± 0.1
2	C_6D_6	2.3	1.0 ± 0.1
3	chlorobenzene-d_5	5.6	1.0 ± 0.1
4	DMSO-d_6	47	2.0 ± 0.3
5	$CDCl_3$	4.8	2.3 ± 0.2
6	CD_3CN	38	2.4 ± 0.1
7	nitrobenzene-d_5	36	3.1 ± 0.3

We investigated the rate of carboxylate exchange as a function of solvent. In these experiments, 1 equiv of **7** and 1 equiv of $Bu_4N(OAc)$ were dissolved in the appropriate solvent in an NMR tube at –38 ºC, and the rate of formation of an equilibrium mixture of **7** and **20** was monitored by ^1H NMR spectroscopy. Intriguingly, k_{obs} for carboxylate exchange did not show a clear correlation with the polarity of the reaction medium (Table 2.2.2). For example, the fastest rate (k_{kel} = 19) was observed in $CDCl_3$ (e = 4.7), while the slowest (k_{rel} = ~0.1)[29] was in toluene-d_8 (e = 2).

Table 2.2.2 Effect of Solvent on the Rate of Carboxylate Exchange from 7

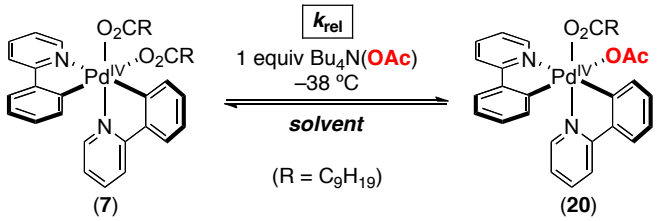

Entry	Solvent	ε	k_{rel}
1	toluene-d_8	2.4	<0.1
2	acetone-d_6	21	1.0 ± 0.1
3	CD_3CN	38	2.0 ± 0.2
4	$CDCl_3$	4.8	19.0 ± 0.1

The solvent data for C–O bond-forming reductive elimination (particularly the low correlation between e and k_{obs}) was initially interpreted as a strong piece of evidence against mechanism **A**.[7,9] However, the results from the corresponding solvent study for carboxylate exchange indicate that this interpretation should be reconsidered.

Mechanism of C–O Bond-Forming Reductive Elimination: Entropy of Activation. Previous work has shown that reductive elimination reactions proceeding via mechanism **A** are often characterized by large negative values of $\Delta S^{\ddagger}$. For example, Canty has reported that C–Se bond-forming reductive elimination from Pd^{IV} has $\Delta S^{\ddagger}$ ranging from –40 to –49 eu, depending on the

reaction solvent.[9b] This has been rationalized on the basis of significant orientation of solvent molecules around the charged transition state.

The rate of C–O bond-forming reductive elimination from **7** was examined over a range of temperatures from 30 to 70 ºC in both $CDCl_3$ and DMSO-d_6 by Dr. Allison Dick. Eyring plots showed that $\Delta S^{\ddagger}$ is close to zero in both solvents ($\Delta S^{\ddagger}$ = –1.4 ± 1.9 eu in $CDCl_3$ and +4.2 ± 1.4 eu in DMSO-d_6). While values of $\Delta S^{\ddagger}$ between 10 and –10 eu are considered difficult to interpret, these values are substantially less negative than those reported by Canty.[27] As such, we initially viewed this data as inconsistent with mechanism **A**.[12]

We conducted similar studies to obtain an Eyring plot for carboxylate exchange. In these experiments, the reaction of **7** with 1.0 equiv of $Bu_4N(OAc)$ in $CDCl_3$ was monitored by ^1H NMR spectroscopy over temperatures ranging from –58 to –38 ºC, and an Eyring plot provided $\Delta S^{\ddagger}$ = –7.2 ± 3 eu. Again, this value is considerably less negative than those reported by Canty,[9b] but is quite similar to that obtained for C–O bond-forming reductive elimination from **7**.[30] The $\Delta S^{\ddagger}$ obtained for both the reductive elimination and the carboxylate exchange are consistent with mechanism **A** if a tight ion is formed between the dissociated carboxylate and ther positive Pd center.

Mechanism of C–O Bond-Forming Reductive Elimination: Acidic Additives. Goldberg has shown that both Brønsted and Lewis acids accelerate C–O and C–C bond-forming reductive elimination from (dppe)$Pt^{IV}(OAc)(Me)_3$ (dppe = diphenylphosphinoethane), which both proceed via mechanism **A**.[7b] For example, the addition of 0.1 equiv of AcOH increased the rate of C–O coupling by a factor of 2, while the use of 0.1 equiv of AgOTf lowered the temperature required for C–C bond-forming reductive elimination from 99 ºC to 25 ºC. Both additives were proposed to act by promoting OAc^- dissociation. On the basis of this report, I reasoned that if mechanism **A** were operative in our system, *both* C–O bond-forming reductive elimination and carboxylate exchange at complex **7** should be accelerated to similar extents by these additives.

We first studied the rate of C–O bond-forming reductive elimination from $(Phpy)_2Pd^{IV}(O_2CC_9H_{19})_2$ (**7**) in the presence of AcOH or AgOTf. The addition of AcOH (2.0 equiv) resulted in a 3.6-fold acceleration of C–O bond-forming reductive elimination (Table 2.2.3, entries 1 and 2), while AgOTf (0.3 equiv) led to a 16-fold increase in k_{obs} for this reaction (Table 2.2.4, entries 1 and 2).

The effect of HOAc and AgOTf on the rate of carboxylate exchange was next determined, and, remarkably, a very similar effect was observed. For example, the addition of AcOH (2.0 equiv) resulted in a 4.5-fold increase in the rate (Table 2.2.3, entry 2), while AgOTf (0.3 equiv) afforded an 8.7-fold increase in k_{obs} for exchange (Table 2.2.4, entry 2). These results are consistent with the hypothesis that carboxylate exchange and C–O bond-forming reductive elimination are mechanistically linked.

Table 2.2.3 Effect of AcOH on C–O Bond-Forming Reductive Elimination and Carboxylate Exchange at 7

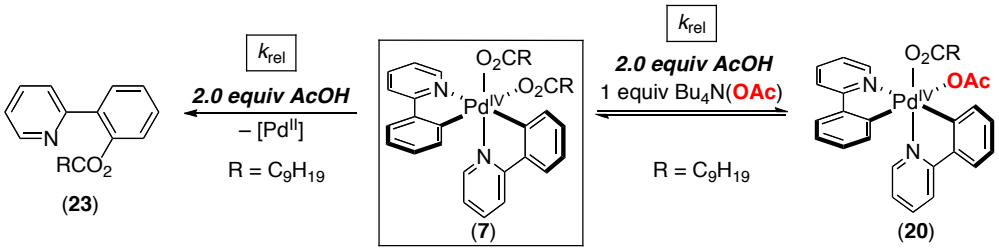

Entry	Acid	k_{rel} C-O coupling	k_{rel} exchange
1	none	**1.0** ± 0.0[a]	**1.0** ± 0.0
2	HOAc	**3.6** ± 0.2[a]	**4.5** ± 0.5[b]

[a] 40 ºC in acetone-d_6; [b] –35 ºC in acetone-d_6;

Table 2.2.4 Effect of AgOTf on C–O Bond-Forming Reductive Elimination and Carboxylate Exchange at 7

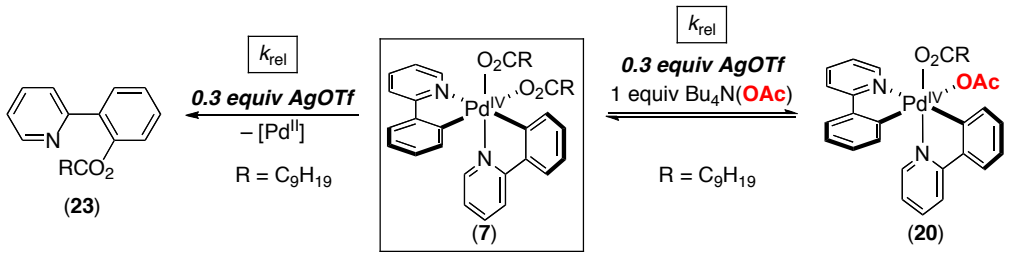

Entry	Acid	k_{rel} C-O coupling	k_{rel} exchange
1	none	**1.0** ± 0.2[a]	**1.0** ± 0.1[b]
2	AgOTf	**16** ± 0.8[a]	**8.7** ± 0.0[b]

[a] 23 °C in $CDCl_3$; [b] –53 °C in $CDCl_3$

Mechanism of C–O Bond-Forming Reductive Elimination: Carboxylate Electronic Effects. A series of Pd^{IV} complexes (**8-18**) were designed to place both σ- and π-electron donating and electron withdrawing substituents on the benzoate ligand. The kinetics of C–O bond-forming reductive elimination from Pd^{IV} complexes **8-18** was then studied at 60 ºC in a solution of 5% v/v C_5D_5N in $CDCl_3$ (Scheme 2.2.12) by Dr. Allison Dick.[28] A Hammett plot of this data showed very good correlation with σ_{para} (R^2 = 0.95) and yielded a ρ value of −1.36 ± 0.04 (Figure 2.2.2).

Scheme 2.2.12 C–O Bond-Forming Reductive Elimination from 8-18

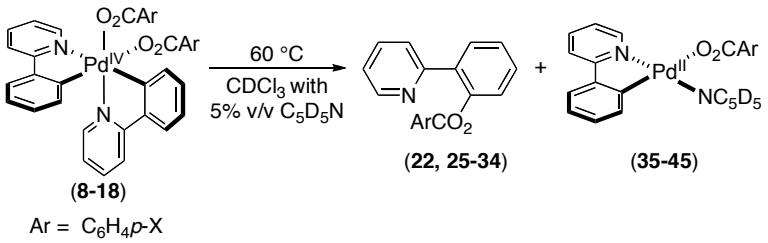

(**8-18**)

Ar = C_6H_4*p*-X

(**22, 25-34**) (**35-45**)

Figure 2.2.2 Hammett Plot for C–O Bond-Forming Reductive Elimination from 8-18

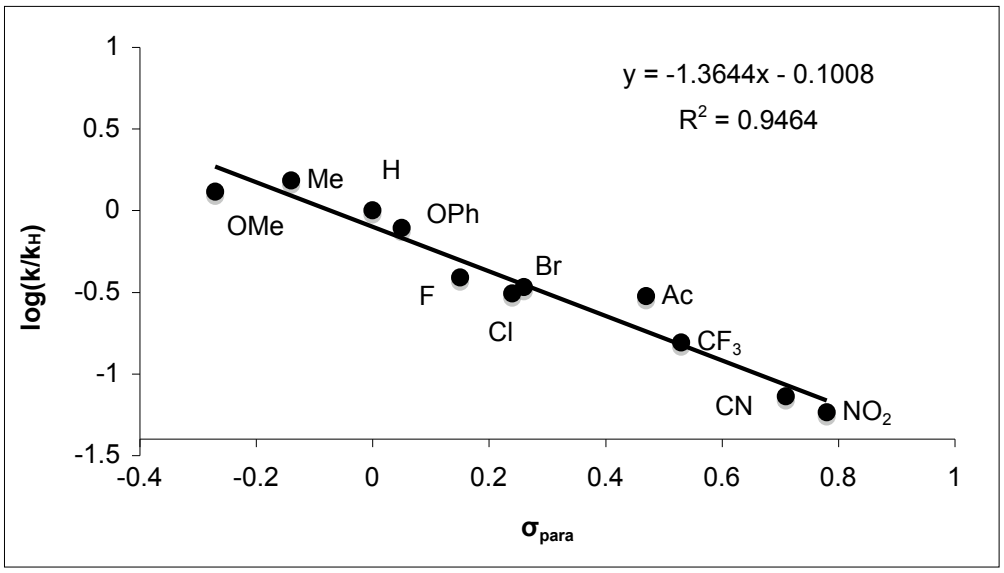

A previous report showed that r = +1.44 for C–O bond-forming reductive elimination from (dppbz)$PtMe_3$(OAr), which proceeds by mechanism **A**.[7b] As such, we initially reasoned that the observed r value of –1.36 provided evidence against an ionic mechanism.[12] However, the overall value of ρ (ρ_{obs}) for a reaction proceeding by mechanism **A** is the sum of ρ_{eq} and ρ_2 (Figure 2.2.3).[31]

The ρ_{obs} of +1.44 in the Pt system was rationalized based on the assumption that $|\rho_{eq}| > |\rho_2|$;[7b] however, since the overall ρ value (ρ_{obs}) is a composite, a positive ρ value is not an inherent feature of such mechanisms.[32] Thus, since all of the possible mechanisms (**A**, **B**, and **C**) involve the carboxylate acting as a nucleophillic partner in a rate-determining C–O bond-forming step (Scheme 2.2.4), the observed negative ρ value is potentially consistent with any of these pathways.

Figure 2.2.3 Values of ρ for Each Step of Mechanism A

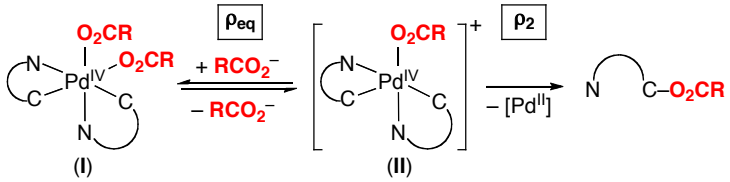

Mechanism of C–O Bond-Forming Reductive Elimination: Arylpyridine Electronic Effects. A series of complexes containing electronically varied arylpyridine ligands **(15,** and **46-50)** were designed to place various electron withdrawing and electron donating substituents *trans* to the Pd-bound carbon atom. The kinetics of C–O bond-forming reductive elimination from **15** and **46**-**50** were studied at 60 ºC in a solution of 5% v/v C_5D_5N in $CDCl_3$ by Dr. Allison Dick. Reductive elimination generally proceeded fastest with electron-withdrawing substituents (Table 2.2.5), although Hammett plots showed only modest correlation with σ_{para} (R^2 = 0.79), s^+ (R^2 = 0.47), and s^- (R^2 = 0.36). This is consistent with the Ar ring acting as the electrophilic partner in C–O coupling.

Table 2.2.5 k_{obs} for Reductive Elimination from $(Arpy)_2Pd^{IV}[O_2C(p\text{-}AcC_6H_4)]_2$

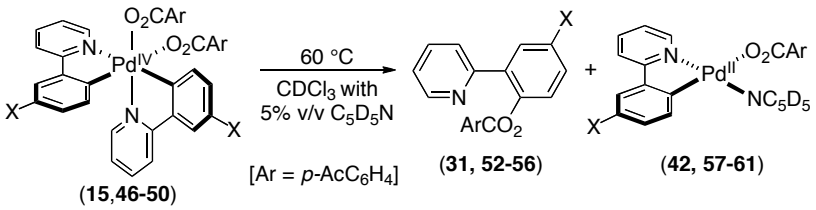

(**15**,**46-50**) (**31, 52-56**) (**42, 57-61**)

Compound	k_{obs} (s^{-1} x 10^5)
*OMe (**46**)	~3[a]
Me (**47**)	4.81
H (**15**)	20.0
F (**48**)	3.64
Cl (**49**)	36.9
*CF_3 (**50**)	~320[a]

[a]These values of k_{obs} are approximate, as samples of **46** and **50** were contaminated with ~10% of inseparable impurities.

***Mechanism of C–O Bond-Forming Reductive Elimination: Ligand Rigidity*.** Originally, it was hypothesized that a decrease in reaction rate with increasing N~C ligand rigidity would provide support for mechanism **C**.[12] Complexes **62**-**64** were designed to systematically vary the flexibility of the tether between the two pyridine rings (Figure 2.2.4). The kinetics of C–O bond-forming

reductive elimination from **62**-**64** was studied by ^{1}H NMR spectroscopy at 50 ºC in a solution of 5% v/v C_5D_5N in $CDCl_3$ by both Dr. Allison Dick and myself. As summarized in Table 2.2.6, the rates of reductive elimination did show a correlation with the rigidity of the N~C ligand. For example, complex **62** reacted twice as fast as **63** and more than 10 times faster than the most rigid **64**.

Figure 2.2.4 Effect of Ligand Rigidity on C–O Bond-Forming Reductive Elimination

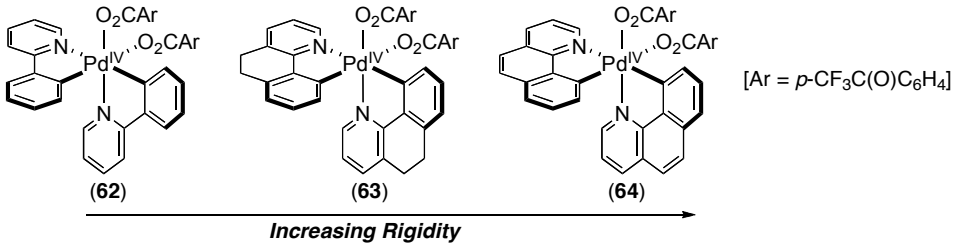

Table 2.2.6 k_{obs} Rate of C–O Bond-Forming Reductive Elimination as a Function of Ligand Rigidity

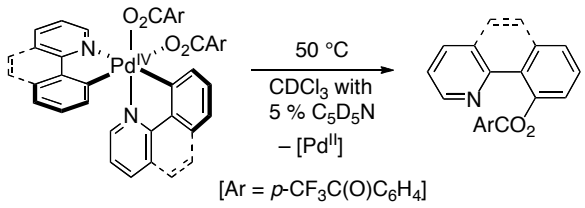

[Ar = *p*-$CF_3C(O)C_6H_4$]

Entry	Complex	k_{rel}
1	**62**	1.9
2	**63**	1.0
3	**64**	~0.1[a]

[a]The slow reaction rate along with competing C–C bond-formation prevented quantitative rate measurement in this system.

As discussed above, it was originally interpreted that these results were most consistent with the chelate dissociation mechanism (**C**).[12,20] However, a number of literature reports have shown that rigid ancillary ligands stabilize Pd^{IV} complexes towards reductive elimination, even when the ligand plays no direct role in the bond-forming process.[10] Therefore, these results do not definitively establish or rule out any of the three mechanistic manifolds.

Summary of Mechanistic Data for C–O Bond-Forming Reductive Elimination. Mechanisms **A**, **B**, or **C** for C–O bond-forming reductive elimination from $(N\sim C)_2Pd^{IV}(O_2CR)_2$ are kinetically indistinguishable; therefore, we have

conducted a series of alternative mechanistic experiments to interrogate this transformation. The original publication on this work suggested that mechanism **C**, chelate dissociation, was most consistent with initial studies of this process.[12] This conclusion was based on 5 key pieces of data: (i) the absence of a clear correlation between k_{obs} and solvent polarity, (ii) the lack of cross-over between free and bound carboxylate, (iii) the small entropy of activation, (iv) the negative ρ value obtained upon substitution of the carboxylate ligand, and (v) the decreased reaction rate with more rigid N~C ligands.[33]

However, we have conducted a variety of new experiments, and these, along with a re-evaluation of the previous data, have led us to conclude that mechanism **A** is, in fact, most likely operating in this system. These new experiments were particularly focused on the exchange of free and bound carboxylate at $(Phpy)_2Pd^{IV}(O_2CR)_2$, which is expected to proceed by an identical mechanism to the first step of mechanism **A**. This exchange occurs at temperatures far below reductive elimination, and shows similar solvent effects and activation parameters to C–O bond-formation.[34] In addition, the rates of carboxylate exchange and of C–O coupling are increased to very similar extents upon addition of AcOH and AgOTf, additives that have both been reported to promote carboxylate dissociation. The C–C bond-forming reactions discussed below offer further evidence in support of mechanism **A**. In addition, they provide a more complete picture of the reactivity of these Pd^{IV} complexes.

2.3 Results and Discussion for C–C Bond-Formation from Pd(IV)

C–C Bond-Forming Reductive Elimination from $(Bzq)_2Pd^{IV}(O_2CR)_2$. In the context of the ligand rigidity studies, we noted that benzo[*h*]quinoline complex **64** reacted to form significant quantities of C–C bond-forming reductive elimination product **66** along with the expected C–O coupled product **65** (Scheme 2.3.1). This result was intriguing, since analogous C–C coupling was not observed in any of the phenylpyridine systems. As such, a series of experiments were designed to further interrogate the mechanism of this process.

Scheme 2.3.1 Competing C–O and C–C Bond-Forming Reductive Elimination from 64

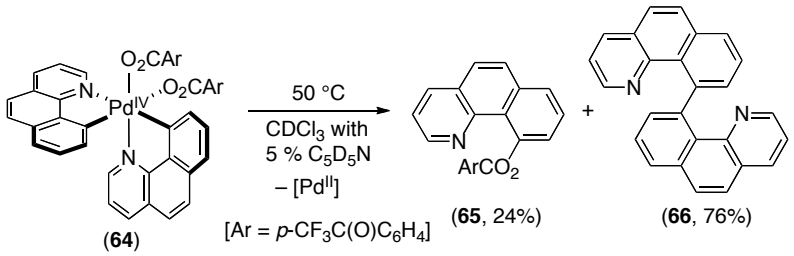

***Mechanism of C–C Bond-Forming Reductive Elimination: Solvent Effects*.** A first study probed the effect of solvent on the relative rates (k_{rel}) of C–C and C–O bond-forming reductive elimination from $(Bzq)_2Pd^{IV}(O_2CC_9H_{19})_2$ (**64**). The values of k_{rel} were determined under a standard set of conditions (80 ºC, 4 h, 15.2 mM) on the basis of the ratio of C–C coupled product **66** to C–O coupled product **65** in the crude reaction mixtures. As summarized in Table 2.3.1, solvent had a significant influence on the product distribution, with the ratio of **68** to **66** ranging from >20 : 1 to 0.25 : 1. While there was no clear relationship between the dielectric constant of the solvent and the product ratio, the largest amounts of **66** were observed in solvents where C–O coupling from the analogous 2-phenylpyridine complex $(Phpy)_2Pd^{IV}(O_2CC_9H_{19})_2$ (**7**) was relatively slow. For example, in benzene and acetone (with k_{rel} = 1 for C–O bond-forming reductive elimination from **7**, Table 2.2.1), >10 : 1 selectivity was observed for **66** (Table 2.3.1, entries 5 and 6). Conversely, in CH_3CN and $CHCl_3$, (solvents where C–O bond-forming reductive elimination from **7** was relatively fast), **65** was the major organic reductive elimination product (entries 1 and 2).

Table 2.3.1 Effect of Solvent on the Product Ratio of Reductive Elimination from 67

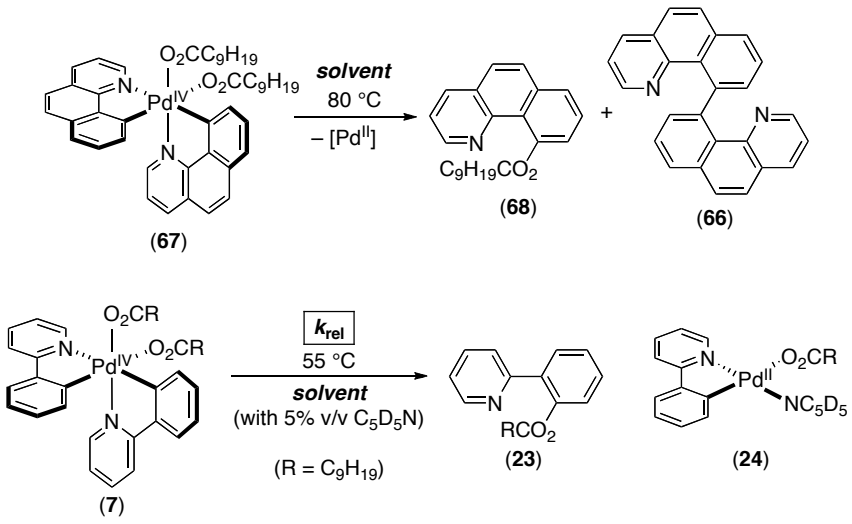

Entry	Solvent	Ratio 66 : 68	k_{rel} for C–O coupling from 7
1	CH_3CN	0.25 : 1	2.4
2	$CHCl_3$	0.77 : 1	2.3
3	nitrobenzene	2.2 : 1	3.1
4	DMSO	3.3 : 1	2.0
5	acetone	13 : 1	1.0
6	benzene	> 20 : 1	1.0

Mechanism of C–C Bond-Forming Reductive Elimination: Acidic Additives. Complex **67** was subjected to standard reductive elimination conditions (80 ºC, 3 h, 15.2 mM in acetone) in the presence of 5.0 equiv of AcOH or 0.10 equiv AgOTf (additives that both accelerate C–O bond-forming reductive elimination from $(Phpy)_2Pd^{IV}(O_2CC_9H_{19})_2$ (**7**)), and the ratio of organic products was determined using ^1H NMR spectroscopy. As summarized in Table 2.3.2, both additives led to a large increase in the relative amount of the oxygenated product **68**. For example, with AcOH, the ratio of **68** to **66** changed from 13 : 1 to 3.6 : 1. The effect was even more dramatic with AgOTf, where the major organic product was **66** (ratio of **68** : **66** = 0.10 : 1).

Table 2.3.2 Effect of Acidic Additives on the Product Ratio of Reductive Elimination from 67

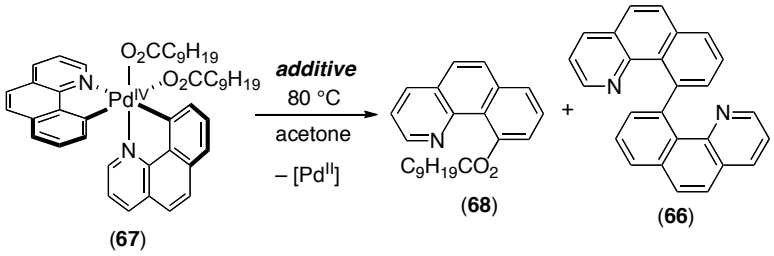

Entry	Additive	Ratio 66 : 68
1	none	13 : 1
2	AcOH (5.0 equiv)	3.6 : 1
3	AgOTf (0.1 equiv)	0.10 : 1

***Mechanism of C–C Bond-Forming Reductive Elimination: Carboxylate Electronics*.** Earlier studies showed that C–O bond-forming reductive elimination from $(Phpy)_2Pd^{IV}(O_2CAr)_2$ is slowed significantly with electron withdrawing benzoate ligands (*c.f.,* Figure 2.2.2), and, as such, we first examined complexes of general structure $(Bzq)_2Pd^{IV}(O_2CAr)_2$, where the substituents on the benzoate ligands were systematically varied. However, the low solubility of these compounds precluded quantitative mechanistic studies. Thus, subsequent efforts aimed to compare $(Bzq)_2Pd^{IV}(O_2CC_9H_{19})_2$ (**73**) to $(Bzq)_2Pd^{IV}(O_2CC_9F_{19})_2$ (**75**), which contains sterically similar but highly electron withdrawing perfluorinated carboxylates. In all of the solvents examined (pyridine-d_5, acetone-d_6, DMSO-d_6, and CD_3CN), electron deficient complex **69** was much less reactive than **67**, and it could be recovered quantitatively from the reaction mixtures following our standard reductive elimination conditions (80 ºC, 3 h). Complete consumption of $(Bzq)_2Pd^{IV}(O_2CC_9F_{19})_2$ required heating at 80 ºC for 3-16 d depending on the solvent. In addition, C–C coupled **66** was the sole organic product in every solvent examined (Table 2.3.3).

Table 2.3.3 Solvent Effects on Product Distribution of Reductive Elimination from Complex 69

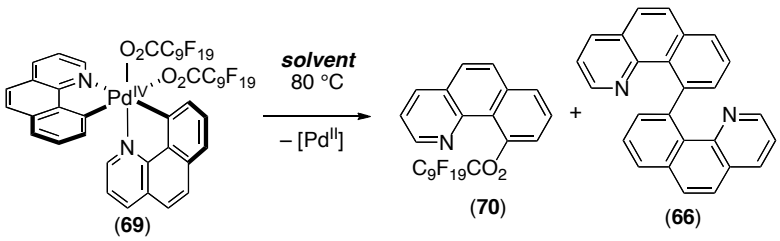

Entry	Solvent	Organic Product
1	pyridine-d_5	**66**
2	acetone-d_6	**66**
3	DMSO-d_6	**66**
4	CD_3CN	**66**

Mechanism of C–C Bond-Forming Reductive Elimination: Added Carboxylate. Under standard reaction conditions (80 ºC, 3 h, 15.2 mM in CH_3CN), **68** was the major product, and the **66** : **68** ratio was 0.2 : 1 as determined by ^1H NMR spectroscopy (Table 2.3.4). However, when 1 equiv of $NBu_4(O_2CC_9H_{19})$ was added, the selectivity completely reversed, and **66** predominated (**66** : **68** ratio = 2 : 1). To confirm that this effect was not just due to the increased ionic strength of the solution, a control experiment was conducted using 1 equiv of NBu_4PF_6. This experiment provided an identical product ratio to the initial reaction (**66** : **68** = 0.2 : 1). Therefore, the reversal in product selectivity is clearly specific to the carboxylate ion.

Table 2.3.4 Effect of $NBu_4(O_2CC_9H_{19})$ on the Product Distribution of Reductive Elimination from 67

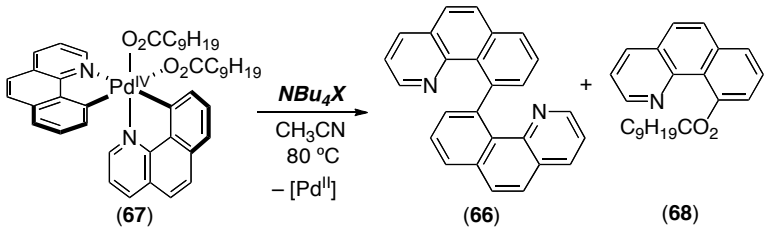

(**67**) (**66**) (**68**)

Entry	Additive	Ratio 66 : 68
1	none	0.2 : 1
2	$NBu_4(O_2CC_9H_{19})$	2 : 1
3	NBu_4PF_6	0.2 : 1

2.4 Mechanistic Discussion and Unifying Experiments for C–O and C–C Bond-Forming Reductive Elimination from Pd^{IV}

Proposed Mechanism for C–C and C–O Bond-Forming Reductive Elimination from $(N\sim C)_2Pd^{IV}(O_2CR)_2$. The solvent, additive, and ligand effect studies, as well as the influence of added carboxylate, all suggest that reductive elimination processes from **67** occur via the pathway outlined in Scheme 2.4.1. This proposal is consistent with all of the mechanistic data and also provides a unifying mechanism for C–O and C–C bond-forming reductive elimination for complexes of general structure $(N\sim C)_2Pd^{IV}(O_2CR)_2$. In this scenario, C–O bond-

forming reductive elimination from **67** proceeds by an analogous mechanism to that proposed for $(Phpy)_2Pd^{IV}(O_2CR)_2$ (via pre-equilibrium carboxylate dissociation followed by C–O coupling, mechanism **A**). In contrast, C–C bond-forming reductive elimination takes place by direct reductive elimination from the 6-coordinate starting material **67**.

Scheme 2.4.1 Proposed Mechanisms for C–C and C–O Bond-Forming Reductive Elimination from $(N\sim C)_2Pd^{IV}(O_2CR)_2$

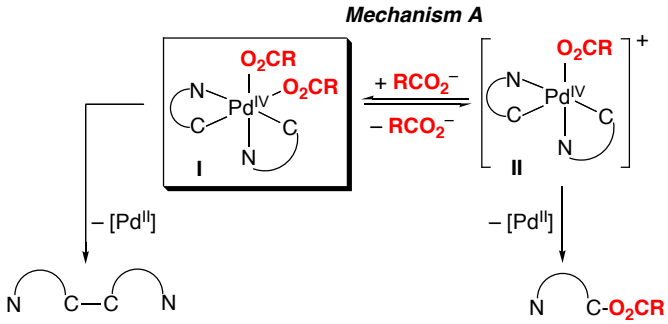

The data presented in this chapter are all consistent with Scheme 2.4.1 In the presence of added carboxylate, the equilibrium for carboxylate dissociation (step *i* of mechanism **A**) should be shifted to the left, thereby leading to increased formation of the C–C coupled product by direct reductive elimination from **I**. Under conditions that accelerate C–O bond-forming reductive elimination by mechanism **A** (*i.e.,* solvents like CH_3CN or $CHCl_3$, additives like HOAc or AgOTf, electron donating carboxylate ligands), the C–O coupled product predominates. In contrast, under conditions shown to slow C–O coupling (*e.g.,* solvents like acetone or benzene, electron withdrawing carboxylate ligands), the C–C coupled product is formed in high yield.

To provide final evidence in support of this mechanistic manifold, we generated $[(Bzq)_2Pd^{IV}(O_2R)]^+$ *in situ* and examined the distribution of organic products from this species. As shown in Scheme 2.4.2, treatment of $(Bzq)_2Pd^{IV}(OAc)(Cl)$ (**71**) with $AgBF_4$ at 80 ºC [conditions that are expected to

afford [$(Bzq)_2Pd^{IV}(OAc)]BF_4$ (**72**)] resulted in rapid C–O bond-forming reductive elimination to afford **73**, *with none of the C–C coupled product **66** observed by ^1H NMR spectroscopy.*[35] This result is in striking contrast to the reaction of **71** in the absence of $AgBF_4$, which yielded a 1 : 0.21 ratio of **73** to **74**, as well as to the reaction of $(Bzq)_2Pd^{IV}(OAc)_2$ (**74**) (which gave a 0.5 : 1 ratio of **73** to **66**). Therefore, it provides a final piece of compelling evidence in support of the proposed mechanism.

Scheme 2.4.2 Effect of $AgBF_4$ on the Product Distribution of Reductive Elimination from 71

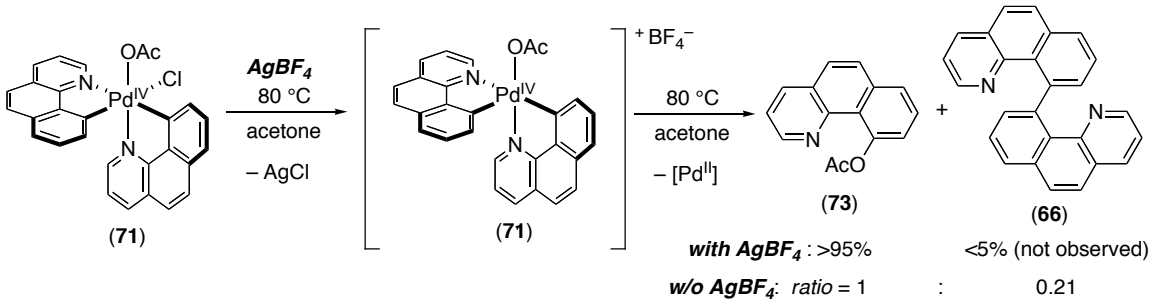

Unified Mechanism: C–C Coupling from Phenylpyridine Complexes. If Scheme 2.4.2 does, in fact, represent a unified mechanism for reductive elimination from $(N\sim C)_2Pd^{IV}(O_2CR)_2$, we reasoned that it should be possible to rationally design conditions to achieve C–C coupling from complexes where N~C = 2-phenylpyridine. Guided by the studies above, we examined conditions under which k_{rel} for C–O bond-forming reductive elimination is predicted to be slow – with a highly electron withdrawing carboxylate ligand and in the presence of an excess of added carboxylate. We was delighted to find that the reaction of $(Phpy)_2Pd^{IV}(O_2CAr)_2$ [Ar = *p*-$CF_3C_6H_4$] in the presence of 5 equiv of $Bu_4N(O_2CAr)$ at 80 ºC in DMSO for 5 h resulted in a 1.6 : 1 mixture of oxygenated product **32** to biaryl product **4** (Scheme 2.4.3). This result demonstrates that perturbations of the ancillary ligand set and additives have similar effects in the 2-phenylpyridine

and benzoquinoline systems, providing support for similar mechanisms in both systems.

Scheme 2.4.3 Effect of $AgBF_4$ on the Product Distribution of Reductive Elimination from 71

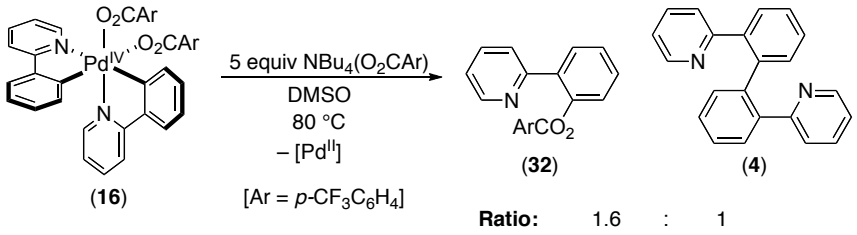

(**16**) [Ar = *p*-$CF_3C_6H_4$] (**32**) (**4**)

Ratio: 1.6 : 1

2.5 Conclusions

This chapter described the synthesis of a series of unusually stable Pd^{IV} complexes of general structure $(N\sim C)_2Pd^{IV}(O_2CR)_2$. These complexes have allowed us to conduct the first detailed mechanistic studies of C–O bond-forming reductive elimination from Pd^{IV} centers. In addition, we have studied competing C–C coupling processes. Based on these investigations, we propose that C–O bond-forming reductive elimination proceeds via an ionic mechanism involving initial carboxylate dissociation, followed by C–O coupling from a 5-coordinate cationic intermediate. In contrast, the C–C bond-forming reaction is believed to involve direct reductive elimination from the octahedral Pd^{IV} starting material. The mechanistic understanding of these processes has facilitated the rational tuning of ancillary ligands and reaction conditions in order to control the ratio of organic products. Current efforts are focused on applying the mechanistic insights obtained from these studies towards the design and optimization of new $Pd^{II/IV}$-catalyzed reactions that form both carbon-oxygen and carbon-carbon bonds.

2.6 Experimental

2.6.1 Synthesis of Pd^{II} Complexes S1-S45[36]

General Procedure. A solution of the aryl bromide (2-3 equiv relative to Pd) in THF or diethyl ether was cooled to –78 oC in a dry ice/acetone bath. *n*-BuLi (1 equiv relative to ligand) or *t*- BuLi (2 equiv relative to ligand) was added dropwise. After stirring at –78 oC for 5-10 min, a solution of $(Et_2S)_2PdCl_2$ in diethyl ether was added. The resulting mixture was stirred at –78 °C for 30-120 min, then the reaction was quenched with water. The reaction mixture was diluted with water, and the palladium(II) product was extracted into CH_2Cl_2 or toluene. The organic extracts were filtered through a plug of aluminum oxide (certified, anhydrous, Fisher A591), the solvent volume was reduced to ~5 mL, and hexanes was added to precipitate the product. The resulting yellow solid was collected by filtration and dried under vacuum to afford the desired bis-cyclometallated complex.

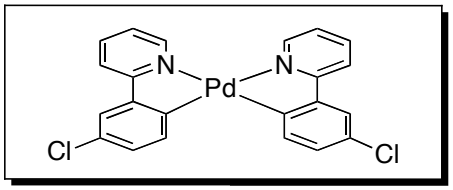

Pd^{II}(Cl-Arpy)$_2$, S1: This complex was synthesized according to the general procedure above. The aryl bromide was dissolved in diethyl ether, *n*-BuLi was used as the lithiating reagent, and the extraction was carried out with CH_2Cl_2. Complex **S1** was obtained in 41% yield as a yellow solid. ^{1}H NMR ($CDCl_3$): δ 8.63 (d, *J* = 5.5 Hz, 1H), 7.91 (d, *J* = 8.0 Hz, 1H), 7.88 (td, *J* = 8.5, 2.5 Hz, 1H), 7.85 (d, *J* = 7.0 Hz, 1H), 7.61 (d, *J* = 2.5 Hz, 1H), 7.32 (ddd, *J* = 7.0, 5.5, 1.5 Hz, 1H), 7.26 (dd, *J* = 8.0, 2.5 Hz, 1H). $^{13}C\{^1H\}$ NMR ($CDCl_3$): δ 164.28, 159.23, 148.32, 148.07, 139.87, 138.60, 130.25, 129.62, 123.34, 122.66, 119.62.

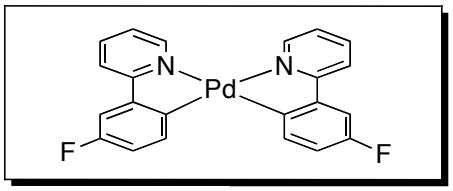

Pd^{II}(F-Arpy)$_2$, S2: This complex was synthesized according to the general procedure above. The aryl bromide was dissolved in diethyl ether, *n*-BuLi was used as the lithiating reagent, and the extraction was carried out with CH_2Cl_2. Complex **S2** was obtained in 43% yield as a yellow solid. ^{1}H NMR ($CDCl_3$): δ 8.64 (d, *J* = 5.5 Hz, 1H), 7.94 (dd, *J* = 8.5, 6.5 Hz, 1H), 7.89 (td, *J* = 7.5, 1.5 Hz, 1H), 7.83 (d, *J* = 8.0 Hz, 1H), 7.36 (dd, *J* = 11.0, 2.0 Hz, 1H), 7.32 (ddd, *J* = 7.5, 5.0, 1.5 Hz, 1H), 7.05 (td, *J* = 9.0, 2.5 Hz, 1H). ^{13}C{^{1}H} NMR (DMSO-d_6): δ 162.81 (d, *J* = 4 Hz), 160.40 (d, *J* = 238 Hz), 156.12 (d, *J* = 3 Hz), 149.04, 147.77 (d, *J* = 6 Hz), 139.28, 138.76 (d, *J* = 6 Hz), 123.52, 119.85, 115.77 (d, *J* = 19 Hz), 110.18 (d, *J* = 21 Hz). ^{19}F NMR ($CDCl_3$): δ –120.48 (dt, *J* = 9.5 Hz, 6.5 Hz).

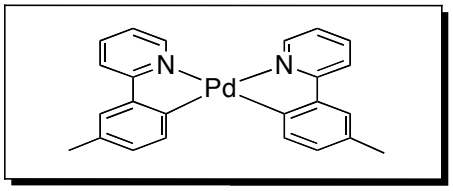

Pd^{II}(Me-Arpy)$_2$, S3: This complex was synthesized according to the general procedure above. The aryl bromide was dissolved in diethyl ether, *n*-BuLi was used as the lithiating reagent, and the extraction was carried out with CH_2Cl_2. Complex **S3** was obtained in 55% yield as a yellow solid. Characterization data matched with those reported previously in the literature.[12]

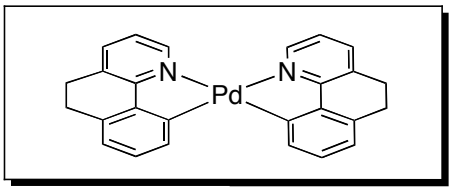

$Pd^{II}(BzqH_2)_2$, S4: This complex was synthesized according to the general procedure above. The aryl bromide was dissolved in THF, *n*-BuLi was used as the lithiating reagent, and the extraction was carried out with CH_2Cl_2. Complex **S4** was obtained in 71% yield as a yellow solid. ^{1}H NMR ($CDCl_3$): δ 8.47 (d, *J* = 4.5 Hz, 1H), 7.92 (d, *J* = 8.0 Hz, 1H), 7.57 (d, *J* = 7.5 Hz, 1H), 7.21 (t, *J* = 7.5 Hz, 1H), 7.15 (dd, *J* = 7.5, 5.5 Hz, 1H), 6.91 (d, *J* = 7.0 Hz, 1H), 3.00 (dd, *J* = 11.5, 4.0 Hz, 2H), 2.96 (dd, *J* = 11.5, 4.0 Hz, 2H). $^{13}C\{^1H\}$ NMR ($CDCl_3$): δ 162.35, 159.76, 145.97, 144.14, 136.90, 136.64, 136.47, 132.52, 129.89, 123.29, 121.68, 28.09, 28.00.

2.6.2 Synthesis of Pd^{IV} Complexes 2, 2-d_6, 47-49,62-64, 69

General Procedure. The appropriate bis-cyclometalated Pd^{II} starting material (0.24 mmol, 1 equiv) and oxidant (1.0-1.1 equiv) were combined in a 50 mL round bottomed flask equipped with a stir bar. CH_2Cl_2 (30 mL) was added, and the mixture was stirred at 25 ºC for between 10 min and 1 h. The solvent was evaporated to a volume of ~5 mL and hexanes (2-5 mL) was added to precipitate the product. The precipitate was collected and then suspended in Et_2O (5-10 mL) and sonicated, leaving a finely suspended powder. This material was collected at the top of a pipette-sized column of Celite and washed with Et_2O (5 mL). The product was then eluted with CH_2Cl_2, and the solvent was removed under vacuum. The Pd^{IV} products were isolated as off-white to yellow powders. If the resulting product was a tacky solid, the solid was washed with hexanes (2 mL) to the remove residual impurities.

Notably, all Pd^{IV} complexes were stored at –35 ºC. HRMS data are reported for each compound and showed loss of one carboxylate ligand (*trans* to the s-aryl group). The characterization of complexes **7-18, 64** was reported previously.[12] In general the Pd^{IV} complexes were insufficiently soluble and/or insufficiently stable to obtain ^{13}C NMR spectral data.

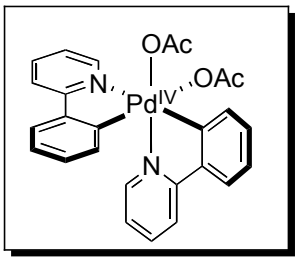

Complex 2: Yield: 81%. ^1H NMR (acetone-d_6): δ 9.45 (d, *J* = 5.5 Hz, 1H), 8.27 (d, *J* = 8.0 Hz, 1H), 8.20 (t, 8.5, 1H), 8.09-8.06 (multiple peaks, 2H), 7.95-7.92 (multiple peaks, 2H), 7.87 (d, *J* = 8.0 Hz, 1H), 7.62 (t, *J* = 6.0 Hz, 1H), 7.58 (d, *J* = 6.0 Hz, 1H), 7.51(t, *J* = 7.5 Hz, 1H), 7.46 (t, *J* = 7.5 Hz, 1H), 7.10-7.08 (multiple peaks, 2H), 6.85 (t, *J* = 8.5 Hz, 1H), 6.30 (d, *J* = 8.5 Hz, 1H), 1.75 (s, 3H), 1.62 (s, 3H). FTIR (KBr): 1654, 1604, 1569, 1484, 1441, 1419, 1366, 1291, 1006, 759 cm^{-1}. HRMS-electrospray (m/z): $[M - OAc]^+$ calcd for $C_{24}H_{19}N_2O_2Pd$, 473.0481; Found, 473.0495.

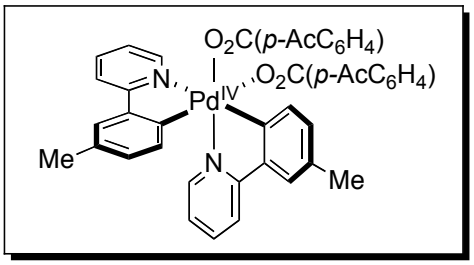

Complex 47: Yield: 63%. ^1H NMR ($CDCl_3$): δ 9.49 (dt, *J* = 5.5, 1.0 Hz, 1H), 8.07-8.02 (multiple peaks, 5H), 7.98 (app. d, *J* = 8.5 Hz, 2H), 7.88 (dt, *J* = 8.5, 1.5 Hz, 2H), 7.82 (app. d, *J* = 8.0 Hz, 2H), 7.80-7.78 (multiple peaks, 2H), 7.58 (d, *J* = 6.0

Hz, 1H), 7.54 (d, *J* = 2.0 Hz, 1H), 7.51 (dd, *J* = 9.0, 5.0 Hz, 1H), 7.49 (d, *J* = 2.0 Hz, 1H), 7.31 (dd, *J* = 8.0, 2.0 Hz, 1H), 6.97 (td, *J* = 6.0, 2.5 Hz, 1H), 6.74 (dd, *J* = 8.0, 1.5 Hz, 1H), 6.39 (d, *J* = 8.0 Hz, 1H), 2.59 (s, 3H), 2.56 (s, 3H), 2.48 (s, 3H), 2.29 (s, 3H). FTIR (KBr): 1683, 1652, 1603, 1558, 1483, 1426, 1260 cm^{-1}. HRMS-electrospray (m/z): $[M - O_2C(p\text{-}AcC_6H_4)]^+$ calcd for $C_{42}H_{34}N_2O_6Pd$ 605.1056; Found, 605.1076.

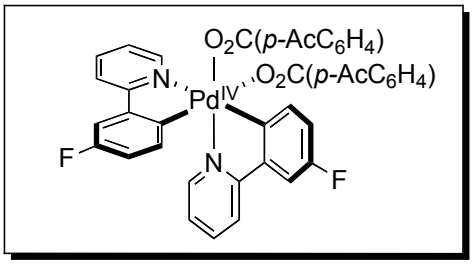

Complex 48: Yield: 77%. ^1H NMR ($CDCl_3$): δ 9.50 (dd, *J* = 5.5, 1.0 Hz, 1H), 8.15-8.11 (multiple peaks, 2H), 8.04 (d, *J* = 8.0 Hz, 1H), 8.01 (d, *J* = 8.0 Hz, 2H), 7.98 (d, *J* = 8.5 Hz, 2H), 7.89 (d, *J* = 8.0 Hz, 2H), 7.87 (m, 1H), 7.84 (d, *J* = 8.0 Hz, 2H), 7.79 (d, *J* = 8.0 Hz, 1H), 7.47 (dd, *J* = 9.5, 3.0 Hz, 1H), 7.44 (dd, *J* = 9.0, 2.5 Hz, 1H), 7.27 (td, *J* = 9.0, 3.0 Hz, 1H), 7.06 (td, *J* = 7.0, 1.5 Hz, 1H), 6.72 (td, *J* = 9.0, 3.0 Hz, 1H), 6.44 (dd, *J* = 9.0, 5.5 Hz, 1H), 2.59 (s, 3H), 2.57 (s, 3H). ^{19}F NMR ($CDCl_3$): δ –114.72 (dt, *J* = 9.0, 6.0 Hz), –116.69 (dt, *J* = 9.0, 6.0 Hz). FTIR (KBr): 1683, 1652, 1604, 1564, 1484, 1464, 1426, 1261 cm^{-1}. HRMS-electrospray (m/z): $[M - O_2C(p\text{-}AcC_6H_4)]^+$ calcd for $C_{40}H_{28}F_2N_2O_6Pd$ 613.0555; Found, 613.0559.

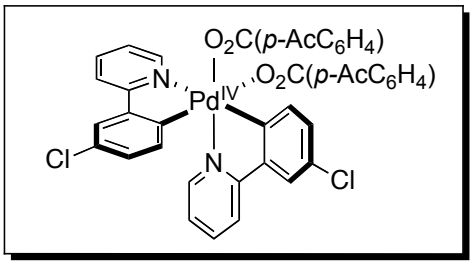

Complex 49: Yield: 70%. ^{1}H NMR ($CDCl_3$): δ 9.48 (dd, *J* = 5.5, 1.0 Hz, 1H), 8.13 (td, *J* = 7.5, 1.5 Hz, 1H), 8.10 (d, *J* = 8.5 Hz, 1H), 8.07 (app. d, *J* = 8.0 Hz, 1H), 8.01 (d, *J* = 8.5 Hz, 2H), 7.98 (d, *J* = 8.5 Hz, 2H), 7.89 (d, *J* = 8.5 Hz, 2H), 7.87 (dd, *J* = 8.0, 1.5 Hz, 1H), 7.84 (d, *J* = 8.0 Hz, 2H), 7.81 (dd, *J* = 8.0, 1.5 Hz, 1H), 7.72 (d, *J* = 2.5 Hz, 1H), 7.70 (d, *J* = 2.5 Hz, 1H), 7.59 (ddd, *J* = 7.5, 5.5, 1.5 Hz, 1H), 7.57 (dd, *J* = 6.0, 1.0 Hz, 1H), 7.49 (dd, *J* = 8.5, 2.5 Hz, 1H), 7.07 (ddd, *J* = 7.5, 6.0, 1.5 Hz, 1H), 6.94 (dd, *J* = 9.0, 2.5 Hz, 1H), 6.43 (d, *J* = 8.5 Hz, 1H), 2.60 (s, 3H), 2.57 (s, 3H). FTIR (KBr): 1683, 1652, 1604, 1558, 1482, 1422, 1262 cm^{-1}. HRMS-electrospray (m/z): $[M - O_2C(p\text{-}AcC_6H_4)]^+$ calcd for $C_{40}H_{28}Cl_2N_2O_6Pd$ 644.9964; Found, 644.9960.

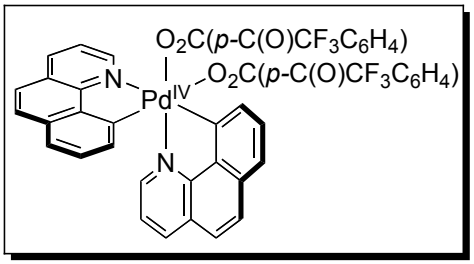

Complex 64: Yield: 91%. ^{1}H NMR (acetone-d_6): δ 9.97 (dd, *J* = 5.0, 1.6 Hz, 1H), 8.76 (dd, *J* = 8.0, 1.5 Hz, 1H), 8.54 (dd, *J* = 8.0, 1.5 Hz, 1H), 8.44 (d, *J* = 7.0 Hz, 1H), 8.14-7.87 (multiple peaks, 12H), 7.66 (d, *J* = 7.6 Hz, 1H), 7.40 (dd, *J* = 8.0, 6.0 Hz, 1H), 7.14 (t, *J* = 8.0, 1H), 6.44 (d, *J* = 7.6, 1H). ^{19}F NMR: (acetone-d_6): δ –72.46 (s, 3F), –72.52 (s, 3F). FTIR (KBr): 1718, 1658, 1620, 1568, 1490, 1455, 1406, 1319 cm^{-1}. HRMS-electrospray (m/z): $[M - O_2C[(p\text{-}C(O)CF_3)C_6H_4] + CH_3OH]^+$ calcd for $C_{44}H_{24}F_6N_2O_6Pd$, 711.0723; Found, 711.0735.

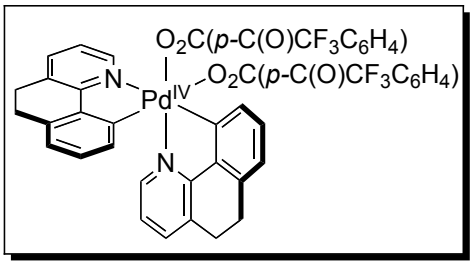

Complex 63: Yield: 82%. ^{1}H NMR ($CDCl_3$): δ 9.33 (d, *J* = 4.5 Hz, 1H), 8.09-8.07 (multiple peaks, 2H), 8.01-8.00 (ap. d, *J* = 9 Hz, 4H), 7.94-7.92 (multiple peaks, 2H), 7.86 (d, *J* = 8.5 Hz, 1H), 7.80 (d, *J* = 7.0 Hz, 1H), 7.53 (d, *J* = 8.0 Hz, 1H), 7.47-7.41 (multiple peaks, 2H), 7.35 (d, *J* = 5.5 Hz, 1H), 7.19 (d, *J* = 7.5 Hz, 1H), 6.92-6.83 (multiple peaks, 3H), 6.34 (d, *J* = 8.0 Hz, 1H). ^{19}F NMR: (acetone-d_6): δ –72.35 (s, 3F), –72.42 (s, 3F). HRMS-electrospray (m/z): [M – O_2C[(*p*-$C(O)CF_3)C_6H_4$] + CH_3OH]$^+$ calcd for $C_{44}H_{28}F_6N_2O_6Pd$, 715.1036; Found, 715.1046.

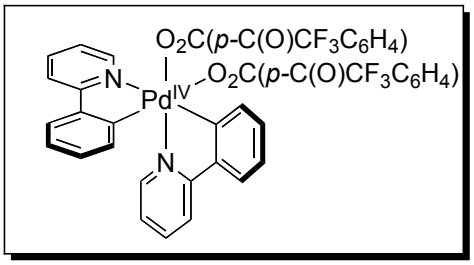

Complex 62: Yield: 71%. ^{1}H NMR (acetone-d_6): δ 9.56 (d, *J* = 5.6 Hz, 1H), 8.38 (d, *J* = 8.4 Hz, 1H), 8.27 (td, *J* = 7.2, 1.6 Hz, 1H), 8.22-8.17 (multiple peaks, 2H), 8.11 (d, *J* = 6.8 Hz, 2H), 8.09-7.30 (multiple peaks, 9H), 7.70 (d, *J* = 5.2 Hz, 1H), 7.70 (dd, *J* = 7.6, 5.6 Hz, 1H), 7.56-7.48 (multiple peaks, 2H), 7.22 (td, *J* = 6.0, 1.6 Hz, 1H), 7.16 (t, *J* = 7.2 Hz, 1H), 6.94 (td, *J* = 8.6, 1.6 Hz, 1H), 6.48 (d, *J* = 8.0 Hz, 1H). ^{19}F NMR (acetone-d_6): δ –72.36 (s, 3F), –72.43 (3F, s). FTIR (KBr): 1717, 1604, 1569, 1485, 1442, 1335, 1185 cm^{-1}. HRMS-electrospray (m/z): [M – O_2C[(*p*-$C(O)CF_3)C_6H_4$] + CH_3OH]$^+$ calcd for $C_{40}H_{24}F_6N_2O_6Pd$ 663.0711; Found, 663.0723.

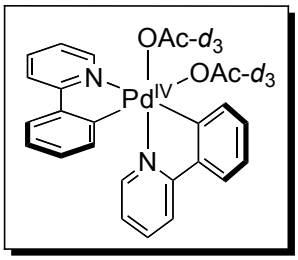

Complex 2-d_6: Yield: 73%. ^{1}H NMR ($CDCl_3$): δ 9.36 (d, *J* = 4.8 Hz, 1H), 8.12 (dd, *J* = 7.8, 1.0 Hz, 1H), 8.10-8.00 (multiple peaks, 2H), 7.76-7.73 (multiple peaks, 2H), 7.55-7.49 (multiple peaks, 3H), 7.44 (td, *J* = 7.5, 1.2 Hz, 1H), 7.07 (td, *J* = 7.5, 1.0 Hz, 1H), 6.90 (m, 1H), 6.85 (ddd, *J* = 8.0, 7.0, 1.5 Hz, 1H), 6.38 (dd, *J* = 8.0, 1.0 Hz, 1H). ^{2}D NMR ($CHCl_3$): δ 1.93 (s, 3H), 1.86 (s, 3H). FTIR (KBr): 1648, 1604, 1570, 1484, 1442, 1353, 1309, 1286, 1007, 760 cm^{-1}. HRMS-electrospray (m/z): $[M - OAc\text{-}d_3]^+$ calcd for $C_{24}H_{16}D_3N_2O_2Pd$, 476.0670; Found, 476.0677.

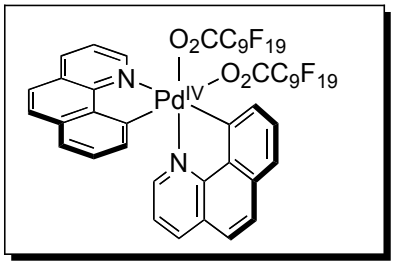

Complex 69: Under the general procedure conditions (above), a mixture of products was formed. Therefore, the reaction was carried out in dry acetone at 45 °C and then worked up according to the general procedure above. Yield: 64%. ^{1}H NMR (acetone-d_6): δ 9.73 (d, *J* = 5.0 Hz, 1H), 8.94 (d, *J* = 8.0 Hz, 1H), 8.62 (d, *J* = 8.0 Hz, 1H), 8.19-8.16 (multiple peaks, 4H), 8.12 (d, *J* = 9.0 Hz, 1H), 8.00-7.94 (multiple peaks, 3H), 7.95 (d, *J* = 9.0 Hz, 1H), 7.86 (d, *J* = 6.0 Hz, 1H), 7.73 (d, *J* = 8.0 Hz, 1H), 7.43 (d, *J* = 5.0 Hz, 1H), 7.41 (d, *J* = 5.0 Hz, 1H), 7.17 (t, *J* = 8.0 Hz, 1H), 6.38 (d, *J* = 8.0 Hz, 1H). ^{19}F NMR (acetone- d_6): δ –81.79 to – 81.85

(multiple peaks, 6F), –116.6 to –116.80 (multiple peaks, 4F), –122.48 to –123.38 (multiple peaks, 24F), –126.88 (br. s, 4F). FTIR (KBr): 1726, 1699, 1660, 1569, 1456, 1408, 1364, 1322, 1210 cm^{-1}. HRMS-electrospray (m/z): $[M - O_2CC_9F_{19}]^+$ calcd for $C_{46}H_{16}F_{38}N_2O_4Pd$ 974.9943; Found, 974.9966.

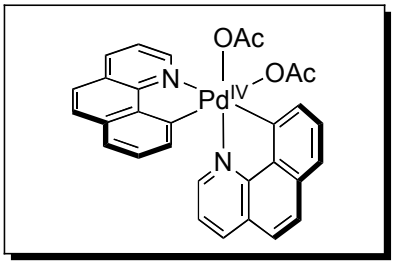

Complex 71: Yield: 71%. ^{1}H NMR (acetone-d_6): δ 9.83 (d, *J* = 5.0 Hz, 1H), 8.77 (d, *J* = 8.0 Hz, 1H), 8.42 (d, *J* = 8.0 Hz, 1H), 8.24 (d, *J* = 8.0 Hz, 1H), 8.08-7.83 (multiple peaks, 7H), 7.69 (d, *J* = 6.0 Hz, 1H), 7.56 (d, *J* = 8.0 Hz, 1H), 7.26 (multiplet, 1H), 7.03 (t, *J* = 8.0 Hz, 1H), 6.24 (d, *J* = 8.0 Hz, 1H), 1.73 (s, 3H), 1.57 (s, 3H). FTIR (KBr): 1646, 1616, 1558, 1405, 1353, 1309, 1283, 914, 836, 667 cm^{-1}. HRMS-electrospray (m/z): $[M - O_2C_2H_3]^+$ calcd for $C_{30}H_{22}N_2O_4Pd$ 521.0481; Found, 521.0489.

2.6.3 Synthesis of $(Phpy)_2Pd(Cl)(OAc)$ (21), $(Phpy)_2Pd(Cl)(OAc\text{-}d_3)$ (S21-d_3) and $(Bzq)_2Pd(Cl)(OAc)$ (73)

General Procedure. The appropriate Pd^{IV} complex [either $(Phpy)_2Pd(OAc)_2$ or $(Phpy)_2Pd(OAc\text{-}d_3)_2$] (0.12 mmol, 1.0 equiv) was dissolved in THF (10 mL). LiCl (52 mg, 1.2 mmol, 10 equiv) was added, and the reaction was stirred for 30 min. The precipitate from the reaction was collected on a frit, washed with THF, and dried under vacuum. The resulting off-white solid was dissolved in acetone (12 mL), and HCl (1 M solution in Et_2O, 100 μL, 0.10 mmol, 0.84 equiv) was added. The mixture was stirred for 3 h, and then the solvent was removed under vacuum to afford the product as a light yellow solid.

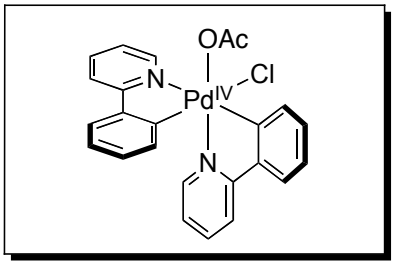

(Phpy)$_2$Pd(Cl)(OAc) (**21**). Yield: 31%. ^{1}H NMR (DMSO-d_6): δ 9.62 (d, *J* = 4.0 Hz, 1H), 8.39 (d, *J* = 8.0 Hz, 1H), 8.31-8.27 (multiple peaks, 2H), 8.08-8.04 (multiple peaks, 2H), 7.97 (d, *J* = 6.5 Hz, 1H), 7.89 (d, *J* = 8.5 Hz, 1H), 7.76 (t, *J* = 7.0 Hz, 1H), 7.51 (t, *J* = 8.0 Hz, 1H), 7.22-7.18 (multiple peaks, 2H), 7.12 (t, *J* = 7.0 Hz, 1H), 6.92 (t, *J* = 7.0, 1H), 6.19 (d, *J* = 8.0 Hz, 1H), 1.72 (s, 3H). FTIR (KBr): 1758, 1650, 1603, 1567, 1464, 1421, 1294 cm^{-1}. HRMS-electrospray (m/z): [M – Cl]$^+$ calcd for $C_{24}H_{19}ClN_2O_2Pd$ 473.0481; Found, 473.0478.

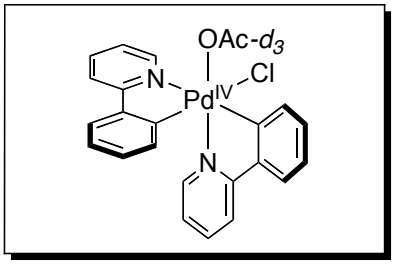

(Phpy)$_2$Pd(Cl)(OAc-*d*$_3$) (**S21-*d*$_3$**). Yield: 43%. ^{1}H NMR (DMSO-d_6): δ 9.61 (d, *J* = 4.0 Hz, 1H), 8.39 (d, *J* = 8.0 Hz, 1H), 8.31-8.24 (multiple peaks, 2H), 8.07-8.02 (multiple peaks, 2H), 7.96 (d, *J* = 7.5 Hz, 1H), 7.88 (d, *J* = 8.5 Hz, 1H), 7.75 (t, *J* = 6.0 Hz, 1H), 7.57 (t, *J* = 8.0 Hz, 1H), 7.49 (t, *J* = 7.5 Hz, 1H), 7.23-7.19 (multiple peaks, 2H), 7.11 (t, *J* = 7.5 Hz, 1H), 6.92 (t, *J* = 8.0 Hz, 1H), 6.19 (d, *J* = 8.0 Hz, 1H). ^{2}H NMR (DMSO): δ 1.99 (s, 3D). FTIR (KBr): 1640, 1602, 1579, 1567, 1484, 1439, 1410, 1305 cm^{-1}. HRMS-electrospray (m/z): [M – Cl]$^+$ calcd for $C_{24}H_{16}D_3ClN_2O_2Pd$ 476.0670; Found, 476.0679.

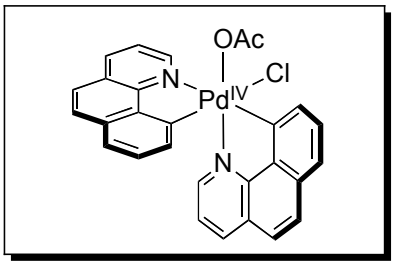

(Bzq)$_2$Pd(Cl)(OAc) (**73**). Yield: 96%. ^{1}H NMR (DMSO-d_6): δ 9.91 (d, *J* = 5.0 Hz, 1H), 8.92 (d, *J* = 8.0 Hz, 1H), 8.60 (d, *J* = 8 Hz, 1H), 8.21-8.15 (multiple peaks, 4H), 8.09 (d, *J* = 9.0 Hz, 1H), 8.03 (t, *J* = 8.0 Hz, 1H), 7.98-7.95 (multiple peaks, 2H), 7.67 (d, *J* = 7.5 Hz, 1H), 7.42-7.40 (multiplet, 1H), 7.35 (d, *J* = 6.0 Hz, 1H), 7.14 (t, *J* = 8.0 Hz, 1H), 6.20 (d, *J* = 8.0 Hz, 1H), 1.74 (s, 3H). FTIR (KBr): cm^{-1}. HRMS-electrospray (m/z): $[M - Cl]^+$ calcd for $C_{28}H_{19}ClN_2O_2Pd$ 521.0481; Found, 521.0488.

2.6.4 Synthesis of Pd^{IV} Complexes 2a-d_3, 2b-d_3 and 6 Containing Mixed Carboxylate Ligands

General Procedure. Complex **21** or **S21-d_3** (0.074 mmol, 1 equiv) and AgO_2CR (0.082 mmol, 1.1 equiv) were dissolved in a 50/50 solution of CH_2Cl_2/EtOAc (16 mL). The reaction mixture was stirred for 1.5 h, and was then filtered through a plug of Celite. The filtrate was concentrated to afford the product as a yellow powder.

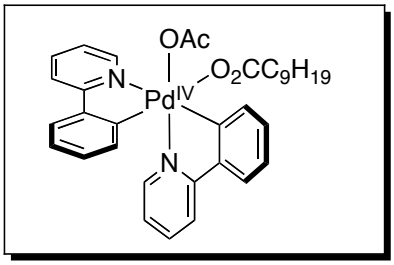

$(Phpy)_2Pd(O_2CC_9H_{19})(OAc)$ (19). Yield: 74%. ^1H NMR ($CDCl_3$): δ 9.39 (d, *J* = 5.0 Hz, 1H), 8.08 (d, *J* = 8.0 Hz, 1H), 8.02-7.98 (multiple peaks, 2H), 7.70 (multiple peaks, *J* = 4.0 Hz, 2H), 7.65-7.61 (multiple peaks, 2H), 7.54 (d, *J* = 6.0 Hz, 1H), 7.50-7.38 (multiple peaks, 2H), 7.40 (t, *J* = 7.0 Hz, 1H), 7.04 (t, *J* = 7.0 Hz, 1H), 6.87-6.82 (multiple peaks, 2H), 6.35 (d, *J* = 8.0 Hz, 1H), 2.07 (t, *J* = 8.0 Hz, 2H), 1.93 (s, 3H), 1.33-0.99 (multiple peaks, 14H), 0.85 (t, *J* = 7.0 Hz, 3H). HRMS-electrospray (m/z): $[M - O_2CC_9H_{19}]^+$ calcd for $C_{24}H_{19}N_2O_2Pd$, 473.0481; Found, 473.0480.

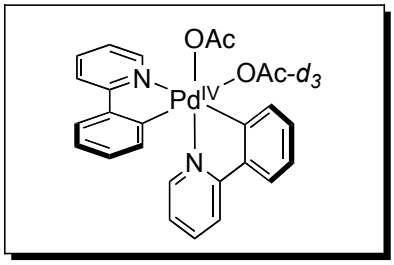

$(Phpy)_2Pd(OAc\text{-}d_3)(OAc)$ (2a-d_3). Yield: 53%. ^1H NMR (acetone-d_6): δ 9.44 (d, *J* = 5.0 Hz, 1H), 8.26 (d, *J* = 8.0 Hz, 1H), 8.19 (t, *J* = 8.0 Hz, 1H), 8.07-8.05 (multiple peaks, 2H), 7.94-7.91 (multiple peaks, 2H), 7.86 (d, *J* = 8.0 Hz, 1H), 7.60 (t, *J* = 5.5 Hz, 1H), 7.57 (d, *J* = 5.5 Hz, 1H), 7.50 (t, *J* = 7.5 Hz, 1H), 7.46-7.43 (multiple peaks, 2H), 7.07 (multiple peaks, 2H), 6.84 (t, *J* = 8.5 Hz, 1H), 6.29 (d, *J* = 8.5 Hz, 1H), 1.73 (s, 3H). ^2H NMR ($CHCl_3$): δ 1.86 (s, 3D). HRMS-electrospray (m/z): $[M - OAc\text{-}d_3]^+$ calcd for $C_{26}H_{19}D_3N_2O_4Pd$ 473.0481; Found, 473.0491.

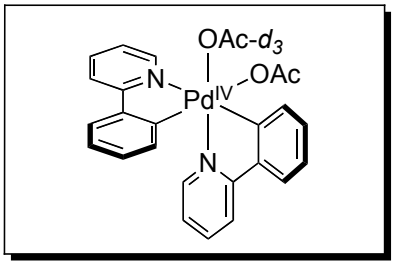

$(Phpy)_2Pd(OAc)(OAc\text{-}d_3)$ (2b-d_3). Yield: 51%. ^1H NMR (acetone-d_6): δ 9.42 (d, *J* = 5.0 Hz, 1H), 8.24 (dd, *J* = 7.0 Hz, 1H), 8.17 (t, *J* = 8.0 Hz, 1H), 8.06-8.03 (multiple peaks, 2H), 7.93-7.88 (multiple peaks, 2H), 7.85 (d, *J* = 8.0 Hz, 1H), 7.60-7.54 (multiple peaks, 2H), 7.50-7.41 (multiple peaks, 2H), 7.07-7.02 (multiple peaks, 2H), 6.82 (t, *J* = 7.0 Hz, 1H), 6.28 (d, *J* = 8.0 Hz, 1H), 1.60 (s, 3H). ^2H NMR ($CHCl_3$): δ 1.94 (s, 3D). HRMS-electrospray (m/z): $[M - OAc]^+$ calcd for $C_{26}H_{19}D_3N_2O_4Pd$ 476.0670; Found, 476.0675.

2.6.5 Characterization of Organic Products of C–O Bond-Forming Reductive Elimination

The organic reductive elimination products were challenging to purify from the crude reaction mixtures. As a result they were synthesized independently according to the general procedure below. In all cases, the products were spectroscopically identical to those observed by ^1H NMR spectroscopy in the reductive elimination reactions.

General Procedure. The appropriate arylpyridine substrate (1.7 mmol, 1.0 equiv), $PhI[O_2C(p\text{-}AcC_6H_4)]_2$ (3.4 mmol, 2.0 equiv), and $Pd(OAc)_2$ (0.05 mmol, 3 mol %) were dissolved in CH_3CN (18 mL) in a 20 mL vial. The vial was sealed with a Teflon-lined cap, and the reaction mixture was heated at 80°C for 12 h. The solvent was removed under vacuum, and the resulting brown residue was re-dissolved in CH_2Cl_2 (15 mL). The organic layer was extracted with saturated $NaHCO_3$ (2 x 30 mL) and then dried over $MgSO_4$. The products were purified by column chromatography.

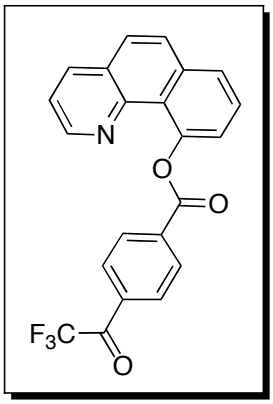

Benzo[h]quinolin-10-yl-4-(2,2,2-trifluoroacetyl)benzoate (65): Yield: 37% of an off-white tacky solid. R_f = 0.1 in 59% hexanes/40% ethyl acetate/1% triethylamine. ^{1}H NMR ($CDCl_3$): δ 8.54 (d, *J* = 4.0 Hz, 1H), 8.33 (dd, *J* = 4.5, 1.5 Hz, 1H), 8.3 (d, *J* = 8.0 Hz, 2H), 8.14 (dd, *J* = 8.0, 1.5 Hz, 1H), 7.93 (d, *J* = 7.0 Hz, 1H) 7.9 (d, *J* = 9.0 Hz, 1H), 7.76 (t, *J* = 8.0 Hz, 1H), 7.73 (d, *J* = 9.0 Hz, 1H), 7.55 (d, *J* = 8.0 Hz, 1H), 7.39 (dd, *J* = 8.0, 4.5, 1H). ^{19}F NMR ($CDCl_3$): δ –71.55 (s, 3F). FTIR (KBr): 1741, 1718, 1595, 1410, 1270, 1190, 1087, 942, 836, 716 cm^{-1}. When this compound was dissolved in DMSO-d_6 (required for sufficient solubility to obtain a ^{13}C NMR spectrum), partial hydration of the trifluoromethylketone was observed. The reductive elimination products from **64** were further characterized by treatment with a solution of NaOH in methanol to convert.

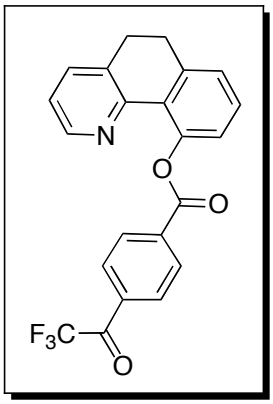

(5,6-Dihydrobenzo[*h*]quinolin-10-yl 4-(2,2,2-trifluoroacetyl)benzoate (S5): Isolated directly from reductive elimination of 63 (0.028 mmol) at 80°C in CH_3CN (1.8 mL) and purified via column chromatography. Yield: 78% of an off-white tacky solid. R_f = 0.2 in 59% hexanes/40% ethyl acetate/1% triethylamine. ^1H NMR ($CDCl_3$): δ 8.38-8.35 (multiple peaks, 2H), 8.18 (d, *J* = 8.0 Hz, 2H), 7.89 (dd, *J* = 5.0, 2.0 Hz, 1H), 7.44 (dd, *J* = 8.0, 2.0 Hz, 1H), 7.36 (t, *J* = 8.0 Hz, 1H), 7.21 (dd, *J* = 6.5, 1.0 Hz, 1H), 7.13 (dd, *J* = 8.0, 1.0 Hz, 1H), 6.95 (dd, *J* = 5.0, 3.0 Hz, 1H), 2.95-2.91 (multiple peaks, 4H). ^{19}F NMR ($CDCl_3$): δ –71.38 (s, 3F). FTIR (KBr): 1744, 1718, 1278, 1227, 1202, 1179, 1141, 1091, 941, 802, 720 cm^{-1}. When this compound was dissolved in DMSO-d_6 (required for sufficient solubility to obtain a ^{13}C NMR spectrum), partial hydration of the trifluoromethylketone was observed. The reductive elimination products were further characterized by treatment with a solution of NaOH in methanol to convert **S5** to 5,6-dihydrobenzo[h]quinolin-10-ol. ^1H NMR ($CDCl_3$): δ 14.01 (s, 1H), 8.30 (d, *J* = 4.5 Hz, 1H), 7.56 (d, *J* = 7.0 Hz, 1H), 7.20-7.16 (multiple peaks, 2H), 6.86 (d, *J* = 8.0 Hz, 1H), 6.69 (d, *J* = 7.0 Hz, 1H), 2.89 (multiplet, 4H). $^{13}C\{^1H\}$ NMR ($CDCl_3$): δ 159.47, 154.68, 144.11, 138.99, 136.34, 131.93, 131.04, 121.52, 118.39, 116.61, 116.01, 28.19, 27.95. HRMS-electrospray (*m/z*): $[M + H]^+$ calcd for $C_{13}H_{11}NO$ 198.0919; Found, 198.0914.

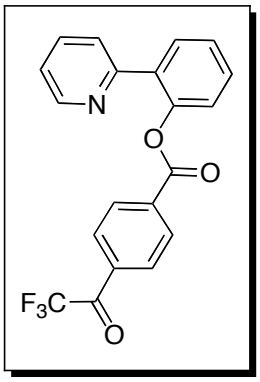

2-(pyridin-2-yl)phenyl 4-(2,2,2-trifluoroacetyl)benzoate (S6): Yield: 26% of an off-white tacky solid. R_f = 0.1 in 59% hexanes/40% ethyl acetate/1% triethylamine. ^{1}H NMR ($CDCl_3$): δ 8.51 (d, *J* = 6.0, 2.0 Hz, 1H), 8.24 (d, *J* = 8.0 Hz, 2H), 8.24 (d, *J* = 8.0 Hz, 2H), 7.74 (dd, *J* = 6.0, 2.0 Hz, 1H), 7.67 (td, *J* = 8.0, 2.0, 1H), 7.55-7.50 (multiple peaks, 2H), 7.44 (td, *J* = 8.0, 1.0 Hz, 1H), 7.33 (dd, *J* = 8.0, 1.0 Hz, 1H), 7.16 (ddd, *J* = 5.0, 3.0, 1.0 Hz, 1H). ^{19}F NMR ($CDCl_3$): δ –71.64 (3F, s). FTIR (KBr): 1733, 1469, 1270, 1180, 1116, 1072, 1053, 1016, 923, 859, 755, 709 cm^{-1}. When this compound was dissolved in DMSO-d_6 (required for sufficient solubility to obtain a ^{13}C NMR spectrum), partial hydration of the trifluoromethylketone was observed. The reductive elimination products were further characterized by treatment with a solution of NaOH in methanol to convert **S6** to 2-(pyridine-2yl)phenol.

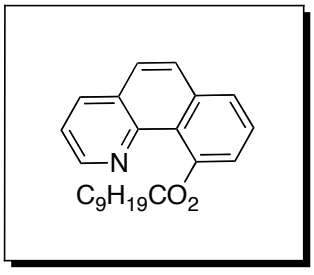

Benzo[*h*]quinolin-10-yl deconate (68): Yield: 36 % of a yellow oil. R_f = 0.2 in 79% hexanes/20% ethyl acetate/1% triethylamine**.** ^{1}H NMR (acetone-d_6): δ 8.99 (dd, *J* = 4.0, 2.0 Hz, 1H), 8.36 (dd, *J* = 8.0, 2.0 Hz, 1H), 7.97-7.94 (multiple

peaks, 2H), 7.85 (d, *J* = 9.0 Hz, 1H) 7.74 (t, *J* = 8.0 Hz, 1H), 7.62 (dd, *J* = 8.0, 4.0 Hz, 1H), 7.40 (dd, *J* = 8.0, 1.0 Hz, 1H), 2.89 (t, *J* = 7.5 Hz, 2H), 1.83 (m, 2H), 1.54 (m, 2H), 1.42-1.29 (multiple peaks, 10H), 0.88 (t, *J* = 7.0 Hz, 3H). $^{13}C\{^{1}H\}$ NMR ($CDCl_3$): δ 173.77, 149.01, 148.18, 145.89, 136.20, 135.87, 128.25, 128.22, 127.43, 126.77, 126.51, 123.63, 122.43, 121.67, 35.06, 32.11, 29.71, 29.67, 29.65, 29.53, 24.90, 22.89, 14.34. FTIR (KBr): 3048, 2925, 2853, 1757, 1622, 1593, 1444, 1403, 1142, 834, 806, 746, 721 cm^{-1}. HRMS-electrospray (*m/z*): $[M + H]^+$ calcd 350.2120 for $C_{23}H_{27}NO_2$; Found, 350.2126.

2.6.5 Characterization of Inorganic Products of C–O Bond-Forming Reductive Elimination

The inorganic reductive elimination products were challenging to purify cleanly from the crude reaction mixtures. As a result they were synthesized independently according to the following three-step sequence. In all cases, the products were spectroscopically identical to those observed by ^{1}H NMR spectroscopy in the reductive elimination reactions.

Scheme 2.6.5.1 Synthesis of Inorganic Products of C–O Bond-Forming Reductive Elimination

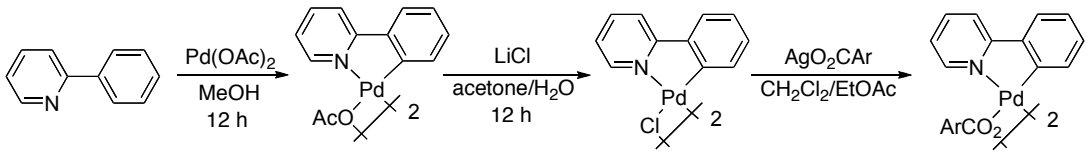

General Procedure. Step 1: The appropriate N~C ligand (0.56 mmol, 1.0 equiv) and Pd(OAc)2 (0.56 mmol, 1.0 equiv) were dissolved in MeOH (8 mL). The orange reaction mixture was allowed to stir for 12 h. The resulting solid precipitate was collected on a frit and washed with hexanes. For further purification, the solid was re-dissolved in CH2Cl2, precipitated with hexanes and dried under vacuum to afford the products as bright yellow solids. Step 2: The yellow solid from step 1 (0.30 mmol, 1.0 equiv) was combined with LiCl (1.45 mmol, 4.8 equiv) in acetone (3.25 mL) and water (325 μL). The reaction mixture was stirred for 12 h. A precipitate was formed and collected on a frit. The product

washed with hexanes and dried under vacuum to afford a pale yellow solid. Step 3: The solid from step 2 (0.25 mmol, 1.0 equiv) was combined with $Ag(O_2CAr)$ (0.62 mmol, 2.5 equiv) in a mixture of CH_2Cl_2 (12 mL) and EtOAc (8 mL). The reaction mixture was stirred for 12 h, then filtered through a plug of celite. The solvent was removed under vacuum, and the resulting residue was recrystallized from CH_2Cl_2/hexanes to afford a bright yellow solid.

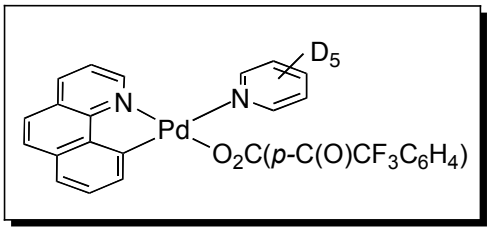

$BzqPd(C_5D_5N)OBz_{C(O)CF3}$ (**S7):** Yield: 56%. ^1H NMR ($CDCl_3$ containing 20% C_5D_5N): δ 8.71 (d, J = 4.8 Hz, 1H), 8.30 (dd, J = 8.4, 1.2 Hz, 1H), 8.26 (d, J = 8.0 Hz, 2H), 8.07 (d, J = 8.0 Hz, 2H), 7.76 (d, J = 8.4 Hz, 1H), 7.63-7.58 (multiple peaks, 2H), 7.45 (dd, J = 8.0, 5.2 Hz, 1H), 7.30 (d, J = 7.2 Hz, 1H), 6.47 (d, J = 7.6 Hz, 1H). ^{19}F NMR ($CDCl_3$): δ –71.44 (s, 3F). FTIR (KBr): 1599, 1555, 1485, 1397, 1205, 1185, 1141, 941, 752 cm^{-1}.

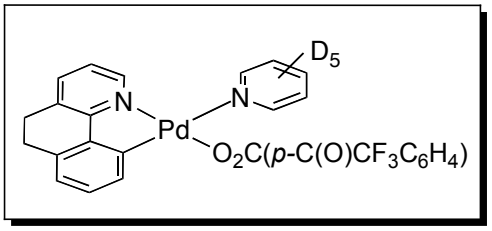

$BzqH_2Pd(C_5D_5N)OBz_{C(O)CF3}$ (**S8):** Yield: 51%. ^1H NMR ($CDCl_3$ containing 20% C_5D_5N): δ 8.27 (d, J = 8.8 Hz, 1H), 8.07 (d, J = 8.4 Hz, 1H), 7.50 (d, J = 7.6 Hz, 2H), 7.00 (t, J = 6.4 Hz, 2H), 6.90-6.86 (multiple peaks, 3H), 6.08 (d, J = 6.4 Hz, 1H), 2.93 (app. s, 4H). ^{19}F NMR ($CDCl_3$): δ –71.57. FTIR (KBr): 1599, 1564, 1479, 1411, 1318, 1159, 720, 534 cm^{-1}.

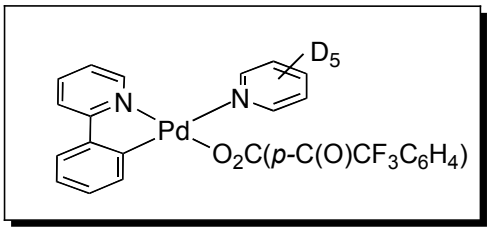

$(Phpy)_2Pd(C_5D_5N)OBz_{C(O)CF3}$ (**S9):** Yield: 43%. ^1H NMR ($CDCl_3$ containing 20% C_5D_5N): δ 8.51 (d, J = 4.4 Hz, 1H), 8.21 (d, J = 7.6 Hz, 2H), 8.05 (d, J = 7.6 Hz, 2H), 7.80 (td, J = 8.0, 1.2 Hz, 1H), 7.68-7.65 (multiple peaks, 2H), 7.47 (d, J = 7.6 Hz, 1H), 7.10-7.07 (multiple peaks, 2H), 6.94 (t, J = 7.8 Hz, 1H), 6.25 (d, J = 8.0 Hz, 1H). ^{19}F NMR ($CDCl_3$): δ –71.50 (s, 3F). FTIR (KBr): 1600, 1556, 1384, 1319, 1164, 1065, 941, 712, 532 cm^{-1}.

Attempts to isolate clean samples of the dimeric Pd^{II} species observed in the reductive elimination of Pd^{IV} complexes 58-60 were hindered by the hazards associated with working with $Ag(O_2C(p\text{-}C(O)AcC_6H_4)$. Although the explosive nature of this salt has not been reported previously, it was found that when dried and exposed to a minor amount of friction, it readily underwent detonation.

2.6.6 General Procedure for Crossover studies

Scheme 2.6.6.1 Cross-over Study of the Reductive Elimination of Complex 2-*d*$_6$

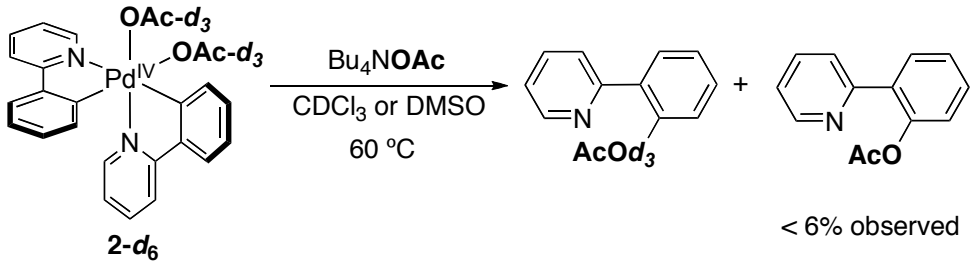

Scheme 2.6.6.2 Cross-over Study of the Reductive Elimination of Complex 2b-*d*$_3$

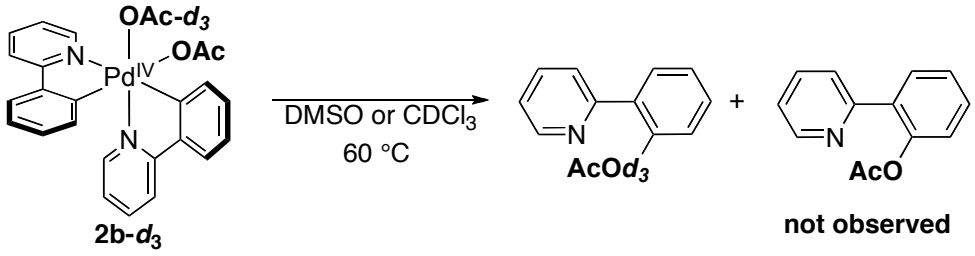

Complex **2-*d*$_6$** or **2b-*d*$_3$** (6.2 mg, 0.012 mmol) was dissolved in DMSO or $CHCl_3$ (0.8 mL) in a 4 mL vial in a N_2-filled drybox. If appropriate, $NBu_4(OAc)$ (18 mg, 0.060 mmol, 5.0 equiv) was added to this solution. The vial was sealed with a Teflon-lined cap, removed from the drybox, and heated at 60 °C for 5 h. The resulting mixture was evaporated to dryness, redissolved in CH_2Cl_2 (3 mL), then filtered through a pipette plug containing 25% poly-4-vinylpyridine and 75% silica gel. The plug was washed with a 9 : 1 solution of hexanes : ethyl acetate that contained 1% triethylamine (~20 mL total volume). The solvent was then

removed under vacuum, and the organic products were analyzed by ^{1}H and ^{2}H NMR spectroscopy. The ratio of **3-*d*$_3$** to **3** was determined by integration of H6 of the pyridine (8.68 ppm) relative to the methyl group of the acetate (2.17 ppm) in $CDCl_3$. Each experiment was carried out in triplicate, and the results reported in the manuscript represent an average of three runs.

2.6.7 Source of error in Kinetics Experiments

Error in the kinetics experiments most likely arises from a slight temperature instability in the NMR spectrometer. Additionally minor inconsistencies in the amount of pyridine added to the reaction have been shown to affect the rate of C–O bond formation. In the case of the carboxylate exchange reactions, the close proximity of the resonances associated with the starting materials and products leads to some error in the integration values. The error was calculated by taking an average of the trials. The standard deviation of the average was then calculated. The average was added to the standard deviation, and the difference and sum of these values were taken against the average to obtain the plus/minus values.

2.6.8 General Procedure for Solvent Study of Kinetics of Carboxylate Exchange

Scheme 2.6.8.1 Eyring Plot for Carboxylate Exchange

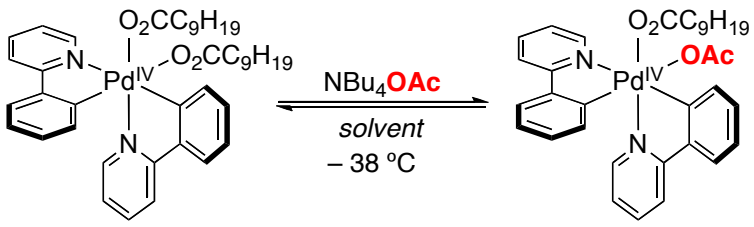

Complex **7** (5.8 mg, 0.0076 mmol, 1.0 equiv) was dissolved in an appropriate deuterated solvent (0.25 mL) in a screw cap NMR tube in a N_2-filled drybox. The NMR tube was sealed with a Teflon-lined cap fitted with a septum, and removed from the drybox. Bu_4NOAc (2.4 mg, 0.0076 mmol, 1.0 equiv) was dissolved in the appropriate deuterated solvent (0.25 mL) in a 4 mL vial, and the vial was sealed with a Teflon-lined cap fitted with a septum and removed from the glovebox. The solution in the NMR tube was frozen in liquid nitrogen, and the [Bu_4NOAc] solution was added via syringe. The NMR tube was placed in the NMR spectrometer where the probe had been pre-cooled to –38 ºC. The sample was allowed to equilibrate in the spectrometer for six minutes before acquiring spectra. The rate of carboxylate exchange was then studied by ^1H NMR spectroscopy at –38 ºC by monitoring the disappearance of the most downfield resonance (9.51 ppm in acetone-d_6, 9.33 in CD_3CN, 9.27 in $CDCl_3$, 9.82 in toluene-d_8). The reaction was followed until it reached equilibrium and then fitted to a first order kinetics plot for a reversible reaction.[37] Each experiment was carried out in duplicate, and the *k* values represent an average of two runs. Notably, when the experiment was run in toluene, no exchange was observed over the course of approximately 6 h at –38 ºC.

2.6.9 General procedure for Eyring Plot for Carboxylate Exchange

Scheme 2.6.9.1 Eyring Plot for Carboxylate Exchange

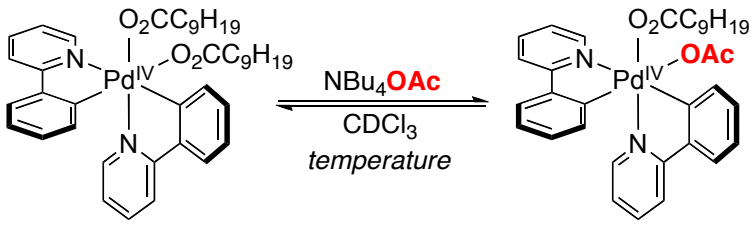

Complex **7** (5.8 mg, 0.0076 mmol, 1.0 equiv) was dissolved in $CDCl_3$ (0.25 mL) in a screw cap NMR tube in a N_2-filled drybox. The NMR tube was sealed with a Teflon-lined cap fitted with a septum, and removed from the drybox. Bu_4NOAc (2.4 mg, 0.0076 mmol, 1.0 equiv) was dissolved in the appropriate deuterated solvent (0.25 mL) in a 4 mL vial, and the vial was sealed with a Teflon-lined cap fitted with a septum and removed from the glovebox. The solution in the NMR tube was frozen in liquid nitrogen, and the [Bu_4NOAc] solution was added via syringe. The NMR tube was placed in the NMR spectrometer where the probe had been pre-cooled to the appropriate temperature. The sample was allowed to equilibrate in the spectrometer for six minutes before acquiring spectra. The rate of carboxylate exchange was then studied by ^1H NMR spectroscopy at –58 ºC, –53 ºC, –50 ºC, –48 ºC and –38 ºC by monitoring the disappearance of the most downfield resonance (9.27 ppm in $CDCl_3$). The reaction was followed until it reached equilibrium and then fitted to a first order kinetics plot for a reversible reaction. The rates shown in Table S2 below are an average of two trials.

Table 2.6.9.1 Rate Data for Carboxylate Exchange at Complex 7 as a Function of Solvent

Solvent	k_{obs} **(s^{-1} x 10^4)**[a]
toluene-d_8	<0.1
acetone-d_6	3.6 ± 0.1
CD_3CN	7.6 ± 0.1
$CDCl_3$	70 ± 0.1

[a] Values represent an average of two kinetics runs

Figure 2.6.9.1 Representative Kinetics Data for Carboxylate Exchange at 7 in CH_3CN at –38 °C

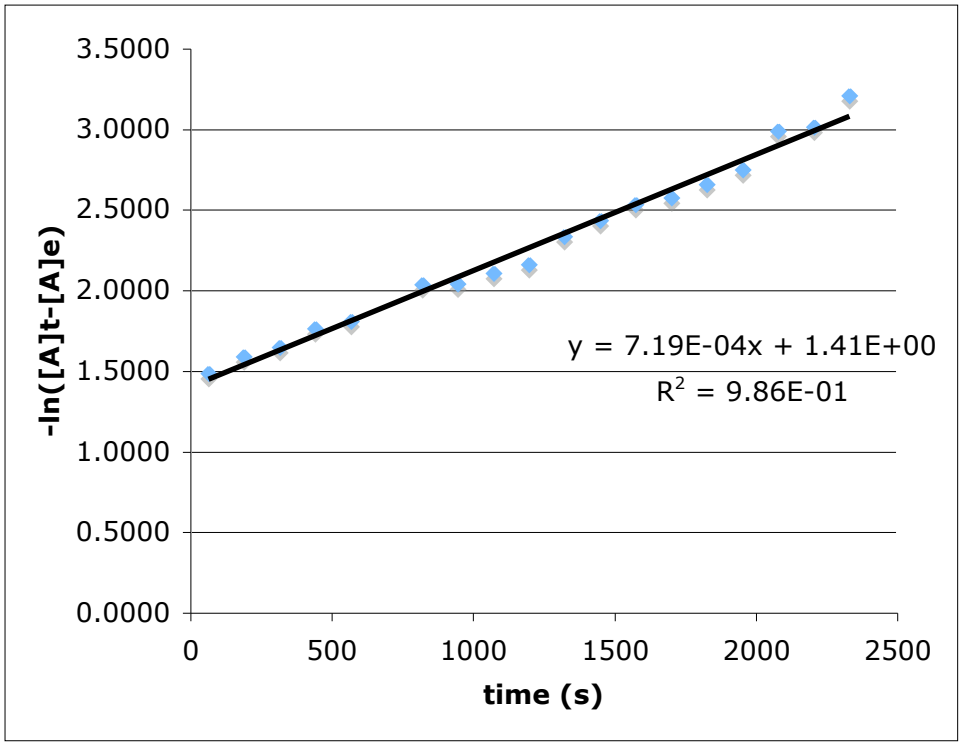

Table 2.6.9.2 Rate Data for Carboxylate Exchange at Complex 7 as a Function of Temperature

Temperature	k_{obs} (s^{-1} x 10^4)[a]
–58 ºC	4.1± 0.1
–53 ºC	5.4± 0.0
–50 ºC	20 ± 0.4
–48 ºC	19 ± 0.5
–38 ºC	70 ± 0.1

[a] Values represent an average of two kinetics runs

Figure 2.6.9.2 Erying Plot for Carboxylate Exchange at 7

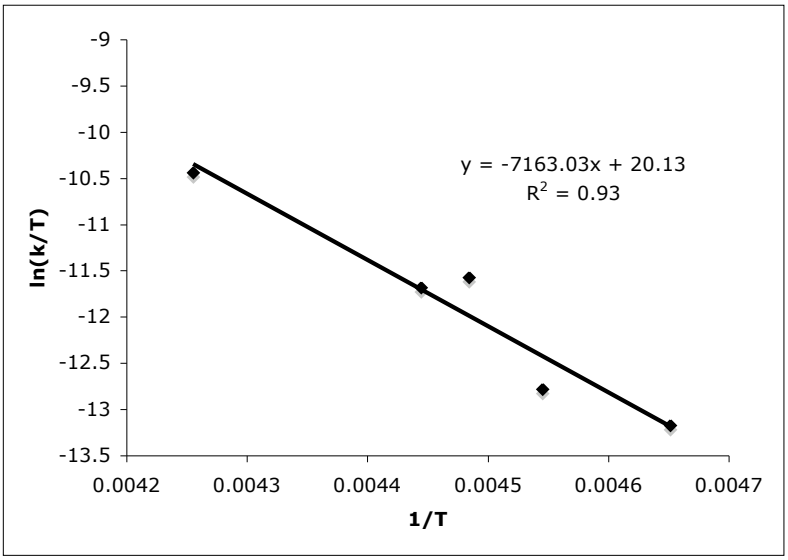

2.6.10 General Procedure for Kinetics with Acidic Additives

Scheme 2.6.10.1 Kinetics with Acetic Acid

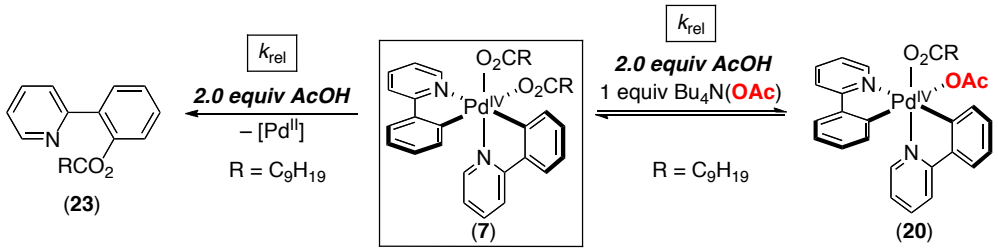

Carboxylate Exchange (HOAc). Complex **7** (5.8 mg, 0.0076 mmol, 1.0 equiv) was dissolved in acetone-d_6 (0.25 mL) in a screw cap NMR tube in a N_2-filled drybox. The NMR tube was sealed with a Teflon-lined cap fitted with a septum, and removed from the drybox. Bu_4NOAc (2.4 mg, 0.0076 mmol, 1.0 equiv) and a stock solution of AcOH (0.25 mL of a 14 mM stock solution in acetone-d_6, 0.0035 mmol, 0.5 equiv) was dissolved in the acetone-d_6 (0.25 mL) in a 4 mL vial, and the vial was sealed with a Teflon-lined cap fitted with a septum and removed from the glovebox. The solution in the NMR tube was frozen in liquid nitrogen, and the [Bu_4NOAc]/acid solution was added via syringe. The NMR tube was quickly shaken and placed in the NMR spectrometer where the probe had been pre-cooled to –35 ºC. The sample was allowed to equilibrate in the spectrometer for six minutes before acquiring spectra. Carboxylate exchange was studied by ^1H NMR spectroscopy by monitoring the disappearance of the most downfield signal (at 9.51 ppm in acetone-d_6). The reaction was followed until it reached equilibrium and then the data was fitted to a first order kinetics plot for a reversible reaction. Each experiment was carried out in duplicate, and the *k* values represent an average of two runs.

Reductive Elimination (HOAc). Complex **7** (5.8 mg, 0.0076 mmol, 1.0 equiv) was dissolved acetone-d_6 (0.5 mL) in a screw cap NMR tube in a N_2-filled drybox. AcOH (0.5 mL of a 7 mM stock solution in acetone-d_6, 0.0035 mmol, 0.5 equiv) was then added. The tube was sealed with a Teflon-lined cap, shaken, and removed from the drybox. The tube was quickly placed in the NMR spectrometer, and the reaction was allowed to equilibrate for six minutes in the spectrometer before acquisition was started. The kinetics of reductive elimination was studied by ^{1}H NMR spectroscopy by monitoring the disappearance of the most downfield signal (at 9.51 ppm in acetone at 40 °C). The data was fit to a first order kinetics plot. Each experiment was carried out in duplicate, and the *k* values represent an average of two runs.

Scheme 2.6.10.2 Kinetics with Silver Triflate

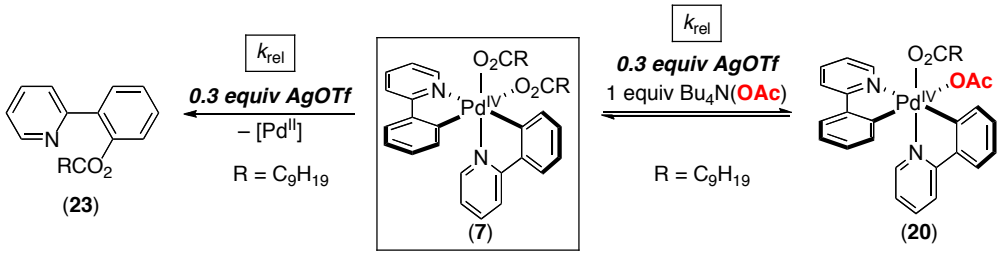

Carboxylate Exchange (AgOTf). Complex **7** (5.8 mg, 0.0076 mmol, 1.0 equiv) was dissolved in $CDCl_3$ (0.25 mL) in a 4 mL vial in a N_2-filled drybox. AgOTf was added to a screw cap NMR tube as a stock solution in THF (40 μL of a 50 mM stock solution, 0.50 mg, 0.002 mmol, 0.3 equiv). The solvent was then removed from the tube under high vacuum. The NMR tube was then transferred into a N_2-filled drybox and Bu_4NOAc (2.4 mg, 0.0076 mmol, 1.0 equiv) dissolved in 0.25 mL of $CDCl_3$ was added to the NMR tube, which was then sealed with a Teflon-lined cap fitted with a septum, and removed from the drybox. This solution was frozen in liquid N_2, and complex **7** (5.8 mg, 0.0076 mmol, 1.0 equiv) was dissolved in $CDCl_3$ (0.25 mL) and added to the NMR tube via syringe. The NMR

tube was quickly shaken and placed in the NMR spectrometer where the probe had been pre-cooled to –53 ºC. The sample was allowed to equilibrate in the spectrometer for six minutes before acquiring spectra. Carboxylate exchange was studied by ^{1}H NMR spectroscopy by monitoring the disappearance of the most downfield signal (9.42 ppm in $CDCl_3$). The reaction was followed until it reached equilibrium and then the data was fitted to a first order kinetics plot for a reversible reaction. Each experiment was carried out in duplicate, and the *k* values represent an average of two runs.

Reductive Elimination (AgOTf). AgOTf was added to a screw cap NMR tube as a stock solution in THF (40 μL of a 50 mM stock solution, 0.50 mg, 0.002 mmol, 0.3 equiv). The solvent was then removed from the tube under high vacuum. The NMR tube was transferred into a N_2-filled drybox. Complex **7** (5.8 mg, 0.0076 mmol, 1.0 equiv) was dissolved in $CDCl_3$ (0.5 mL) in a 4 mL vial and then transferred to the screw cap NMR tube that contained the AgOTf. The tube was sealed with a Teflon-lined cap, shaken, and removed from the drybox. The tube was quickly placed in the NMR spectrometer, and the reaction was allowed to equilibrate for six minutes in the spectrometer before acquisition was started. The kinetics of reductive elimination were studied by ^{1}H NMR spectroscopy by monitoring the disappearance of the most downfield signal (9.42 ppm in $CDCl_3$ at 23 °C). The data was fit to a first order kinetics plot. Each experiment was carried out in duplicate, and the *k* values represent an average of two runs.

Table 2.6.10.1 Effect of AcOH on C–O Bond-Forming Reductive Elimination and Carboxylate Exchange at 7

	Rate of Carboxylate Exchange	Rate of C–O Reductive Elimination
Additive	**k (s^{-1} x 10^4), -35 °C**	**k (s^{-1} x 10^4), 40 °C**
AcOH	15.0	1.3
no AcOH	3.3	0.82
acceleration	**4.5** ± 0.7	**3.6** ± 0.4

[a] 40 ºC in acetone-d_6; [b] –35 ºC in acetone-d_6;

Table 2.6.10.2 Effect of AgOTf on C–O Bond-Forming Reductive Elimination and Carboxylate Exchange at 7

	Rate of Carboxylate Exchange	Rate of C–O Reductive Elimination
Additive	**k (s^{-1} x 10^4), -53 °C**	**k (s^{-1} x 10^4), 23 °C**
AgOTf	54	4.0
no AgOTf	6.2	0.26
acceleration	**8.7** ± 0.1	**16** ± 0.8

[a] 23 ºC in $CDCl_3$; [b] –53 ºC in $CDCl_3$

Figure 2.6.10.1 Representative Kinetics Data for Reductive Elimination of 7 with AcOH

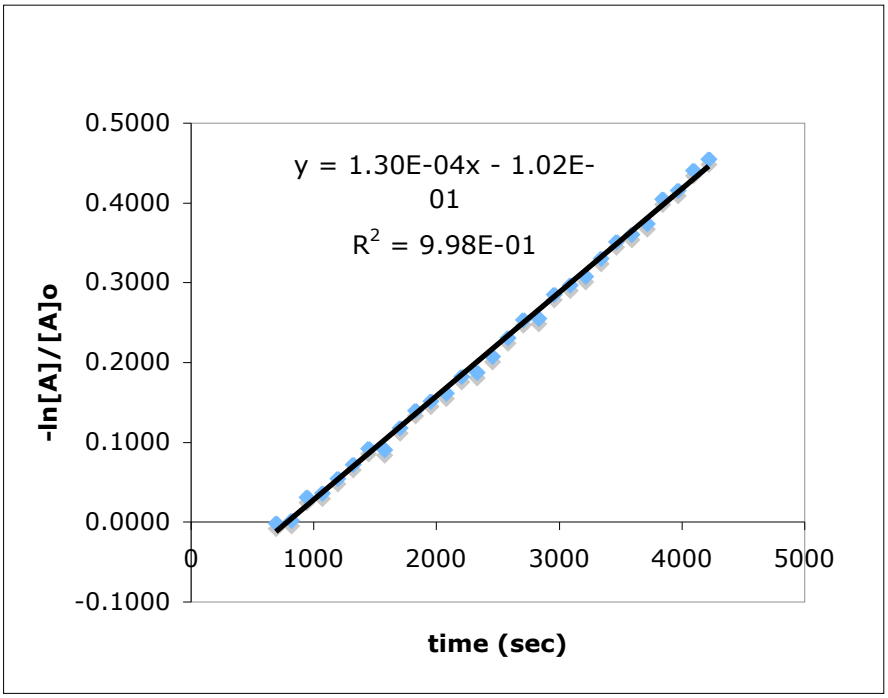

Figure 2.6.10.2 Representative Kinetics Data for Carboxylate Exchange at 7 with AgOTf

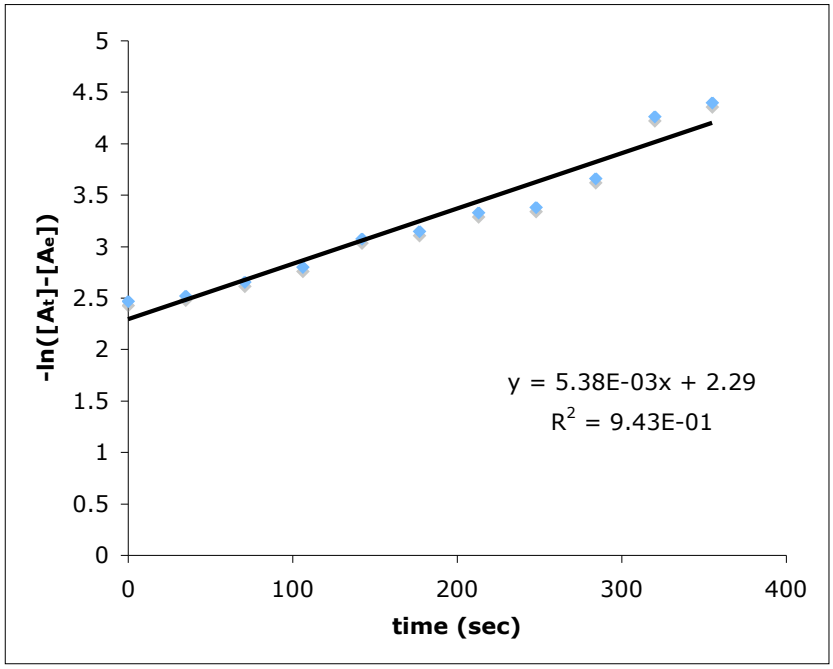

2.6.11 General Procedure for Studies of Arylpyridine Electronics

Scheme 2.6.11.1 Study of Arylpyridine Electronics

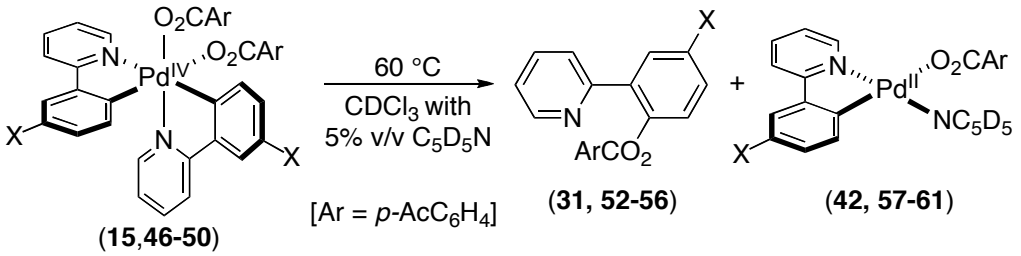

The Pd^{IV} complex (0.0076 mmol) was dissolved in $CDCl_3$ containing 5% by volume pyridine-d_5 (0.5 mL) in a screw cap NMR tube in a N_2-filled drybox. The tube was sealed with a Teflon-lined cap and removed from the drybox. The kinetics of carboxylate exchange were studied by ^1H NMR spectroscopy at 60 ºC by monitoring the disappearance of the most downfield resonance and the most upfield aromatic resonance of each complex. The rates of disappearance from these peaks were averaged. The data are summarized in Table 2.6.11.1. The data was fitted to a Hammett Plot with σ_{para} but only gave a moderate R squared value.

Table 2.6.11.1 Data for Hammett Plot of Arylpyridine Electronics

Compound	k_{obs} (s^{-1} x 10^5)	σ_{para}
*OMe	3.08	–0.27
Me	4.81	–0.14
H	20.0	0.00
F	3.64	0.15
Cl	36.9	0.24
*CF_3	323	1.4

* These complexes were studied but clean samples were not obtained.

Figure 2.6.11.1 Hammett Plot with σ_{para}

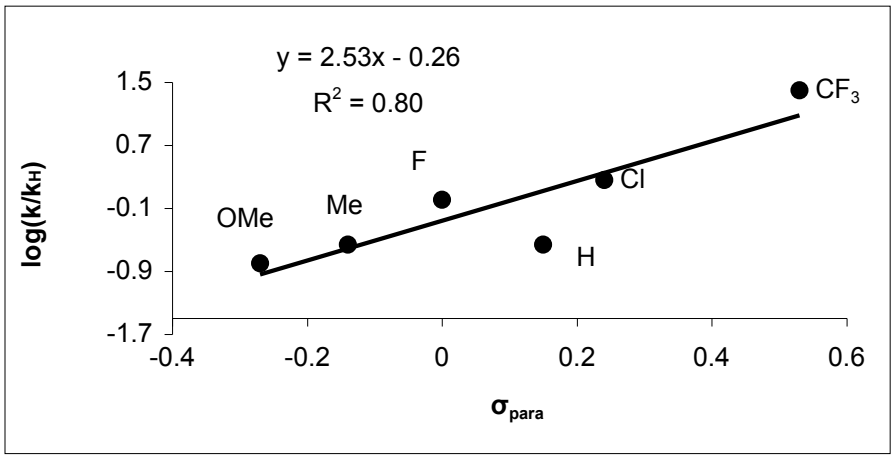

2.6.12 General Procedure for Rigidity Kinetics and C-O vs. C-C Product Formation

Scheme 2.6.12.1 Study of Arylpyridine Electronics

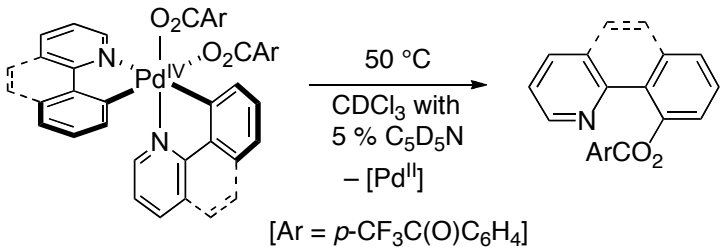

Effect of Ligand Rigidity on Rate of Reductive Elimination. The Pd^{IV} complex (0.0076 mmol) was dissolved in $CDCl_3$ containing 5% by volume pyridine-d_5 (0.5 mL) in a screw cap NMR tube in a N_2-filled drybox. The tube was sealed with a Teflon-lined cap and removed from the drybox. The kinetics of reductive elimination was studied by ^1H NMR spectroscopy at 50 ºC by monitoring the disappearance of the most downfield resonance associated with each Pd^{IV} complex. Two trials were run and the rates of disappearance from the runs were averaged. The data are summarized in Table S6.

Table 2.6.12.1 Data for Ligand Rigidity Kinetics

Substrate	k_{obs} (s^{-1} x 10^5)	k_{rel}
62	1.96 ± 0.1	1.9
63	1.06 ± 0.1	1.0
64	N/A	~0.1*

***** The slow reaction rate along with competing C–C bond-formation prevented quantitative rate measurement in this system.

2.6.13 Competing C–C and C–O Bond-Forming Reductive Elimination

Observation of Competing C–O and C–C Bond-Forming Reductive Elimination from 64. Complex **64** (0.0076 mmol) was dissolved in $CHCl_3$ containing 5% by volume pyridine (0.5 mL) in a 4 mL vial in a drybox. The vial was sealed with a Teflon-lined cap, removed from the drybox, and heated at 50 ºC for 4 d. The solvent was removed under vacuum, and the resulting residue was taken up in CH_2Cl_2 (1 mL) and filtered through a plug containing 25% poly-4-vinylpyridine and 75% Celite. The plug was washed with CH_2Cl_2 (10 mL), the solvent was removed under vacuum, and the reaction was analyzed by ^1H NMR spectroscopy in $CDCl_3$. The ratio of C–O to C–C products for reductive elimination from **64** was determined by integration of signals at 8.54 ppm for **65** (C–O) and at 7.74 ppm for **66** (C–C). The results listed below represent the average of two trials.

Table 2.6.13.1 Competing C–O and C–C Bond-Forming Reductive Elimination from 64

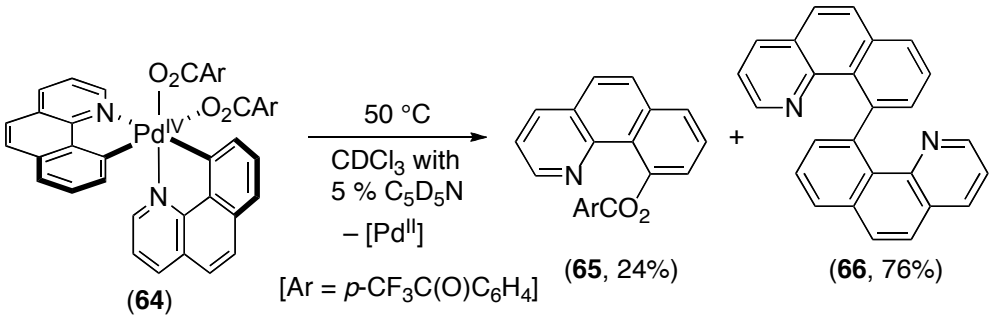

Complex	yield 65 : yield 66
64	24% : 76%

average of two trials

2.6.14 Effect of Solvent on the Ratio of C–C versus C–O Bond-Forming Reductive Elimination

Complex **67** (6.1 mg, 0.0076 mmol) was dissolved in the appropriate solvent (0.5 mL) in a 4 mL vial in a drybox. The vial was sealed with a Teflon-lined cap, removed from the drybox, and heated at 80 ºC for 4 h. The solvent was removed under vacuum, and the resulting residue was taken up in CH_2Cl_2 (1 mL), and filtered through a plug containing 25% poly-4-vinylpyridine and 75% Celite. The plug was washed with CH_2Cl_2 (10 mL), the solvent was removed under vacuum, and the reaction was analyzed by ^{1}H NMR spectroscopy in acetone-d_6. The ratio of C–C to C–O products was determined by integration of signals at 8.93 ppm for **68** (C–O) and at 7.98-8.08 ppm for **66** (C–C). The results listed below represent the average of two trials.

Table 2.6.14.1 Effect of Solvent on the Product Ratio of Reductive Elimination from 67

Solvent	Ratio 66 : 68
CH_3CN	0.25 : 1.0
$CHCl_3$	0.77 : 1.0
nitrobenzene	2.2 : 1.0
DMSO	3.3 : 1.0
acetone	13 : 1.0
benzene	> 20 : 1

* average of two trials

2.6.15 Effect of Carboxylate on the Ratio of C–C versus C–O Bond-Forming Reductive Elimination

Scheme 2.6.15.1 Effect of Carboxylate on the Ratio of C–C versus C–O Bond-Forming Reductive Elimination from 69

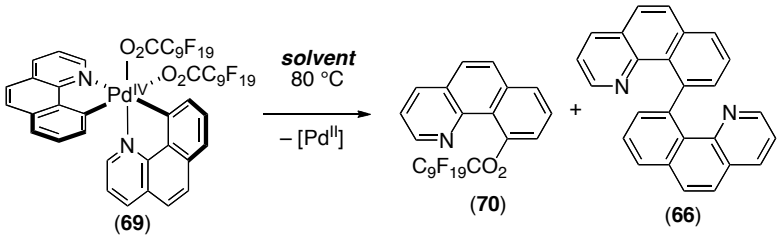

Complex **69** (11.3 mg, 0.0076 mmol) was dissolved in the appropriate solvent (0.5 mL) in a 4 mL vial in a drybox. The vial was sealed with a Teflon-lined cap, removed from the drybox, and heated at 80 ºC for 8 d. The solvent was removed under vacuum, and the resulting residue was taken up in CH_2Cl_2 (1 mL), and filtered through a plug containing 25% poly-4-vinylpyridine and 75% Celite. The plug was washed with CH_2Cl_2 (10 mL), the solvent was removed under vacuum, and the reaction was analyzed by ^1H NMR spectroscopy in acetone-d_6. In all cases, the sole product observed was **66** (C–C).

Table 2.6.15.1 Solvent Effects on Product Distribution of Reductive Elimination from Complex 69

Solvent	Product
pyridine-d_5	**66**
acetone-d_6	**66**
DMSO-d_6	**66**
CD_3CN	**66**

2.6.16 Effect of Additives on the Relative Rates of C–C versus C–O Bond-Forming Reductive Elimination

Additive = AcOH. Complex **67** (6.1 mg, 0.0076 mmol, 1.0 equiv) was dissolved in acetone (0.5 mL) in a 4 mL vial in a drybox. AcOH (2.2 μL, 0.038 mmol, 5 equiv) was added, and then the vial was sealed with a Teflon-lined cap, removed from the drybox, and heated at 80 ºC for 3 h. The solvent was removed under vacuum, and the resulting residue was taken up in CH_2Cl_2 (1 mL), and filtered through a plug containing 25% poly-4-vinylpyridine and 75% Celite. The plug was washed with CH_2Cl_2 (10 mL), the solvent was removed under vacuum, and the reaction was analyzed by ^{1}H NMR spectroscopy in acetone-d_6. The ratio of C–C to C–O products was determined by integration of signals at 8.93 ppm for **68** (C–O) and at 7.98-8.08 ppm for **66** (C–C). The results listed below represent the average of two trials.

Additive = AgOTf. AgOTf was transferred to a 4 mL vial as a stock solution in THF (15.5 μL of a 50 mM stock solution, 0.20 mg, 0.00078 mmol, 0.1 equiv). The THF was removed under vacuum and then this vial was taken into the glove box. Complex **67** (6.1 mg, 0.0076 mmol, 1.0 equiv) and acetone were added to the vial, which was then sealed with a Teflon-lined cap, removed from the drybox, and heated at 80 ºC for 3 h. The solvent was removed under vacuum, and the resulting residue was taken up in CH_2Cl_2 (1 mL), and filtered through a plug containing 25% poly-4-vinylpyridine and 75% Celite. The plug was washed with CH_2Cl_2 (10 mL), the solvent was removed under vacuum, and the reaction was analyzed by ^{1}H NMR spectroscopy in acetone-d_6. The ratio of C–C to C–O products was determined by integration of signals at 8.93 ppm for **68** (C–O) and at 7.98-8.08 ppm for **66** (C–C). The results shown in Table S10 represent the average of two trials.

Table 2.6.16.1 Effect of Acidic Additives on the Product Ratio of Reductive Elimination from 67

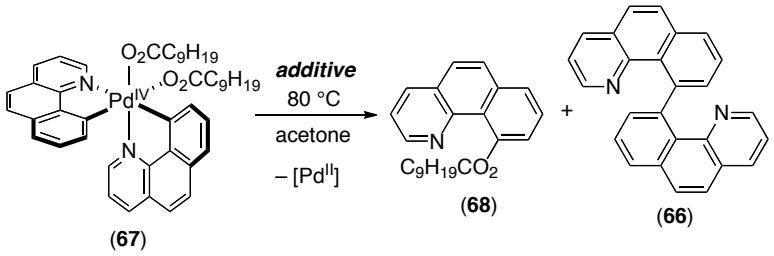

Entry	Additive	Ratio 66 : 68
1	none	13 : 1
2	AcOH (5.0 equiv)	3.6 : 1
3	AgOTf (0.1 equiv)	0.10 : 1

* average of two trials

Additive = NBu_4X. Complex **67** (6.1 mg, 0.0076 mmol, 1.0 equiv) was dissolved in CH_3CN (0.5 mL) in a 4 mL vial in a drybox. BuN_4X (0.0076 mmol, 1.0 equiv) was added. The vial was sealed with a Teflon-lined cap, removed from the drybox, and heated at 80 ºC for 3 h. The solvent was removed under vacuum, and the resulting residue was taken up in CH_2Cl_2 (1 mL), and filtered through a plug containing 25% poly-4-vinylpyridine and 75% Celite. The plug was washed with CH_2Cl_2 (10 mL), the solvent was removed under vacuum, and the reaction was analyzed by ^{1}H NMR spectroscopy in acetone-d_6. The ratio of C–C to C–O products was determined by integration of signals at 8.93 ppm for **68** (C–O) and at 7.98-8.08 ppm for **66** (C–C). The results listed in Table S11 represent the average of two trials.

Table 2.6.16.2 Effect of $NBu_4(O_2CC_9H_{19})$ on the Product Distribution for Reductive Elimination from 67

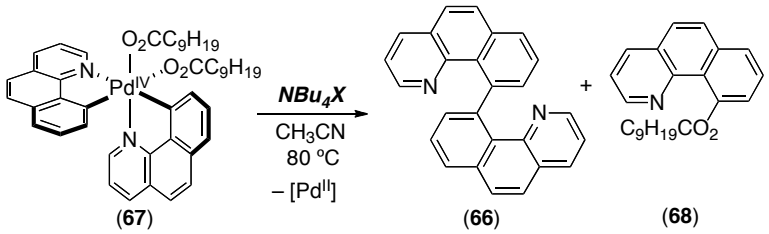

Entry	Additive	Ratio 66 : 68
1	none	0.2 : 1
2	$Bu_4N(O_2CC_9H_{19})$	2 : 1
3	$Bu_4N(PF_6)$	0.2 : 1

* average of two trials

2.6.17 Study of the Reductive Elimination from 71 with $AgBF_4$

Scheme 2.6.17.1 Reductive Elimination from 74 in Acetone

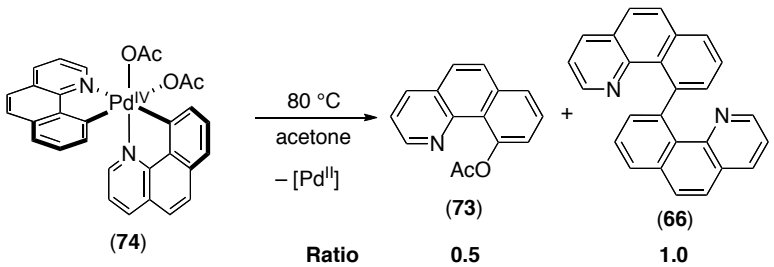

Scheme 2.6.17.2 Reductive Elimination from 71 in Acetone

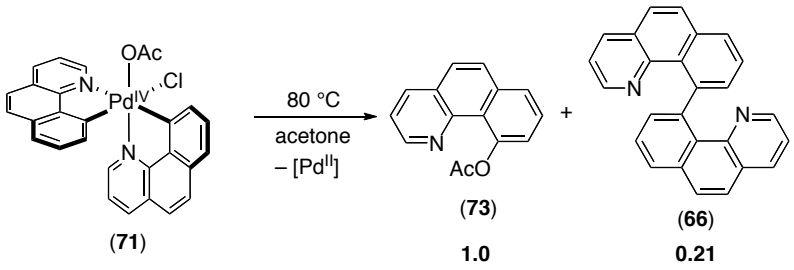

(**71**) (**73**) (**66**)

1.0 **0.21**

Scheme 2.6.17.3 Reductive Elimination from 71 with $AgBF_4$ in Acetone

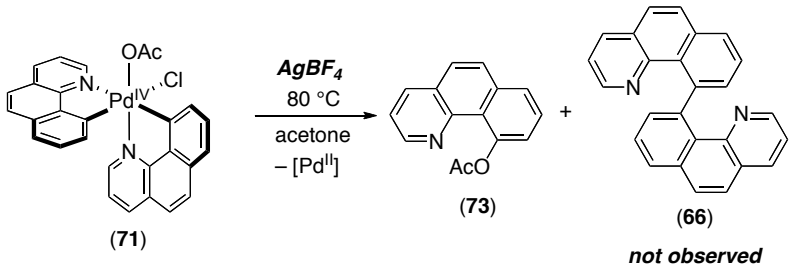

(**71**) (**73**) (**66**)

not observed

Complex **71** (4.2 mg, 0.0076 mmol, 1.0 equiv) or complex **74** (4.4 mg, 0.0076 mmol, 1.0 equiv) was dissolved in acetone (0.5 mL) in a 4 mL vial. The vial was sealed with a Teflon-lined cap and heated at 80 ºC for 3 h. The solvent was removed under vacuum, and the resulting residue was taken up in CH_2Cl_2 (1 mL), and filtered through a plug containing 25% poly-4-vinylpyridine and 75% Celite. The plug was washed with CH_2Cl_2 (10 mL), the solvent was removed under vacuum, and the reaction was analyzed by ^1H NMR spectroscopy in $CDCl_3$. The ratio of C–C to C–O products was determined by integration of signals at 7.61 ppm for **68** (C–O) and at 7.98-8.08 ppm for **66** (C–C). The

hydrolysis product was observed in varying quantities after workup, when this was the case the integral at 8.84 ppm (for the OH product) was added to the peak for product **68**. The ratios listed represent the average of two trials.

Complex **73** (4.2 mg, 0.0076 mmol, 1.0 equiv) was dissolved in acetone (0.5 mL) in a 4 mL vial. $AgBF_4$ (1.5 mg, 0.0076 mmol, 1.0 equiv) was added to the vial and then, was sealed with a Teflon-lined cap and heated at 80 ºC for 3 h. The solvent was removed under vacuum, and the resulting residue was taken up in CH_2Cl_2 (1 mL), and filtered through a plug containing 25% poly-4-vinylpyridine and 75% Celite. The plug was washed with CH_2Cl_2 (10 mL), the solvent was removed under vacuum, and the reaction was analyzed by ^1H NMR spectroscopy in $CDCl_3$. The ratio of C–C to C–O products was determined by integration of signals at 7.61 ppm for **68** (C–O) and at 7.98-8.08 ppm for **66** (C–C). The hydrolysis product was observed in varying quantities after workup, when this was the case the integral at 8.84 ppm (for the OH product) was added to the peak for product **68**. The ratios listed represent the average of two trials.

2.6.18 Observation of C–C Bond-Forming Reductive Elimination at Phenylpyridine Complex 16

Scheme 2.6.18.1 C–C Bond-Forming Reductive Elimination at Phenylpyridine Complex 16

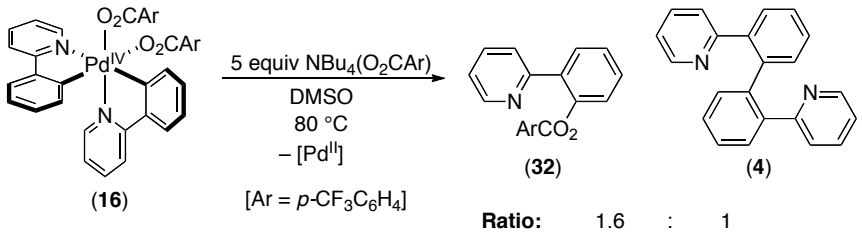

Complex **16** (6.8 mg, 0.0080 mmol, 1.0 equiv) was dissolved in DMSO (0.5 mL) in a 4 mL vial in a drybox. $Bu_4N(O_2C(p\text{-}CF_3C_6H_4))$ (19 mg, 0.039, 5.0 equiv) was added. The vial was sealed with a Teflon-lined cap, removed from the drybox, and heated at 80 ºC for 5 h. The solvent was removed under vacuum, and the resulting residue was taken up in CH_2Cl_2 (2 mL), and filtered through a plug containing 25% poly-4-vinylpyridine and 75% Celite. The plug was washed with CH_2Cl_2 (12 mL), the solvent was removed under vacuum, and the reaction was analyzed by ^1H NMR spectroscopy in acetone-d_6. The ratio of C–C to C–O products was determined by integration of signals at 8.48 ppm for **32** (C–O) and at 8.36 ppm for **4** (C–C). The results listed below represent the average of two trials.

Table 2.6.18.1 Data for C-C vs. C-O Product Formation with Additive

Trial	Ratio 32 : 4
Additive	1.0 : 1.6
No Additive	0.0 : 1.0

* average of two trials

2.7 References and Footnotes

1. For directed C–H bond acetoxylation with $ArI(OAc)_2$, see: a) Dick, A. R.; Hull, K. L.; Sanford, M. S. *J. Am. Chem. Soc.* **2004***, 126*, 2300. b) Desai, L. V.; Hull, K. L.; Sanford, M. S. *J. Am. Chem. Soc.* **2004***, 126*, 9542. c) Kalyani, D.; Sanford, M. S. *Org. Lett.* **2005***, 7*, 4149. d) Kalberer, E. W.; Whitfield, S. R.; Sanford, M. S. *J. Mol. Catal., A* **2006***, 251*, 108. e) Desai, L. V.; Stowers, K. J.; Sanford, M. S. *J. Am. Chem. Soc.* **2008**, *130*, 13285.

2. For examples of directed C–H bond acetoxylation with other oxidants, see: a) Giri, R.; Liang, J.; Lei, J. G.; Li, J. J.; Wang, D. H.; Chen, X.; Naggar, I. C.; Guo, C.; Foxman, B. M.; Yu, J. Q. *Angew. Chem., Int. Ed.* **2005**, *44*, 7420. b) Desai, L. V.; Malik, H. A.; Sanford, M. S. *Org. Lett.* **2006***, 8*, 1141. c) Reddy, B. V. S.; Reddy, L. R.; Corey, E. J. *Org. Lett.* **2006**, *8*, 3391. d) Wang, G. W.; Yuan, T. T.; Wu, X. L. *J. Org. Chem.* **2008**, *73*, 4717.

3. For examples of other $Pd^{II/IV}$-catalyzed acetoxylation reactions using $PhI(OAc)_2$, see: a) Alexanian, E. J.; Lee, C.; Sorensen, E. J. *J. Am. Chem. Soc.* **2005**, *127*, 7690. b) Liu, G.; Stahl, S. S. *J. Am. Chem. Soc.* **2006**, *128*, 7179. c) Desai, L. V.; Sanford, M. S. *Angew. Chem., Int. Ed.* **2007**, *46*, 5737. d) Li, Y.; Song, D.; Dong, V. M. *J. Am. Chem. Soc.* **2008**, *130*, 2962.

4. A related mechanism was also proposed for the $Pd(OAc)_2$-catalyzed acetoxylation of benzene with $PhI(OAc)_2$. See: Yoneyama, T.; Crabtree, R. H. *J. Mol. Catal. A* **1996**, *108*, 35.

5. a) Matsunaga, P. T.; Hillhouse, G. K. *J. Am. Chem. Soc.* **1993**, *115*, 2075. b) Matsunaga, P. T.; Mavropoulos, J. C.; Hillhouse, G. K. *Polyhedron* **1995**, *14*, 175. c) Han, R.; Hillhouse, G. L. *J. Am. Chem. Soc.* **1997**, *119*, 8135. d) Koo, K.; Hillhouse, G. L. *Organometallics* **1998**, *17*, 2924.

6. a) Komiya, S.; Akai, Y.; Yamamoto, T.; Yamamoto, A. *Organometallics* **1985**, *4*, 1130. b) Mann, G.; Hartwig, J. F. *J. Am. Chem. Soc.* **1996**, *118*, 13109. c)

Widenhoefer, R. A.; Zhong, H. A.; Buchwald, S. L. *J. Am. Chem. Soc.* **1997**, *119*, 6787. d) Widenhoefer, R. A.; Buchwald, S. L. *J. Am. Chem. Soc.* **1998**, *120*, 6504. e) Mann, G.; Incarvito, A. L.; Rheingold, A. L.; Hartwig, J. F. *J. Am. Chem. Soc.* **1999**, *121*, 3224. f) Shelby, Q.; Katoaka, N.; Mann, G.; Hartwig, J. F. *J. Am. Chem. Soc.* **2000**, *122*, 10718. g) Mann, G.; Shelby, Q.; Roy, A. H.; Hartwig, J. F. *Organometallics* **2003**, *22*, 2775. h) Stambuli, J. P.; Weng, Z.; Incarvito, C. D.; Hartwig, J. F. *Angew. Chem., Int. Ed.* **2007**, *46*, 7674.

7. a) Williams, B. S.; Holland, A. W.; Goldberg, K. I. *J. Am. Chem. Soc.* **1999***, 121*, 252. b) Williams, B. S.; Goldberg, K. I. *J. Am. Chem. Soc.* **2001***, 123*, 2576. c) Vedernikov, A. N.; Binfield, S. A.; Zavalij, P. Y.; Khusnutdinova, J. R. *J. Am. Chem. Soc.* **2006**, *128*, 82. d) Khusnutdinova, J. R.; Zavalij, P. Y.; Vedernikov, A. N. *Organometallics* **2007**, *26*, 3466. e) Khusnutdinova, J. R.; Newman, L. L.; Zavalij, P. Y.; Lam, Y.-F.; Vedernikov, A. N. *J. Am. Chem. Soc.* **2008**, *130*, 2174. f) Smythe, N. A.; Grice, K. A.; Williams, B. S.; Goldberg, K. I. *Organometallics* **2009***, 28*, 277.

8. a) Canty, A. J.; Traill, P. R.; Skelton, B. W.; White, A. H. *J. Organomet. Chem.* **1992**, *433*, 213. b) Canty, A. J.; Jin, H.; Roberts, A. S.; Skelton, B. W.; White, A. H. *Organometallics* **1996***, 15*, 5713. c) Yamamoto, Y.; Ohno, T.; Itoh, K. *Angew. Chem., Int. Ed.* **2002***, 41*, 3662. d) Yamamoto, Y.; Kuwabara, S.; Matsuo, S.; Ohno, T.; Nishiyama, H.; Itoh, K. *Organometallics* **2004***, 23*, 389.

9. For examples where Pd^{IV} complexes containing O-donor ligands were detected at low temperature, see: a) Canty A. J.; Jin, H. *J. Organomet. Chem.* **1998**, *565*, 135. b) Canty, A. J.; Jin, H.; Skelton, B. W.; White, A. H. *Inorg. Chem.* **1998**, *37*, 3975. c) Canty, A. J.; Done, M. C.; Skelton, B. W.; White, A. H. *Inorg. Chem. Commun.* **2001**, *4*, 648. d) Canty, A. J.; Denney, M. C.; Skelton, B. W.; White, A. H. *Organometallics* **2004**, *23*, 1122.

10. For examples of rigid bidentate ligands stabilizing Pd^{IV} complexes, see: a) Canty, A. J. *Acc. Chem. Res.* **1992**, *25*, 83. b) van Asselt, R.; Rijnberg, E.; Elsevier, C. J. *Organometallics* **1994**, *13*, 706. c) Canty, A J.; van Koten, G. *Acc.*

Chem. Res. **1995**, *28*, 406. d) Suginome, M.; Kato, Y.; Takeda, N.; Oike, H.; Ito, Y. *Organometallics* **1998***, 17*, 495. e) Campora, J.; Palma, P.; del Rio, D.; Lopez, J. A.; Alvarez, E.; Connelly, N. G. *Organometallics* **2005***, 24*, 3624.

11. For the first example of the use of multiple strongly σ-donating alkyl ligands to stabilize a Pd^{IV} center, see: Byers, P. K.; Canty, A. J.; Skelton, B. W.; White, A. H. *J. Chem. Soc., Chem. Commun.* **1986**, 1722.

12. Dick, A. R.; Kampf, J.; Sanford, M. S. *J. Am. Chem. Soc.* **2005**, *127*, 12790.

13. For more recent reports of related Pd^{IV} complexes stabilized by cyclometalated ligands, see: a) Whitfield, S. R.; Sanford, M. S. *J. Am. Chem. Soc.* **2007**, *129*, 15142. b) Furuya, T.; Ritter, T. *J. Am. Chem. Soc.* **2008**, *130*, 10060.

14. Jolliet, P.; Gianini, M.; von Zelewsky, A.; Bernardinelli, G.; Stoeckli-Evans, H. *Inorg. Chem.* **1996***, 35*, 4883.

15. a) Goldberg, K. I.; Yan, J.; Winter, E. L. *J. Am. Chem. Soc.* **1994**, *116*, 1573. b) Goldberg, K. I.; Yan, J.; Breitung, E. M. *J. Am. Chem. Soc.* **1995**, *117*, 6889.

16. Pawlikowski, A. V.; Getty, A. D.; Goldberg, K. I. *J. Am. Chem. Soc.* **2007**, *129*, 10382.

17. Yahav-Levi, A.; Goldberg, I.; Vigalok, A.; Vedernikov, A. N. *J. Am. Chem. Soc.* **2008**, *130*, 724.

18. Driver, M. S.; Hartwig, J. F. *J. Am. Chem. Soc.* **1997***, 119*, 8232.

19. a) Baranano, D.; Hartwig, J. F. *J. Am. Chem. Soc.* **1995***, 117*, 2937. b) Mann, G.; Baranano, D.; Hartwig, J. F.; Rheingold, A. L.; Guzei, I. A. *J. Am. Chem. Soc.* **1998***, 120*, 9205.

20. a) Crumpton, D. M.; Goldberg, K. I. *J. Am. Chem. Soc.* **2000***, 122*, 962. b) Crumpton-Bregel, D. M.; Goldberg, K. I. *J. Am. Chem. Soc.* **2003***, 125*, 9442. c)

Arthur, K. L.; Wang, Q. L.; Bregel, D. M.; Smythe, N. A.; O'Neill, B. A.; Goldberg, K. I.; Moloy, K. G. *Organometallics* **2005***, 24*, 4624.

21. Stang, P. J.; Boehshar, M.; Wingert, H.; Kitamura, T. *J. Am. Chem. Soc.* **1988***, 110*, 3272.

22. Fu, J.; Li, Z.; Liang, S.; Guo, Q.; Lui, L. *Organometallics* **2008**, *27*, 3736.

23. Crabtree, R. H.; *The Organometallic Chemistry of Transition Metals*; John Wiley & Sons, Inc: Hoboken, NJ, 2005; Fourth Edition.

24. Whitfield, S. R. Ph.D. Thesis, University of Michigan, 2008.

25. These complexes were synthesized by reaction of $(Phpy)_2Pd^{IV}(Cl)(OAc)$ or $(Phpy)_2Pd^{IV}(Cl)(OAc\text{-}d_3)$ with the corresponding silver carboxylate. See Supporting Information for full details.

26. Byers, P. K.; Canty, A. J.; Crespo, M.; Puddephatt, R. J.; Scott, J. D. *Organometallics* **1988**, *7*, 1363.

27. Isaacs, N. S. *Physical Organic Chemistry, 2nd Edition*; Pearson Education: New York, 1995.

28. Initial investigations revealed that clean first order kinetics were not observed in some solvents, and we hypothesized that this might be due to initial formation of a highly reactive 3-coordinate Pd^{II} species after loss of the organic product **12**. Closely related challenges have been observed in reductive elimination reactions from Pd^{II} centers (for example, see ref. 19a) and have been resolved by the addition of external ancillary ligands, which serve to trap unsaturated intermediates. Similarly, we found that the addition of 5% of pyridine-d_5 to the reductive elimination reactions of **8** in each solvent resulted in clean first order kinetics over greater than three half-lives. Qualitative time studies showed that added pyridine had little effect on the relative rate in each of the solvents studied.

29. Carboxylate exchange in toluene progressed too slowly to measure quantitatively at –38 °C (*i.e.,* no observable exchange occurred after 6 h).

30. More investigation is needed to understand why the entropy of activation is so small in this system. See ref. 36 for a possible explanation.

31. Exner, O. Correlation Analysis of Chemical Data; Plenum Press: New York, 1988.

32. Reductive elimination reactions from $(Phpy)_2Pd^{IV}(O_2CAr)_2$ have the added complication that these complexes contain two different carboxylate ligands. If mechanism **A** were operating, these two ligands would serve two very different roles in the first step of the reaction – one would dissociate to form an anion (stabilized by electron withdrawing groups), while the other would remain bound to cationic intermediate **II** (stabilized by electron donating groups).

33. Calculations on C–O bond-forming reductive elimination reactions from **15** (ref. 22) suggested that mechanisms **A** and **B** are relatively close in energy ($\Delta G^{\ddagger}$ = 31.4 kcal/mol and 26.4 kcal/mol, respectively). In contrast, mechanism **C** was calculated to have a much larger activation energy of 44.3 kcal/mol.

34. While the observed solvent effects and activation parameters are somewhat unexpected for a system involving ionic intermediates, they may result from an unusually early or late transition state that has relatively little charge buildup.

35. Only C–O coupled products were observed in this reaction; however, both acetoxylated product **73** and the corresponding phenol (presumably formed by ester hydrolysis under the reaction conditions) were observed.

36. Jolliet, P.; Gianini, M.; von Zelewsky, A.; Bernardinelli, G.; Stoeckli-Evans, H. *Inorg. Chem.* **1996**, *35*, 4883-4888.

37. Espenson, J. H. Reversible and Concurrent Reactions. *Chemical Kinetics and Reaction Mechanisms*, Second Edition; Speer J. B., Morriss, J. M., Eds.; McGraw-Hill in Advanced Chemistry; McGraw-Hill, Inc.: New York, NY, 1995; 46-47.

Chapter 3: Investigations of Reactivity and Mechanism of sp^3 C–X Bond Forming Reductive Elimination from Pd^{IV} Complexes

3.1 Introduction

The development of new transition metal-catalyzed methods for incorporating sp^3-C–heteroatom (C–X) bonds into organic molecules is a challenging feat in organic synthesis.[1] The widespread importance of sp^3-C–X bonds in pharmaceuticals, argochemicals and commodity chemicals make novel methodology for the facile construction of these functionalities particularly interesting.[1] Over the past several years, there has been significant progress made in the development of catalytic reactions that incorporate sp^3-C–X bonds into molecules through C–H activation/functionalization manifolds.[2] Elegant methodology has been developed for the installation of sp^3-C–X bonds (C–O, C–I), while advances for the incorporation of sp^3-C–Cl, C–F and C–N bonds still remain limited.[2] These reactions are typically thought to involve high oxidation state Pd intermediates and proceed via $Pd^{II/IV}$ catalytic systems. The final step of the aforementioned $Pd^{II/IV}$ catalytic reactions hinges on reductive elimination from high oxidation state Pd as the key transformation for the product release step to generate the sp^3-C–X bonds. Scheme 3.1.1 depicts an example of a catalytic reaction that converts a sp^3-C–H (**I-1**) bond directly to a sp^3-C–OAc (**I-3**) bond via reductive elimination from a proposed Pd^{IV} intermediate (**I-2**).[3] Despite the limited reports of sp^3-C–Cl, C–F and C–N bond formation from Pd^{IV}, high oxidation state Pd catalysis remains an attractive means for constructing challenging kinds of

bonds because of the large thermodynamic driving force for the reduction of Pd^{IV} to Pd^{II}.[4]

Scheme 3.1.1 Proposed Pd^{IV} Intermediate in a Catalytic Alkane C–H Acetoxylation Reaction

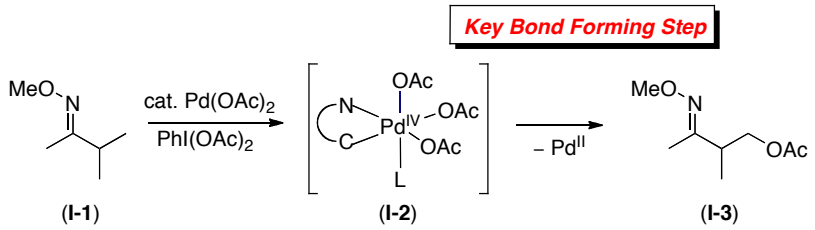

Studying reactivity directly at a Pd^{IV} center is critical to understanding how the product release occurs to afford sp^3-C–X bonds. Ultimately, knowledge of reactivity at a Pd^{IV} center that furthers the understanding of how the formation of sp^3-C–X bonds proceeds can lead to the improvement of known reactions as well as launch innovative advancement of catalytic reactions in this area.[6] Our group as well as the Ritter group have conducted extensive mechanistic investigations at monomeric Pd^{IV} and dimeric Pd^{III} for sp^2-C–O, C–Cl, C–F and C–CF_3 bond formation from characterized and observable/isolable complexes.[7,8,9] The results have provided valuable insights into how catalytic reactions might be improved or broadened. In all of these cases, reversible dissociation of a ligand from an octahedral Pd^{IV} compound (**I-4**) to generate a five coordinate Pd^{IV} species (**I-5**) preceded bond-forming reductive elimination to afford either sp^2-C–O_2CR, C–F or C–CF_3 bonds (**I-6**). This type of dissociative mechanism (whether of an ionic or neutral ligand) was favored over a concerted reductive elimination from a coordinately saturated Pd^{IV} complex (Scheme 3.1.2).

Scheme 3.1.2 General Depiction of Proposed Mechanisms for sp^2-C–O_2CR, C–F and C–CF_3 Reductive Elimination from Observable Pd^{IV} Complexes

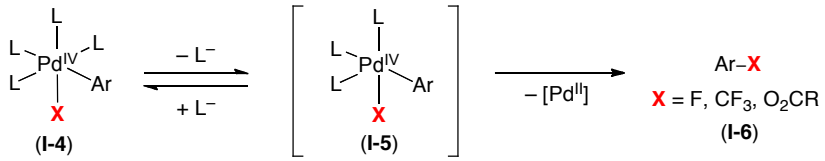

However, while many advances have been made in the development of Pd^{IV} systems to study sp^2-C–X reductive elimination, there have not been rigorous mechanistic studies of analogous sp^3-C–X bond formation from Pd^{IV}.[10] There are several distinct mechanistic questions to be addressed in this area that could impact the advancement of catalytic $Pd^{II/IV}$ catalysis. For instance, if a dissociative mechanism is at play, sp^3-C–X bond formation from Pd^{IV} could potentially proceed via two different pathways. As depicted in Scheme 4.1.3, after a pre-equilibrium dissociation occurred to generate a five coordinate intermediate (**I-8**), reductive elimination from this species might occur through a concerted reductive elimination (**I**) or, alternatively, by an S_N2 type attack (**II**) of X^- on the σ-alkyl ligand. Pathway (**II**) for sp^3-C–X bond formation differs from the possible reaction routes for sp^2-C–X bond formation. Typically, S_N2 mechanisms are not thought to be feasible for sp^2-C–X reductive elimination because there are not available orbitals for the nucleophile to participate in backside attack.[11] If pathway **(II**) were operative for sp^3-C–X reductive elimination, it would be particularly intriguing to probe if an external nucleophile could be used to install a functional group into the product instead of being constrained to the functionality derived from the oxidant. Therefore, understanding the mechanism of sp^3-C–X reductive elimination reactions might allow for cheaper/alternative oxidants and reagents to be considered for catalytic reactions.

Scheme 3.1.3 Possible Pathways for sp^3-C–X Bond Formation via a Dissociative Mechanism

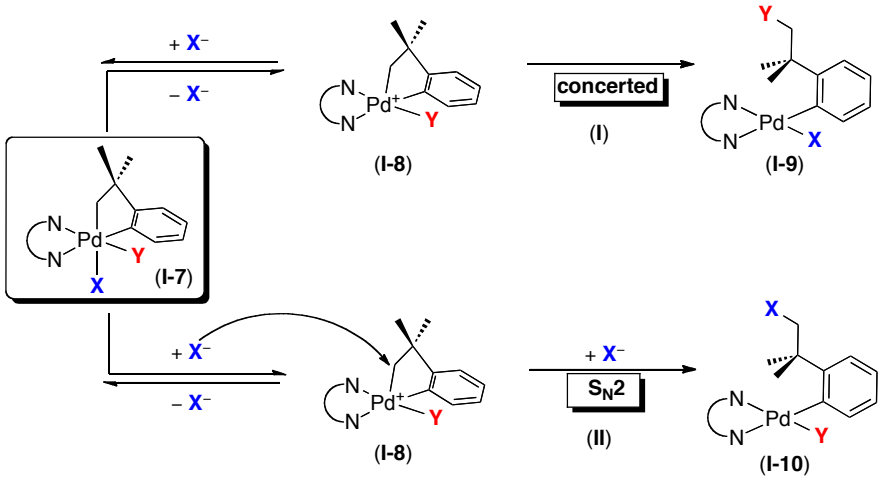

Secondly, it would be appealing to explore the competition between sp^2 versus sp^3-C–X reductive elimination from Pd^{IV} complexes. If one could develop a stoichiometric system to allow for this competition to take place for a variety of C–X reductive elimination reactions, this might allow for predictions of reactivity in catalytic reactions. In 2004 studies by Canty examined C–Se bond formation from the mixed alkyl/aryl Pd^{IV} complex (bpy)$Pd^{IV}(CH_3)(p\text{-}CH_3OC_6H_4)(p\text{-}ClC_6H_4Se)_2$ (**I-11**).[12] Complex **I-11** allowed for direct comparison of the relative rates of sp^2 versus sp^3 C–Se coupling. As shown in Scheme 3.1.4, only CH_3–Se(p-ClC_6H_4) (**I-12**) was detected, demonstrating that sp^3-C–Se coupling is considerably faster in this system. Canty's result, however, is in contrast to what has been observed for reductive elimination reactions from Pd^{II}, which typically exhibit significantly faster aryl–X reductive elimination compared to alkyl–X bond formation.[35] Thus, it would be useful to identify other sp^2/sp^3-C–X systems that would allow us to further explore if a preference for sp^3-C–X over sp^2-C–X coupling is a general attribute of Pd^{IV}.

Scheme 3.1.4 Study of Competitive sp^3 versus sp^2-C–Se Bond Formation from Palladium^{IV} by Canty

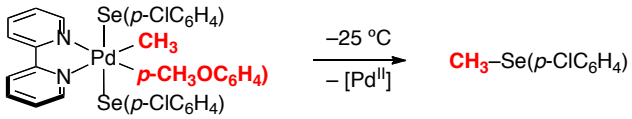

(**I-11**) (**I-12**)

For the decision of what type of complex might satisfy the desired design criteria for the observation and study of sp^3-C–X bond formation from Pd^{IV}, we examined the types of sp^3-C–X reductive elimination reactions have been observed from Pd^{IV} complexes previously. In the literature there are limited examples of sp^3-C–X bond formation (C–I, C–Cl, C–S and C–Se) from observable Pd^{IV} complexes, and most proceed in low yield.[10] For example, in 1994 Elsevier reported CH_3–I formation from (*p*-Tol-BIAN)$Pd^{IV}(CH_3)_3I$ (*p*-Tol-BIAN= bis(*p*-tolylimino)acenaphthene) at 20 ºC in 15 % yield.[13] The major product in this system was ethane, resulting from C–C coupling (80-90%). Canty also reported C–I reductive elimination from (bpy)$Pd^{IV}(C_4H_8)(CH_2CH_3)I$ to generate iodohexane in low yield (9%).[14] Most recently, Canty and coworkers demonstrated that the oxidation of (bpy)$Pd^{II}(CH_3)_2$ (**I-13**) with I_2 at –50 ºC in acetone-d_6 affords the diorgano Pd^{IV} complex (bpy)$Pd^{IV}(I)_2(CH_3)_2$ (**I-14**).[15] This species was too unstable to isolate, and, upon warming to –10 ºC, it underwent clean and highly selective C–I bond-forming reductive elimination to generate CH_3I (**I-16**) and (bpy)$Pd^{II}(CH_3)(I)$ (**I-15**) (Scheme 3.1.5). Additionally, Canty also reported an example of sp^3-C–Se and also C–S bond formation from $TpPd^{IV}(CH_3)_2(SePh)$ (Tp = tris(pyrazol-1-yl)borate). The corresponding thiophenolate was also synthesized and underwent reductive elimination to afford CH_3-SePh (40%) and CH_3-SPh (52%).[16] Lastly, Vincente reported the only example of sp^3-C–Cl bond formation, which was from a bimetallic Pd^{IV}-Pd^{IV} species at –25 ºC.[17]

Scheme 3.1.5 Reported Example sp^3 C–I Reductive Elimination from Pd^{IV}

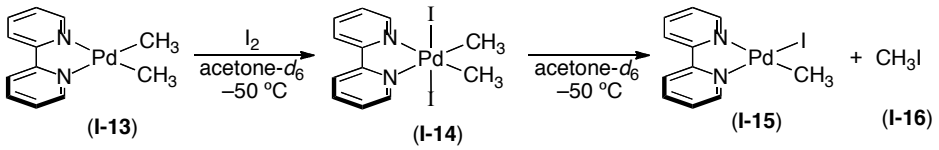

(**I-13**) (**I-14**) (**I-15**) (**I-16**)

Target Complex. This chapter aims to identify isolable/observable complexes that react to afford various types of sp^3-C–X bonds via reductive elimination. Ideally, these reactions should proceed cleanly so that their mechanism maybe investigated. Lastly, it would be interesting to identify a system to directly compare sp^3 versus sp^2 reductive elimination from Pd^{IV}. A common feature of the aforementioned known complexes by Canty and Elsevier that yield sp^3-C–I, C–S and C–Se reductive elimination is that they contain a N~N bidentante or N~N~N tridentante ligand to stabilize the Pd^{IV} complexes. Therefore, we hypothesized that either 2,2'-bipyridine (bpy) or 2,2'-bis(4-*tert*-butylbipyridine (dtbpy) ligand would be effective supporting ligands for our target complex. We began studies with the Pd^{II} precursor used by Carmona and co-workers (**I-18**). However, instead of replacing COD (1,5-cyclooctadiene) with the Tp ligand, we utilized an N~N bidentante ligand (**I-19**, **I-20**) (Scheme 3.1.6). Importantly, compound **I-18** is easily accessible via the reaction of $(COD)Pd^{II}Cl_2$ with the commercial Grignard reagent $C_6H_4C(CH_3)_2CH_2MgCl$.

Scheme 3.1.6 Pd^{II} Starting Material Inspired by Carmona Synthesis

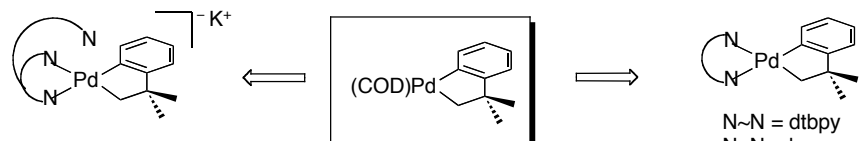

N~N~N = $[HB(C_3N_2H_3)_3]$ (**I-17**) (**I-18**) (**I-19, I-20**)

The following Sections (3.2–3.7) describe the reactivity of Pd^{IV} complexes derived from **I-19** and **I-20** (Scheme 3.1.7). These undergo selective sp^3-C–F, C–N, C–O_2CR, C–Cl and C–C bond-forming reductive elimination. Also, this work reports the first detailed mechanistic studies of sp^3-C–X bond formation from Pd^{IV}.

Scheme 3.1.7 Proposed Oxidation of I-19, I-20

(I-19, I-20) (I-21)

3.2 Study of sp^3 C–F Bond Forming Reductive Elimination from Pd^{IV}

Introduction. The development of transition-metal catalyzed reactions for C–F bond formation has been an area of intense research over the past decade.[18] Traditionally, the C–F coupling step of these sequences has proven challenging due to the high kinetic barrier for C–F bond-forming reductive elimination from most transition metal centers.[19] The approach in the Sanford laboratory to address this has been through the use of Pd^{II} catalysts in conjunction with F^+-based oxidants. As shown in Scheme 3.2.1, we were able to fluorinate 8-methylquinoline at the benzylic position with 10 mol % of $Pd(OAc)_2$ and *N*-fluoro-2,4,6-trimethylpyridinium tetrafluoroborate (NFTPB). Since 2006, a variety of other Pd^{II}-catalyzed reactions with F^+ reagents have been developed that introduce fluorine at both sp^2- and sp^3-carbon centers.[20-23] These transformations have been proposed to proceed via C–F bond-forming reductive elimination from transient, highly reactive Pd^{IV}(F)(alkyl/aryl) intermediates.

Scheme 3.2.1 Catalytic sp^3 C–F Functionalization

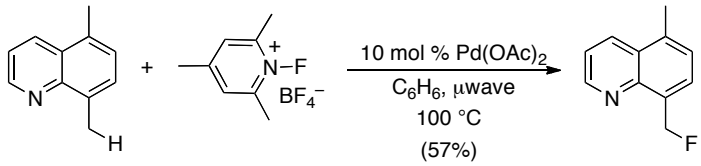

A detailed understanding of the high valent Pd intermediates involved in the key C–F bond-forming step has lagged considerably behind catalytic reaction development. In particular, the feasibility of sp^3-C–F bond formation from Pd^{IV} (a crucial step in Pd-catalyzed benzylic/alkyl C-H fluorination[21c] as well as olefin fluorination reactions)[22] has not yet been established. Several recent reports have described detailed investigations of related sp^2-C–F bond-forming reductive elimination from Pd^{IV}(F)(Aryl) complexes.[24] In addition, both Vigalok[25] and Gagne[26] have demonstrated that related Pt^{II} alkyl complexes react stoichiometrically with F^+ reagents to form alkyl fluorides. Both groups proposed sp^3-C–F bond-forming reductive elimination from a high valent Pt center as a key step; however, no intermediates were isolated in either of these transformations. Our goal was to design a system where we could access Pd^{IV} alkyl fluoride complexes and directly study their reactivity towards C–F bond-forming reductive elimination.[27] We report herein the first direct observation of this important transformation from a group 10 metal center.

Results. We targeted the cyclometalated bipyridine Pd^{II} complex **1**[28] as a precursor to stable Pd^{IV} alkyl fluoride adducts. The oxidation of **1** with *N*-fluoro-2,4,6-trimethylpyridinium triflate (NFTPT)[29] afforded the Pd^{IV} product **2** in 94% yield. The triflate ligand of **2** was highly labile and could be displaced by pyridine or water to generate the cationic products **3** and **4**, respectively (Scheme 3.2.2). The Pd^{IV} products **2-4** were all formed as a single detectable stereoisomer (as determined by ^{1}H NMR spectroscopic analysis). Notably, unlike most other palladium-fluoride complexes,[30] **2**-**4** are not sensitive to water. They were

routinely synthesized under ambient conditions and could be stored on the bench top for several hours (and in a –35 ºC freezer for several weeks) without noticeable decomposition. The fluoride ligand of **2-4** appears as a sharp doublet at –336.17 ppm (J = 15 Hz) in the ^{19}F NMR spectrum. In all cases, the fluoride is coupled to one of the α-hydrogens of the σ-alkyl ligand. The sharpness of this ^{19}F NMR signal as well as the insensitivity of the complex to adventitious moisture both suggest against interactions of the fluoride ligand with H_2O in solution. The result demonstrates that the triflate counter ion is not essential component for the stablization of these cationic Pd^{IV} complexes.

Scheme 3.2.2 Synthesis of Pd^{IV} Fluoride Complexes 2-4

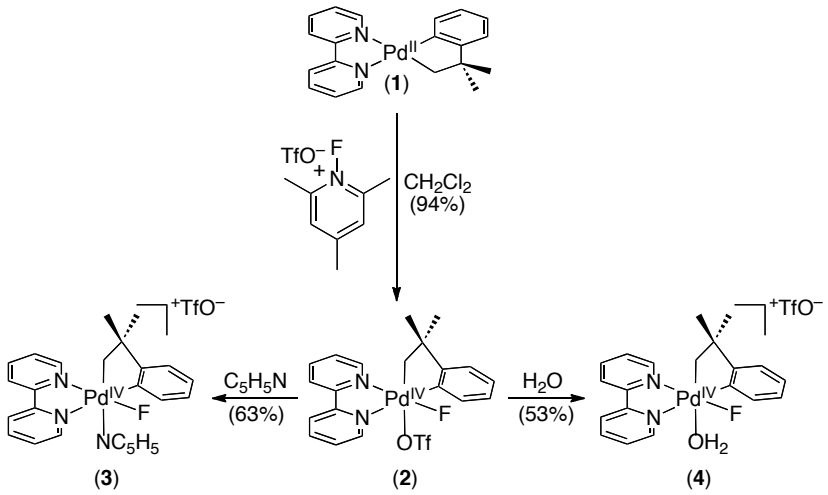

X-ray quality crystals of **4** were obtained by slow diffusion of pentane into a solution of **3** in wet acetone at –35 °C. The crystal structure of **4** shows that the σ-alkyl group of the cyclometalated ligand is *trans* to the labile H_2O ligand, while the σ-aryl and fluoride are trans to the bipyridine (Figure 3.2.1). The Pd–F bond length of complex **4** (1.979 Å) is shortened in comparison to bond lengths reported for other known Pd^{IV}–F complexes (1.983, 1.999 and 2.040 Å).[23,37] Notably, in contrast to complex **4**, these complexes display water sensitivity

suggesting a possible correlation between the reduced Pd–F bond length observed for **4** and its remarkable water stability.

Figure 3.2.1 ORTEP of Complex 4

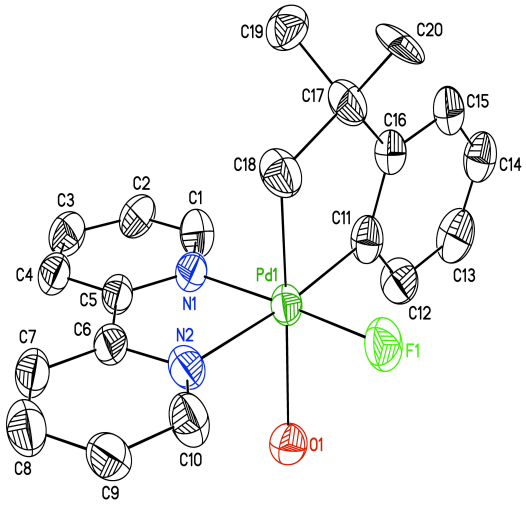

Thermal ellipsoids are drawn at 50 % probability, and hydrogen atoms are omitted for clarity. Selected bond lengths (Å): Pd–F(1) 1.979(5), Pd–C(11) 2.008(9), Pd–N(1) 2.015(7), Pd–C(18) 2.025(9), Pd–N(2) 2.151(8), Pd–O(1) 2.229(6), C(11)–C(16) 1.383(13), C(17)–C(18) 1.522(13) Selected bond angles (deg): F(1) –Pd–C(11) 85.9(3), F(1) –Pd–N(1) 175.8(3), C(11) –Pd–N(1) 98.3(3), F(1)–Pd–C(18) 89.2(3), F(1)–Pd–N(2) 96.1(2), F(1)–Pd–O(1) 90.1(2), C(11) –Pd–O(1) 100.6(3), N(1)–Pd–O(1) 89.8(2).

The triflate ligand of **2** could also be readily replaced with fluoride. For example, the treatment of **1** with NFTPT for 15 min followed by the addition of 1.6 equiv of NMe_4F afforded the difluoride complex **5** in 93% yield (Scheme 3.2.3). The ^{19}F NMR spectrum of **5** shows two distinct fluorine resonances, a doublet at –201.42 ppm and a doublet of doublets at –336.73 ppm. Complex **5** could also

be prepared in high yield by the direct reaction of Pd^{IV} triflate complex **2** with 1.6 equiv of NMe_4F.

Scheme 3.2.3 Synthesis of Pd^{IV} bis-fluoride Complex 5

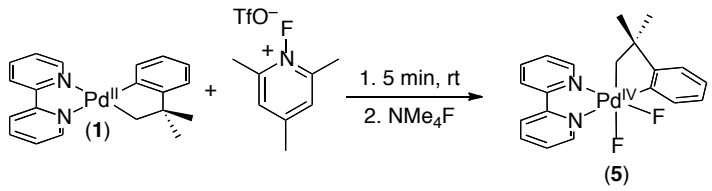

The difluoride Pd^{IV} complex **5** displayed very different properties than **2-4**. Complex **5** was extremely sensitive to water, and attempts to synthesize **5** without rigorous exclusion of moisture resulted in the formation of complex mixtures of unidentified products. Given the strong *trans* influence of the σ-alkyl ligand, the *trans*-fluoride of **5** is likely labile and highly susceptible to interactions with H_2O.

We next sought to study the reactivity of these Pd^{IV} fluoride complexes towards C–F bond-forming reductive elimination. There are several potential challenges to consider for these transformations. First, **2-5** all contain both sp^2-C and sp^3-C ligands; thus, it was not clear that selectivity could be achieved in the reductive elimination processes. Second, sp^3-C-heteroatom bond-forming reductive eliminations from Pd^{IV} generally proceed by outer-sphere mechanisms involving S_N2-type attack of a nucleophile on the sp^3-C–Pd^{IV} bond.[30] However, it is well-known in organic chemistry that fluoride is a poor nucleophile for S_N2 reactions,[31] suggesting that such a pathway might not be viable in these systems. In addition, the high degree of β-substitution at the sp^3-C–Pd bond in **2-5** was expected to further disfavor S_N2-type processes.

We were pleased to find that, despite these potential challenges, both **3** and **5** underwent clean C–F bond-forming reductive elimination at 80 ºC. Heating **3** for 30 min at 80 ºC produced **6** in 93% yield (Scheme 3.2.4 a); **3-BF_4** showed similar reactivity, forming **6**-**BF_4** in 58% yield. Similarly, **5** converted cleanly to **7**

upon heating at 80 ºC for 15 min (87%) (Scheme 3.2.4 b).[32] *These are the first directly observable examples of sp^3-C–F bond-forming reductive elimination from palladium(IV).* Remarkably, the reactions were both highly selective for sp^3-C–F coupling, and the analogous aryl fluorides **6-b** and **7-b** was not detected under any conditions examined. This is a reversal of the 'normal' selectivity of reductive elimination. For example, at Pd^{II} and most other metal centers sp^2-C ligands are typically much more reactive towards reductive elimination than their sp^3-C analogues.[34] This result highlights an important and complementary feature of Pd^{IV}-mediated fluorinations[20-22] compared to analogous transformations at Pd^{II} centers.[19]

Scheme 3.2.4 sp^3-C–F Bond-Forming Reductive Elimination from 3 and 5

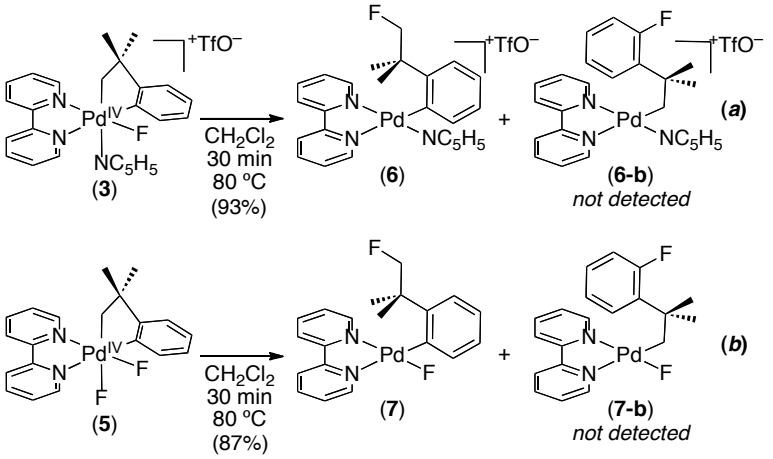

A ^{19}F NMR array for the conversion of **3-BF$_4$** to **6-BF$_4$** is shown in Figure 4.2.2. The disappearance of starting material proceeded with clean first order kinetics (k_{obs} = 3.5 x 10^{-4} s^{-1} at 45 ºC), and no intermediates were detected in this reaction. The rate of C–F bond-forming reductive elimination from **3-BF$_4$** slowed dramatically upon the addition of pyridine. For example, in the absence of added pyridine, reductive elimination was complete after 30 min at 80 ºC. In contrast,

under analogous conditions but with 50 equiv of added pyridine, no reaction was observed. A quantitative study of k_{obs} versus [pyridine] was conducted. As shown in Figure 3.2.3, an excellent linear fit was observed for a plot of k_{obs} versus $1/[C_5D_5N]$.

Figure 3.2.2 ^{19}F NMR Array Spectrum of Reductive Elimination from 3-BF_4

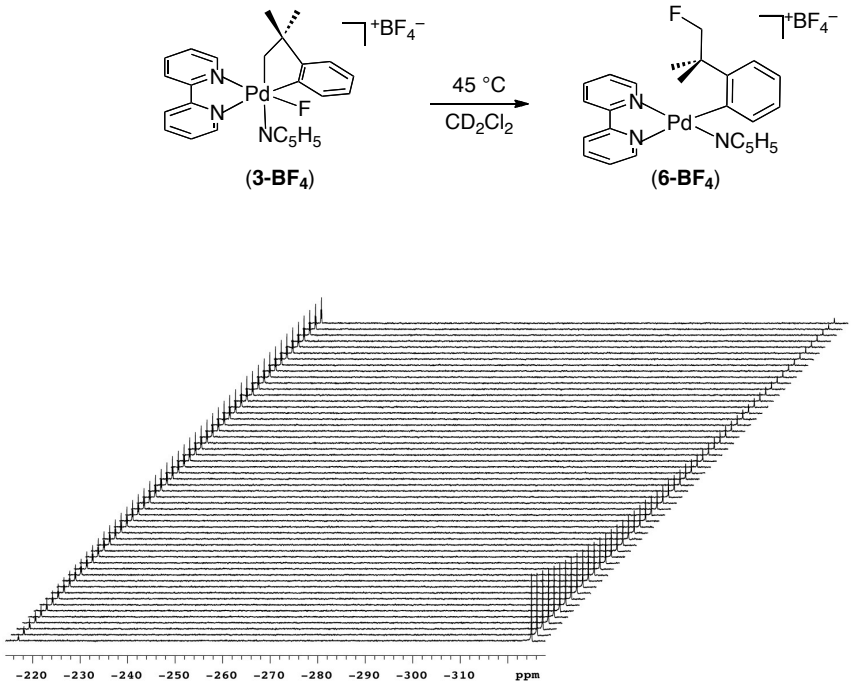

(**3-BF_4**) (**6-BF_4**)

Figure 3.2.3 Plot of k_{obs} Versus 1/[C_5D_5N] for Reductive Elimination from 3-BF_4 to Form 6-BF_4 in CD_2Cl_2 at 45 ºC. y = (5.65×10^{-7})x – 1.39×10^{-5}; R^2 = 0.979

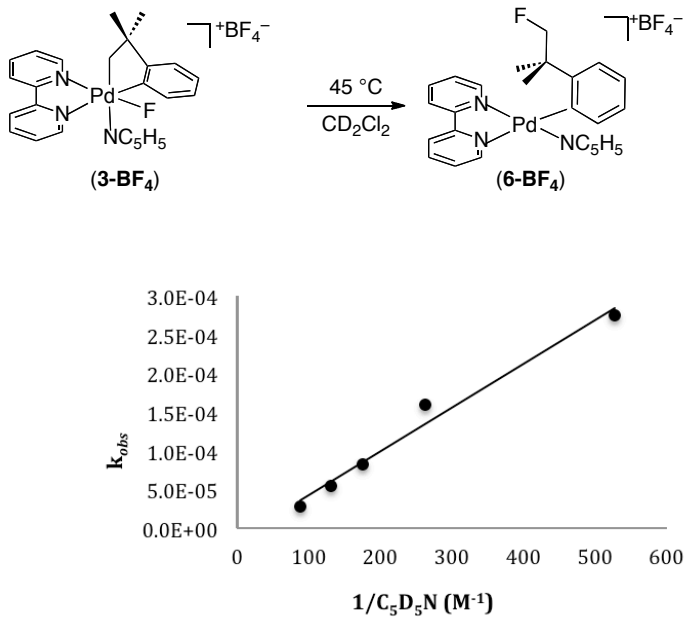

Mechanistic Discussion. On the basis of these studies, we propose that C–F bond-forming reductive elimination proceeds by the mechanism shown in Scheme 4.2.5. The inverse 1st order dependence on [pyridine] implicates dissociation of the pyridine ligand prior to the rate-determining step. Following this dissociation, C–F coupling could potentially occur either by direct reductive elimination from **8** (shown in Scheme 3.2.5, (a)) or via dissociation of fluoride from **8** to generate a Pd^{IV} dication followed by S_N2-type attack of F^- on the σ-alkyl ligand (Scheme 3.2.5, (b)). While we cannot definitively distinguish these possibilities at this time, we favor the direct reductive elimination pathway for several reasons. First, as discussed above, fluoride is generally a poor nucleophile for S_N2 reactions, and S_N2 is typically very slow in systems with high degrees of β-substitution.[32] Second, dissociation of fluoride to generate a dicationic Pd^{IV} species is expected to be highly unfavorable, particularly in the

non-polar solvent CH_2Cl_2.[35] Finally, stereochemical studies have implicated direct sp^3-C–F bond-forming reductive elimination (with retention of configuration at carbon) at related Pt^{IV} and Au^{III} centers.[26,27]

Scheme 3.2.5 Proposed reaction pathway for complex 3

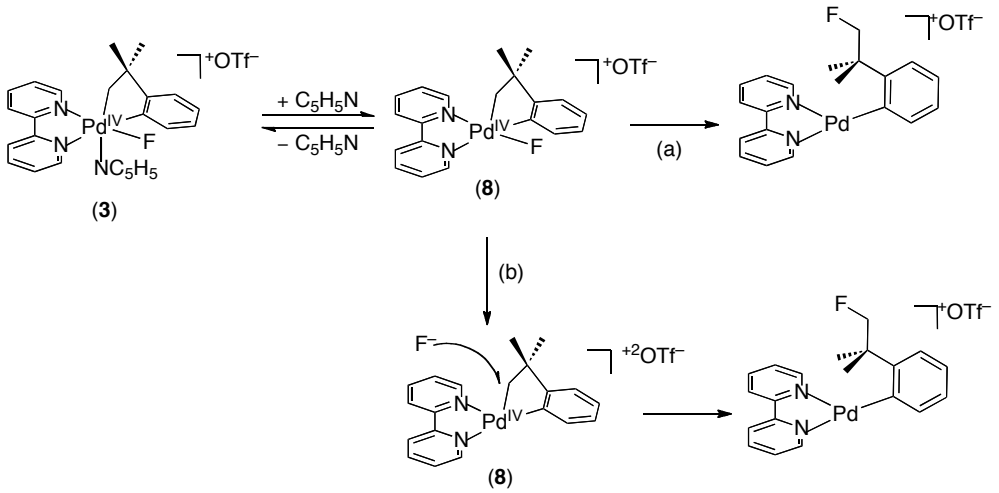

In this Section, we demonstrated the synthesis of a series of Pd^{IV} fluoride complexes, including several (**2-4**) that are remarkably insensitive to water. *Additionally, we report the first directly observable example of sp^3-C–F bond formation from a group 10 metal center.* This reaction proceeds with exquisite selectivity for sp^3-C–F bond formation despite the potential for competing sp^2-C–F coupling. Preliminary studies are consistent with a mechanism involving direct C–F bond-formation rather than S_N2-type attack on the Pd^{IV}-alkyl. We anticipate that further investigations of this and related systems will inform the development of new $Pd^{II/IV}$-catalyzed alkane/alkene fluorination processes.

3.3 Study of sp^3 C–N Bond Forming Reductive Elimination from Pd^{IV}

Introduction. As discussed in the previous section, C–F bond formation from transition metal complexes is difficult to achieve. First, fluorine is a poor nucleophile and, also, it is highly electronegative and thus, forms highly polarized bonds with Pd. Both of these attributes contribute to the attenuated ability of fluorine to undergo reductive elimination reactions.[33] Although we were able to identify conditions to promote C–F bond formation from complexes **3**, **3-BF_4** and **5**, we now sought to utilize the mitigated reactivity of the $Pd^{IV}F$ complexes to achieve sp^3-C–N bond formation, another challenging transformation.

One of the obstacles of generating C–N bonds from Pd^{IV} complexes is that there are limited accounts of oxidants that can oxidize Pd^{II} to Pd^{IV} with delivery of a nitrogen containing ligand. Although NBS (*N*-bromosuccinimide) and NCS (*N*-chlorosuccinimide) have been shown to stoichiometrically generate Pd^{IV} from Pd^{II}, incorporation of a succinimide moiety into the organic product limits the generality of the kinds of C–N bonds that can be formed through such a method.[38] The exploration of other ways for achieving C–N bonds from Pd^{IV} remains underdeveloped.

Another challenge for incorporating C–N bonds into molecules by $Pd^{II/IV}$ catalysis arises from competitive reductive elimination reactions with other nucleophiles that preferentially form C–X bonds over the desired C–N bond.[39] These other "X" type groups that compete with C–N bond formation are typically delivered to the metal center via an oxidant. Therefore, we thought that we might be able to exploit the reduced reactivity of fluorine and attain C–N bond formation by using NFTPT as an oxidant and delivering a F^- ligand, which is a poor nucleophile for reductive elimination. Yu has achieved catalytic success for intramolecular C–N amination with this strategy.[40] As shown in Scheme 3.3.1, he was able to demonstrate the use 2.0 equiv of NFTPT with phenyltriflamide (**9**) and 10 mol% of $Pd(OAc)_2$ to afford functionalized indoline (**10**) with no observation of the possible aryl fluorination products (**11**) and (**12**).

Scheme 3.3.1 Yu's Catalytic Intramolecular C–N Amination Reaction

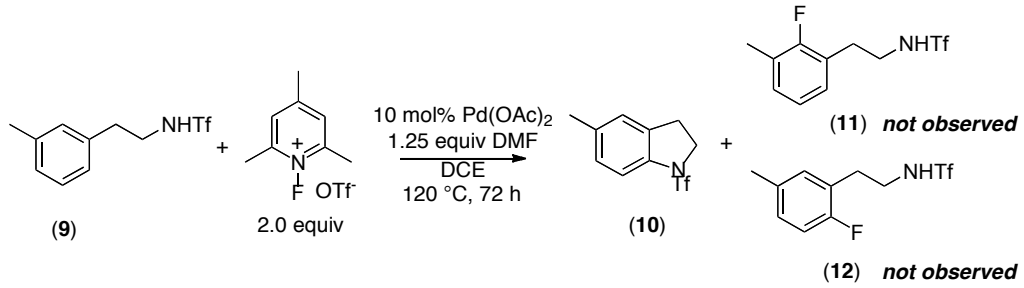

It would be useful to explore this approach directly at an isolated Pd^{IV} center so that the catalytic methodology might be expanded to include intermolecular versions of Yu's reaction. By understanding how this reactivity takes place, we might be able to understand the factors and reaction pathways that control C–N versus C–F reductive elimination from Pd^{IV}.

If we could design a system to study sp^3-C–N bond formation from Pd^{IV} this would add significantly to the known accounts of this type of reaction from a group 10 metal center. Not only are examples of C–N bond formation from characterized Pd^{IV} complexes exceptionally rare, but also, the demonstration of sp^3-C–N bond formation from group 10 metals is extremely limited. Our group documented the only report of sp^2 C–N bond formation from a well defined Pd^{IV} complex. Dr. Salena Whitfield reported that thermolysis of (2-phpy)$_2$$Pd^{IV}$Cl(succinimide) (**13**) in C_5H_5N to afforded dimer **16** in 81% yield along with 6% of 2-phpy-Cl (C–Cl) (**14**) and 8% of 2-phpy-suc (C–N) (**15**).[38]

Scheme 3.3.2 sp^2 C–N Reductive Elimination from 13

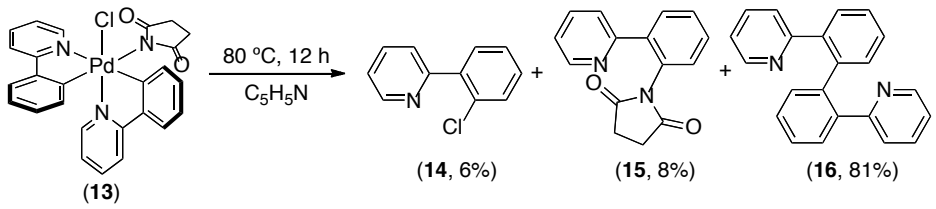

As mentioned above, accounts of sp^3-C–N reductive elimination from late transition metal centers remain even scarcer. In 2007 Goldberg described the first well characterized illustration of this type of reaction. She reported the formation of N-methylsulfonamides (**20**) and ethane via the thermolysis of the isolated Pt^{IV} complexes with the general structure *fac*-(dppbz)$PtMe_3(NHSO_2R)$ (dppbz = *o*-bis(diphenylphosphino)benzene (**18**).[41] The amide ligand was delivered to Pt via reaction with complex **17** and the appropriate amide with generation of water as a by-product (Scheme 3.3.2). The mechanism of C–N bond formation from the Pt^{IV} complexes was proposed to involve a pre-equilibrium dissociation of the sulfamide ligand, followed by nucleophilic S_N2 attack of the dissociated amide on a methyl ligand (Scheme 3.3.2, pathway (**b**)). Additionally, it was shown that the C–C reaction to yield ethane proceeded through the same intermediate (**19**), but reductive elimination occurred directly from the five coordinate intermediate (pathway (**a**)). The authors were able to inhibit C–C bond formation and generate C–N coupled products in high yields (65%) by adding excess of the sulfonamide anion under thermolysis conditions in benzene. A similar mechanism to the one that is outlined in Scheme 4.3.2 (pathway (**b**)) has also been observed for C–O[42] and C–I[43] reductive elimination reactions from related Pt^{IV} species. Thus the authors propose that this type of reaction pathway might be 'general' for alkyl C–X reductive elimination reactions from Pt^{IV}.

Scheme 3.3.2 Synthesis and Competitive Reductive Elimination of 18

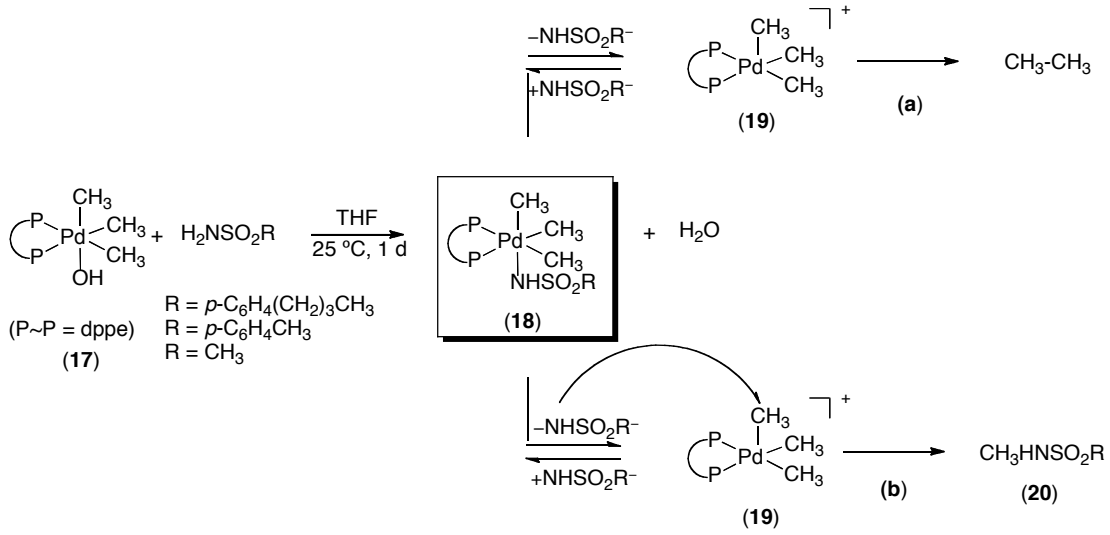

Additionally, Hillhouse has reported oxidatively-induced alkyl C–N bond formation from Ni^{II} to produce cyclic amines in high yields. Analogous reactions of acyclic Ni^{II} complexes have also been disclosed, but proceeded in low yields.[44] Mechanisms involving sp^3-C–N reductive elimination from transient Ni^{III} intermediates were proposed. Reports of Rh^{III} porphyrin complexes that undergo intramolecular nucleophilic attack of an amino group on an alkyl ligand of the porphyrin have been reported.[45] Most recently in 2010, Hartwig described sp^3-C–N bond-formation from Pd^{II} benzyl amido complexes.[46] It was determined that reductive elimination was slightly influenced by the electronic properties of the amido group and that electron donating groups on the amido ligand reacted faster than electron poor groups.

Since there are limited accounts of this type of reaction, it would be valuable to develop and study Pd^{IV} systems that undergo alkyl C–N bond formation.

Results. We demonstrated in Section 4.2 that complex **2** could be synthesized from the reaction of **1** with NFTPT and that the triflate ligand could be readily displaced (Scheme 3.2.2). Next, we wanted to investigate replacing

the triflate ligand of complex **2** with an amide in order to explore sp^3-C–N bond formation from Pd^{IV}. The amides that we tested for this reaction were benzenesulfonamide and 2,2,2-trifluoroacetamide. These substrates are particularly interesting because electron deficient amides are difficult to install via $Pd^{0/II}$ catalysis[47] and, also alkylsulfonamide linkages are easily deprotected to reveal free amines.[33]

Scheme 3.3.3 Reaction of 21 with NFTPT

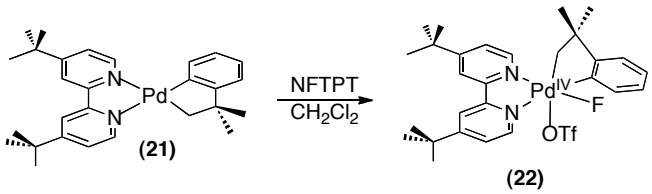

For the next series of studies we decided to synthesize and use complexes **21** and **22** because of the increased solubility of dtbpy-ligated complexes. Complex **21** readily reacted with NFTPT to yield Pd^{IV} complex **22** in 96% yield (Scheme 3.3.3). To screen for sp^3 C–N reductive elimination, we first combined Pd^{II} complex **21** (1.0 equiv) with NFTPT (1.0 equiv) and benzenesulfonamide (2.0 equiv) and allowed the reaction mixture to stir at 25 °C for 12 h in MeOH. This resulted in an unidentifiable array of products along with unreacted benzenesulfonamide. We hypothesized that complex **21** and NFTPT react to generate **22** *in situ*, although as we observed with complex **3** in Section 4.2, the decomposition of complex **22** was perhaps the source of the intractable mixtures of compounds. This result was suggestive that benzenesulfonamide was not binding to the Pd^{IV} complex and that a base stronger than MeOH might be necessary to deprotonate the amide and faciliate reactivity.

Therefore, we decided to use Cs_2CO_3 to facilitate deprotonation of the amide in MeCN (both benzenesulfonamide and 2,2,2-trifluoroacetamide are soluble in MeCN and the Cs_2CO_3 is semi-soluble). Thus, we stirred benzenesulfonamide (4.0 equiv) with Cs_2CO_3 (4.0 equiv) at 65 °C in MeCN for 1

h, then, added **21** and NFTPT to the reaction mixture. The reaction was heated for 12 h and afforded **23** in 71% yield (Scheme 3.3.4 (a)). Furthermore, the ^{19}F NMR spectra displayed no fluorine peaks corresponding to sp^3 or sp^2-C-F products. This same system also worked for 2,2,2-trifluoroacetamide and produced the C–N product **24** in 29% yield (Scheme 3.3.4 (b)). *Compounds **23** and **24** are unusual examples of products derived from sp^3-C-N reductive elimination.* Notably, there was not a fluorine ligand on the isolated product perhaps indicative of the known lability of Pd^{II} fluorides.

Scheme 3.3.4 Reaction of 21 with NFTPT, Cs_2CO_3 and Amide

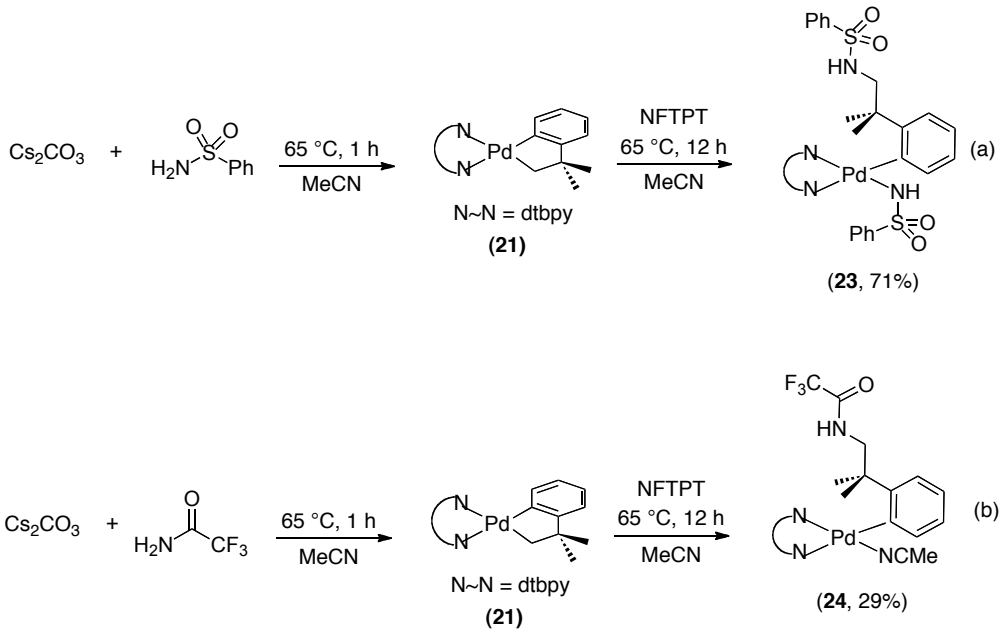

After identifying reaction conditions to achieve sp^3-C–N bond formation without any apparent competitive C–F products, we sought to investigate if we could observe Pd^{IV} intermediates in this system. Since Pd^{IV} complexes containing monodentate amido ligands are extremely rare, we wanted to understand if C–N bond formation in this system was derived from a Pd^{IV} complex that contained an amide ligand or if the product was obtained through an external attack without

direct displacement of the triflate. Thus, we combined 3.0 equiv of the sulfonamide and 3.0 equiv of Cs_2CO_3 and allowed the reagents to stir in MeCN for 1 h at 65 °C to facilitate deprotonation. The solution was cooled and complex **22** was added to the reaction. Gratifyingly, complexes **25** and **26** were isolated from the reaction mixture in 45% and 32% isolated yield, respectively (Scheme 3.3.5). Purification/isolation of these complexes proved challenging due to the removal of the excess amide. In order to test if this was the cause of the low yields, we carried out the reaction of **22** with Cs_2CO_3/NH_2R via ^1H NMR spectroscopy with an internal standard. Within 5 min at 25 °C, both reactions proceeded in high yields to affording **25** in 82% yield and **26** in 79% yield as determined by ^1H NMR spectroscopic analysis.

These complexes were fairly robust and could be isolated on the bench top under ambient conditions as well as stored in the freezer at –35 °C for up to a month without observable decomposition. Characterization via ^1H NMR and ^{19}F NMR spectroscopy proved diagnostic for complexes **25** and **26**. For example in the ^1H NMR spectra, complex **25** showed a broad singlet at 3.53 ppm for the hydrogen of the sulfonamide, a distinct doublet of doublets (J = 15 Hz, 7 Hz) for one of the methylene protons at 3.97 ppm, and a multiplet at 3.02 ppm for the other methylene proton. The 15 Hz coupling constant is reflected in the ^{19}F NMR spectrum where the Pd^{IV}–F resonance appears as a doublet (J = 15 Hz) at –339.66 ppm. Similar ^1H NMR and ^{19}F NMR spectrum were observed for complex **26**.

Scheme 3.3.5 Reaction of 22, Cs_2CO_3 and Amide

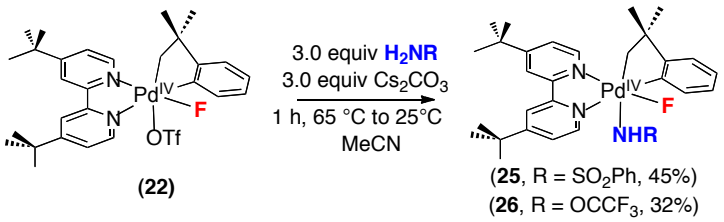

(**22**)

(**25**, R = SO_2Ph, 45%)
(**26**, R = $OCCF_3$, 32%)

Interestingly, thermolysis of the isolated complexes (**25** and **26**) afforded mixtures of both C–N and C–F reductive elimination products in an approximately 0.5: 1.0 ratio at 65 °C within 15 min. Although the reductive elimination products in Scheme 4.3.6 were not isolated, the coupling constants and splitting patterns in the ^{1}H and ^{19}F NMR spectra are consistent with two products that each contain either a sp^3-C–F or sp^3-C–N bond. Further, studies are underway to definitively characterize these products. This result was drastically different than the clean C–N bond formation that we observed in Scheme 3.3.4. However, the reaction in Scheme 3.3.4 contained both excess amide and Cs_2CO_3, which might account for the difference in reactivity observed upon the thermolysis of the isolated complexes.

Scheme 3.3.6 Distribution of Products from the Reductive Elimination of 25 and 26

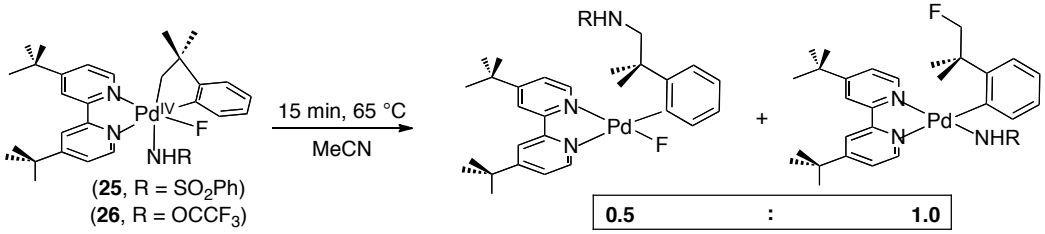

To further investigate what might be contributing to the distribution of C–N and C–F products in Scheme 3.3.6, we followed the reaction of **22** with amide and Cs_2CO_3 via ^{1}H NMR spectroscopy. The amide and Cs_2CO_3 were heated at 65 °C in MeCN for 1 h, then complex **22** was added to a cooled solution and within 5 min at 25 °C complex **25** was formed. After 2 h complex **25** reacted cleanly to afford the C–N reductive elimination product **23** in 70% (Scheme 3.3.7) (similar results were observed from the formation of **24** (48%)). Not only did this reaction with excess amide and Cs_2CO_3 provide a different product distribution than the reaction in Scheme 4.3.4, it also proceeded much slower. For example, the reaction in Scheme 3.3.7 took 2 h at 65 °C for the complete decomposition of

25 or **26** as compared to the reaction shown in Scheme 3.3.6, which took 15 mins at 65 °C for the disappearance of complex **25** or **26**. As shown in Figure 3.3.1, thermolysis of **25** with excess amide and Cs_2CO_3 at 65 °C proceeded with a clean first order decay (k_{obs} = 1.1x 10^{-4} s^{-1}) to afford the C–N reductive elimination product **23**. *This reaction is the first demonstration of sp^3 C–N bond formation from a characterized Pd^{IV} complex and the only example of high yielding C–N reductive elimination from Pd^{IV}.*

Scheme 3.3.7 Reaction of 25 with Excess Cs_2CO_3 and Benzenesulfonamide

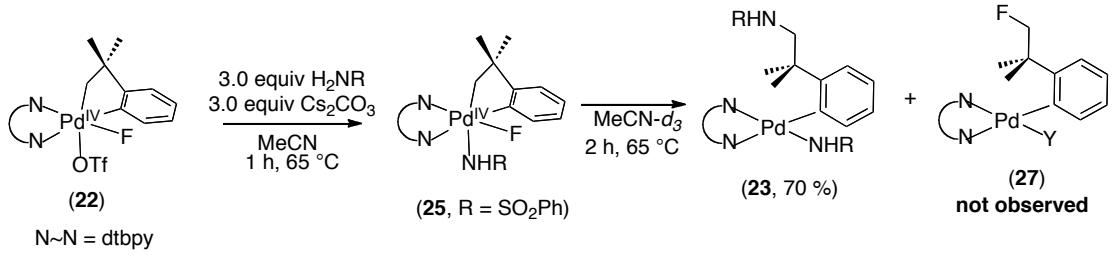

Figure 3.3.1 First Order Decay of 25 in the Presence of Excess Cs_2CO_3 and Benzenesulfonamide

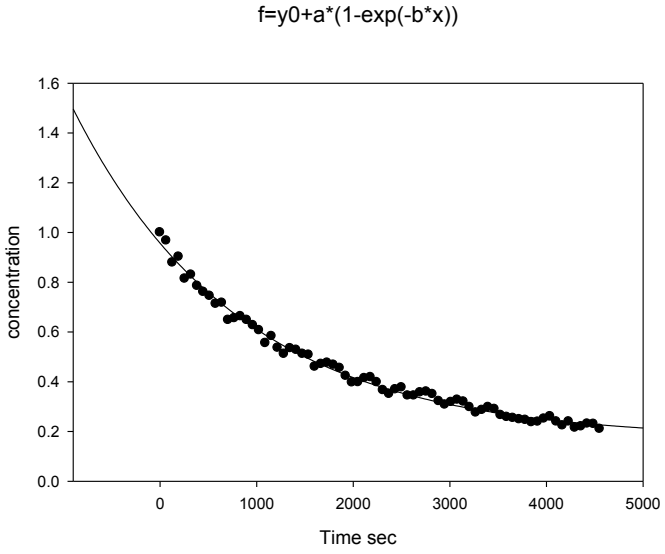

3.4 Reactivity of Complex X to Form sp^3 C–Cl and C–O Bonds and General Insights into sp^3 C–X Reductive Elimination from Pd^{IV}-F Complexes

Introduction. As demonstrated in sections 3.2 and 3.3, we identified systems to study unprecedented sp^3-C–F and C–N reductive elimination from Pd^{IV}. Next, we wanted to explore if this ligand systems could be used to explore other types of C–X reductive elimination from Pd^{IV}.

Replacement of Triflate with Cl and OAc. Our first goal was to replace the triflate ligand of complex **2** with Cl^- or AcO^- to observe either sp^3-C–Cl and C–OAc reductive elimination from Pd^{IV}. Gratifyingly, complex **2** reacted cleanly with NBu_4OAc and NBu_4Cl to afford **28** and **29** (Scheme 3.4.1). These complexes were formed in high yield (91% and 90%, respectively), but could not be isolated due to their low stability in solution (*vide infra).* Based on Figure 3.2.1, we reasoned that the new ligand (AcO^- or Cl^-) was incorporated onto the complex in the position that is *trans* to the σ-alkyl ligand, replacing the labile triflate ligand. Complexes **28** and **29** underwent thermal decomposition via C–X bond-forming reductive elimination. This transformation was highly selective for sp^3-C–X bond formation; furthermore, the group *trans* to the σ-alkyl ligand reacted selectivity. *The formation of compound **30** is the first reported example of sp^3-C–O bond formation from high oxidation state Pd. Additionally, the decomposition of **29** to **31** documents the first sp^3-C–Cl reductive elimination from a monometallic Pd^{IV} species.* Notably, complexes **28** and **29** were significantly less stable than complexes **5**, **3** and **3-BF_4**, suggestive that sp^3-C–Cl and C–OAc reductive elimination is significantly more facile than sp^3-C–F coupling from Pd^{IV}.

Scheme 3.4.1 Sp^3 C–OAc and C–Cl Bond Formation from Pd^{IV}

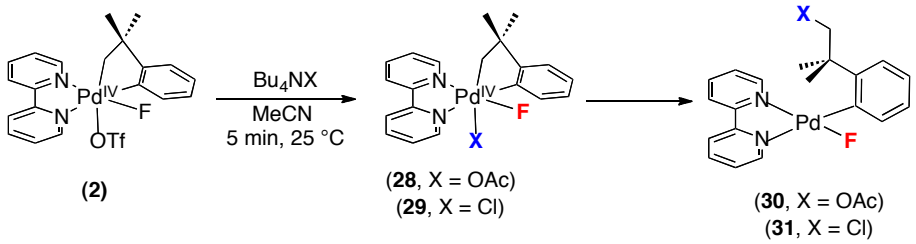

Analysis of Reactivity of Pd^{IV} Complexes for sp^3-C–X Reductive Elimination. Compounds **5**, **25, 28-dtbpy** and **29-dtpy** provide an excellent series of complexes to compare and contrast four types of sp^3-C–X (F, NHR, OAc, Cl) reductive elimination reactions from Pd^{IV}. Regardless of the X type ligand at the Pd^{IV} center, sp^3-C–X reductive elimination occurs exclusively from all of these complexes. Also, the type of ligand on the complex in this series appears to control the relative stability of complexes. These reactions were carried out with *in situ* generation of the desired Pd^{IV} complexes, since complexes **28-dtbpy** and **29-dtbpy** were unstable to isolation. Additionally, 3.0 equiv of excess nucleophile delivered via NBu_4OAc, NBu_4NCl, $C_6H_7NO_2S/Cs_2CO_3$ or NMe_4F was used because those conditions resulted in clean formation of **23** from **25** without any competing sp^3-C–F coupling. Complex **22** was subjected to 3.0 equiv of either NBu_4OAc, NBu_4NCl, $C_6H_7NO_2S/Cs_2CO_3$ or NMe_4F in MeCN and the relative rates of reductive elimination were monitored. The Pd^{IV} compound **28-dtbpy** was most reactive, with complete conversion to sp^3 reductive elimination product **30** in 1 h at 25 °C. Next, **29-dtbpy** fully reacted to afford **31** in 2 h at 25 °C. After 2 h at 25 °C, complexes **5** and **25** appeared mostly unreacted, so they were heated to 65 °C. Within 45 min at 65 ºC, **5** converted to completely **7**. Finally, complex **25** required 2 h at 65 ºC to generate the reductive elimination product **23**. The reactivity of complexes **5**, **25, 28-dtbpy, 29-dtbpy** shows the following trend: sp^3 C–O > C–Cl > C–F > C–N. Interestingly, this observation also tracks with the catalytic development in the area of $Pd^{II/IV}$ catalysis with C–O and C–Cl bond forming reactions being more prevalent in the literature than C–N and C–F bond forming reactions.

Scheme 3.4.2 Relative Stability of Complexes that undergo Sp^3 C–X Reductive Elimination from Pd^{IV}

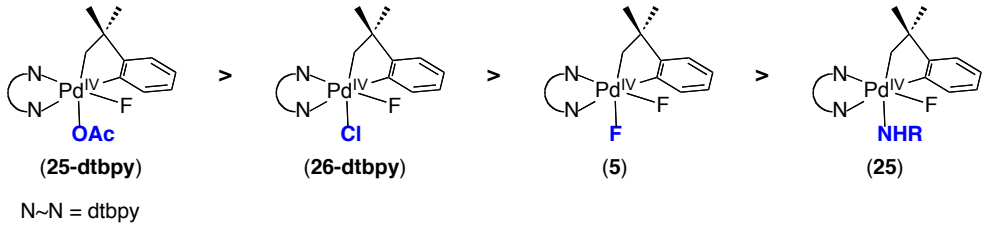

A general mechanism for sp^3-C–O, C–Cl and C–N bond formation is proposed. Bond-forming reductive elimination from complexes **25, 26, 28** and **29** is most consistent with a mechanism involving pre-equilibrium dissociation of a ligand followed by nucleophilic S_N2 attack of the dissociated ligand on the σ-alkyl carbon of the complex (Scheme 3.4.3).

Scheme 3.4.3 General S_N2 Mechanism for Reactivity from Complexes 25, 26, 28 and 29

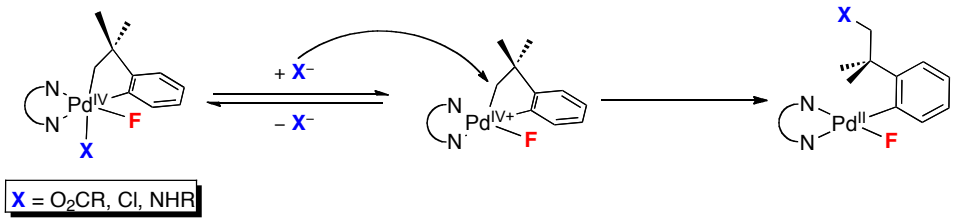

Alternatively, C–F reductive elimination from complexes **3** and **3-BF_4**, most reasonably occurs via dissociation of pyridine followed by concerted reductive elimination from Pd^{IV} to form sp^3-C–F reductive elimination products. This mechanism is similar to what Goldberg observed for sp^3-C–C bond formation from Pt^{IV} complexes.[48] Additionally, reductive elimination from complex **5** to afford C–F bond formation might occur by either the pathway in Scheme 3.4.3 or 3.4.4 or potentially both.

Scheme 3.4.4 General Concerted Mechanism for Reactivity from Complexes 3 and 3-BF_4

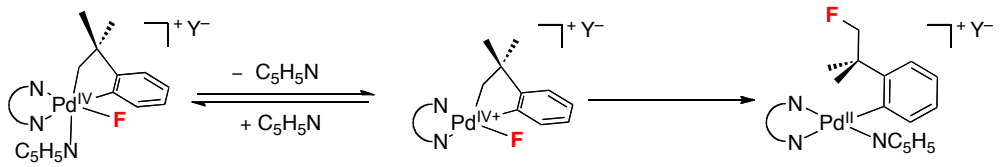

As discussed in the introduction (Scheme 3.1.2) the studies that have been done for sp^2-C–F, C–CF_3 and C–O reductive elimination from Pd^{IV} involve a pre-equilibrium dissociation of a ligand followed by bond formation from a five coordinate intermediate. Therefore, the data in the literature and the results presented in this chapter suggest that the favored pathway for both sp^2 and sp^3-C–X bond formation from an octahedral Pd^{IV} complex involves dissociation of a ligand prior to reductive elimination. The new reactions presented in this document substantially add to the known examples of sp^3-C–X reductive elimination from characterized Pd^{IV} complexes, as results are the first examples of high yielding sp^3 C–X bond formation from Pd^{IV}.

Oxidation with Iodosylbenzene. Lastly, our results in this section suggest that the functionality of the C–X reductive elimination products do not need to be derived directly from the oxidant. This is because of the preference for sp^3-C–X coupling to proceed via a S_N2 mechanism and also due to the lability of ligands observed at Pd^{IV} complexes. Therefore, we sought to investigate using PhIO as an oxidant with nucleophiles such as Cl^- or AcO^- delivered via tetrabutylammonium salts to achieve sp^3-C–Cl and C–OAc products from **21**. We combined 2.0 equiv of either NBu_4Cl or NBu_4OAc with complex **21** in CH_2Cl_2 and then added 1.0 equiv of PhIO. After 12 h at 65 °C we observed formation of **32** (49%) and **33** (75%). Alternatively under analogous conditions, sp^3-C–F and C–N products were not observed by this method. This result is interesting because it implies that we are able to achieve products where the functionality in the product comes from an external nucleophile.

Scheme 3.4.4 Reaction of 21 with PhIO and NBu_4X

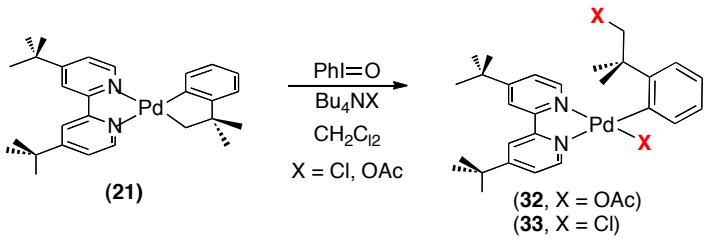

3.5 Reactivity of Complex 1 and 21 with Non-Fluorine Containing Oxidants

Oxidation of 21 with PhI(X)$_2$. Next, we wanted to explore the oxidation of **21** with various oxidants that do not deliver a fluorine ligand to the metal. Typically, fluorine is thought to stabilize high oxidation state metals since fluorine forms a highly polarized bond with the metal and also it is a relatively poor nucleophile for reductive elimination. Therefore, we thought that it would be interesting to explore the reactivity of complexes that did not contain a fluorine ligand. We wanted to explore whether complex **21** would react with other oxidants to form stable/isolable complexes. Since these complexes might be more reactive, we sought to explore whether these complexes would undergo sp^2 or sp^3 or mixtures of C–X reductive elimination reactions.

Thus, we carried out several reactions of Pd^{II} complex **21** with oxidants of the general structure $PhI(X)_2$. The first reaction explored was the oxidation of complex **21** with 1 equiv of $PhI(OAc)_2$. Upon combining the reagents an immediate color change from dark to light yellow occurred. Analysis of the reaction mixture by ^1H NMR spectroscopy indicated clean formation of one product that contained an unsymmetrical ligand environment for the dtbpy ligand as well as two distinct acetate resonances. The methylene protons of the carbon ligand appeared as two doublets at 5.41 and 4.48 ppm with J = 10 Hz. Given the instability of complex **28**, we reasoned that the isolated compound was most likely the Pd^{II} reductive elimination product (**32**) as opposed to the Pd^{IV} diacetate

complex (**I**) (Scheme 3.5.1). If this were the case, the ^{1}H NMR spectrum suggested that sp^{3}-C–OAc reductive elimination was the only product formed in this reaction.

X-ray quality crystals of **32-bpy** (the reaction of **1** with PhI(OAc)$_2$ was used for the isolation of **32-bpy** to facilitate crystallization) were obtained by slow diffusion of pentanes into a DCE solution of this compound at −35 °C. The crystal structure confirmed that **32** is the Pd^{II} product of sp^{3}-C–OAc bond-forming reductive elimination (Figure 3.5.1). Based on the previous results, we postulated that PhI(OAc)$_2$ oxidized complex **1** to intermediate **I** (Scheme 3.5.1), which underwent facile sp^{3}-C–O reductive elimination at 25 °C to yield product (**32**). Next, we sought to examine whether this reactivity was general for a series of hypervalent iodine reagents oxidants. As depicted in Table 3.5.1, oxidants with electron rich and electron deficient carboxylate substituents gave similar results of high yielding sp^{3} C–O reductive elimination products (**34**-**37**) in 92-61% yield. Additionally, PhI(Cl)$_2$ displayed similar reactivity with sp^{3}-C–Cl bond formation occurring rapidly to afford complex **33** (98% yield).

Scheme 3.5.1 Reaction of 1 with PhI(OAc)$_2$

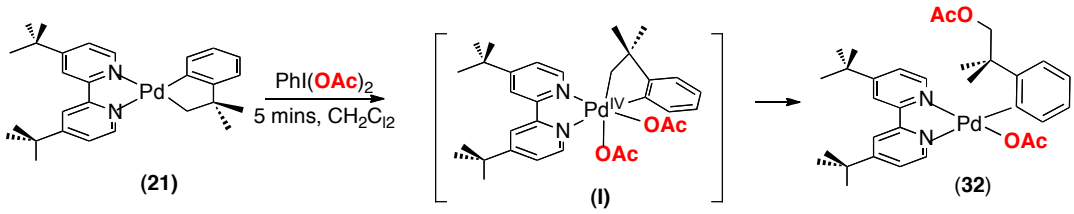

Figure 3.5.1 ORTEP Plot of 32

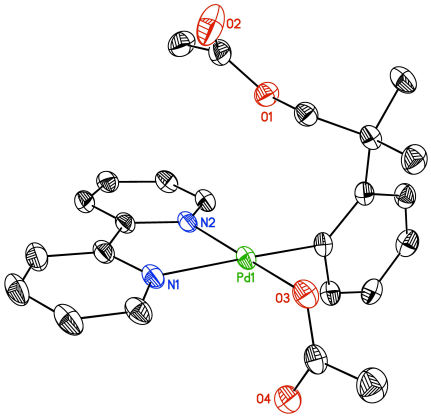

Table 3.5.1 Oxidation of 21 with $PhI(X)_2$ Oxidants

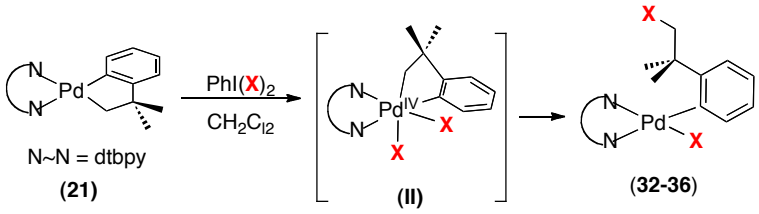

X	Product	Yield (%)
OAc	**32**	81
TFA	**34**	61
$O_2CC_9F_{19}$	**35**	92
$O_2CC_6H_4$*p*-OMe	**36**	86
$O_2CC_6H_4$*p*-OAc	**37**	83
Cl	**33**	98

Next, we chose to investigate if a Pd^{IV} intermediate could be observed via low temperature NMR spectroscopy. The reaction of **21** with $PhI(Cl)_2$ was studied at temperatures as low as –60 °C. A possible Pd^{IV} intermediate was observed,

but within several minutes complete conversion to **33** occurred. Next, the reaction of **21** with $PhI(OAc)_2$ was investigated at low temperature. However, even at –60 °C no intermediate was observed. Additionally, at 10 °C the conversion of **21** to **32** occurred within 10 min without any observable intermediates.

Taking into consideration the work we conducted in Chapter 2 on the mechanism of sp^2-C–O bond formation from Pd^{IV} complexes, we hypothesized that reacting **21** with an oxidant that contained an electron deficient carboxylate might allow for the observation of a Pd^{IV} intermediate. We showed in Chapter 2 that Pd^{IV} complexes with electron deficient ligands undergo slower rates of reductive elimination than complexes with electron rich carboxylates. Therefore, we combined **21** with $PhI(O_2CC_9F_{19})_2$ to observe a possible Pd^{IV} intermediate (**II**). At –30 °C, only unreacted starting material **21** was detected. However, at –10 °C a mixture of **38** and **35** was observed. Furthermore, after 30 min at 0 °C, **38** completely converted to **35**. Thus, this result gives support that a Pd^{IV} complex (**II**) is formed prior to reductive elimination from **21** for products **32-37**.

Scheme 3.5.2 Low Temperature Reaction of 21 with $PhI(O_2CC_9F_{19})_2$

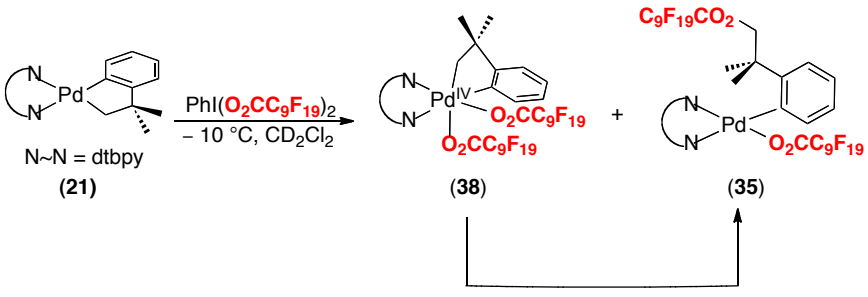

Oxidation with CH_3I. Next, we were intrigued by the reaction of CH_3I with complex **1**. There have been studies involving competitive C–I (CH_3I) and C–C (ethane) reductive elimination from di and trimethyl Pd^{IV} and Pt^{IV} complexes. It has been shown by Goldberg that complex *fac*-$L_2Pt(CH_3)_3I$ (L_2 = bis(diphenylphosphino)ethane) (**39**) reacts to undergo C–I reductive elimination

yielding CH_3I as the kinetic product.[43] This is thought to be formed via a mechanism involving a reversible dissociation of I^- followed by S_N2 attack of I^- on an alkyl group of the Pt^{IV} complex (**40**). C–C reductive elimination from this complex to produce ethane is the thermodynamic product with the same initial first step of reversible dissociation of I^- followed by concerted C–C coupling from the Pt^{IV} complex (**40**). One key piece of data in their mechanistic analysis was the observation of significant rate inhibition of formation of the C–C product with added NaI. Additionally, Canty has studied the reductive elimination reaction of $bpyPd^{IV}(CH_3)_3I$ and $bpyPd^{IV}(CH_3)_2(I)_2$. He showed that $bpyPd^{IV}(CH_3)_3I$ underwent exclusive C–C reductive elimination while the di-methyl complex ($bpyPd^{IV}(CH_3)_2(I)_2$) afforded C–I reductive elimination.[49]

Scheme 3.5.3 Low Temperature Reaction of 21 with $PhI(O_2CC_9F_{19})_2$

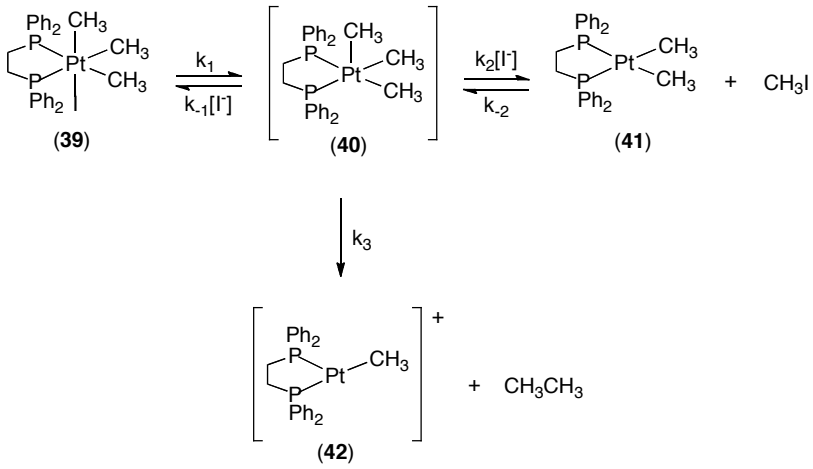

Thus, we were curious about whether competitive C–C and C–I reductive elimination from complex **21** upon reaction with CH_3I would be observed and how the mechanism of these transformations would compare to the reported reaction from *fac*-$L_2Pt(CH_3)_3I$. When CH_3I was combined with complex **21**, the yellow solution immediately turned light red with concurrent consumption of the starting material to form compound **43** in 81% yield (Scheme 3.5.3). This reaction was

once again selective for sp^3 bond formation over sp^2 and interestingly, C–C reductive elimination completely out-competed C–I reductive elimination.

If reductive elimination in this system is occurring via a similar mechanism to the complexes previously discussed in this chapter, a pre-equilibrium dissociation of a ligand prior to reductive elimination is probable. Since dissociation of a CH_3 group seems unlikely, we hypothesized a pre-equilibrium dissociation of I^- followed by a concerted reductive elimination from a five coordinate Pd^{IV} intermediate might be taking place. This mechanism would imply that the concerted C–C reductive elimination takes place faster than an S_N2 nucleophilic attack by the dissociated iodide, which is similar to what Goldberg observed for ethane formation from *fac*-$L_2Pt(CH_3)_3I$ (L_2 = bis(diphenylphosphino)ethane). This theory was tested by studying k_{obs} for the consumption of **21** with 1.0 equiv of CH_3I at 5 °C in the presence of varying equivalents of NBu_4I. An excellent linear fit was observed for an inverse dependence on the concentration of [I^-]. Thus C-C bond formation in this reaction most likely occurs via the mechanism outlined in Scheme 4.5.4, where **21** is oxidized to (**III**) and dissociation of I^- to generate the five coordinate intermediate (**IV**) proceeds concerted sp^3 C–C reductive elimination.

Scheme 3.5.4 Reaction of 21 with CH_3I

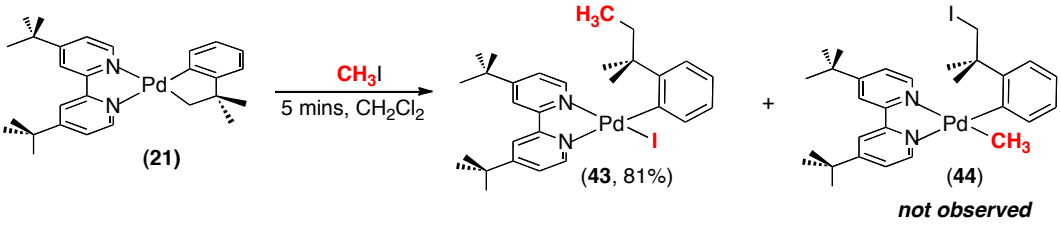

Figure 3.5.2 Plot of k_{obs} verse 1/[NBu_4I] for reductive elimination from 21 to form 43 in CD_2Cl_2 at 5 °C. y = (3.17×10^{-4})x – 1.92×10^{-3}); R^2 = 0.988.

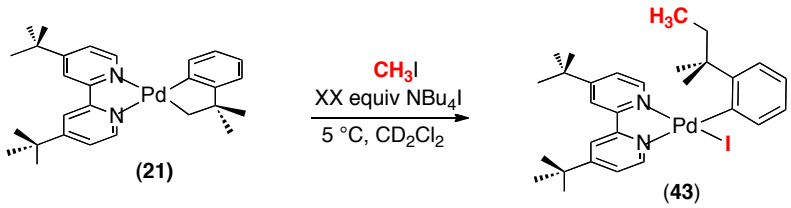

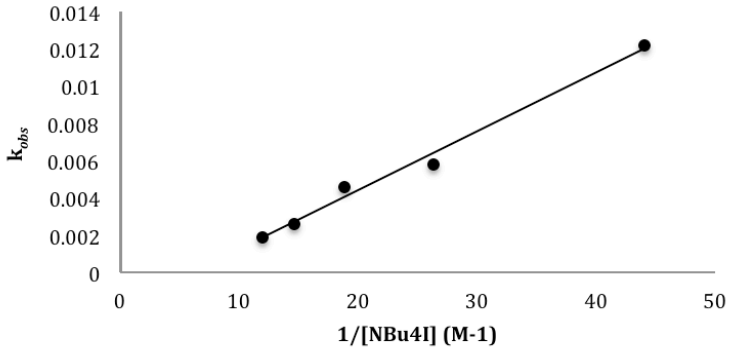

Scheme 3.5.5 Proposed Mechanism of the Reaction of 21 with CH_3I

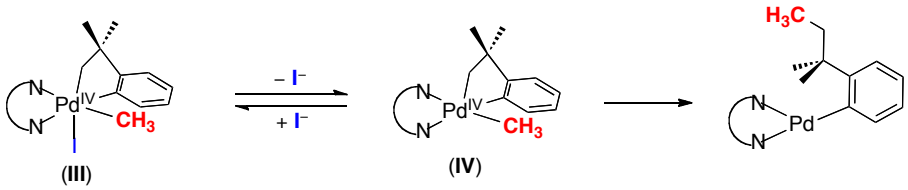

In conclusion this chapter demonstrated the first high yielding examples of sp^3-C–X bond formation from Pd^{IV} complexes. Interestingly, it was determined that in certain cases an S_N2 mechanism is feasible for reductive elimination from a Pd^{IV} center. Given this observation we were able to demonstrate that the nucleophile that participates in the reductive elimination reaction can be derived from sources other than the oxidant. Additionally, it is important to note that complexes that contained a fluoride ligand were remarkably more stable than complexes that contained other X type ligands.

3.6 Experimental Data and Characterization of Complexes

General Procedures

NMR spectra were obtained on a Varian vnmrs 700 (699.76 MHz for ^{1}H; 175.95 MHz for ^{13}C), a Varian Inova 400 (399.96 MHz for ^{1}H; 376.34 MHz for ^{19}F; 100.57 MHz for ^{13}C), a Varian vnmr500 (500.09 MHz for ^{1}H; 470.56 MHz for ^{19}F; 125.75 MHz for ^{13}C), or a Varion MR400 (400.53 MHz for ^{1}H; 376.87 MHz for ^{19}F; 100.71 MHz for ^{13}C) spectrometer. ^{1}H, ^{19}F and ^{13}C chemical shifts are reported in parts per million (ppm) relative to TMS, with the residual solvent peak used as an internal reference. ^{19}F NMR spectra are referenced on a unified scale, where the single primary reference is the frequency of the residual solvent peak in the ^{1}H NMR spectrum. ^{1}H and ^{19}F multiplicities are reported as follows: singlet (s), doublet (d), doublet of doublets (dd), quartet (q), multiplet (m), and broad resonance (br). Mass spectral data were obtained on a Micromass magnetic sector mass spectrometer or on a Micromass LCT mass spectrometer in electrospray ionization mode.

Materials and Methods

Bipyridine (bpy) and 2-methyl-2-phenylpropyl magnesium chloride were obtained from Aldrich. 1-Fluoro-2,4,6-trimethylpyridinium triflate (NFTPT) and 1-fluoro-2,4,6-trimethylpyridinium tetrafluoroborate (NFTPB) were obtained from TCI America. Unless otherwise noted, all reagents were used as received. NMR solvents were obtained from Cambridge Isotope Laboratories. All other solvents were obtained from Fisher Chemicals. Tetrahydrofuran was purified using an Innovative Technologies (IT) solvent purification system consisting of a copper catalyst, activated alumina, and molecular sieves.

Section 3.2 Characterization and Experimental Procedures

Synthesis of Pd^{II} Complex 1

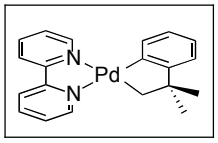

Complex 1. $Pd^{II}(CH_2CMe_2\text{-}o\text{-}C_6H_4)(COD)$ (720 mg, 2.08, 1.0 equiv) was combined with 2,2′-bipyridine (325 mg, 2.08 mmol, 1.0 equiv) in CH_2Cl_2 (200 mL), and the reaction mixture allowed to stir for 30 min. The solution was concentrated under vacuum (to 5 mL), and hexanes (30 mL) was added to precipitate the product. Complex **1** was isolated as a bright yellow solid (737 mg, 90% yield). ^{1}H NMR (500 MHz [D_3]chloroform, 25 °C): δ = 9.25 (d, *J* = 5 Hz, 1H), 8.80 (d, *J* = 5 Hz, 1H), 8.07-8.05 (multiple peaks, 2H), 7.99-7.93 (multiple peaks, 2H), 7.56-7.53 (multiple peaks, 2H), 7.47 (t, *J* = 7 Hz, 1H), 7.01-6.99 (multiple peaks, 2H), 6.87 (t, *J* = 5 Hz, 1H), 2.46 (s, 2H), 1.43 (s, 6H). ^{13}C NMR (125 MHz [D_3]chloroform, 25 °C): δ = 168.71, 158.54, 154.73, 154.21, 150.43, 149.37, 137.11, 134.35, 128.18, 125.42, 125.13, 123.72, 122.76, 121.34, 121.04, 121.00, 46.96, 44.97, 33.35 (two overlapping carbons). HRMS-electrospray (m/z): $[M + H]^+$ calcd for $C_{20}H_{20}N_2Pd$, 395.0734; Found, 395.0746.

Synthesis of Pd^{IV} Complexes 2-5

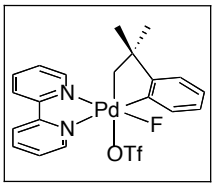

Complex 2. Compound **1** (70 mg, 0.18 mmol, 1.0 equiv) and NFTPT (52 mg, 0.18 mmol, 1.0 equiv) were combined in CH_2Cl_2 (15 mL), and this mixture was stirred for 15 min. The solvent was removed by rotary evaporation, and the resulting yellow oil was washed with diethyl ether (15 mL). The solid material was then dissolved in CH_2Cl_2 (1 mL), and diethyl ether (10 mL) was added to precipitate the product. The precipitate was collected and dried under vacuum to afford **2** as a light yellow solid (96 mg, 94% yield). ^{1}H NMR (400 MHz [D_3]acetonitrile, 25 °C): δ = 8.96 (d, *J* = 5 Hz, 1H), 8.58-8.56 (multiple peaks, 2H), 8.43 (t, *J* = 8 Hz, 1H), 8.34 (t, *J* = 8 Hz, 1H), 8.03-7.99 (multiple peaks, 2H), 7.78 (d, *J* = 8 Hz, 1H), 7.61 (t, *J* = 6 Hz, 1H), 7.34 (d, *J* = 8 Hz, 1H), 7.29 (d, *J* = 8 Hz, 1H), 7.13 (d, *J* = 8 Hz, 1H), 4.80 (dd, J *J* = 15, 5 Hz, 1H), 4.24 (app. br. s, 1H), 1.45 (s, 3H), 1.12 (s, 3H). ^{19}F NMR (376 MHz [D_3]acetonitrile, 25 °C): δ = –79.11 (s, 3F), –336.17 (d, *J* = 15 Hz, 1F). ^{13}C NMR data could not be obtained due to the instability of the complex over the timescale required for the experiment. HRMS-ESI (m/z): $[M - OTf]^+$ calcd for $C_{20}H_{20}FN_2Pd$ 413.0640; Found, 413.0644.

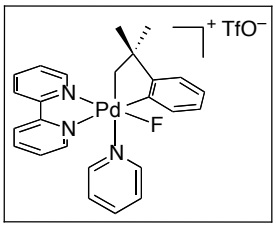

Complex 3. Compound **1** (120 mg, 0.3 mmol, 1.0 equiv), NFTPT (88 mg, 0.3 mmol, 1.0 equiv), and C_5H_5N (49 μL, 0.6 mmol, 2.0 equiv) were combined in

CH_2Cl_2 (15 mL), and this mixture was stirred for 15 min. The solvent was removed by rotary evaporation, and the resulting yellow oil was washed with diethyl ether (10 mL). The solid material was then dissolved in CH_2Cl_2 (2 mL), and diethyl ether (25 mL) was added to precipitate the product. The precipitate was collected and dried under vacuum to afford **3** as an off-white solid (125 mg, 63% yield). ^{1}H NMR (700 MHz [D_2]dichloromethane, 25 °C): δ = 8.93-8.91 (multiple peaks, 2H), 8.72 (d, *J* = 8 Hz, 1H), 8.48 (t, *J* = 8 Hz, 1H), 8.29 (t, *J* = 8 Hz, 1H), 8.24 (app. br. s, 2H), 8.07 (d, *J* = 6 Hz, 1H), 7.88 (t, *J* = 8 Hz, 1H), 7.77 (t, *J* = 6 Hz, 1H), 7.64 (t, *J* = 6 Hz, 1H), 7.47-7.44 (multiple peaks, 2H), 7.24 (t, *J* = 7 Hz, 1H), 7.05 (d, *J* = 8 Hz, 1H), 7.01 (t, *J* = 8 Hz, 1H), 6.66 (d, *J* = 8 Hz, 1H), 4.72 (dd, *J* = 15, 6 Hz, 1H), 3.89 (app. br. s, 1H), 1.50 (s, 3H), 1.13 (s, 3H). ^{19}F NMR (376 MHz [D_2]dichloromethane, 25 °C): δ = –78.97 (s, 3F), –324.80 (d, J = 15 Hz, 1F). ^{13}C NMR data could not be obtained due to the instability of the complex over the timescale required for the experiment. HRMS-ESI (m/z): [M + H]$^+$ calcd for $C_{26}H_{24}F_4N_3O_3PdS$ 642.0660; Found, 642.0669.

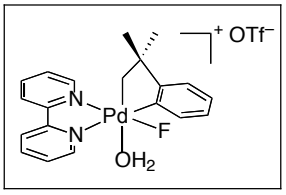

Complex 4. Compound **2** (11 mg, 0.02 mmol) was dissolved in acetone (1.5 mL) in a 3 mL vial. The vial was then placed in a 20 mL vial containing pentane and sealed with a Teflon-lined cap. The vial was placed in a –35 ºC freezer until yellow crystals formed. The solvent was decanted, and the crystals were washed with pentanes (3 mL), CH_2Cl_2 (3 mL), and acetone (3 mL). The crystals were then collected and dried under vacuum to afford **4** as a bright yellow solid (5.2 mg, 53% yield). ^{1}H NMR (500 MHz [D_6]dimethyl sulfoxide, 25 °C): δ = 9.04 (d, *J* = 5 Hz, 1H), 8.91-8.89 (multiple peaks, 2H), 8.56 (t, *J* = 8 Hz, 1H), 8.47 (t, *J* = 8 Hz, 1H), 8.10 (t, *J* = 6 Hz, 1H), 7.86 (d, *J* = 7 Hz, 1H), 7.78 (t, *J* = 6 Hz, 1H), 7.72 (d, *J* = 7 Hz, 1H), 7.31 (d, *J* = 8 Hz, 1H), 7.27 (d, *J* = 8 Hz, 1H), 7.14 (d, *J* = 7 Hz,

1H), 4.61 (dd, *J* = 15, 5 Hz, 1H), 4.23 (d, *J* = 5 Hz, 1H), 3.31 (broad s) 1.45 (s, 3H), 1.13 (s, 3H). ^{19}F NMR (376 MHz [D_6]dimethyl sulfoxide, 25 °C): δ = –77.91 (s, 3F), –328.96 (d, *J* = 15 Hz, 1F). ^{13}C NMR data could not be obtained due to the instability of the complex over the timescale required for the experiment. HRMS-ESI (m/z): [M – H_2O – OTf]$^+$ calcd for $C_{20}H_{20}FN_2Pd$ 413.0640; Found, 413.0656.

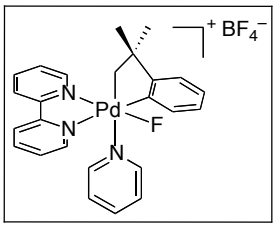

Complex 3-BF_4. Compound **1** (552 mg, 1.4 mmol, 1.0 equiv), NFTPB (259 mg, 1.4 mmol, 1.0 equiv), and C_5H_5N (225 μL, 2.8 mmol, 2.0 equiv) were combined in CH_2Cl_2 (50 mL), and this mixture was stirred for 15 min. The solvent was removed by rotary evaporation, and the resulting yellow oil was washed with diethyl ether (20 mL). The solid material was then dissolved in CH_2Cl_2 (3 mL), and diethyl ether (25 mL) was added to precipitate the product. The precipitate was collected and dried under vacuum to afford **3-BF_4** as an off-white solid (486 mg, 58% yield). ^{1}H NMR (400 MHz [D_2]dichloromethane, 25 °C): δ = 8.91 (d, *J* = 5 Hz, 1H), 8.79 (d, *J* = 8 Hz, 1H), 8.62 (d, *J* = 8 Hz, 1H), 8.47 (d, *J* = 8 Hz, 1H), 8.29 (d, *J* = 8 Hz, 1H), 8.23 (app. br. s, 2H), 8.07 (d, *J* = 6 Hz, 1H), 7.88 (t, *J* = 8 Hz, 1H), 7.77 (t, *J* = 5 Hz, 1H), 7.64 (t, *J* = 7 Hz, 1H), 7.45 (t, *J* = 7 Hz, 2H), 7.24 (t, *J* = 7 Hz, 1H), 7.05 (d, *J* = 7 Hz, 1H), 7.01 (t, *J* = 8 Hz, 1H), 6.65 (d, *J* = 8 Hz, 1H), 4.72 (dd, *J* = 15, 6 Hz, 1H), 3.88 (app. br. s, 1H), 1.49 (s, 3H), 1.13 (s, 3H). ^{19}F NMR (376 MHz [D_2]dichloromethane, 25 °C): δ = –152.48 (s, 4F), –324.80 (d, *J* = 15 Hz, 1F). ^{13}C NMR data could not be obtained due to the instability of the complex over the timescale required for the experiment. HRMS-ESI (m/z): [M – pyridine – BF_4]$^+$ calcd for $C_{20}H_{20}FN_2Pd$ 413.0640; Found, 413.0645.

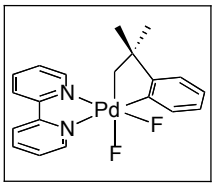

Complex 5. Compound **2** (310 mg, 0.54 mmol, 1.0 equiv) and Me_4NF (52 mg, 0.86 mmol, 1.6 equiv) were combined in dry CH_2Cl_2 (15 mL), and this mixture was stirred for 15 min in the glovebox. The solution turned dark orange with a dark solid precipitate. The reaction was filtered through celite, and the solvent was removed under vacuum. The resulting yellow oil was dissolved in DCE (4 mL), and pentane (30 mL) was added to precipitate the product. The precipitate was collected and dried under vacuum to afford **5** as a light yellow solid (190 mg, 77% yield, along with 19 % Me_4NBF_4 as determined by ^{1}H NMR). ^{1}H NMR (500 MHz [D_2]dichloromethane, 25 °C): δ = δ 9.06 (d, *J* = 5 Hz, 1H), 8.43 (d, *J* = 8 Hz, 1H), 8.40 (d, *J* = 8 Hz, 1H), 8.14-8.08 (multiple peaks, 2H), 8.01 (t, *J* = 8 Hz, 1H), 7.95 (d, *J* = 8 Hz, 1H), 7.74 (d, *J* = 6 Hz, 1H), 7.31 (t, *J* = 6 Hz, 1H), 7.24-7.16 (multiple peaks, 2H), 6.95 (d, *J* = 8 Hz, 1H), 4.11 (m, 1H), 3.51 (dd, *J* = 6, 3 Hz, 1H), 1.39 (s, 3H), 1.02 (s, 3H). ^{19}F NMR (470 MHz [D_2]dichloromethane, 25 °C): δ = –201.42 (d, *J* = 51 Hz, 1F), –336.71 (dd, *J* = 51, 14 Hz, 1F). HRMS-ESI (m/z): $[M - F]^+$ calcd for $C_{20}H_{20}FN_2Pd$ 413.0645; Found, 413.0640.

Synthesis of Pd^{II} Reductive Elimination Products

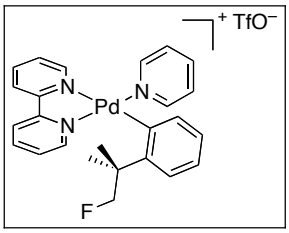

Complex 6. Compound **3** (30 mg, 0.06 mmol) was dissolved CH_2Cl_2 (10 mL). The reaction was stirred for 30 min at 80 °C. The solvent was removed by rotary

evaporation, and the resulting yellow oil was dissolved in CH_2Cl_2 (1 mL), and precipitated with pentane (15 mL). The precipitate was collected and dried under vacuum to afford **6** as a tacky yellow solid (28 mg, 93% yield). ^{1}H NMR (500 MHz [D_3]chloroform, 25 °C): δ = 8.88 (d, *J* = 8 Hz, 2H), 8.56 (d, *J* = 8 Hz, 1H), 8.53 (d, *J* = 8 Hz, 1H), 8.22 (t, *J* = 8 Hz, 1H), 8.16 (t, *J* = 8 Hz, 1H), 8.04-7.99 (multiple peaks, 2H), 7.77 (d, *J* = 5 Hz, 1H), 7.68-7.61 (multiple peaks, 2H), 7.56 (d, *J* = 6 Hz, 1H), 7.32 (t, *J* = 6 Hz, 1H), 7.22 (t, *J* = 8 Hz, 1H), 7.11-7.08 (multiple peaks, 2H), 4.69 (dd, *J* = 48, 9 Hz, 1H), 4.53 (dd, *J* = 48, 9 Hz, 1H), 1.68 (s, 3H), 1.61 (s, 3H). ^{19}F NMR (470 MHz [D_3]chloroform, 25 °C): δ = –78.99 (s, 1F), –217.01 (t, *J* = 48 Hz, 1F). ^{13}C NMR (125 MHz [D_3]chloroform, 25 °C): δ = 156.40, 153.70, 152.45, 152.25, 150.41, 148.29, 148.13, 141.10, 140.82, 139.70, 132.91, 128.34, 128.07, 126.94, 126.86, 126.48 (q, J = 322 Hz, 1C), 126.38, 125.27, 124.04, 124.01, 92.21 (d, J = 177 Hz, 1C), 40.91, 40.76, 27.60. HRMS-ESI (m/z): [M – C_5H_5N – OTf]$^+$ calcd for $C_{20}H_{20}FN_2Pd$ 413.0645; Found, 413.0643.

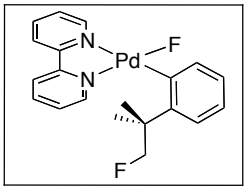

Complex 8. Compound **7** (20 mg, 0.04 mmol, 1.0 equiv) was dissolved in dry CH_2Cl_2 (6 mL) under N_2. The reaction was stirred for 15 min at 80 ºC. The solvent was removed by rotary evaporation, the resulting yellow oil was dissolved in CH_2Cl_2 (1 mL), and the product was precipitated with pentane (15 mL). The precipitate was collected and dried under vacuum to afford **8** as a tacky yellow solid (18 mg, 90% yield). ^{1}H NMR (700 MHz [D_2]dichloromethane, 25 °C): δ = 9.16 (d, *J* = 5 Hz, 1H), 8.75 (d, *J* = 5 Hz, 1H), 8.15-8.13 (multiple peaks, 2H), 8.06-8.01 (multiple peaks, 2H), 7.61 (t, *J* = 5 Hz, 1H), 7.53 (d, *J* = 6 Hz, 1H), 7.51 (d, *J* = 8 Hz, 1H), 6.99 (t, *J* = 7 Hz, 1H), 6.95 (t, *J* = 8 Hz, 1H), 6.86 (d, *J* = 7 Hz, 1H), 4.54 (dd, *J* = 49, 9 Hz, 1H), 4.51 (dd, *J* = 49, 9 Hz, 1H), 1.39 (s, 3H), 1.38 (s, 3H). ^{19}F NMR (376 MHz [D_2]dichloromethane, 25 °C): δ = –151.89 (s, 1F), –

214.87 (t, *J* = 49 Hz, 1F). ^{13}C NMR (175 MHz [D_3]chloroform, 25 °C): δ = 163.45, 160.98, 155.59, 155.19, 151.02, 150.11, 138.42, 138.37, 135.29, 126.46, 126.24, 125.22, 123.63, 123.25, 122.27, 122.20, 95.39 (d, J = 176 Hz, 1C), 36.62, 36.60, 25.63. HRMS-APCI (m/z): $[M - F]^+$ calcd for $C_{20}H_{20}FN_2Pd$ 413.0640; Found, 413.0641.

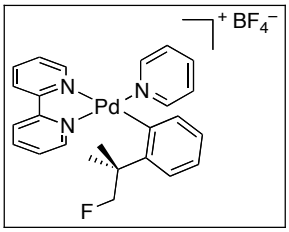

Complex 6-BF_4. Compound **3-BF_4** (30 mg, 0.05 mmol) dissolved combined in CH_2Cl_2 (10 mL). The reaction was stirred for 30 min at 80 °C. The solvent was removed by rotary evaporation, and the resulting yellow oil was dissolved in CH_2Cl_2 (1 mL), and precipitated with pentane (15 mL). The precipitate was collected and dried under vacuum to afford **6-BF_4** as a tacky yellow solid (26 mg, 87% yield). ^{1}H NMR (700 MHz [D_2]dichloromethane, 25 °C): δ = 8.85-8.83 (multiple peaks, 2H), 8.48-8.45 (multiple peaks, 2H), 8.16-8.11 (multiple peaks, 2H), 8.01-7.96 (multiple peaks, 2H), 7.75 (d, *J* = 5 Hz, 1H), 7.63 (d, *J* = 7 Hz, 1H), 7.62-7.58 (multiple peaks, 2H), 7.52 (d, *J* = 6 Hz, 1H), 7.27 (t, *J* = 6 Hz, 1H), 7.19 (d, *J* = 8 Hz, 1H), 7.08-7.05 (multiple peaks, 2H), 4.68 (dd, *J* = 48 Hz, J = 9 Hz, 1H), 4.50 (dd, *J* = 48 Hz, *J* = 9 Hz, 1H), 1.64 (s, 3H), 1.40 (s, 3H). ^{19}F NMR (376 MHz [D_3]chloroform, 25 °C): δ = –152.42 (s, 1F), –216.08 (t, *J* = 48 Hz, 1F). ^{13}C NMR (125 MHz [D_3]chloroform, 25 °C): δ = 156.03, 153.23, 151.87 (two overlapping carbon's), 150.16, 147.91, 140.67, 140.49, 139.35, 132.58, 127.94, 127.74, 126.60 (two overlapping carbon's), 126.42, 126.00, 124.87, 123.55, 123.47, 93.31 (d, J = 176 Hz, 1C), 40.53, 40.40, 27.19. HRMS-ESI (m/z): $[M - C_5H_5N - BF_4]^+$ calcd for $C_{20}H_{20}FN_2Pd$ 413.0645; Found, 413.0655.

Determining Order in Pyridine with 3-BF_4 at 45 °C in CD_2Cl_2

Complex **3-BF_4** (4.4 mg, 0.00758 mmol, 1.0 equiv) and C_5D_5N (0.001895 to 0.0114 mmol, 3.8 mM to 20.0 mM) were combined in a screw cap NMR tube and dissolved in CD_2Cl_2 (0.5 mL). An internal standard (2-nitrobenzotrifluoride) was added (20 μl of a stock solution in CD_2Cl_2, 0.00758, 1 equiv) and the tube was sealed with a Teflon®-lined cap. The tube was immediately placed in an NMR spectrometer with the temperature pre-equilbrated to 45 °C, and the reaction was allowed to equilibrate for 2 min. The rate of reductive elimination was monitored by ^{19}F NMR spectroscopy by monitoring the disappearance of the starting material. The reaction was followed to between 2-3 half lives, and the data was plotted as –ln[**3-BF_4**/**3-BF_4**^{o}] versus time. A representative kinetics run is shown in Figure 3.5.1 The values of k_{obs} for each [pyridine] are reported in Table 3.5.1.

Table 3.6.1. Rate as a Function of [C_5D_5N] at 45 °C

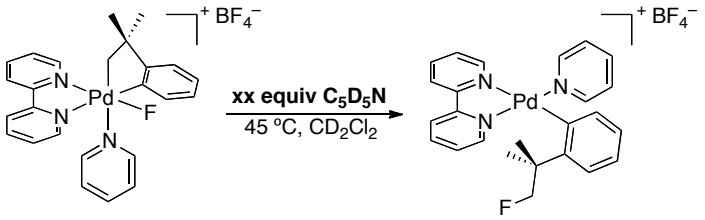

equiv C_5D_5N	[C_5D_5N]	[1/C_5D_5N]	k_{obs}
0.25	0.001895	528	2.75×10^{-4}
0.5	0.00379	264	1.6×10^{-4}
0.75	0.00568	176	5.51×10^{-5}
1	0.00758	132	8.02×10^{-5}
1.5	0.114	88	2.81×10^{-5}

Figure 3.6.1. Representative Rate Data (Reductive Elimination from 3-BF_4 in the Presence of 11.4 mM C_5D_5N)

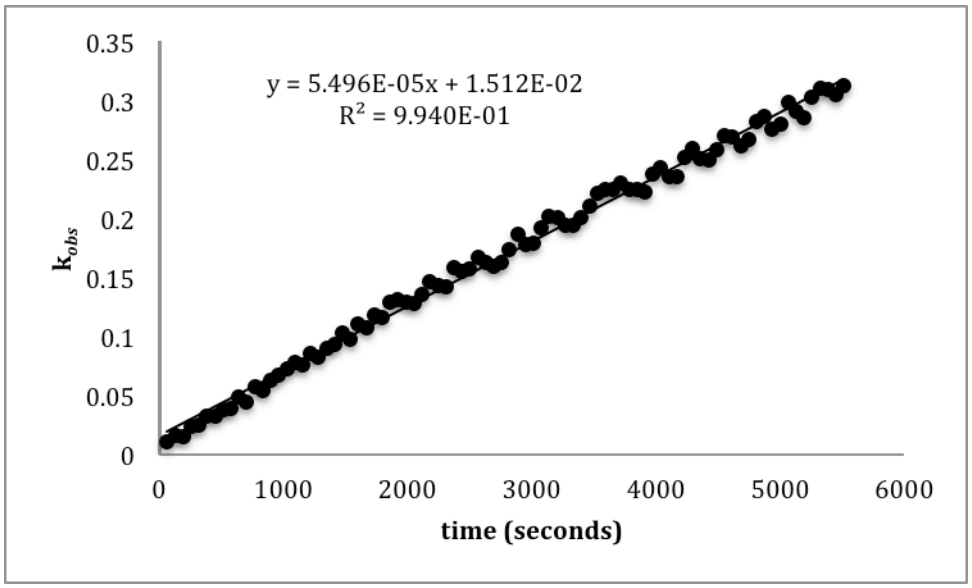

X-ray Crystallography Details

Yellow cubes of **4** were grown from an acetone/pentanes solution at –35 °C. A crystal of dimensions 0.10 x 0.10 x 0.10 mm was mounted on a Bruker SMART APEX CCD-based X-ray diffractometer equipped with a low temperature device and fine focus Mo-target X-ray tube (l = 0.71073 A) operated at 1500 W power (50 kV, 30 mA). The X-ray intensities were measured at 85(1) K; the detector was placed at a distance 5.055 cm from the crystal. A total of 4717 frames were collected with a scan width of 0.5° in w and 0.45° in phi with an exposure time of 30 s/frame. The integration of the data yielded a total of 119486 reflections to a maximum 2q value of 56.64° of which 7429 were independent and 7186 were greater than 2s(I). The final cell constants (Table 1) were based on the xyz centroids of 9866 reflections above 10s(I). Analysis of the data showed negligible decay during data collection; the data were processed with SADABS and corrected for absorption. The structure was solved and refined with the Bruker SHELXTL (version 2008/4) software package, using the space group Pca2(1) with Z = 4 for the formula $C_{33}H_{26}BN_3F_4Cl_2Pd$. All non-hydrogen atoms were refined anisotropically with the hydrogen atoms placed in idealized positions. Full matrix least-squares refinement based on F^2 converged at R1 = 0.0219 and wR2 = 0.0533 [based on I > 2sigma(I)], R1 = 0.0232 and wR2 = 0.0542 for all data. Additional details are presented in **Table S2** and are available in the corresponding CIF file (deposited in the Cambridge Structural Database: CCDC 852596).

Sheldrick, G.M. SHELXTL, v. 2008/4; Bruker Analytical X-ray, Madison, WI, 2008.

Saint Plus, v. 7.60A, Bruker Analytical X-ray, Madison, WI, 2009.

Sheldrick, G.M. SADABS, v. 2008/1. Program for Empirical Absorption Correction of Area Detector Data, University of Gottingen: Gottingen, Germany, 2008.

Table 3.6.2 Crystal data and structure refinement for 5.

Empirical formula	C21 H22 F4 N2 O4 Pd S
Formula weight	580.87
Temperature	85(2) K
Wavelength	1.54178 A
Crystal system, space group	Triclinic, P-1
Unit cell dimensions	a = 9.3652(2) A alpha = 94.404(7) deg.
	b = 11.5602(3) A beta = 108.848(8) deg.
	c = 11.9928(8) A gamma = 111.654(8) deg.
Volume	1113.33(8) A^3
Z, Calculated density	2, 1.733 Mg/m^3
Absorption coefficient	8.196 mm^-1
F(000)	584
Crystal size	0.18 x 0.12 x 0.09 mm
Theta range for data collection	4.00 to 68.17 deg.
Limiting indices	-11<=h<=11, -13<=k<=13, -11<=l<=12
Reflections collected / unique	16877 / 3453 [R(int) = 0.0504]
Completeness to theta = 68.17	84.7 % (96% complete to 0.86 A).

Absorption correction	Semi-empirical from equivalents
Max. and min. transmission	0.686 and 0.557
Refinement method	Full-matrix least-squares on F^2
Data / restraints / parameters	3453 / 0 / 375
Goodness-of-fit on F^2	1.261
Final R indices [I>2sigma(I)]	R1 = 0.0688, wR2 = 0.2137
R indices (all data)	R1 = 0.0699, wR2 = 0.2141
Largest diff. peak and hole	2.236 and -1.268 e.A^-3

Section 3.3-3.5 Characterization and Experimental Procedures

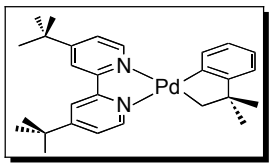

Complex 21. (COD)Pd^{II}(CH_2CMe_2-*o*-C_6H_4) (104 mg, 0.30, 1.0 equiv) was combined with 4,4′-di-*tert*-butylbipyridine (80 mg, 0.30 mmol, 1.0 equiv) in CH_2Cl_2 (120 mL) and allowed to stir for 30 min at rt. The reaction was concentrated under vacuum to 5 mL and ~30 mL of hexanes was added to precipitate the product. **21** was isolated as a bright yellow solid (147 mg, 97% yield). ^{1}H NMR ($CDCl_3$): δ 9.11(d, *J* = 6 Hz, 1H), 8.55 (d, *J* = 6 Hz, 1H), 7.98-7.97 (multiple peaks, 2H), 7.55 (d, *J* = 8 Hz, 1H), 7.53 (d, *J* = 6 Hz, 1H), 7.43 (d, *J* = 6 Hz, 1H), 7.00 (app. t, 2H), 6.87 (d, *J* = 8 Hz, 1H), 2.43 (s, 2H), 1.44 (s, 6H), 1.43 (s, 9H), 1.42 (s, 9H). ^{13}C NMR ($CDCl_3$): δ 169.09, 161.95, 161.87, 159.24, 155.35, 154.86, 150.38, 149.32, 134.79, 123.92, 122.90, 122.78, 122.54, 121.58, 117.94, 117.84, 47.27, 44.84, 35.19, 35.17, 33.76, 31.07, 30.30, 30.27. HRMS-electrospray (m/z): $[M+H]^+$ calcd for $C_{28}H_{36}N_2Pd$, 507.1986; Found, 507.2000.

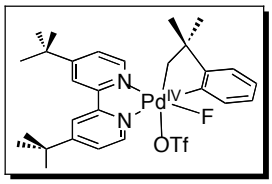

Complex 22. Compound **21** (510 mg, 1.01 mmol, 1.0 equiv) and NFTPT (291 mg, 1.01 mmol, 1.0 equiv) were combined in CH_2Cl_2 (15 mL), and this mixture was stirred for 15 min. The solvent was removed by rotary evaporation, and the resulting yellow oil was washed with diethyl ether (30 mL). The solid material was then dissolved in CH_2Cl_2 (5 mL), and diethyl ether (25 mL) was added to precipitate the product. The precipitate was collected and dried under vacuum to

afford **22** as a light yellow solid (644 mg, 94% yield). ^{1}H NMR (CD_3CN): δ 8.80 (d, *J* = 6 Hz, 1H), 8.52 (s, 1H), 8.48 (s, 1H), 7.95 (d, *J* = 6 Hz, 1H), 7.83 (d, *J* = 6 Hz, 1H), 7.66 (d, *J* = 6 Hz, 1H), 7.54 (d, *J* = 7 Hz, 1H), 7.32 (t, *J* = 7 Hz, 1H), 7.25 (t, *J* = 8 Hz, 1H), 7.09 (d, *J* = 8 Hz, 1H), 4.72 (dd, *J* = 15, 6 Hz, 1H), 4.12 (app. br. s, 1H), 1.52 (s, 9H), 1.43 (s, 9H), 1.41 (s, 3H), 1.09 (s, 3H).. ^{19}F NMR (CD_3CN): δ –79.56 (s, 3F), –335.43 (d, *J* = 15 Hz, 1F). ^{13}C NMR data could not be obtained due to the instability of the complex over the timescale required for the experiment. HRMS-ESI (m/z): $[M - CF_3O_3S]^+$ calcd for $C_{28}H_{36}FN_2Pd$ 525.1897; Found, 525.1890.

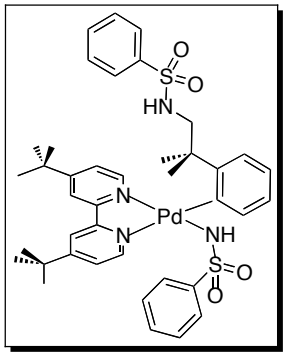

Complex 23. Cs_2CO_3 (24 mg, 0.074 mmol, 2.0 equiv) and benzenesulfonamide (12 mg, 0.074 mmol, 2.0 equiv) were combined in MeCN (3.0 mL) at 65 °C and allowed to stir for 1 h. The solution was allowed to cool and complex **22** (25 mg, 0.037 mmol, 1.0 equiv) was added to the reaction mixture. The reaction was heated at at 65 °C for 12 h. The solvent was removed by rotary evaporation and diethyl ether was added to the yellow sticky solid. The solution was decanted and the solvent was removed by rotary evaporation. The yellow solid was dissolved in 2 mL of diethyl ether and precipitated with pentanes (~ 6 mL). Compound **23** solid was collected as a yellow solid. (14 mg, 46% yield). ^{1}H NMR (CD_3CN): δ 9.16 (d, *J* = 6 Hz, 1H), 8.39 (d, *J* = 6 Hz, 1H), 8.30 (d, *J* = 6 Hz, 1H), 7.88-7.84 (multiple peaks, 2H), 7.75 (d, *J* = 6 Hz, 1H), 7.63-7.55 (multiple peaks, 3H), 7.51 (d, *J* = 6 Hz, 1H), 7.31 (d, *J* = 6 Hz, 1H), 7.14 (d, *J* = 7 Hz, 1H), 7.06-7.03

(multiple peaks, 2H), 6.84 (t, *J* = 8 Hz, 1H), 6.80 (t, *J* = 6 Hz, 1H), 6.73 (d, *J* = 8 Hz, 1H), 5.65 (br. s, 2H), 2.80 (d, *J* = 11, 1H), 2.36 (d, *J* = 11, 1H), 1.45 (s, 9H), 1.43 (s, 3H), 1.38 (s, 9H), 1.24 (s, 3H). ^{13}C NMR (CD_3CN): δ 164.50, 164.38, 156.82, 153.74, 153.48, 151.66, 150.99, 149.57, 143.57, 135.73, 132.86, 129.86, 129.61(overlapping carbons, 2C), 128.06, 127.92, 126.45, 125.41, 124.06, 123.65, 123.35, 121.21, 120.69, 119.55, 57.16, 44.30, 35.97, 35.90, 32.32, 30.05, 29.86, 27.27. HRMS-ESI (m/z): $[M - C_6H_6NO_2S]^+$ calcd for $C_{34}H_{42}N_3O_2PdS$ 662.2027; Found, 662.2040.

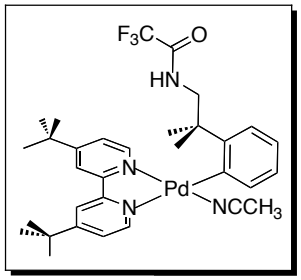

Complex 24. Cs_2CO_3 (36 mg, 0.111 mmol, 3.0 equiv) and 2,2,2-trifluoroacetamide (13 mg, 0.111 mmol, 3.0 equiv) were combined in MeCN (4.0 mL) at 65 °C and allowed to stir for 1 h. The solution was allowed to cool and complex **22** (25 mg, 0.037 mmol, 1.0 equiv) was added to the reaction mixture. The reaction was heated at 65 °C for 12 h. The solvent was removed by rotary evaporation and diethyl ether was added to the white solid. The solution was decanted and the solvent was removed by rotary evaporation (2X). The white solid was dissolved in 2 mL of diethyl ether and precipitated with pentanes (~ 6 mL). Complex **24** was collected as a white solid. (6 mg, 23% yield). ^{1}H NMR (CD_3CN): δ 8.47 (d, *J* = 6 Hz, 1H), 8.39 (d, *J* = 5 Hz, 1H), 8.36-8.35 (multiple peaks, 2H), 7.70 (d, *J* = 6 Hz, 1H), 7.59 (d, *J* = 6 Hz, 1H), 7.40-7.39 (multiplet, 1H), 7.09-7.05 (multiple peaks, 3H), 3.62 (d, *J* = 13, 1H), 3.02 (d, *J* = 13, 1H), 2.30 (s, 3H), 2.18 (s, 1H), 1.48 (s, 3H), 1.47 (s, 9H), 1.45 (s, 3H), 1.44 (s, 9H). ^{13}C NMR (CD_3CN): δ 164.42, 164.25, 160.98 (q, *J* = 31 Hz, 1H), 156.00, 153.27, 153.16, 150.96, 149.62, 148.83, 135.73, 133.72, 125.38, 123.88, 123.60, 123.51,

121.80, 120.20 98 (q, *J* = 289 Hz, 1H), 120.41, 119.72, 42.87, 35.50, 35.44, 29.46, 29.32, 27.38. HRMS-ESI (m/z): $[M - CH_3CN]^+$ calcd for $C_{30}H_{37}F_3N_3OPd$ 618.1929; Found, 618.1929. *At this time the counterion on this complex has not been determined.*

Scheme 3.6.1 Synthesis of Complexes 25, 26, 28 and 29

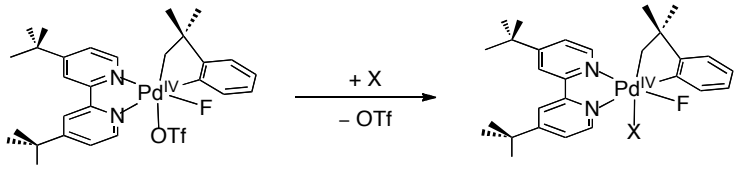

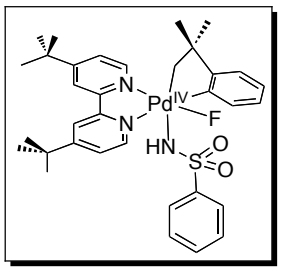

Complex 25. Cs_2CO_3 (22 mg, 0.066 mmol, 2.0 equiv) and benzenesulfonamide (10 mg, 0.066 mmol, 3.0 equiv) were combined in MeCN (2.0 mL) at 65 °C and allowed to stir for 1 h. The solution was allowed to cool and complex **22** (15 mg, 0.022 mmol, 1.0 equiv) was added to the reaction mixture. The reaction was shaken for ~ 1 min and then filtered over a pipette filled with celite. The filtrate was collected and the solvent was removed by rotary evaporation. Diethyl ether (2 mL) was added to the yellow solid and decanted into a vial. The solvent was removed by rotary evaporation. Diethyl ether (2 mL) was added to the yellow solid and decanted into a vial. The solvent was removed by rotary evaporation. The solid was dissolved in (0.5 mL) CH_2Cl_2 and allowed to crystalize by diffusion

with pentanes at -35 °C. The yellow solid was collected (7 mg, 45% yield). ^{1}H NMR (CD_3CN): δ 8.56 (d, *J* = 6 Hz, 1H), 8.40-8.38 (multiplet, 1H), 8.07 (s, 1H), 8.03 (s, 1H), 7.91-7.88 (multiple peaks, 3H), 7.68 (d, *J* = 6 Hz, 1H), 7.57 (d, *J* = 8 Hz, 1H), 7.43 (d, *J* = 7 Hz, 1H), 7.24-7.22 (multiple peaks, 2H), 6.98-6.95 (multiple peaks, 3H), 3.97 (dd, *J* = 15, 7 Hz, 1H), 3.35 (s, 1H), 3.02 (d, *J* = 7 Hz, 1H), 1.48 (s, 9H), 1.43 (s, 9H), 1.46 (s, 3H), 1.33 (s, 3H). ^{19}F NMR (CD_3CN): δ –335.43 (d, *J* = 15 Hz, 1F). HRMS-ESI (m/z): $[M - C_6H_4NO_2S]^+$ calcd for $C_{28}H_{36}FN_2Pd$ 525.1897; Found, 525.1906.

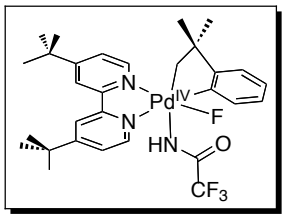

Complex 26. Cs_2CO_3 (29 mg, 0.089 mmol, 3.0 equiv) and 2,2,2-trifluoroacetamide (10 mg, 0.089 mmol, 3.0 equiv) were combined in MeCN (2.5 mL) at 65 °C and allowed to stir for 2 h. The solution was allowed to cool and complex **22** (20 mg, 0.03 mmol, 1.0 equiv) was added to the reaction mixture. The reaction was shaken for ~ 1 min and then filtered over a pipette filled with celite. The filtrate was collected and the solvent was removed by rotary evaporation. CH_2Cl_2 (2 mL) was added to the off white solid and decanted into a vial. The solvent was removed by rotary evaporation and petroleum ether (3 mL) was added to the vial and the solution was decanted. The solvent was removed by rotary evaporation and the solid was dissolved in (0.5 mL) chlorobenzene and allowed to crystalize by diffusion with pentanes at -35 °C. The filtrate was removed from the solid/crystals and the solvent was removed by rotary evaporation to afford an off white solid (6 mg, 32% yield). ^{1}H NMR (CD_3CN): δ 8.73 (d, *J* = 6 Hz, 1H), 8.43 (s, 1H), 8.38 (s, 1H), 7.93 (d, *J* = 6 Hz, 1H), 7.85 (d, *J* = 6 Hz, 1H), 7.72 (d, *J* = 8 Hz, 1H), 7.54 (d, *J* = 7 Hz, 1H), 7.40 (d, *J* = 6 Hz, 1H),

7.22 (t, *J* = 7 Hz, 1H), 7.16 (d, *J* = 8 Hz, 1H), 7.02 (d, *J* = 8 Hz, 1H), 4.72 (dd, *J* = 15, 7 Hz, 1H), 4.12 (d, *J* = 7 Hz, 1H), 3.02 (s, 1H), 1.52 (s, 9H), 1.43 (s, 9H), 1.41 (s, 3H), 1.09 (s, 3H). ^{19}F NMR (CD_3CN): δ –79.56 (s, 3F), –339.67 (d, *J* = 15 Hz, 1F). ^{13}C NMR data could not be obtained due to the instability of the complex over the timescale required for the experiment. HRMS-ESI (m/z): $[M - C_2HF_3NO]^+$ calcd for $C_{28}H_{36}FN_2Pd$ 525.1897; Found, 525.1901. HRMS-ESI (m/z): $[M - F]^+$ calcd for $C_{30}H_{37}F_3N_3OPd$ 618.1924; Found, 618.1910.

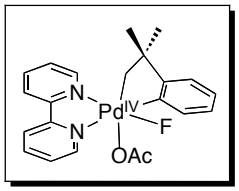

Complex 28. Compound 2 (4.3 mg, 0.008 mmol, 1.0 equiv) was dissolved in CD_3CN (0.25 mL) and frozen with liquid nitrogen in a screw cap NMR tube sealed with a Teflon-lined cap. A solution of Bu_4NOAc (2.3 mg, 0.008 mmol, 1.0 equiv) in CD_3CN (0.25 mL) with CH_2Cl_2 as an internal standard was added to the NMR tube and frozen with liquid nitrogen. The reaction mixture was allowed to warm to room temperature in the NMR probe. After 5 min, a spectrum was acquired. The reaction was repeated three times and the yield is an average of the three trials. Yield: 90% as determined by ^{1}H NMR spectroscopic analysis of the crude reaction mixture. ^{1}H NMR (CD_3CN): δ 8.89 (d, *J* = 5 Hz, 1H), 8.52 (multiple peaks, 2H), 8.37-8.29 (multiple peaks, 2H), 7.95 (multiple peaks, 2H), 7.76 (t, *J* = 6 Hz, 1H), 7.55 (t, *J* = 8 Hz, 1H), 7.29-7.18 (multiple peaks, 2H), 7.07 (t, *J* = 7 Hz, 1H), 4.74 (dd, *J* = 15, 6 Hz, 1H), 4.17 (multiplet, 1H), 2.18 (s, 3H), 1.58 (s, 3H), 1.33 (s, 3H). ^{19}F NMR (CD_3CN): δ –329.56 (d, *J* = 15 Hz, 1F). *^{13}C NMR data could not be obtained due to the instability of the complex over the timescale required for the experiment.*

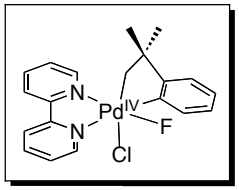

Complex 29. Compound 2 (4.3 mg, 0.008 mmol, 1.0 equiv) and Bu_4NCl (2.1 mg, 0.008 mmol, 1.0 equiv) were dissolved in CD_3CN (0.5 mL) with CH_2Cl_2 as an internal standard. After 5 minutes at 25 °C the reaction was analyzed by ^1H NMR spectroscopy. The reaction was repeated three times, and the yield is an average of the three trials. Yield: 91% as determined by ^1H NMR spectroscopic analysis of the crude reaction mixture. ^1H NMR (CD_3CN): δ 8.95 (d, *J* = 5 Hz, 1H), 8.50-8.47 (multiple peaks, 2H), 8.32 (t, *J* = 6 Hz, 1H), 8.29 (t, *J* = 6 Hz, 1H), 8.20 (t, *J* = 8 Hz, 1H), 7.99 (d, *J* = 6 Hz, 1H), 7.87 (d, *J* = 5 Hz, 1H), 7.47 (t, *J* = 7 Hz, 1H), 7.26-7.16 (multiple peaks, 2H), 7.03 (d, *J* = 7 Hz, 1H), 4.58 (dd, *J* = 15, 6 Hz, 1H), 3.84 (multiplet, 1H), 1.05 (s, 3H), 0.70 (s, 3H). ^{19}F NMR (CD_3CN): δ–337.49 (d, *J* = 15 Hz, 1F). ^{13}C NMR data could not be obtained due to the instability of the complex over the timescale required for the experiment.

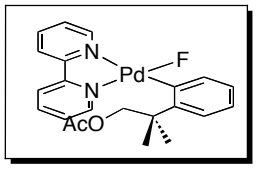

Complex 30. Compound 2 (4.3 mg, 0.008 mmol, 1.0 equiv) and Bu_4NOAc (2.3 mg, 0.008 mmol, 1.0 equiv) were dissolved in CD_3CN (0.5 mL) with CH_2Cl_2 as an internal standard. This reaction was stirred for 2 h to yield compound 30. The reaction was repeated three times and the yield is an average of the three trials. Yield: 77% as determined by ^1H NMR spectroscopic analysis of the crude reaction mixture. ^1H NMR (CD_3CN): δ 8.43 (d, *J* = 5 Hz, 1H), 8.28 (d, *J* = 8 Hz, 1H), 8.23 (d, *J* = 8 Hz, 1H), 8.16 (t, *J* = 8 Hz, 1H), 8.04 (t, *J* = 8 Hz, 1H), 7.97 (d, *J* = 7 Hz, 1H), 7.64 (t, *J* = 6 Hz, 1H), 7.48 (d, *J* = 6 Hz, 1H), 7.28 (t, *J* = 7 Hz, 1H), 7.16 (d, *J* = 8 Hz, 1H), 6.95 (t, J = 7 Hz, 1H), 6.87 (t, *J* = 8 Hz, 1H), 5.17 (d, *J* =

11 Hz, 1H), 4.55 (d, *J* = 11 Hz, 1H), 1.84 (s, 3H), 1.64 (s, 3H), 1.76 (s, 3H). ^{19}F NMR (MeCN) –30 °C: δ –146.54 (broad s, 1F). *This compound could not be isolated cleanly from the mixture without decomposition. Therefore it was converted to compound* ***S1*** *for complete characterization.*

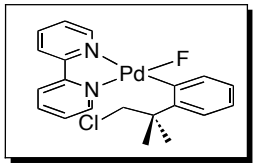

Complex 31. Compound 2 (4.3 mg, 0.008 mmol, 1.0 equiv) and Bu_4NCl (2.1 mg, 0.008 mmol, 1.0 equiv) were dissolved in CD_3CN (0.5 mL) with CH_2Cl_2 as an internal standard. This reaction was stirred for 2 h at 25 ºC to yield compound 31. The reaction was repeated three times and the yield is an average of the three trials. Yield: 63% as determined by ^1H NMR spectroscopic analysis of the crude reaction mixture. ^1H NMR (CD_3CN): δ 9.15 (d, *J* = 5 Hz, 1H), 8.36-8.25 (multiple peaks, 2H), 8.19 (t, *J* = 8 Hz, 1H), 8.10 (t, *J* = 8 Hz, 1H), 7.78 (d, J= *J* = 8 Hz, 1H), 7.72 (t, *J* = 7 Hz, 1H), 7.55 (d, *J* = 7 Hz, 1H), 7.36 (t, *J* = 5 Hz, 1H), 7.26 (d, *J* = 8 Hz, 1H), 6.99 (t, *J* = 8 Hz, 1H), 6.92 (t, *J* = 8 Hz, 1H), 4.58 (d, *J* = 11 Hz, 1H), 4.10 (d, *J* = 11 Hz, 1H), 1.85 (s, 3H), 1.70 (s, 3H). *This compound could not be isolated cleanly from the mixture without decomposition. Therefore it was converted to compound* ***S2*** *for complete characterization.*

Scheme 3.6.2 Synthesis and Characterization of Complexes S1 and S2 Derived from 30 and 31

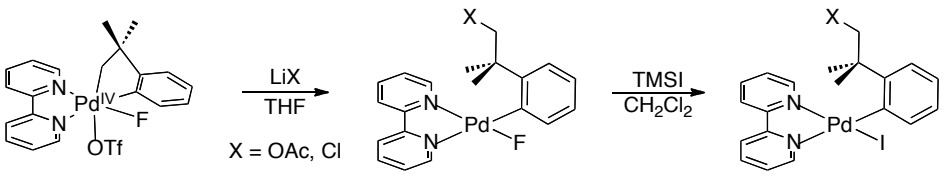

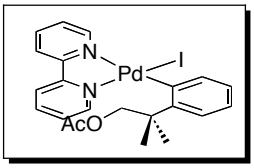

Complex S1. Compound **2** (50 mg, 0.09 mmol, 1.0 equiv) and LiOAc (7.6 mg, 0.12 mmol, 1.3 equiv) were combined in THF (10 mL), and this reaction mixture was stirred for 1 h at 25 ºC. The reaction mixture was filtered through celite, and the solvent was removed by rotary evaporation. The resulting yellow oil was dissolved in MeCN (5 mL) and TMSI (13 μL, 0.09 mmol, 1.0 equiv) was added. The solvent was removed by rotary evaporation. The yellow oil was washed with diethyl ether (10 mL), dissolved in CH_2Cl_2 (2 mL), and then the product was precipitated with pentane (15 mL). The resulting solid was collected, and MeCN (1 mL) was added. The solid was collected and dried under vacuum to afford **S1** as a tacky yellow solid (18 mg, 35% yield). ^{1}H NMR (CD_2Cl_2): δ 9.65 (d, *J* = 5 Hz, 1H), 8.11-8.05 (multiple peaks, 2H), 8.03 (t, *J* = 8 Hz, 1H), 8.00 (t, *J* = 7 Hz, 1H), 7.78 (d, *J* = 8 Hz, 1H), 7.58 (t, *J* = 5 Hz, 1H), 7.32-7.30 (multiple peaks, 2H), 7.24 (d, *J* = 8 Hz, 1H), 6.94 (t, *J* = 7 Hz, 1H), 6.83 (t, *J* = 7 Hz, 1H), 4.73 (d, *J* = 11 Hz, 1H), 4.51 (d, *J* = 11 Hz, 1H), 1.80 (s, 3H), 1.69 (s, 3H), 1.59 (s, 3H). ^{13}C NMR ($CDCl_3$): δ 171.05, 158.97, 153.28, 153.10, 150.07, 138.35, 137.17, 127.77, 127.14, 126.74, 126.05, 125.10, 124.75, 124.14, 123.26, 121.67, 121.39, 74.25, 38.94, 21.95, 19.32. HRMS-ESI (m/z): $[M - I]^+$ calcd for $C_{22}H_{23}N_2O_2Pd$ 453.0789; Found, 453.0791.

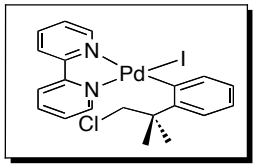

Complex S2. Compound **2** (50 mg, 0.09 mmol, 1.0 equiv) and LiCl (4.9 mg, 0.12 mmol, 1.3 equiv) were combined in THF (10 mL), and this reaction mixture was stirred for 1 h at 25 ºC. The reaction was filtered through celite, and the solvent was removed by rotary evaporation. The resulting yellow oil was dissolved in MeCN (5 mL), and TMSI (13 μL, 0.09 mmol, 1.0 equiv) was added. The solvent was removed by rotary evaporation. The yellow oil was washed with diethyl ether (10 mL), dissolved in CH_2Cl_2 (2 mL), and then the product was precipitated with pentane (15 mL). The solid was collected, and MeCN (1 mL) was added After filtration over a small pad of celite, the filtrate was collected and the solvent was removed by rotary evaporation. The solid was collected and dried under vacuum to afford **S2** as a tacky yellow solid (24 mg, 48% yield). ^{1}H NMR (CD_2Cl_2): δ 9.58 (d, J = 5 Hz, 1H), 8.03-8.00 (multiple peaks, 2H), 7.97 (t, v = 8 Hz, 1H), 7.92 (t, *J* = 8 Hz, 1H), 7.72 (d, *J* = 8 Hz, 1H), 7.51 (t, *J* = 5 Hz, 1H), 7.29 (d, *J* = 8 Hz, 1H), 7.24 (t, *J* = 6 Hz, 1H), 7.17 (d, *J* = 8 Hz, 1H), 6.87 (t, *J* = 7 Hz, 1H), 6.77 (t, *J* = 8 Hz, 1H), 4.22 (d, *J* = 11 Hz, 1H), 3.91 (d, *J* = 11 Hz, 1H), 1.70 (s, 3H), 1.67 (s, 3H). ^{13}C NMR (CD_2Cl_2): δ 157.62, 155.83, 154.62, 151.87, 150.55, 144.13, 140.40, 140.34, 138.87, 129.62, 128.40, 128.05, 125.80, 124.86, 123.58, 123.38, 59.29, 42.40, 30.80 (two overlapping carbon's). HRMS-ESI (m/z): $[M - I]^+$ calcd for $C_{20}H_{20}ClN_2Pd$ 429.0344; Found, 429.0348.

Scheme 3.6.3 Reaction of 21 with Oxidants

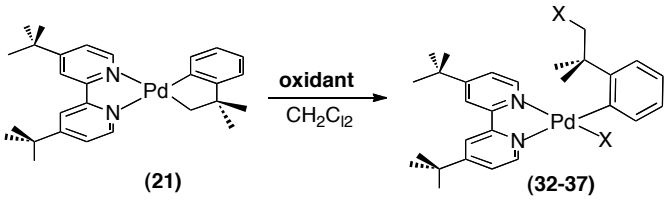

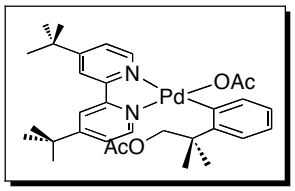

Complex 32. Compound **21** (200 mg, 0.395, 1.0 equiv) was combined with $PhI(OAc)_2$ (127 mg, 0.395 mmol, 1.0 equiv) in CH_2Cl_2 (100 mL), and the reaction mixture allowed to stir for 15 min. The solution was concentrated under vacuum to ~2 mL and diethyl ether (20 mL) was added to precipitate the product. Complex **32** was isolated as a pale yellow solid (130 mg, 53% yield). ^{1}H NMR (MeCN): δ 8.33 (d, *J* = 6 Hz, 1H), 8.29 (s, 1H), 8.23 (s, 1H), 7.98 (d, *J* = 6 Hz, 1H), 7.69 (d, *J* = 6 Hz, 1H), 7.38-7.30 (multiple peaks, 2H), 7.18 (d, *J* = 8 Hz, 1H), 6.97 (t, *J* = 7 Hz, 1H), 6.87 (t, *J* = 7 Hz, 1H), 5.41 (d, J = 10 Hz, 1H), 4.48 (d, J = 10 Hz, 1H), 1.86 (s, 3H), 1.76 (s, 3H), 1.65 (s, 3H), 1.64 (s, 3H), 1.47 (s, 9H), 1.38(s, 9H). ^{13}C NMR ($CDCl_3$): δ 176.38, 171.18, 165.07, 164.60, 156.75, 154.02, 152.07, 151.87, 150.49, 148.72, 136.42, 127.01, 124.37, 124.34, 124.31, 123.93, 120.90, 120.40, 74.52, 40.17, 36.12, 36.10, 30.19, 29.99, 28.12, 27.69, 23.90, 20.80. HRMS-electrospray (m/z): $[M - OAc]^+$ calcd for $C_{30}H_{39}N_2O_2Pd$, 565.2051; Found, 565.2041.

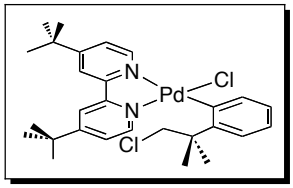

Complex 33. Compound **21** (200 mg, 0.394 mmol, 1.0 equiv) and $PhICl_2$ (110 mg, 0.394 mmol, 1.0 equiv) were combined in CH_2Cl_2 (40 mL), and the resulting solution was stirred for 15 min. The reaction mixture was concentrated to ~4 mL, and hexanes (~30 mL) was added to precipitate the product. The precipitate was collected and dried under vacuum to afford **33** was isolated as a bright yellow solid (223 mg, 98% yield). ^{1}H NMR ($CDCl_3$): δ 9.16 (d, *J* = 6 Hz, 1H), 7.95 (multiple peaks, 2H), 7.84 (d, *J* = 8 Hz, 1H), 7.54 (d, J = 6 Hz, 1H), 7.46 (d, *J* = 6 Hz, 1H), 7.26-7.19 (multiple peaks, 2H), 6.96 (t, *J* = 7 Hz, 1H), 6.90 (t, J = 7 Hz, 1H), 4.76 (d, *J* = 11 Hz, 1H), 3.93 (d, *J* = 11 Hz, 1H), 1.81 (s, 3H), 1.78 (s, 3H), 1.43 (s, 9H), 1.37 (s, 9H). ^{13}C NMR ($CDCl_3$): δ 163.59, 163.16, 155.76, 153.49, 151.53, 149.36, 148.79, 148.03, 134.97, 127.42, 124.85, 123.55 overlapping carbons, 2C), 123.52, 118.36, 117.80, 57.88, 41.28, 35.55 (2C, overlapping), 30.46, 30.27, 29.03, 28.81. HRMS-EI (m/z): $[M+]^+$ calcd for $C_{29}H_{39}Cl_2N_2Pd$, 591.1525; Found, 591.1518.

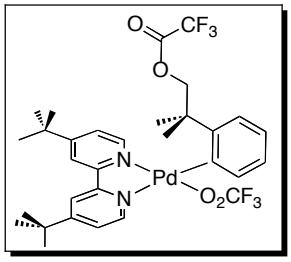

Complex 34. Compound **21** (80 mg, 0.158, 1.0 equiv) was combined with $PhI(O_2CCF_3)_2$ (68 mg, 0.158 mmol, 1.0 equiv) in CH_2Cl_2 (50 mL), and the reaction mixture allowed to stir for 15 min. The solution was concentrated under vacuum. Then, ~1 mL CH_2Cl_2 was added to the yellow oil and diethyl ether (20 mL) was added to precipitate the product. Complex **21** was isolated as a pale yellow solid (72 mg, 61% yield). ^{1}H NMR (acetone): δ 8.60 (s, 1H), 8.56 (s, 1H),

8.22 (d, *J* = 6 Hz, 1H), 7.96 (d, *J* = 8 Hz, 1H), 7.83 (d, *J* = 6 Hz, 1H), 7.44-7.38 (multiple peaks, 2H), 7.13 (d, *J* = 8 Hz, 1H), 6.93 (t, *J* = 7 Hz, 1H), 6.83 (t, *J* = 7 Hz, 1H), 5.42 (d, *J* = 11 Hz, 1H), 4.91 (d, *J* = 11 Hz, 1H), 1.76 (s, 3H), 1.68 (s, 3H), 1.42 (s, 9H), 1.36 (s, 9H). ^{19}F NMR (MeCN): δ –78.17(s, 3F), –78.73 (s, 3F). HRMS-electrospray (m/z): [M – $C_2O_2F_3$]$^+$ calcd for $C_{31}H_{40}F_3N_2O_2Pd$, 619.1764; Found, 619.1780.

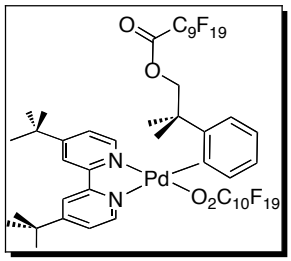

Complex 35. Compound **21** (30 mg, 0.059, 1.0 equiv) was combined with $PhI(O_2C_{10}F_{19})_2$ (73 mg, 0.059 mmol, 1.0 equiv) in CH_2Cl_2 (40 mL), and the reaction mixture allowed to stir for 15 min. The solution was concentrated under vacuum. Then, ~1 mL CH_2Cl_2 was added to the yellow oil and pentanes (20 mL) was added to precipitate the product. Complex **35** was isolated as a pale yellow solid (74 mg, 81% yield). ^{1}H NMR ($CDCl_3$): δ 8.30 (d, *J* = 6 Hz, 1H), 7.97 (d, *J* = 8 Hz, 1H), 7.95 (s, 1H), 7.92 (s, 1H), 7,53 (d, *J* = 6 Hz, 1H), 7.44 (d, *J* = 6 Hz, 1H), 7.15 (d, *J* = 6 Hz, 1H), 7.09 (d, *J* = 7 Hz, 1H), 6.94 (t, *J* = 7 Hz, 1H), 6.88 (t, *J* = 8 Hz, 1H), 5.47 (d, *J* = 11 Hz, 1H), 4.67 (d, *J* = 11 Hz, 1H), 1.75 (s, 3H), 1.69 (s, 3H), 1.41 (s, 9H), 1.34 (s, 9H). ^{19}F NMR (CD_2Cl_2): δ –82.49 to – 82.51 (multiple peaks, 6F), –117.35 (br. s, 2F), –120.08 (br. s, 2F), –123.54 to –124.51 (multiple peaks, 24F), –127.90 (br. s, 4F). ^{13}C NMR (CD_2Cl_2): δ 165.98, 165.65, 163.19 (t, *J* = 25 Hz, 1C), 159.56 (t, *J* = 30 Hz, 1C), 157.83, 154.71, 153.30, 150.07, 149.61, 149.26, 138.99, 136.67, 126.08, 126.02, 125.53, 125.41, 120.61, 120.12, 119.49 (t, *J* = 34 Hz, 1C), 117.85 (t, *J* = 27 Hz, 1C), 114.11-109.61 (b peaks, 16 C), 41.29, 37.09, 36.99, 31.56, 31.35, 28.65, 28.30, 26.61. HRMS-

electrospray (m/z): $[M - C_{10}F_{19}O_2]^+$ calcd for $C_{38}H_{36}F_{19}N_2O_2Pd$, 1019.1503; Found, 1019.1518.

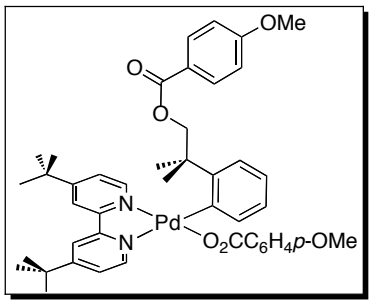

Complex 36. Compound **21** (15 mg, 0.03, 1.0 equiv) was combined with $PhI(O_2CC_6H_4p\text{-}OMe)_2$ (15 mg, 0.03 mmol, 1.0 equiv) in CH_2Cl_2 (15 mL), and the reaction mixture allowed to stir for 15 min. The solution was concentrated under vacuum to ~2 mL and diethyl ether (20 mL) was added to precipitate the product. Complex **36** was isolated as a pale yellow solid (14 mg, 72% yield). ^{1}H NMR ($CDCl_3$): δ 8.41 (d, *J* = 6 Hz, 1H), 8.21 (d, *J* = 7 Hz, 1H), 8.00 (app. d, *J* = 8 Hz, 2H), 7.89 (s, 1H), 7.81 (s, 1H), 7.72 (app. d, *J* = 8 Hz, 2H), 7.44 (d, *J* = 6 Hz, 1H), 7.30-7.23 (multiple peaks, 2H), 6.98 (t, *J* = 6 Hz, 1H), 6.90 (t, *J* = 6 Hz, 1H), 6.83-6.76 (multiple peaks, 3H), 6.60 (d, *J* = 6 Hz, 1H), 6.00 (d, *J* = 10 Hz, 1H), 4.49 (d, *J* = 10 Hz, 1H), 1.94 (s, 3H), 1.71 (s, 3H), 1.38 (s, 9H), 1.16(s, 9H). ^{13}C NMR ($CDCl_3$): δ 172.79, 165.93, 163.25, 163.10, 162.54, 161.10, 155.93, 153.20, 151.69, 151.04, 149.30, 148.82, 135.73, 132.08, 131.54, 131.37, 129.32, 126.29, 124.19, 123.79, 123.15, 123.11, 118.39, 117.80, 113.50, 112.55, 74.55, 55.44, 55.22, 35.47, 35.17, 34.68, 30.39, 30.02, 28.34, 27.63. HRMS-electrospray (m/z): $[M - C_8H_7O_3]^+$ calcd for $C_{36}H_{43}N_2O_3Pd$, 657.2309; Found, 657.2328.

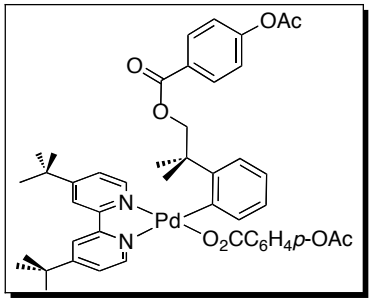

Complex 37. Compound **21** (20 mg, 0.039, 1.0 equiv) was combined with $PhI(O_2CC_6H_4p\text{-}OMe)_2$ (17 mg, 0.039 mmol, 1.0 equiv) in CH_2Cl_2 (15 mL), and the reaction mixture allowed to stir for 30 min. The solution was concentrated under vacuum. Then, diethyl ether (5 mL) was added to the yellow oil and decanted. Pentanes (5 mL) was added to the reaction and decanted. Complex **37** was isolated as a pale yellow solid (28 mg, 83% yield). ^{1}H NMR (MeCN): δ 8.28-8.27 (multiple peaks, 2H), 8.17 (d, *J* = 2 Hz, 1H), 8.05 (dd, *J* = 7 Hz, *J* = 2 Hz, 1H), 7.98-7.96 (multiple peaks, 2H), 7.79-7.78 (multiple peaks, 2H), 7.75 (d, *J* = 8 Hz, 1H), 7.61 (dd, *J* = 6 Hz, *J* = 2 Hz, 1H), 7.35 (d, *J* = 6 Hz, 1H), 7.28 (dd, *J* = 8 Hz, *J* = 2 Hz, 1H), 7.18 (t, *J* = 8 Hz, 1H), 7.13-7.12 (multiple peaks, 2H), 7.01-6.97 (multiple peaks, 3H), 6.88-6.86 (multiple peaks, 2H), 6.04 (d, *J* = 11 Hz, 1H), 4.61 (d, *J* = 11 Hz, 1H), 2.27 (s, 3H), 2.25 (s, 3H), 1.80 (s, 1H), 1.77 (s, 1H), 1.43 (s, 9H), 1.22 (s, 9H). NMR (MeCN): δ 171.57, 170.78, 170.05, 170.03, 169.68, 166.54, 166.38, 165.78, 164.45, 156.57, 155.11, 153.95, 153.12, 152.00, 151.74, 150.39, 148.54, 138.08, 136.29, 134.88, 131.29, 128.63, 127.09, 124.44, 124.42, 124.13, 124.06, 122.67, 121.58, 120.99, 120.40, 75.34, 40.37, 36.16, 35.87, 30.11, 29.81, 28.31, 28.22, 27.72, 20.96. HRMS-electrospray (m/z): $[M + H]^+$ calcd for $C_{46}H_{48}N_2O_8Pd$, 863.2518; Found, 863.2539.

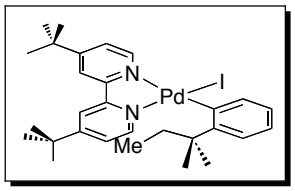

Complex 42. Compound **21** (50 mg, 0.0986, 1.0 equiv) was combined with MeI (6 μL, 0.0986 mmol, 1.0 equiv) in CH_2Cl_2 (20 mL), and the reaction mixture allowed to stir for 15 min. The solution was concentrated under vacuum to ~2 mL and pentane (10 mL) was added to precipitate the product. Complex **38** was isolated as a pale yellow solid (52 mg, 81% yield). ^{1}H NMR (CD_2Cl_2): δ 9.50 (d, *J* = 6 Hz, 1H), 8.15 (d, *J* = 6 Hz, 1H), 7.94 (app. s, 2H), 7.47 (d, *J* = 6 Hz, 1H), 7.37 (d, *J* = 6 Hz, 1H), 7.17 (d, *J* = 6 Hz, 1H), 6.96 (app. s, 3H), 2.73 (s, 2H), 2.71 (s, 3H), 1.67 (s, 6H), 1.39 (s, 9H), 1.38 (s, 9H). ^{13}C NMR (CD_2Cl_2): δ 162.09, 162.00, 155.71, 153.02, 152.08, 149.49, 147.94, 136.90, 132.37, 125.65, 124.92 (2 overlapping C's), 123.28, 122.18, 118.06, 117.28, 120.90, 120.40, 41.66, 34.98 (2 overlapping C's), 33.58 (2 overlapping C's), 30.04, 29.90, 26.39, 24.02. HRMS-electrospray (m/z): $[M - I]^+$ calcd for $C_{29}H_{39}N_2Pd$, 521.2154; Found, 521.2143.

Scheme 3.6.4 Reaction 21 with NFTPT, Cs_2CO_3 and Amide

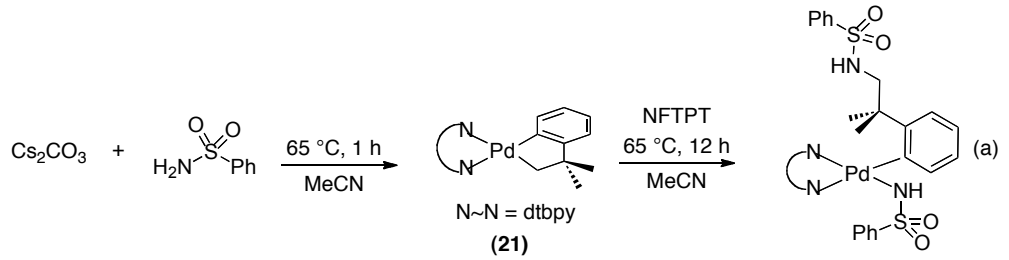

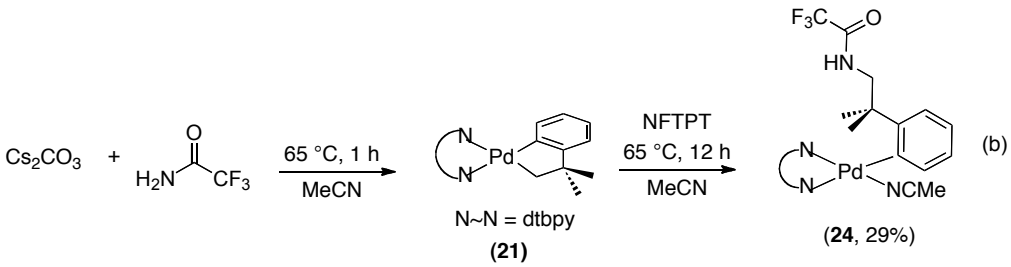

Cs_2CO_3 (10 mg, 0.031 mmol, 4.0 equiv) and benzenesulfonamide (4.8 mg, 0.031 mmol, 4.0 equiv) were combined in MeCN (0.5 mL) (with nitrotoluene as a standard) at 65 °C and allowed to stir for 1 h. The solution was allowed to cool and complex **21** (3.8 mg, 0.0075 mmol, 1.0 equiv) and NFTPT (2.2 mg, 0.0075 mmol, 1.0 equiv) was added to the reaction mixture. The reaction was heated at 65 °C for 12 h. The yield (71% an average of two trials) of **25** was determined by ^{1}H NMR spectroscopy.

Cs_2CO_3 (10 mg, 0.031 mmol, 4.0 equiv) and 2,2,2-trifluoroacetamide (3.4 mg, 0.031 mmol, 4.0 equiv) were combined in MeCN (0.5 mL) (with nitrotoluene as a standard) at 65 °C and allowed to stir for 1 h. The solution was allowed to cool and complex **21** (3.8 mg, 0.0075 mmol, 1.0 equiv) and NFTPT (2.2 mg, 0.0075 mmol, 1.0 equiv) was added to the reaction mixture. The reaction was heated at

65 °C for 12 h. The yield (29% an average of two trials) of **26** was determined by ^{1}H NMR spectroscopy.

Scheme 3.6.5 ^{1}H NMR Reaction 22 with NFTPT, Cs_2CO_3 and Amide

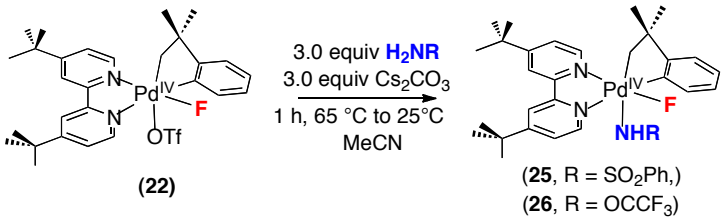

Cs_2CO_3 (7.4 mg, 0.023 mmol, 3.0 equiv) and benzenesulfonamide (3.6 mg, 0.023 mmol, 3.0 equiv) were combined in MeCN (0.5 mL) (with nitrotoluene as a standard) at 65 °C and allowed to stir for 1 h. The solution was allowed to cool and complex **22** (5.1 mg, 0.0076 mmol, 1.0 equiv) was added to the reaction mixture. The yield (82%) of **25** was determined by ^{1}H NMR spectroscopy.

Cs_2CO_3 (7.4 mg, 0.023 mmol, 3.0 equiv) and 2,2,2-trifluoroacetamide (2.6 mg, 0.023 mmol, 3.0 equiv) were combined in MeCN (0.5 mL) (with nitrotoluene as a standard) at 65 °C and allowed to stir for 1 h. The solution was allowed to cool and complex **22** (5.1 mg, 0.0076 mmol, 1.0 equiv) was added to the reaction mixture. The yield (79%) of **26** was determined by ^{1}H NMR spectroscopy.

Scheme 3.6.6 Distribution of Products from the Reductive Elimination of 25 and 26

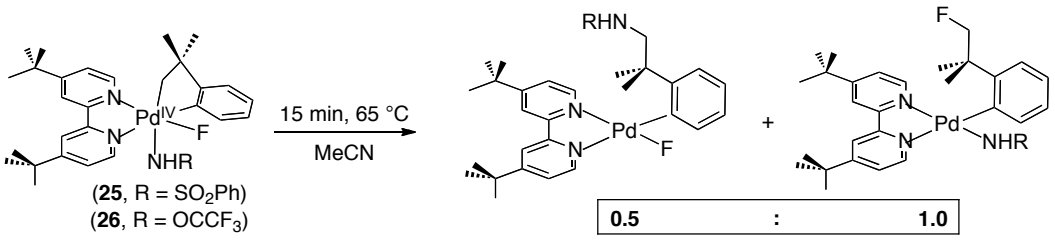

Complex **25** (4.8 mg, 0.007 mmol) was dissolved in MeCN (0.5 mL) (with nitrotoluene as a standard) and heated at 65 °C for 15 min. The ratio of sp^3-C–N and sp^3-C–F reductive elimination products was determined by ^1H NMR spectroscopy. Although the sp^3-C–N and sp^3-C–F products were not isolated from the reaction mixture, the products analyzed were determined to be either the sp^3-C–N and sp^3-C–F by the coupling constant and splitting pattern in the ^1H NMR.

Complex **26** (5.0 mg, 0.0075 mmol) was dissolved in MeCN (0.5 mL) (with nitrotoluene as a standard) and heated at 65 °C for 15 min. The ratio of sp^3-C–N and sp^3-C–F reductive elimination products was determined by ^1H NMR spectroscopy. Although the sp^3-C–N and sp^3-C–F products were not isolated from the reaction mixture, the products analyzed were determined to be either the sp^3-C–N and sp^3-C–F by the coupling constant and splitting pattern in the ^1H NMR.

Scheme 3.6.7 Reductive Elimination of 25 and 26 with Excess Cs_2CO_3 and Amide

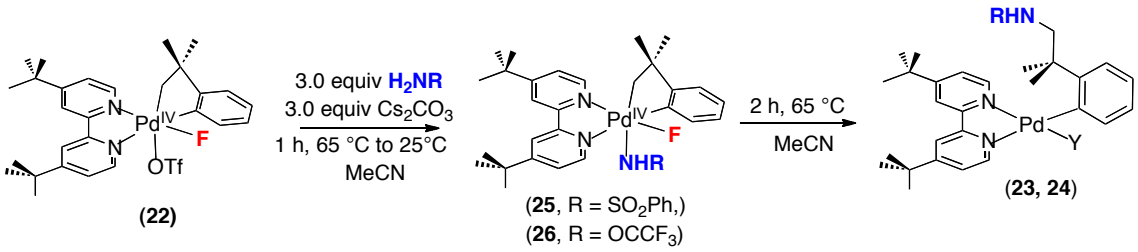

Cs_2CO_3 (7.4 mg, 0.023 mmol, 3.0 equiv) and benzenesulfonamide (3.6 mg, 0.023 mmol, 3.0 equiv) were combined in MeCN (0.5 mL) (with nitrotoluene as a

standard) at 65 °C and allowed to stir for 1 h. The solution was allowed to cool and complex **22** (5.1 mg, 0.0076 mmol, 1.0 equiv) was added to the reaction mixture. The reaction was heated at 65 °C for 2 h. The yield (70%) of **23** was determined by ^{1}H NMR spectroscopy.

Cs_2CO_3 (7.4 mg, 0.023 mmol, 3.0 equiv) and 2,2,2-trifluoroacetamide (2.6 mg, 0.023 mmol, 3.0 equiv) were combined in MeCN (0.5 mL) (with nitrotoluene as a standard) at 65 °C and allowed to stir for 1 h. The solution was allowed to cool and complex **22** (5.1 mg, 0.0076 mmol, 1.0 equiv) was added to the reaction mixture. The reaction was heated at 65 °C for 2 h. The yield (48%) of **24** was determined by ^{1}H NMR spectroscopy.

Figure 3.6.2 Representative Rate Data of Decompostion of 25

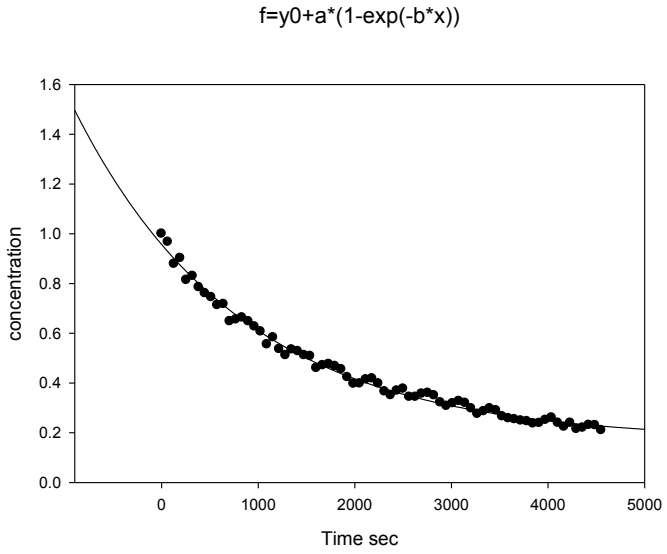

Scheme 3.6.7 Reaction of 21 with PhIO and NBu_4X

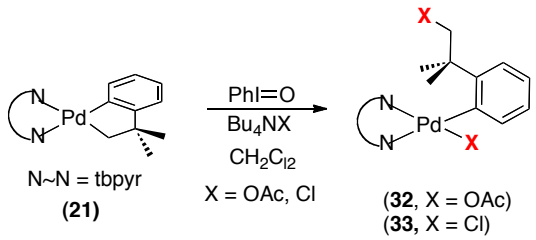

Complex **21** (3.8 mg, 0.0075, 1.0 equiv) was combined with iodosylbenzene (3.3 mg, 0.0082, 1.1 equiv) and either NBu_4OAc (6.3 mg, 0.021 mmol, 3.0 equiv) or NBu_4Cl (6.2 mg, 0.021 mmol, 3.0 equiv) and heated at 65 °C for 2 h in CH_2Cl_2 (0.5 mL) with DCE as an internal standard. For product **32** the peak at 9.05 ppm in the ^1H NMR spectrum was integrated relative to the standard and two trials gave an average yield of 76%. For product **33** the peak at 9.09 ppm in the ^1H NMR spectrum was integrated relative to the standard and two trials gave an average yield of 46%.

Scheme 3.6.8 Low Temperature Reaction of 21 with $PhI(O_2CC_9F_{19})_2$

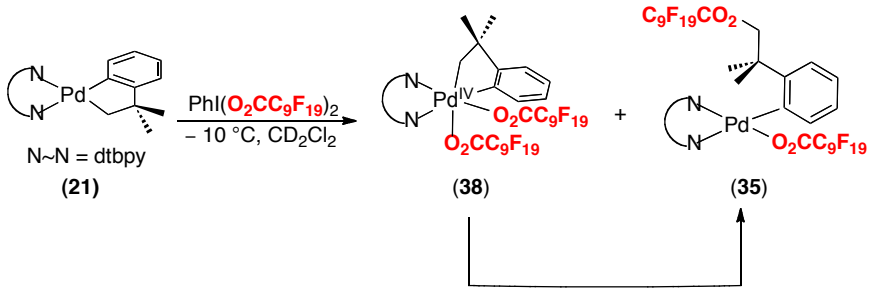

Complex **21 (**3.8 mg, 0.0076, 1.0 equiv) was dissolved in (0.25 mL) of CD_2Cl_2 and placed in a Teflon screw cap NMR tube and frozen with liquid nitrogen. $PhI(O_2CC_9F_{19})_2$ (9.3 mg, 0.0076 mmol, 1.0 equiv) was dissolved in (0.25 mL) of CD_2Cl_2 and placed in a Teflon screw cap NMR tube and frozen on top of the solution of complex **21** with liquid nitrogen. The reaction was allowed to warm in the NMR spectrometer and monitored via ^1H NMR spectroscopy.

Scheme 3.6.9 Reaction of 21 with CH_3I and XX equiv NBu_4I

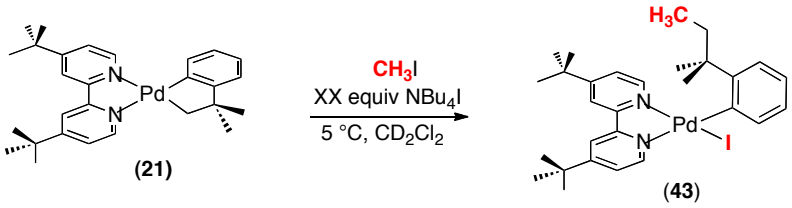

Determining Order in NBu_4I with 21 and CH_3I at 5 °C in CD_2Cl_2

Complex **21** (3.8 mg, 0.0076 mmol, 1.0 equiv) and CH_3I (0.43 μL, 0.0076 mmol, 1.0 equiv) were combined in CD_2Cl_2 (0.25 mL) and placed in a screw cap NMR tube, then frozen with liquid nitrogen. NBu_4I (0.0227 to 0.0834 mmol, 45 mM to 167 mM) and CD_2Cl_2 (0.25 mL) were combined in the same screw cap NMR tube and frozen on top of the layer with complex **21** and CH_3I. An internal standard (dichloroethane) was added (20 μl of a stock solution in CD_2Cl_2, 0.00758, 1 equiv) and the tube was sealed with a Teflon®-lined cap. The NMR tube was allowed to thaw and then immediately placed in an NMR spectrometer with the temperature pre-equilbrated to 5 °C, and the reaction was allowed to equilibrate for 2 min. The rate of reductive elimination was monitored by ^{19}H NMR spectroscopy by monitoring the disappearance of the starting material (**21**). The reaction was followed to between 2-3 half lives, and the data was plotted as –

ln[**21**/**21º**] versus time. A representative kinetics run is shown in Figure 3.6.3. The values of k_{obs} for each [pyridine] are reported in Table 3.6.2.

Table 3.6.3 Rate as a Function of [NBu4I] at 5 °C

equiv NBu_4I	$[NBu_4I]$	$[1/NBu_4I]$	k_{obs}
3.0	0.0227	44.05	1.22×10^{-2}
5.0	0.0379	26.38	5.8×10^{-3}
7.0	0.0531	18.83	4.6×10^{-3}
9.0	0.0682	14.66	2.6×10^{-3}
11.0	0.0834	11.99	1.9×10^{-3}

Figure 3.6.3 Representative Rate Data (Reductive Elimination from 21 with CH_3I in the Presence of 106 mM NBu_4I)

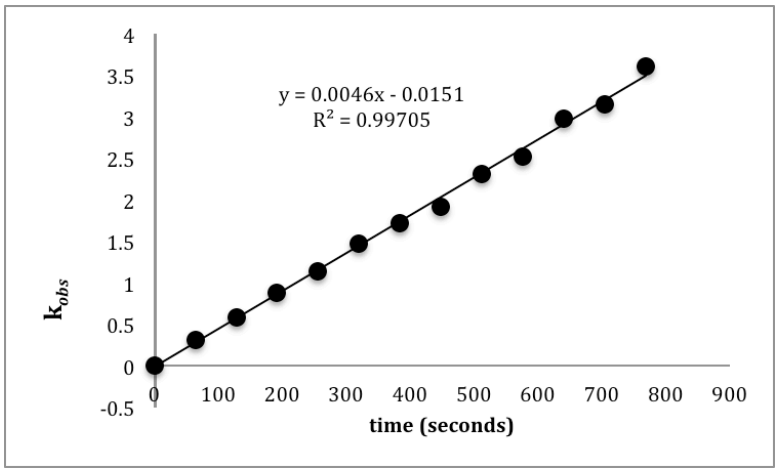

3.7 References and Footnotes

1. (a) Kakiuchi, F.; Chatani, N. *Adv. Synth. Catal.* **2003**, *345*, 1077. (b) Labinger, J. A.; Bercaw, J. E. *Nature* **2002**, *417*, 507. (c) Shilov, A. E.; Shul'pin, G. B. *Chem. Rev.* **1997**, *97*, 2879.

2. Lyons T. W.; Sanford, M. S. *Chem. Rev.* **2010**,*110*,1147.

3. Desai, L. V.; Hull, K. L.; Sanford, M. S. *J. Am. Chem. Soc.* **2004**, *126*, 9542.

4. (a) Huheey, J. E. *Inorganic Chemistry: Principles of Structure & Reactivity*, 5th ed.; Addison-Wesley: **2009**. (b) James, A. M.; Lord, M. P. *Macmillan's Chemical and Physical Data*; Macmillan: London, **1992**.

5. Sehnal, P.; Taylor, R. J. K.; Fairlamb, I. J. S. *Chem. Rev.*, **2010**, *110*, 824.

6. (a) Powers, D. C.; Ritter, T. *Top. Organomet. Chem.* **2011**, *35*, 129. (b) Xu, L. M.; Li, B. J.; Yang, Z.; Shi, Z. J. *Chem. Soc. Rev.* **2010**, *39*, 712. (c) Sehnal, P.; Taylor, R. J. K.; Fairlamb, I. J. S. *Chem. Rev.* **2010**, *110*, 824. (d) Deprez, N. R.; Sanford, M. S. *Inorg. Chem.* **2007**, *46*, 1924. (e) Muniz, K. *Angew. Chem. Int. Ed.* **2009**, *48*, 9412. (f) Canty, A. J. *Dalton Trans.* **2009**, *47*, 10409.

7. (a) Racowski J. M.; Dick A. R.; Sanford M. S. *J. Am. Chem. Soc.* **2009**, *131*, 10974. (b) Dick A. R.; Kampf, J. W.; Sanford, M. S. *J. Am. Chem. Soc*., **2005**, *127*, 12790. (c) Powers, D. C.; Benitez, D.; Tkatchouk, E.; Goddard, III W. A.; Ritter T. *J. Am. Chem. Soc.* **2010**, *132*, 14092.

8. (a) Furuya, T.; Ritter, T. *J. Am. Chem. Soc.* **2008**, *130*, 10060. (b) Furuya, T.; Ritter, T. *J. Am. Chem. Soc.,* **2008** 130, 12834. (c) Furuya, T.; Benitez, D.; Tkatchouk, E.; Strom, A. E.; Tang, P.; Goddard, III W. A.; Ritter, T. *J. Am. Chem. Soc.*, **2010**, *132*, 3793. (d) Furuya. T; Benitez, D.; Tkatchouk, E.; Strom, A. E.; Tang, P.; Goddard, III W.A.; Ritter, T. *J. Am. Chem. Soc.*, **2010**, *132*, 5922.

9. (a) Ye, Y.; Ball, N. D.; Kampf, J. W.; Sanford, M. S. *J. Am. Chem. Soc.* **2010**, *132*, 14682. (b) Ball, N. D.; Kampf, J. W.; Sanford, M. S. *J. Am. Chem. Soc.* **2010**, *132*, 2878. (c) Ball, N. D.; Gary, J. B.; Ye, Y.; Sanford, M. S. *J. Am. Chem. Soc.* **2011**, *133*, 7577.

10. Racowski, J. M.; Sanford, M. S. *Top. Organomet. Chem.*, **2011**, *53*, 61.

11. Loudon, G. M. *Organic Chemistry*, 4th ed.; Oxford University Press: **2002,** 360-371.

12. Canty, A. J.; Denney, M. C.; Skelton, B. W.; White, A. H. *Inorg. Chem. Commun.,* **2004**, *4*, 648.

13. van Asselt, R.; Rijnberg, E.; Elsevier, C. J. *Organometallics*, **1994**, *13*, 706.

14. Canty, A. J.; Hoarse, J. L.; Davies, N. W.; Traill, P. R. *Organometallics*, **1998**, *17*, 2046.

15. Canty, A. J.; Denney, M. C.; Skelton, B. W., White, A. H. *Organometallic,s* **2004**, *23*, 1122.

16. Canty, A. J.; Jin, H. *J. Organomet. Chem.,* **1998**, *565*, 135.

17. Vincente, J.; Chicote, M. T.; Lagunas, M. C.; Jones, P. G.; Bembenek, E. *Organometallics*, **1994**, *13*, 1243.

18. Reviews: a) K. M. Engle, T. S. Mei, X. Wang, J. Q. Yu *Angew. Chem.* **2011**, *123*, 1514-1528; *Angew. Chem., Int. Ed.* **2011**, *50*, 1478-1491. b) T. Furuya, A. S. Kamlet, T. Ritter *Nature*, **2011**, *473*, 470-477. c) V. V. Grushin *Acc. Chem. Res.* **2010**, *43*, 160-171. d) A. Vigalok, A. W. Kaspi, *Top. Organomet. Chem.* **2010**, *31*, 19-38.

19. $Pd^{0/II}$ catalysis for sp^2-C–F bond formation: a) T. J. Maimone, P. J. Milner, T. Kinzel, Y. Zhang, M. K. Takase, S. N. Buchwald, *J. Am. Chem. Soc.* **2011**, asap article. b) M. H. Katcher, A. Sha, A. G. Doyle, *J. Am. Chem. Soc.* **2011**, *133*, 15902-15905. c) T. Noel, T. J. Maimone, S. L. Buchwald, *Angew. Chem.* **2011**, *123*, 9062-9065; *Angew. Chem. Int. Ed.* **2011**, *50*, 8900-8903. d) C. Hollingworth, A. Hazari, M. N. Hopkinson, M. Tredwell, E. Benedetto, M. Huiban, A. D. Gee, J. M. Brown, V. Gouverneur, *Angew. Chem.* **2011**, *123*, 2661-2665; *Angew. Chem. Int. Ed.* **2011**, *50*, 2613-2617. c) M. H. Katcher; A. G. Doyle, *J. Am. Chem. Soc.* **2010**, *132*, 17402-17404. d) D. A. Watson, M. Su, G. Teverovskiy, Y. Zhang, J. Garcia-Fortanet, T. Kinzel, S. L. Buchwald *Science* **2009**, *321*, 1661-1664.

20. Other recent examples of metal-catalyzed fluorination reactions: a) T. Xu, X. Mu, H. Peng, G. Liu, *Angew. Chem. Int. Ed.* **2011**, *123*, 8326-8329; *Angew. Chem. Int. Ed.* **2011**, *50*, 8176-8179. b) P. Tang, T. Furuya, T. Ritter *J. Am. Chem. Soc.* **2010**, *132*, 12150-12154. c) J. A. Kalow, A. G. Doyle, *J. Am. Chem. Soc.* **2010**, *132*, 3268-3269. d) Review on Au-catalyzed fluorination reactions: M. N. Hopkinson, A. G. Gee, V. Gouverneur, *Isr. J. Chem.* **2010**, *50*, 675-690.

21. Pd-catalyzed C-H fluorination with F^+ reagents: a) K. S. L. Chan, M. Wasa, X. Wang, J. Q. Yu, *Angew. Chem.* **2011**, *123*, 9247-9250; *Angew. Chem. Int. Ed.* **2011**, *50*, 9081-9084. b) X. Wang, T. S. Mei, J. Q. Yu *J. Am. Chem. Soc.* **2009**, *131*, 7520-7521. c) K. L. Hull, W. Q. Anani, M. S. Sanford *J. Am. Chem. Soc.* **2006**, *128*, 7134-7135.

22. Pd-catalyzed olefin aminofluorination with F^+ reagents: T. Wu, G. Yin, G. Liu, *J. Am. Chem. Soc.* **2009**, *131*, 16354-16355.

23. Stoichiometric aryl–F coupling from Pd^{II}/F^+: T. Ritter *Angew. Chem.* **2008**, *120*, 6082-6085; *Angew. Chem. Int. Ed.* **2008**, *47*, 5993-5996.

24. a) T. Furuya, D. Benitez, E. Tkatchouk, A. E. Strom, P. Tang, W.A. Goddard III, T. Ritter *J. Am. Chem. Soc.* **2010**, *132*, 3793-3807. b) N. D. Ball, M. S. Sanford *J. Am. Chem. Soc.* **2009**, *131*, 3796-3797.

25. A.W. Kaspi, I. Goldberg, A. Vigalok, *J. Am. Chem. Soc.* **2010**, *132*, 10626-10627.

26. S. B. Zhao, J. J. Becker, M. R. Gagne, *Organometallics* **2011**, *30*, 3926-3929.

27. For a recent example of sp^3-C–F bond-forming reductive elimination from *in situ* generated Au^{III} complexes, see: N. P. Mankad, F. D. Toste *Chem. Sci.* **2011**, advance article.

28. For the microscopic reverse (oxidative addition of sp^3-C–F bonds), see: J. Choi, D. Y. Wang, S. Kundu, Y. Choliy, T. J. Emge, K. Krough-Jespersen, A. S. Goldman *Science* **2011**, *332*, 1545-1548.

29. J. Campora, J. A. Lopez, P. Palma, D. Rio, E. Carmona, P. Valerga, C. Graiff, A. Tiripicchio, *Inorg. Chem.* **2001**, *40*, 4116-4126.

30. Use of NFTPT to access high oxidation state Pd complexes: a) J. M. Racowski, N. D. Ball, M. S. Sanford, *J. Am. Chem. Soc.* **2011**, *133*, asap article. b) N. D. Ball, J. B. Gary, Y. Ye, M. S. Sanford, *J. Am. Chem. Soc.* **2011**, *133*, 7577-7584.

31. V. V. Grushin, *Chem.-Eur. J.* **2002**, *8*, 1006-1014.

32. a) P. Sehnal, R. J. K. Taylor, I. J. S. Fairlamb, *Chem. Rev.* **2010**, *110*, 824-889. b) J. M. Racowski. M. S. Sanford *Top. Organomet. Chem.* **2010**, *53*, 63-84.

33. M. B. Smith, J. March, *March's Advanced Organic Chemistry: Reactions, Mechanisms and Structure*: Wiley: New York, **2007**.

34. Thermolysis of complexes **2** and **4** yielded complex and intractable mixtures of products. We hypothesize that this may be due to decomposition of the initially formed reductive elimination products (analogues of **6** and **7**), since these Pd^{II} species would contain highly labile OH_2 and/or OTf ligands.

35. J. F. Hartwig *Organotransition Metal Chemistry: From Bonding to Catalysis* University Science Books: Sausalito, 2010, p. 332-333.

36. Crabtree, R. H. *The Organometallic Chemistry of Transition Metals* John Wiley & Sons: Hoboken, NJ 2005. b) P. R. Mitchel, P. V. Parish *J. Chem. Educ.* **1969**, *46*, 811-814.

37. Ball, N. D.; Sanford, M. S. *J. Am. Chem. Soc.* **2009**, *131*, 3796-3797.

38. Whitfield, S. R.; Sanford, M. S. *J. Am. Chem. Soc.* **2007**, *129*, 15142-15143.

39. Engle, K. M.; Mei, T. S.; Wang, X.; Yu, J. Q. *Angew. Chem. Int. Ed.* **2011**, *50*, 1478-1491.

40. Mei, X.; Wang, J. Q.; Yu, J. Q. *J. Am. Chem. Soc.* **2009**, *131*, 10806-10807.

41. Pawlikowski, A. V.; Getty, A. D.; Goldberg, K. I. *J. Am. Chem. Soc.* **2007**, *129*, 10382-10393.

42. (a) Williams, B. S.; Holland, A. W.; Goldberg, K. I. *J. Am. Chem. Soc.* **1999**, *121*, 252. (b) Williams, B. S.; Goldberg, K. I. *J. Am. Chem. Soc.* **2001**, *123*, 2576.

43. (a) Goldberg, K. I.; Yan, J.; Winter, E. L. J. Am. Chem. Soc. 1994, 116, 1573. (b) Goldberg, K. I.; Yan, J.; Breitung, E. M. *J. Am. Chem. Soc.* 1**995**, *117*, 6889.

44. (a) Koo, K.; Hillhouse, G. I. *Organometallics* **1995**, *14*, 4421. (b) Koo, K.; Hillhouse, G. I. *Organometallics* **1996**, *15*, 2669.

45. Sanford, M. S.; Groves, J. T. *Angew. Chem., Int. Ed*. **2004**, *43*, 588.

46. Marquard, S. L.; Rosenfeld, D. C.; Hartwig, J. F. *Angew. Chem.* **2010**, *122*, 805-808.

47. Fujita, K; Yamashita, M.; Puschmann, F.; Alvarez-Falcon, M. M.; Incarvito, C. D.; Hartwig, J. F. *J. Am. Chem. Soc.* **2006**, *128*, 9044-9045.

48. Crumpton, D. M.; Goldberg, K. I. *J. Am. Chem. Soc.* **2000**, *122*, 962.

49. (a) Byers, P. K.; Canty, A. J.; Skelton, B. W.; White, A. H. *J. Chem. Soc. Chem. Commun.,* **1986**, 1722. (b) Canty, A. J.; Denney, M. C., Skelton, B. W.; White, A. H. *Organometallics*, **2004**, *23*, 1122.

Chapter 4: C–H Bond Activation at Palladium^{IV} Centers

4.1 Introduction

Over the past decade, high oxidation state palladium catalysis has found increasingly diverse applications in organic synthesis.[1] The development of new transformations in this area has been guided by fundamental studies of Pd^{III} and Pd^{IV} model complexes, which have provided key insights into the unique reactivity and mechanisms accessible at high valent palladium centers.[1,2] To date, these model studies have primarily focused on reductive elimination from Pd^{III} and/or Pd^{IV} species.[1,2] In contrast, the possibility of other organometallic transformations at high oxidation state Pd has not been explored in detail. This is likely due to the assumption that reductive elimination occurs much faster than competing reactions.fr

Very recently, several groups have proposed a new reaction – C–H activation at a transient Pd^{IV} intermediate – as a key step in catalysis.[3-7] This novel mode of reactivity has been implicated in four different catalytic contexts: (*i*) the oxidative dimerization of 2-arylpyridine derivatives,[3] (*ii*) the carboamination of olefins,[4] (*iii*) the acetoxylation of allylic C–H bonds,[5] and (*iv*) the C–H arylation of naphthalene.[6,7] Remarkably, many of these catalytic reactions proceed under unusually mild conditions[3-5] and/or exhibit unprecedented site selectivities (Scheme 4.1.1).[3,4,6] These results suggest that harnessing C–H activation at Pd^{IV} could provide opportunities for achieving distinct and highly complementary reactivity relative to analogous and more common transformations at Pd^{II} centers.

Scheme 4.1.1 Catalytic Reactions in which C–H Activation at Pd^{IV} Proposed as a Key Step

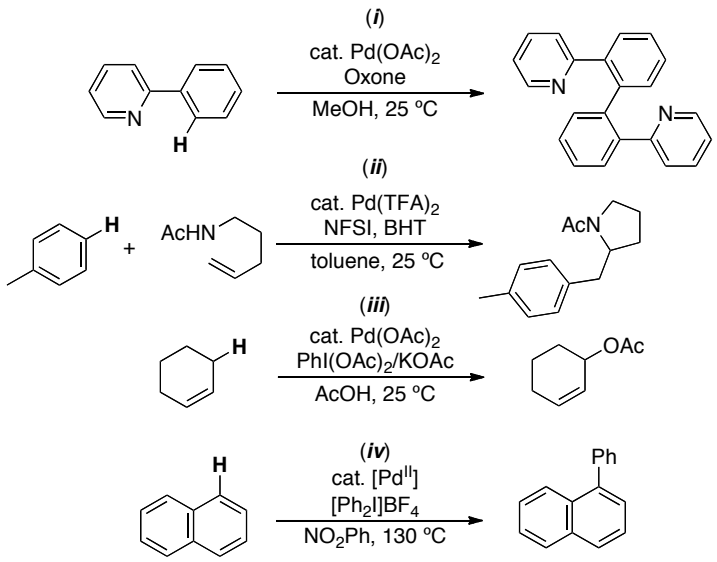

While the reports described above have proposed C–H activation at Pd^{IV} during catalysis, until this work there was no literature precedent for such a transformation. As such, my goal was to design model systems to demonstrate the viability of this reaction and to probe reactivity and site selectivity in this context.[8,9] This work demonstrates that, with appropriate choice of supporting ligands, C–H activation at a Pd^{IV} center can proceed rapidly at temperatures as low as –40 °C. Furthermore, we showed that the site selectivity of this transformation can be dramatically different than that at analogous Pd^{II} complexes. The results demonstrated in this chapter provide a novel platform for incorporating C–H activation at a Pd^{IV} center as a step in new catalytic processes.

In order to observe and study C–H activation at Pd^{IV}, it was critical to slow competing C–X bond-forming reductive elimination (k_{RE}) while increasing the relative rate of the desired C–H activation process (k_{C-H}) (Scheme 4.1.2).

Scheme 4.1.2. Competing Reductive Elimination versus C–H Activation at Pd^{IV}

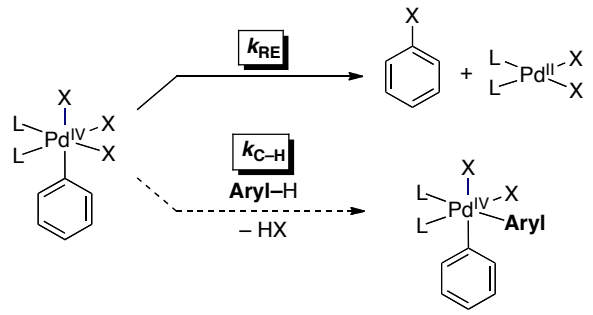

4.2 Initial Results

Our first attempt to observe C–H activation (*intermolecular*) at Pd^{IV} involved complexes of an analogous structure to the compounds that I synthesized and isolated in Chapter 2. I reasoned that Pd^{IV} complex $(N\sim C)_2Pd^{IV}(Cl)_2$ (**I-1**) (N~C = 2-phenylpyridine) might serve as an attractive target. I reasoned that the chloride ligands could serve two appealing purposes. First, complex **I-1** been shown to require higher temperatures to undergo bond-forming reductive elimination than related $(N\sim C)_2Pd^{IV}(OAc)_2$.[10] Thus, **I-1** might permit for the C–H activation event to out-compete reductive elimination. Secondly, the incorporation of chloride ligands onto the complex would allow for easy abstraction with a silver salt. This would open a coordination site on the metal and hopefully allow for the desired C–H activation reaction to take place.

Gratifyingly, the treatment of complex **I-1** with 1.0 equiv of AgOTf and 2.0 equiv of pyridine resulted in the successful synthesis and isolation of complex **I-2** (Scheme 4.2.1)**.** Crystallization of complex **I-2** was achieved by slow diffusion of hexanes into a chlorobenzene solution at –35 °C (Figure 4.2.1). The crystal structure shows a cationic Pd^{IV} center where the chloride substituent was replaced with a pyridine ligand at the site on the complex that is *trans* to the σ-aryl carbon.

Scheme 4.2.1 Synthesis of Complex I-2

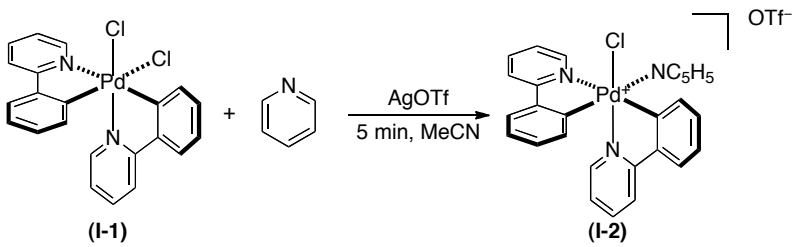

Figure 4.2.1 ORTEP of Complex I-2 (Triflate Counterion Omitted for Clarity)

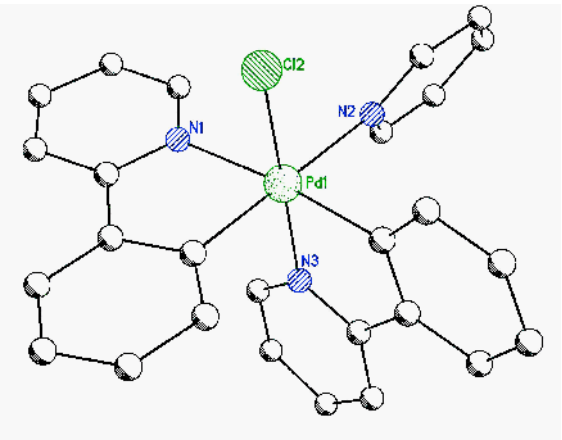

Unfortunately, when complex **I-2** was screened for the intermolecular C–H activation reaction with various arenes (1,2-dimethoxybenzene, aniline, toluene, benzene, (trifluoromethyl)bezene, etc) over a range of temperatures and solvents only C–Cl and C–C reductive elimination products were observed (Scheme 4.2.2).

Scheme 4.2.2 Screen for Intermolecular C–H Activation with I-2

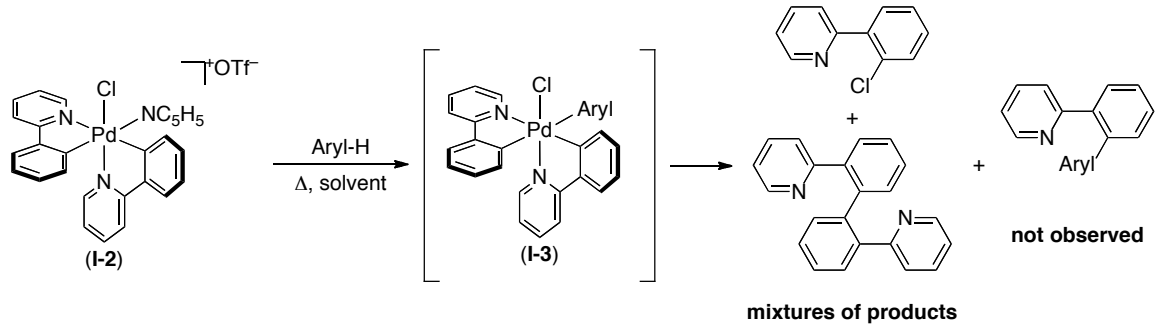

At this point, we considered the need for a more stable Pd^{IV} complex that would not undergo the undesired reductive elimination event so easily. Therefore, we searched the literature for a relatively stable cationic Pd^{IV} complex and found complex **I-4**, which had been previously synthesized by Campora and co-workers.[11] The trispyrazolylborate ligand has been shown to impart significant stability to high oxidation state palladium, while we reasoned that the pyridine ligand might be easily replaced with an arene substrate. Complex **I-4** was indeed highly stable towards reductive elimination. However, in the presence of various arene substrates, the complex was either unreactive or decomposed into a complex mixture of unidentifiable products (Scheme 4.2.3).

Scheme 4.2.3 Screen for Intermolecular C–H Activation with I-4

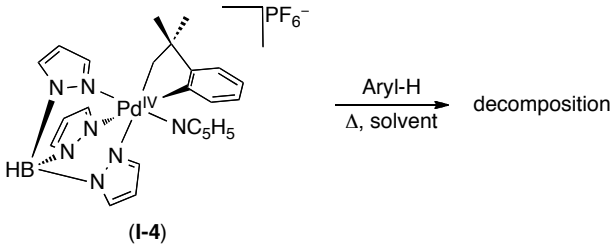

4.3 Results

On the basis of the previous mentioned considerations and unsuccessful attempts at intermolecular C–H activation, we initiated investigations of oxidatively-induced *intramolecular* C–H activation at complex **1** (Scheme 4.3.1). This Pd^{II} starting material contains a rigid bidentate sp^2 N-donor ligand [2,2'-di-*tert*-butylbipyridine (dtbpy)] and a chloride. Both of these ligands are known to slow reductive elimination (k_{RE}) from high valent Pd intermediates,[13-15] often enabling detection/isolation of Pd^{III} or Pd^{IV} species.[1,2,13-15] In addition, the tethered aryl C–H bond could undergo sp^2 C–H activation to afford a favorable 5-membered palladacycle. The intramolecular nature of this C–H cleavage event is expected to increase k_{C-H}.[12]

We first examined the oxidation of **1** with $PhICl_2$, since this reagent is known to react with Pd^{II} starting materials to yield isolable Pd^{IV} products.[15] As shown in Scheme 4.3.1, the reaction produced two major inorganic compounds: $Pd^{II}Cl_2$(dtbpy) (**2**, 83% yield) and complex **3** (16% yield). Both **2** and **3** are Pd^{II} species rather than the desired Pd^{IV} products; however, **3** is remarkable in that it contains a σ-aryl rather than a σ-alkyl ligand bound to Pd. We hypothesized that **2** and **3** might be formed from transient Pd^{IV} intermediate **I**, which could undergo competing sp^3-C–Cl bond-forming reductive elimination (to liberate **2**) and C–H activation/sp^3-C–Cl bond-formation to generate **3**. While these were promising initial results, complex **3** remained a minor side product under all conditions examined. Additionally, efforts to observe Pd^{IV} intermediates **I** and/or **II** were unsuccessful in this system.

Scheme 4.3.1 Oxidation of 1 with $PhICl_2$: Formation of 2 and 3 (N~N = dtbpy)

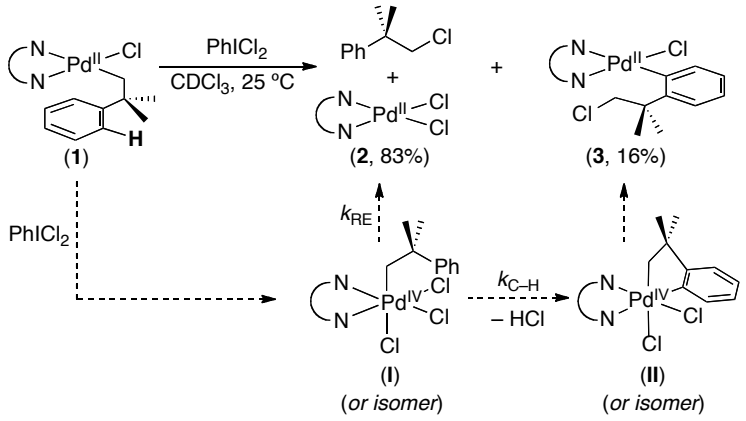

The results in Scheme 4.3.1 suggest that k_{RE} is significantly faster than $k_{C–H}$ for intermediate **I**. We reasoned that this problem could be addressed by: (1) replacing the chloride with an X-type ligand that is less prone to reductive elimination and (2) limiting the conformational flexibility of the tethered C–H substrate. As such, guided by the work of my group member and co-author on this published manuscript, Dr. Nicholas Ball, we next targeted $Pd^{II}(CF_3)(2\text{-}PhC_6H_4)(dtbpy)$ (**4**) as a Pd^{II} starting material. Dr. Nicholas Ball observed an interesting result when he treated complex **4** with *N*-fluoro-2,4,6-trimethylpyridinium triflate (NFTPT) and hypothesized that C–H activation might be occurring on the *ortho*-phenyl ring of the complex. The incorporation of the CF_3 ligand was a particularly important design feature, since several recent reports have shown that $Pd^{IV}(CF_3)(Aryl)$ complexes can be stable to reductive elimination at or above room temperature.[16] Complex **4** was prepared in 58% yield by the reaction of $Pd^{II}(I)(2\text{-}PhC_6H_4)(dtbpy)$ with $CsF/TMSCF_3$ in THF.

The treatment of **4** with 1 equiv of $PhICl_2$ in MeCN at 25 °C for 35 min resulted in a color change from pale yellow to dark yellow along with the formation of products **5-Cl**, **6**, and **7** in 81%, 12%, and 11% yield as determined by ^1H NMR spectroscopic analysis of the crude reaction mixture (Scheme 3.3.2).

Complex **5-Cl** was isolated in 77% yield by recrystallization from CH_2Cl_2/Et_2O. Characterization of **5-Cl** by NMR spectroscopy, mass spectrometry, and X-ray crystallography (of a close analogue, *vide infra*) revealed that this is an octahedral Pd^{IV} complex containing a cyclometalated biphenyl ligand. This indicates that the desired C–H activation event has occurred.

Scheme 4.3.2 Oxidation of 4 with $PhICl_2$

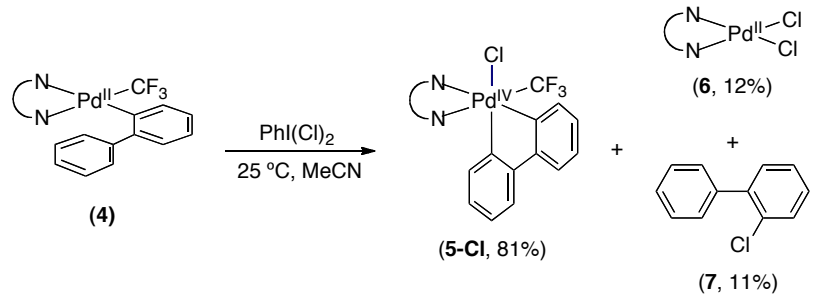

In order to gain insights into the mechanism of the C–H activation process, we monitored the reaction of **4** with d_5-$PhICl_2$ at –30 ºC in CD_3CN (Scheme 4.3.3). ^1H and ^{19}F NMR analysis showed fast consumption of starting material, and the formation of a transient intermediate **8**.[17] Upon warming to RT, this intermediate decayed over 35 min with 1st order kinetics to form a mixture of **5-Cl** and **6** (final ratio of **5-Cl** : **6** = 1.0 : 0.27 under these conditions). Intermediate **8** shows resonances associated with 15 aromatic protons, and a ^1H-^1H COSY allowed assignment of five distinct protons on the pendant phenyl ring.[18] This indicates that this ring is not yet cyclometalated (and also shows that rotation about the aryl-aryl bond is slow on the NMR timescale). ^{19}F-^{13}C HMBC further confirmed that **8** contains a single σ-aryl ligand, as the CF_3 fluorines showed only one correlation with an aromatic carbon. In contrast, two ^{19}F-^{13}C HBMC correlations were observed for the cyclometalated product **5-Cl**. Finally, a DOSY experiment showed that **5-Cl** and **8** have nearly identical diffusion coefficients at

–15 ºC, indicating that these complexes have similar hydrodynamic radii. This is consistent with the formulation of **8** as a monomeric octahedral complex.

Mass spectrometry experiments provided further insights into the molecular structure of **8**. ESI-MS showed a peak at 631.1312, which corresponds to the mass of $[Pd(CF_3)(2\text{-}PhC_6H_4)(Cl)(dtbpy)]^+$. Notably, electrospray ionization commonly results in loss of one X-type ligand from Pd^{IV} complexes.[2g] For example, ESI-MS of **5-Cl** affords a peak at 595.1560, corresponding to the mass of $[\mathbf{5\text{-}Cl}–Cl]^+$. MALDI, a softer ionization technique, resulted in a peak at 667.1, which corresponds to $[Pd(CF_3)(2\text{-}PhC_6H_4)(Cl)_2(dtbpy)+H]^+$.

Scheme 4.3.3 Low temperature NMR study of reaction of 4 with d_5-$PhICl_2$

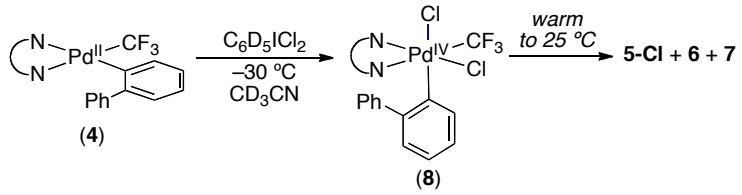

All of the NMR and MS data presented above are consistent with formulation of intermediate **8** as a Pd^{IV} complex of general structure $Pd^{IV}(CF_3)(2\text{-}PhC_6H_4)(Cl)_2(dtbpy)$. The diamagnetic nature of this complex clearly indicates that it is not a monomeric Pd^{III} species. The NMR diffusion experiment along with MALDI MS data provide evidence against alternative formulations as a Pd^{III} dimer or a square planar Pd^{II} complex.[19] *Overall, the characterization data are fully consistent with the C–H activation event occurring at Pd^{IV} intermediate **8***, thereby representing the first demonstration that high oxidation state Pd can mediate this transformation.

We next explored the reaction of **4** with other $2e^-$ oxidants. While no reaction was observed with iodobenzene diacetate ($PhI(OAc)_2$, Table 4.3.1, entry 3),[2g] both iodobenzene bistrifluoroacetate $PhI(TFA)_2$ and *N*-fluoro-2,4,6-trimethylpyridinium triflate (NFTPT)[16] reacted with **4** within 10 min at rt to afford

cyclometalated Pd^{IV} complexes where X = trifluoroacetate and triflate (**5-TFA** and **5-OTf**, respectively). The structure of the trifluoroacetate complex was confirmed by X-ray crystallography, and an ORTEP picture of **5-TFA** is shown in Figure 4.3.1. Consistent with the solution NMR data, the crystal structure shows an unsymmetrical ligand environment around the octahedral Pd^{IV} center, with the trifluoroacetate group *trans* to one σ-aryl ligand and the trifluoromethyl group *trans* to one N of the dtbpy (Figure 4.3.1).

Table 4.3.1 Variation of Oxidant (N~N = dtbpy)

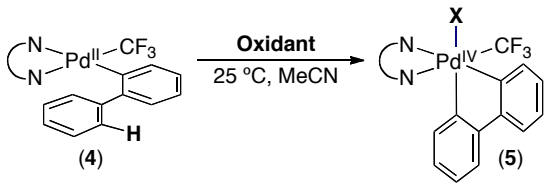

Entry	Oxidant	X (Product)	Yield (%)
1	$PhICl_2$	Cl (**5-Cl**)	77
2	$PhI(TFA)_2$	TFA (**5-**	73
3	$PhI(OAc)_2$	OAc (**5-OAc**)	nr[a]
4	NFTPT	OTf (**5-OTf**)	86

[a] No reaction observed after 12 h at 25 °C.

Figure 4.3.1 ORTEP Plot of 5-TFA

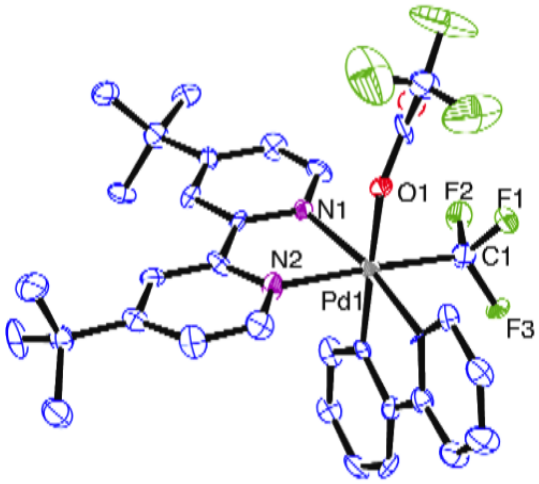

Substrate **9** was also examined in order to probe the accessibility of a six-membered palladacycle (Scheme 4.3.4). In this case, reaction with $PhICl_2$ for 10 min at 25 ºC returned the *ortho*-chlorinated Pd^{II} product **10** in 95% yield. This result suggests that a 6-membered palladacycle was generated, but that the resulting Pd^{IV} intermediate underwent rapid C–Cl bond-forming reductive elimination under the reaction conditions.[20]

Scheme 4.3.4 Oxidation of 9 with $PhI(Cl)_2$

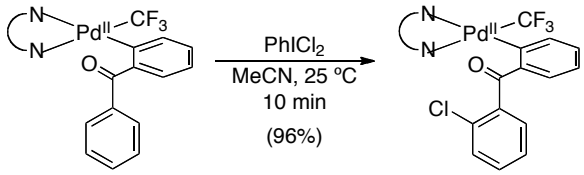

Finally, we conducted a series of experiments to compare this C–H activation at Pd^{IV} to analogous transformations at Pd^{II} centers. A σ-aryl ligand derived from 2-iodo-3,5'-dimethyl-1,1'-biphenyl (ligand abbreviated σ-DMB) was

used, since it contains two sterically and electronically differentiated sites for C–H activation (H_A and H_B**)**. As shown in Scheme 3.3.5, the treatment of σ-DMB complex **11** with NFTPT at rt in MeCN produced a 1.7 : 1 mixture of two isomeric products **12-OTf** and **13-OTf** in 64% yield.[21,22] While **12-OTf/13-OTf** could not be completely separated, the mixture was characterized using a variety of two-dimensional NMR experiments (see section 4.4). In addition, treatment of **12-OTf/13-OTf** with NaCl afforded the corresponding chloride complexes (**12-Cl/13-Cl)**, and the structure of the major isomer was definitively established by X-ray crystallography. As shown in Figure 4.3.2, the X-ray structure confirms that **12-Cl** (and by analogy **12-OTf**) is the product of C–H activation at H_A.

Scheme 4.3.5 Site Selectivity of C–H Activation at Pd^{IV}

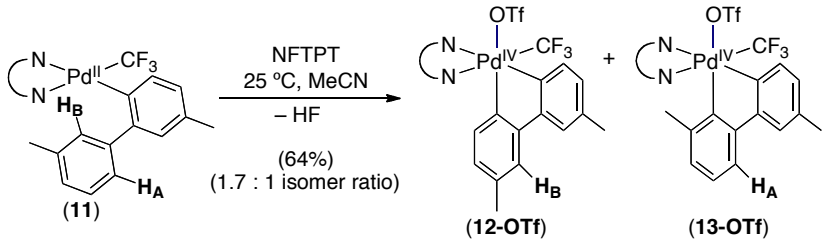

Figure 4.3.2 ORTEP Plot of **12-Cl**

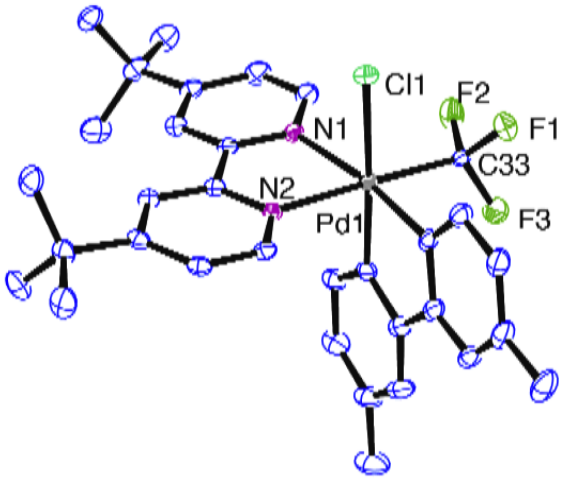

For comparison, we examined an analogous cyclopalladation reaction at the Pd^{II} σ-DMB complex **14-F** (Scheme 4.3.6), which was generated *in situ* by the treatment of **14-I** with AgF. Cyclopalladation at **14-F** was sluggish at room temperature and required heating to 60 ºC in benzene for 4 h to proceed to completion. Furthermore, this reaction afforded >10 : 1 selectivity for activation of the less sterically hindered C–H bond (H_A).[23] This selectivity is similar to that observed in numerous other cyclopalladation reactions at Pd^{II} centers, but very different from that observed in Scheme 4.3.5 (1.7 : 1).[24] The significant difference in both rate and selectivity for this C–H activation at Pd^{II} versus Pd^{IV} highlights the dissimilarity of these processes, and highlights the potential value of Pd^{IV}-mediated C–H activation in catalysis.

Scheme 4.3.6 Site Selectivity of C–H Activation at Pd^{IV}

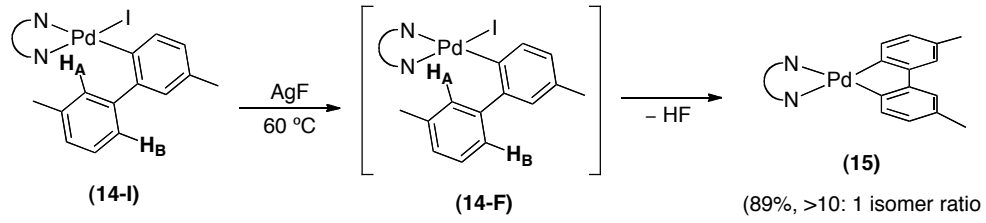

4.3 Conclusions

In summary, this chapter describes the first observation and study of C–H activation at Pd^{IV}. This transformation was achieved by designing model complexes in which the rate of reductive elimination is slowed relative to that of the desired competing C–H activation process. Remarkably, the C–H activation reaction can proceed under mild conditions and with different site selectivity than analogous transformations at Pd^{II}. Investigations are underway to elucidate the mechanism of C–H activation at Pd^{IV} and to identify further intra- and intermolecular examples of this new reaction. We anticipate that such studies will ultimately enable the rational incorporation of Pd^{IV}-mediated C–H activation into Pd-catalyzed processes.

4.4 Experimental

The palladium(II) complexes $Pd(dba)_2$ [dba = dibenzylideneacetone],[25] $(COD)Pd(Cl)_2$ [COD = 1,5-cyclooctadiene] and $(COD)Pd(CH_2CMe_2\text{-}o\text{-}C_6H_4)$ were prepared according to literature procedures. $(PPh_3)_2Pd(Cl)_2$ was purchased from Strem Chemicals. Aryl iodides, anilines and boronic acids were purchased from commercial sources. $TMSCF_3$ was obtained from Matrix Chemicals. Di-*tert*-butylbipyridine (dtbpy) and 2-methyl-2-phenylpropyl magnesium chloride were obtained from Aldrich. 1-Fluoro-2,4,6-trimethylpyridinium triflate (NFTPT) was obtained from TCI America. $PhICl_2$ was prepared via a modification of a literature procedure.[26] $PhI(TFA)_2$ was purchased from Acros Organics. Unless otherwise noted, all reagents were used as received. NMR solvents were obtained from Cambridge Isotope Laboratories. All other solvents were obtained from Fisher Chemicals. Tetrahydrofuran was purified using an Innovative Technologies (IT) solvent purification system consisting of a copper catalyst, activated alumina, and molecular sieves.

4.4.1 Synthesis of Precursors to Organic Ligands

Scheme 4.4.1.1 Synthesis of S2

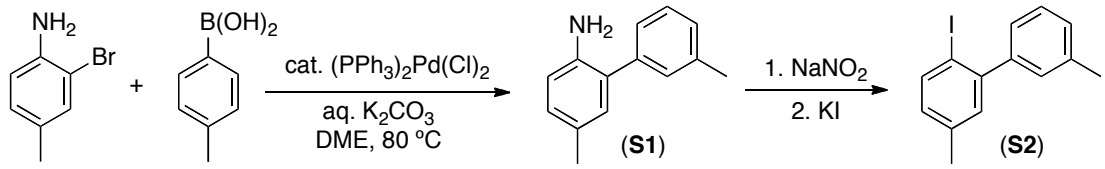

Compound S1. 2-Bromo-4-methylaniline (4.3 g, 18 mmol, 1.0 equiv), *m*-tolyboronic acid (4.1 g, 21 mmol, 1.2 equiv), $(PPh_3)_2Pd(Cl)_2$ (0.270 g, 3.4 mmol, 0.02 equiv), and a 2M solution of K_2CO_3 in water (45 ml) were combined in dimethoxyethane (200 mL). The resulting biphasic reaction mixture was stirred overnight at 80 °C. The reaction mixture was cooled to room temperature and then extracted with ether (3 x 30 mL). The organic extracts were combined, dried over $MgSO_4$, and filtered through a plug of Celite. The product was purified by column chromatography to afford **S1** as a yellow oil (3.16 g, 89% yield, R_F = 0.34 in 1:9 ethyl acetate:hexanes). ^{1}H NMR ($CDCl_3$): δ 7.29 (t, *J* = 8 Hz, 1H), 7.24-7.22 (multiple peaks, 2H), 7.13 (d, *J* = 8 Hz, 1H), 6.96-6.93 (multiple peaks, 2H), 6.67 (d, *J* = 8 Hz, 1H), 3.62 (br s, 2H), 2.38 (s, 3H), 2.26 (s, 3H). ^{13}C NMR ($CDCl_3$): δ 140.94, 139.60, 138.39, 130.92, 129.79, 128.89, 128.62, 127.87 (2 overlapping C's), 127.80, 126.05, 115.74, 21.47, 20.42. HRMS-electrospray (m/z): $[M+H]^+$ calcd for $C_{14}H_{15}N$, 198.1277; Found, 198.1276.

Compound S2. Aniline **S1** (2.36 g, 7.73 mmol, 1.0 equiv) was dissolved in ethanol (40 mL). A solution of $NaNO_2$ (2.36 g, 7.73 mmol, 1.0 equiv) in water (4 mL) was added slowly over 10 min. The reaction mixture was cooled to 0 ºC, and concentrated HCl (10 mL) was added over 30 min. A solution of KI (2.30 g, 14.0 mmol, 1.8 equiv) in water (4 mL) was then added, and the reaction mixture was

removed from the ice bath and allowed to stir at 25 °C for 2 h. The reaction mixture was extracted with ethyl acetate (3 x 45 mL), and the organic extracts were washed with a saturated solution of $NaHSO_3$ (2 x 60 mL). The organic layer was separated and dried over $MgSO_4$. The product was purified by column chromatography to afford **S2** as a colorless oil (1.02 g, 43% yield, R_F = 0.23 in hexanes). ^{1}H NMR ($CDCl_3$): δ 7.78 (d, *J* = 8 Hz, 1H), 7.29 (t, *J* = 8 Hz, 1H), 7.18 (d, *J* = 8 Hz, 1H), 7.12-7.11 (multiple peaks, 3H), 6.84 (d, *J* = 8 Hz, 1H), 2.39 (s, 3H), 2.31 (s, 3H). ^{13}C NMR ($CDCl_3$): δ 146.51, 144.18, 139.21, 138.05, 137.52, 131.05, 129.94, 129.69, 128.26, 127.77, 126.36, 94.48, 21.49, 20.91. HRMS-electrospray (m/z): $[M]^+$ calcd for $C_{14}H_{13}I$, 308.0062; Found, 308.0065.

4.4.2 Synthesis of Palladium(II) Starting Materials

Scheme 4.4.2.1 Synthesis of Complex 1

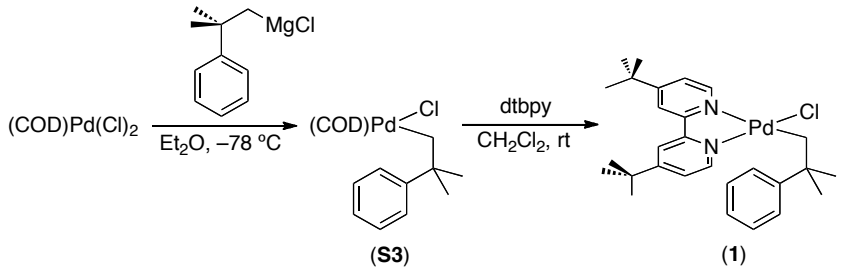

Complex S3. **S3** was prepared using a modification of a literature procedure.[11] To a –78 ºC solution of $(COD)Pd(Cl)_2$ (3.5 g, 12.2 mmol, 1.0 equiv) in Et_2O (60 mL) was added 2-methyl-2-phenylpropyl magnesium chloride (24.5 mL of a 2.0 M solution in Et_2O, 12.2 mmol, 1.0 equiv). The reaction mixture was stirred for 12 h at 25 ºC. The solvent was removed via rotary evaporation, the black solids were dissolved in CH_2Cl_2 (100 mL), and this suspension was filtered through a plug of Celite. The resulting yellow solution was concentrated to ~6 mL, and petroleum ether (~60 mL) was added to precipitate a yellow solid. The precipitate was collected and dried under vacuum to afford **S3** as an off-white solid (3.69 g, 79% yield). ^{1}H NMR ($CDCl_3$): δ 7.56 (d, *J* = 8 Hz, 2H), 7.33 (t, *J* = 8 Hz, 2H), 7.21 (t, *J* = 8 Hz, 1H), 5.84 (br s, 2H), 4.39 (br s, 2H), 2.56 (s, 2H), 2.25 (s, 4H) 2.24 (s, 4H), 1.55 (s, 6H). ^{13}C NMR ($CDCl_3$): δ 151.52, 128.32, 126.03, 125.82, 125.12, 101.16, 47.57, 42.13, 32.41,31.34, 31.34, 31.06, 27.1. Anal. Calc. for $C_{18}H_{25}ClPd$ with ~15 % H_2O as determined by ^{1}H NMR: C, 55.99, H, 6.61; Found: C, 55.97, H, 6.57.

Complex 1. **S3** (613 mg, 1.77 mmol, 1.0 equiv) and 4,4′-di-*tert*-butylbipyridine (473 mg, 1.77 mmol, 1.0 equiv) were combined in CH_2Cl_2 (120 mL), and the reaction mixture was allowed to stir for 30 min at rt. The solvent was

concentrated under vacuum to ~5 mL, and hexanes (~30 mL) was added to precipitate the product. The precipitate was collected and dried under vacuum to afford **1** as a bright yellow solid (893 mg, 93% yield). ^{1}H NMR (CD_2Cl_2): δ 9.08 (d, *J* = 6 Hz, 1H), 7.95 (d, *J* = 6 Hz, 1H), 7.92 (s, 1H), 7.87 (s, 1H), 7.66 (app d, *J* = 8 Hz, 2H), 7.53 (d, *J* = 8 Hz, 1H), 7.07 (d, *J* = 8 Hz, 1H), 7.02 (app t, *J* = 8 Hz, 2H), 6.88 (d, *J* = 8 Hz, 1H), 2.24 (s, 2H), 1.55 (s, 6H), 1.39 (s, 9H), 1.35 (s, 9H). ^{13}C NMR ($CDCl_3$): δ 162.69, 161.64, 155.66, 152.83, 152.01, 149.06, 149.00, 127.03, 126.76, 124.57, 123.17, 122.42, 117.80, 117.13, 41.47, 37.22, 35.26, 35.08, 31.19, 30.30, 30.17, 30.07. HRMS-electrospray (m/z): $[M–Cl]^+$ calcd for $C_{28}H_{37}ClN_2Pd$, 507.1986; Found, 507.1999.

4.4.3 Synthesis of Authentic Sample of 3

Scheme 4.4.3.1 Synthesis of 3

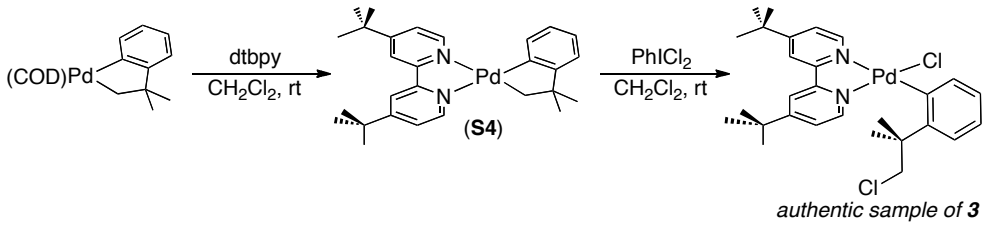

Complex S4. (COD)Pd^{II}(CH_2CMe_2-*o*-C_6H_4) (104 mg, 0.30, 1.0 equiv) was combined with 4,4′-di-*tert*-butylbipyridine (80 mg, 0.30 mmol, 1.0 equiv) in CH_2Cl_2 (120 mL) and allowed to stir for 30 min at rt. The reaction was concentrated under vacuum to 5 mL and ~30 mL of hexanes was added to precipitate the product. **S4** was isolated as a bright yellow solid (147 mg, 97% yield). ^{1}H NMR ($CDCl_3$): δ 9.11(d, *J* = 6 Hz, 1H), 8.55 (d, *J* = 6 Hz, 1H), 7.98-7.97 (multiple peaks, 2H), 7.55 (d, *J* = 8 Hz, 1H), 7.53 (d, *J* = 6 Hz, 1H), 7.43 (d, *J* = 6 Hz, 1H), 7.00 (app. t, 2H), 6.87 (d, *J* = 8 Hz, 1H), 2.43 (s, 2H), 1.44 (s, 6H), 1.43 (s, 9H), 1.42 (s, 9H). ^{13}C NMR ($CDCl_3$): δ 169.09, 161.95, 161.87, 159.24, 155.35,

154.86, 150.38, 149.32, 134.79, 123.92, 122.90, 122.78, 122.54, 121.58, 117.94, 117.84, 47.27, 44.84, 35.19, 35.17, 33.76, 31.07, 30.30, 30.27. HRMS-electrospray (m/z): $[M+H]^+$ calcd for $C_{28}H_{36}N_2Pd$, 507.1986; Found, 507.2000.

Complex 3. An authentic sample of **3** was prepared by the reaction of **S4** with $PhICl_2$ as described below. **S4** (200 mg, 0.394 mmol, 1.0 equiv) and $PhICl_2$ (110 mg, 0.394 mmol, 1.0 equiv) were combined in CH_2Cl_2 (40 mL), and the resulting solution was stirred for 15 min. The reaction mixture was concentrated to ~4 mL, and hexanes (~30 mL) was added to precipitate the product. The precipitate was collected and dried under vacuum to afford **3** was isolated as a bright yellow solid (223 mg, 98% yield). ^{1}H NMR ($CDCl_3$): δ 9.16 (d, *J* = 6 Hz, 1H), 7.95 (multiple peaks, 2H), 7.84 (d, *J* = 8 Hz, 1H), 7.54 (d, *J* = 6 Hz, 1H), 7.46 (d, *J* = 6 Hz, 1H), 7.26-7.19 (multiple peaks, 2H), 6.96 (t, *J* = 7 Hz, 1H), 6.90 (t, *J* = 7 Hz, 1H), 4.76 (d, *J* = 11 Hz, 1H), 3.93 (d, *J* = 11 Hz, 1H), 1.81 (s, 3H), 1.78 (s, 3H), 1.43 (s, 9H), 1.37 (s, 9H). ^{13}C NMR ($CDCl_3$): δ 163.59, 163.16, 155.76, 153.49, 151.53, 149.36, 148.79, 148.03, 134.97, 127.42, 124.85, 123.55 (2 overlapping C's), 123.52, 118.36, 117.80, 57.88, 41.28, 35.55 (2 overlapping C's), 30.46, 30.27, 29.03, 28.81. HRMS-electrospray (m/z): $[M]^+$ calcd for $C_{29}H_{39}Cl_2N_2Pd$, 591.1525; Found, 591.1518.

4.4.4 Synthesis of Authentic Sample of 6

Scheme 4.4.4.1 Synthesis of 6

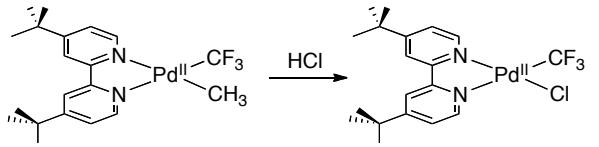

*authentic sample of **6***

Complex 6. HCl (40 μl of a 2 M solution in Et_2O, 2.0 equiv) was added to a solution of $Pd(CH_3)(CF_3)(dtbpy)$[27] (18 mg, 0.04 mmol, 1.0 equiv) in CH_2Cl_2 (10 mL). The reaction was stirred for 5 min, and then the solvent was removed under reduced pressure. The yellow residue was taken up in CH_2Cl_2 (1 mL), and hexanes (~8 mL) was added to precipitate the product. The resulting solids were collected on a fritted filter and dried under vacuum to afford **6** as a light yellow solid (13 mg, 69% yield). ^{1}H NMR (CD_3CN): δ 9.08 (d, *J* = 7 Hz, 1H), 8.68 (d, *J* = 7 Hz, 1H), 8.21 (s, 1H), 8.16 (s, 1H), 7.61-7.58 (multiple peaks, 2H), 1.36 (s, 9H), 1.34 (s, 9H). ^{13}C NMR ($CDCl_3$): δ 164.68, 164.45, 156.05, 154.34 (q, J = 277 Hz), 154.23, 152.48, 150.12, 124.15, 123.51, 118.85, 117.97, 35.62 (2 overlapping C's), 30.35, 30.24. HRMS-electrospray (m/z): $[M–Cl]^+$ calcd for $C_{19}H_{24}ClF_3N_2Pd$, 443.0932; Found, 443.0926.

4.4.5 General procedures for the synthesis of Pd(Aryl)(I)(dtbpy) and Pd(Aryl)(CF_3)(dtbpy)

Scheme 4.4.5.1 General Synthetic Scheme for Pd(Aryl)(I)(dtbpy) and Pd(Aryl)(CF_3)(dtbpy)

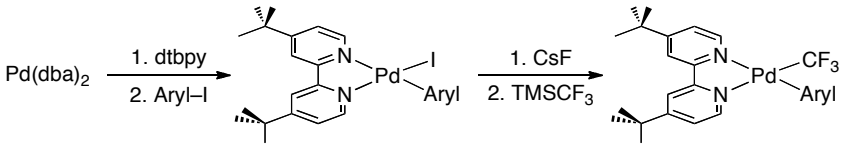

General Procedure: Under nitrogen, $Pd(dba)_2$ (3.0 g, 5.23 mmol, 1 equiv) was weighed into a 250 mL round bottom flask and dissolved in THF (75 mL). The ligand dtbpy (3.7 g, 6.6 mmol, 2.6 equiv) was added, and the resulting mixture was stirred at 25 ºC for 15 min. The aryl iodide (14.6 mmol, 2.8 equiv) was added, and the reaction mixture was warmed to 60 °C for 3 h. In air, the reaction

mixture was filtered through a plug of Celite, and the solvent was removed under reduced pressure. The resulting solid was washed with hexanes (3 x 50 mL) and then with a 50:50 mixture of ether and hexanes (~400 mL) to completely remove residual dibenzylidene acetone. The product was then redissolved in CH_2Cl_2 (20 mL) and stirred with activated charcoal for 30 min. This suspension was then filtered through a plug of Celite, and the solvent was removed *in vacuo* to yield the products.

General procedure: Under N_2, Pd(Aryl)(I)(dtbpy) (1.5-1.6 mmol, 1 equiv) and CsF (3 equiv) were dissolved in THF (0.145 M) in a 25 mL Schlenk flask. The resulting suspension was stirred for 10 min, and then Me_3SiCF_3 (2 equiv) was added. The reaction was stirred vigorously at 22 ºC for 3 h. The solvent was then removed under reduced pressure. CH_2Cl_2 (15 mL) was added to dissolve the product, and the resulting suspension was filtered through a plug of Celite. The plug was washed with of CH_2Cl_2 (2 x 5mL), the filtrate was concentrated under reduced pressure to (~2 mL), and hexanes (60 mL) was added to precipitate the product. The resulting solids was collected on a fritted filter, washed with hexanes (3 x 10 mL) and dried *in vacuo*.

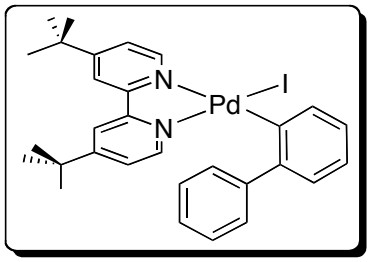

Complex S5. **S5** was prepared using the general procedure above and was isolated as an orange solid (1.6 g, 44% yield). ^{1}H NMR ($CDCl_3$): δ 9.48 (d, *J* = 6 Hz, 1H), 8.01 (app s, 2H), 7.82 (s, 1H), 7.78 (s, 1H), 7.72 (d, *J* = 8 Hz, 1H), 7.47-7.40 (multiple peaks, 2H), 7.25-7.18 (multiple peaks, 3H), 7.09-6.97 (multiple peaks, 4H), 1.38 (s, 9H), 1.33 (s, 9H). ^{13}C NMR ($CDCl_3$): δ 162.71, 162.62,

155.50, 153.60, 152.58, 149.28, 145.85, 145.69, 145.02, 138.73, 129.91, 129.10, 127.11, 125.51, 124.73, 123.62, 123.45, 123.05, 117.83, 117.65, 35.25, 35.24, 30.21, 30.06. HRMS-electrospray (m/z): $[M+Na]^+$ calcd for $C_{30}H_{33}IN_2Pd$, 677.0621; Found, 677.0646.

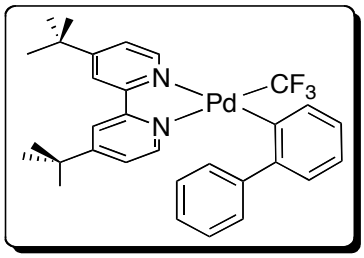

Complex 4. Complex **4** was prepared using the general procedure above and was isolated as a yellow solid (530 mg, 58% yield). ^{1}H NMR ($CDCl_3$): δ 8.97 (d, *J* = 6 Hz, 1H), 7.94-7.92 (mulptile peaks, 2H), 7.88 (s, 1H), 7.82-7.79 (multiple peaks, 2H), 7.53 (d, *J* = 6 Hz, 1H), 7.48 (d, *J* = 6 Hz, 1H), 7.31 (d, *J* = 8 Hz, 1H), 7.19-7.05 (multiple peaks, 6H),1.40 (s, 9H), 1.32 (s, 9H). ^{19}F NMR ($CDCl_3$): δ –20.00 (m, 3F). ^{13}C NMR ($CDCl_3$): δ 162.90, 162.83, 154.97, 154.14, 151.54 (q, *J* = 4 Hz), 150.10, 147.01, 146.27, 136.82, 135.33 (q, *J* = 364 Hz), 129.17, 128.25, 127.08, 125.28, 124.80, 123.31, 123.19, 122.79, 117.81, 117.46, 35.21, 35.16, 30.18, 30.08. HRMS-electrospray (m/z): $[M+Na]^+$ calcd for $C_{31}H_{33}F_3N_2Pd$, 619.1528; Found, 619.1547.

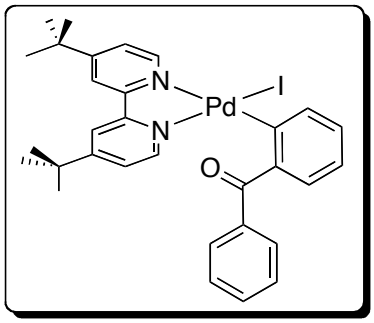

Complex S6. **S6** was prepared using the general procedure above, except that

the reaction was conducted at 50 ºC to minimize impurities. The product was isolated as a yellow solid (1.44 g, 92% yield). ^{1}H NMR (CD_3CN): δ 9.15 (d, *J* = 7 Hz, 1H), 8.22 (app s, 2H), 7.67 (d, *J* = 6 Hz, 1H), 7.60 (d, *J* = 8 Hz, 1H), 7.57-7.55 (multiple peaks, 2H), 7.48 (d, *J* = 6 Hz, 1H), 7.30 (d, *J* = 8 Hz, 1H), 7.28-7.22 (multiple peaks, 3H), 7.13-7.11 (multiple peaks, 2H), 7.04 (t, *J* = 8 Hz, 1H), 1.44 (s, 9H), 1.43 (s, 9H). ^{13}C NMR ($CDCl_3$): δ 200.65, 162.92, 162.91, 155.57, 153.82, 152.31, 149.71, 149.40, 145.49, 139.10, 137.91, 131.39, 130.58, 129.22, 129.08, 127.36, 123.38, 123.28, 121.99, 118.33, 117.87, 35.32, 35.24, 30.22, 30.14. IR (thin film): n 2965.1, 1649.7, 1612.9, 1447.8, 1285.9, 921.5, 735.8, 700.1, 633.7 cm^{-1}. HRMS-electrospray (m/z): $[M–I]^+$ calcd for $C_{31}H_{33}IN_2OPd$, 555.1622; Found, 555.1626.

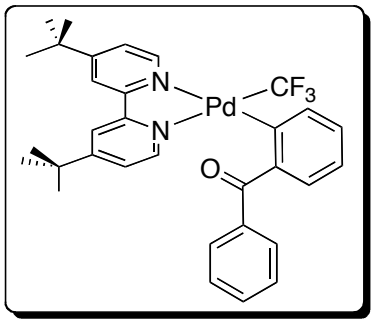

Complex 9. Complex **6** was prepared using the general procedure above and was isolated as a yellow solid (1.56 g, 96% yield). ^{1}H NMR (CD_3CN, 23 ºC): δ 8.64 (br s, 1H), 8.22 (app br s, 2H), 7.80 (d, *J* = 8 Hz, 1H), 7.74-7.58 (br s, 1H) 7.54-7.50 (multiple peaks, 3H), 7.44-7.39 (multiple peaks, 2H), 7.27 (t, *J* = 8 Hz, 1H), 7.23 (t, *J* = 6 Hz, 1H) 7.12 (t, *J* = 7 Hz, 1H), 7.10-7.07 (multiple peaks, 2H), 1.43 (br s, 18H). The broad resonances observed in the room temperature ^{1}H NMR spectrum was considerably sharper at –30 ºC. ^{1}H NMR (CD_3CN, –30 °C): δ 8.63 (1H, broad s), 8.26 (2H, multiple peaks), 7.80 (1H, broad s), 7.67 (1H, broad s), 7.61(1H, broad s), 7.54-7.52 (2H, multiple peaks), 7.40-7.36 (2H, multiple peaks), 7.29-7.25 (2H, multiple peaks), 7.15-7.08 (3H, multiple peaks), 1.44 (s, 9H), 1.40 (s, 9H). ^{19}F NMR (CD_3CN, 23 ºC): δ –21.18 (s, 3F). ^{13}C NMR ($CDCl_3$,

23 ºC): δ 201.51, 163.20, 161.39, 154.71 (br s, 2C), 150.70 (br s, 2C), 144.74, 139.46, 139.34, 137.01, 134.29 (q, *J* = 365 Hz), 131.09, 130.11, 129.98, 129.11, 129.03, 128.28, 127.95, 127.18 (2 overlapping C's), 123.03, 121.97, 117.98, 35.16 (2 overlapping C's), 30.05, 29.96. ^{13}C NMR ($CDCl_3$ –30 °C): 201.51, 163.20, 161.39, 154.71, 154.02, 150.70, 150.04, 144.74, 139.46, 139.34, 137.01, 134.29 (q, *J* = 365 Hz), 131.09, 130.11, 129.98, 129.11, 129.03, 128.28, 127.95, 127.18 (2 overlapping C's), 123.03, 121.97, 117.98, 35.16 (2 overlapping C's), 30.05, 29.96. IR (thin film): ν 2966.5, 1658.0, 1612.6, 1480.9, 1449.6, 1090.2, 736.2, 702.1 cm^{-1}. HRMS-electrospray (m/z): $[M–CF_3]^+$ calcd for $C_{32}H_{33}F_3N_2OPd$, 555.1622; Found, 555.1631.

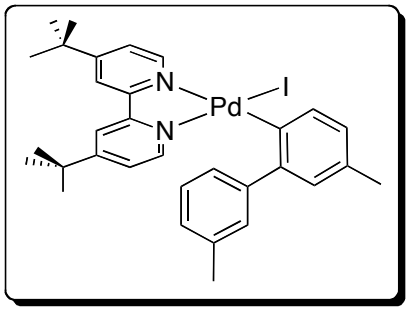

Complex S7. Complex **S7** was prepared using the general procedure above and was isolated as a light orange solid (676 mg, 33% yield). ^{1}H NMR (CD_3CN): δ 9.32 (d, *J* = 6 Hz, 1H), 8.17 (s, 1H), 8.11 (s, 1H), 7.79 (d, *J* = 8 Hz, 1H), 7.73 (s, 1H), 7.61 (d, *J* = 6 Hz, 1H), 7.47-7.39 (multiple peaks, 4H), 7.07-7.04 (multiple peaks, 2H), 6.89 (d, *J* = 8 Hz, 1H), 6.83 (d, *J* = 8 Hz, 1H), 2.36 (s, 3H), 2.17 (s, 3H), 1.40 (s, 9H), 1.35 (s, 9H). ^{13}C NMR ($CDCl_3$): δ 161.72, 161.58, 154.50, 152.69, 151.58, 148.44, 144.64, 143.98, 139.99, 137.54, 135.27, 131.46, 129.70, 129.07, 126.24, 125.97, 125.20, 124.89, 122.60, 122.04, 116.82, 116.71, 34.31 (2 overlapping C's), 29.30, 29.17, 20.28, 19.71. HRMS-electrospray (m/z): $[M–I]^+$ calcd for $C_{32}H_{37}IN_2Pd$, 555.1992; Found, 555.2004.

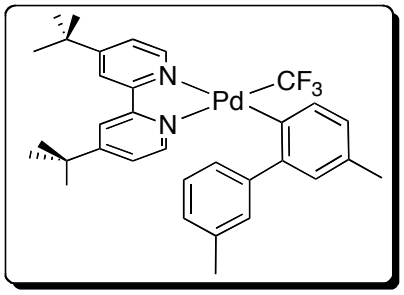

Compound 11. Complex **11** was prepared using the general procedure above and was isolated as a yellow solid (82 mg, 39% yield). ^{1}H NMR (CD_3CN): δ 8.80 (d, *J* = 6 Hz, 1H), 8.33 (s, 1H), 8.23 (s, 1H), 7.66 (d, *J* = 6 Hz, 1H), 7.63-7.61 (multiple peaks, 2H), 7.48 (d, *J* = 8 Hz, 1H), 7.38 (d, *J* = 8 Hz, 1H), 7.31 (d, *J* = 6 Hz, 1H), 6.98 (s, 1H), 6.88 (t, *J* = 6 Hz, 1H), 6.75 (t, *J* = 8 Hz, 1H), 6.70 (t, *J* = 8 Hz, 1H), 2.21 (s, 3H), 2.05 (s, 3H), 1.33 (s, 9H), 1.23 (s, 9H). ^{19}F NMR ($CDCl_3$): δ –20.40 (s, 3F). ^{13}C NMR ($CDCl_3$): δ 162.80, 162.70, 154.78, 154.09, 151.28, 149.97, 146.80, 146.03, 136.47, 136.02, 135.51 (q, *J* = 363 Hz), 131.85, 130.14, 129.19, 128.97, 126.60, 125.77 (2 overlapping C's), 123.06, 122.55, 120.87, 117.62, 117.29, 35.12, 35.04, 30.03, 29.96, 21.07, 20.79. HRMS-electrospray (m/z): $[M–H]^+$ calcd for $C_{33}H_{37}F_3N_2Pd$, 623.1865; Found, 623.1865.

4.4.6 Reactions Discussed in Section 3.3

Scheme 4.4.6.1 Reaction of 1 with $PhICl_2$

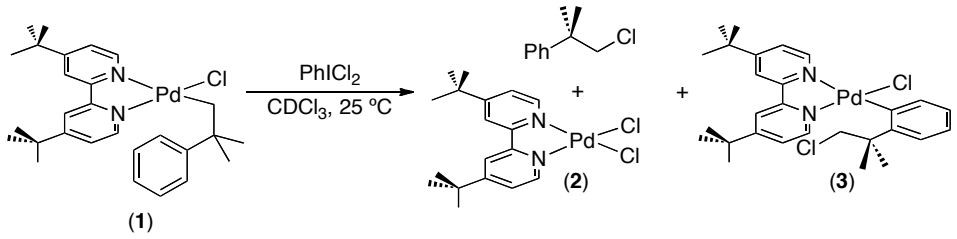

Procedure: Complex **1** (4.1 mg, 0.00758 mmol, 1.0 equiv), $PhICl_2$ (2.1 mg, 0.00758, 1.0 equiv), and an internal standard ($C_2H_4Cl_2$, 0.00758 mmol, added from a stock solution of $C_2H_4Cl_2$ in $CDCl_3$) were combined in $CDCl_3$ (0.5 mL) at room temperature. This mixture was allowed to stand for 10 min and was then analyzed by ^1H NMR spectroscopy. The yields of products **2** and **3** were determined by ^1H NMR integration relative to the internal standard. As discussed above, an authentic sample of **3** was synthesized to confirm the identity of this product. Complex **2** was identified by comparison to literature data.[28] The chlorinated organic product (1-chloro-2-methylpropan-2-yl)benzene was detected by GCMS after (1) evaporation of the reaction solvent under a stream of N_2 followed by (2) extracting the resulting residue with pentane (2 mL) to dissolve the organic materials.

4.4.7 Procedure for the Reaction of 4 with $PhICl_2$ to form 5-Cl, 6, and 7

Scheme 4.4.7.1 Reaction of 4 with $PhICl_2$ to form 5-Cl, 6, and 7

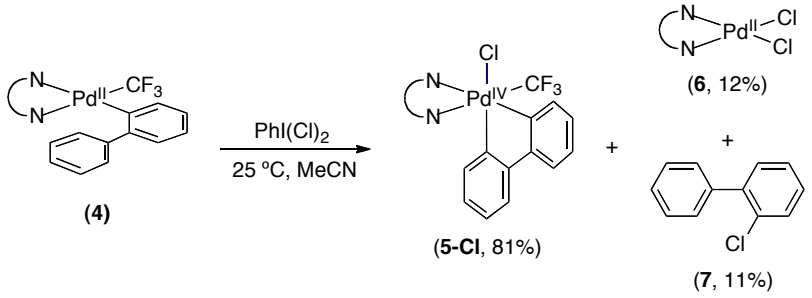

Complex 5-Cl (NMR-scale reaction). Complex **4** (9.1 mg, 0.015 mmol, 1.0 equiv) and $PhICl_2$ (4.2 mg, 0.015 mmol, 1.0 equiv) were combined in MeCN (0.5 mL) with DCE (1.0 equiv) as the internal standard and this mixture was stirred for 35 min at RT Analysis of the crude reaction mixture by ^1H NMR spectroscopy

showed 81% yield of **5-Cl** along with 12% yield of **6**. The crude yield of **7** (11%) was determined from a separate reaction run in parallel. In this latter case, the volatiles were removed under vacuum, the resulting solids were sonicated with hexanes, and this mixture was filtered through a pipette plug of celite. The filtrate was collected, the solvent was removed under vacuum, and the yield of **7** was determined by ^{1}H NMR spectroscopy.

Complex 5-Cl (Isolation of product). Complex **4** (27 mg, 0.048 mmol, 1.0 equiv) and $PhICl_2$ (13 mg, 0.048 mmol, 1.0 equiv) were combined in MeCN (18 mL), and this mixture was stirred for 35 min at RT. The solvent was removed by rotary evaporation. The resulting yellow solids were washed with pentanes (2 x 20 mL). The residue was then dissolved in CH_2Cl_2 (2 mL), and ether (10 mL) was to precipitate the product. The precipitate was collected and dried under vacuum to afford **5-Cl** as a light yellow solid (24 mg, 77% yield). ^{1}H NMR (CD_3CN): δ 9.21 (d, *J* = 6 Hz, 1H), 8.50 (s, 1H), 8.42 (d, *J* = 8 Hz, 1H), 8.36 (s, 1H), 7.95 (d, *J* = 6 Hz, 1H), 7.68 (d, *J* = 8 Hz, 1H), 7.57-7.54 (multiple peaks, 2H), 7.40-7.36 (multiple peaks, 2H), 7.21 (t, *J* = 8 Hz, 1H), 7.08 (t, *J* = 6 Hz, 1H), 6.73 (t, *J* = 8 Hz, 1H), 6.49 (d, *J* = 8 Hz, 1H), 1.54 (s, 9H), 1.34 (s, 9H). ^{19}F NMR (CD_3CN): δ –21.37 (s, 3F). ^{13}C NMR (CD_2Cl_2): δ 169.46 (q, *J* = 6 Hz), 167.19 (q, *J* = 6 Hz), 165.12, 165.01, 153.75, 153.43, 150.66 (q, *J* = 5 Hz), 148.72, 148.63, 148.07, 134.55, 129.82, 128.53, 127.77, 127.29, 126.66, 125.69, 124.94, 123.32 (q, *J* = 365 Hz), 123.23, 123.11, 120.63, 120.46, 36.19, 36.01, 30.76, 30.55. HRMS-electrospray (m/z): $[M–Cl]^+$ $C_{31}H_{32}F_3N_2ClPd$, 595.1552; Found, 595.1558.

4.4.8 Reaction of 4 with $C_6D_5ICl_2$ and Characterization Data for 8

Scheme 4.4.8.1 Reaction of 4 with $C_6D_5ICl_2$

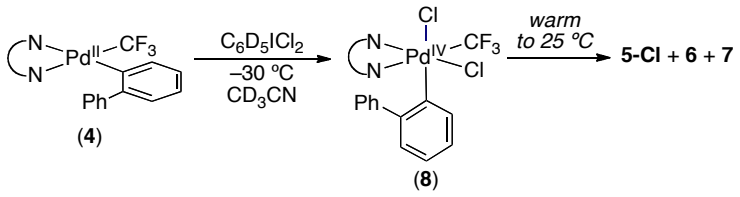

Complex 8. Complex **4** (9.1 mg, 0.015 mmol, 1 equiv) was dissolved in CD_3CN (0.35 mL), and the resulting solution was added to an NMR tube and then frozen in LN_2. A solution of $C_6D_5ICl_2$ (4.1 mg, 0.015 mmol, 1 equiv) in CD_3CN (0.25 mL) was then added to the NMR tube at LN_2 temperature (such that it froze on top of the first solution). The sample was immediately placed into an NMR spectrometer where the probe temperature was set to 25 ºC, –15 ºC, –20 ºC or –30 ºC. The sample was allowed to equilibrate for 3 min and then data acquisition was initiated. The observed ratio of **8** : **5-Cl** after 3 min depended on the probe temperature. This ratio was 1 : 1 at 25 ºC, 3 : 1 at –20 ºC and 3.3 : 1 at –30 ºC. For all the NMR characterization experiments described below, the NMR tube was warmed to 25 ºC before being placed in the spectrometer at low temperature, such that characterization was performed on a 1: 1 mixture of **8** : **5-Cl**.

At –30 ºC, a 3.3 : 1 mixture of **8** : **5-Cl** was observed at t=0. Compound **8** is stable for at least 1 h at –30 ºC, and the ratio of **8** : **5-Cl** did not change over this time. Therefore, it is most probable that the initially formed **5-Cl** is not generated via intermediate **8**. Instead, it appears to be formed from some other undetected intermediate in the oxidation reaction.

Warming the mixture of **8**/**5-Cl** to 0 ºC or 25 ºC resulted in the

disappearance of **8** and growth of **5-Cl** and **6**. The decay of **8** was first order, and plots of [**8**] versus time at 0 ºC and 25 ºC are shown in Figures 3.4.8.1 and 3.4.8.2.

Figure 4.4.8.1 Decay of Intermediate 8 at 0 ºC ([8] versus time)

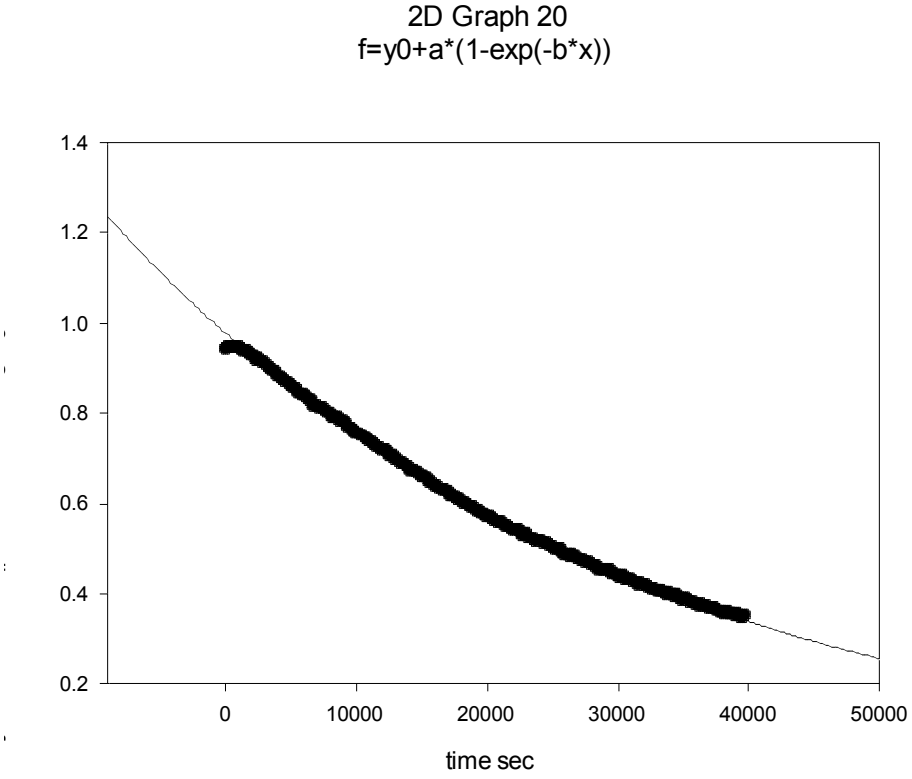

Fit to: f=y0+a*(1-exp(–b*x))

Parameter	Value	StdErr	CV(%)	Dependencies
y0	9.775e-1	1.360e-3	1.391e-1	0.9084933
a	-1.001e+0	1.006e-2	1.005e+0	0.9902510
b	2.551e-5	4.453e-7	1.746e+0	0.9931995

R^2=0.999

Figure 4.4.8.2 Decay of Intermediate 8 at 25 ºC ([8] versus time)

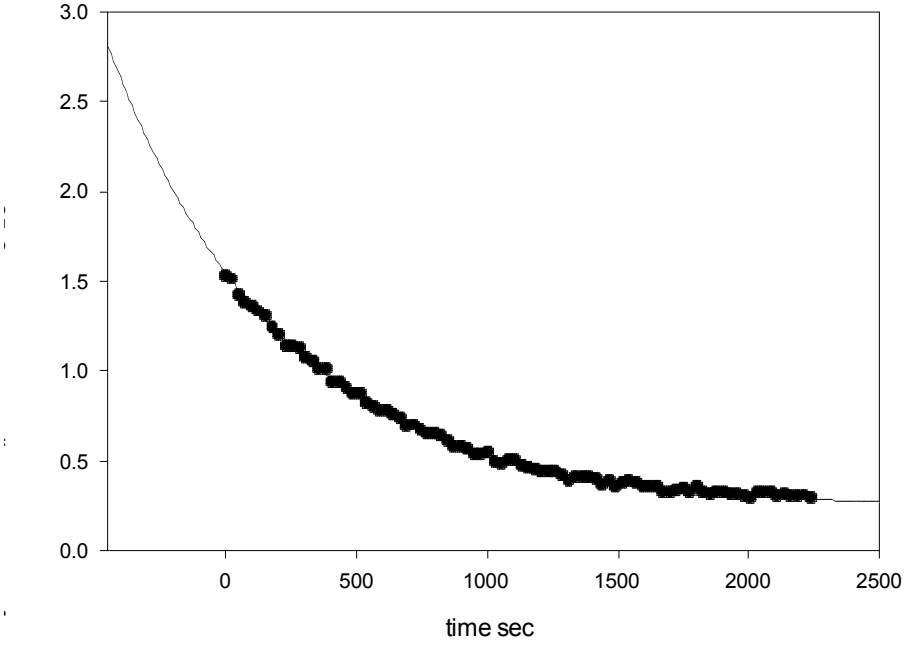

Fit to: f=y0+a*(1-exp(–b*x))

Parameter	Value	StdErr	CV(%)	Dependencies
y0	1.550e+0	6.530e-3	4.213e-1	0.9377485
a	-1.307e+0	6.219e-3	4.756e-1	0.8800414
b	1.497e-3	2.051e-5	1.370e+0	0.8835136

R^2=0.998

Characterization of 8. Complex **8** was characterized using a variety of NMR and mass spectroscopy techniques, which are described in detail below.

HRMS-electrospray. Complex **4** (4.5 mg, 0.0076 mmol, 1 equiv) was dissolved in CH_3CN (0.35 mL). This solution was added to a solution of $C_6H_5ICl_2$ (2.1 mg, 0.0076 mmol, 1 equiv) in CH_3CN (0.25 mL). The resulting sample was immediately subjected to analysis via electrospray ionization mass spectrometry. HRMS-electropray (m/z): $[M–Cl]^+$ calcd for $C_{31}H_{33}ClF_3N_2Pd$, 631.1319; Found, 631.1312.

Scheme 4.4.8.2 Reaction of 4 with $C_6D_5ICl_2$

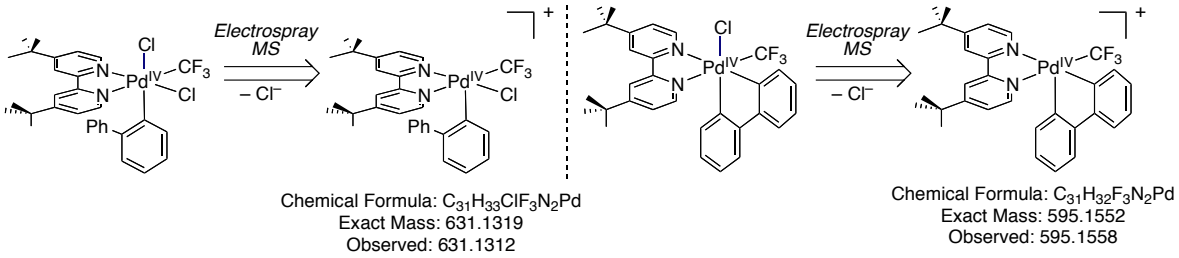

MALDI-TOF (IIN). Complex **4** (4.5 mg, 0.0076 mmol, 1 equiv) was dissolved in CH_3CN (0.35 mL). This solution was added to a solution of $C_6H_5ICl_2$ (2.1 mg, 0.0076 mmol, 1 equiv) in CH_3CN (0.25 mL). The resulting sample was immediately subjected to analysis via MALDI-TOF MS with dithranol as the matrix. MS (MALDI-TOF, IIN): 666.1 $[M+H]^+$.

NMR characterization – general information: In each case, the spectrum is shown below the characterization data. Notably, in all cases, **8** was observed as a mixture with C–H activation product **5-Cl**. Where relevant, accompanying text and/or figures are included to highlight important conclusions from each

experiment.

^{19}F NMR spectrum of **8** (CD_3CN, 25 ºC): δ ^{19}F NMR ($CDCl_3$): δ –19.08 (s, 3F), –20.34 (s, 3F). *This spectrum shows the presence of a mixture of intermediate **8** and product **5-Cl**. No starting material (–20.00 ppm) is observed.*

Figure 4.4.8.3 ^{19}F NMR spectrum of 8

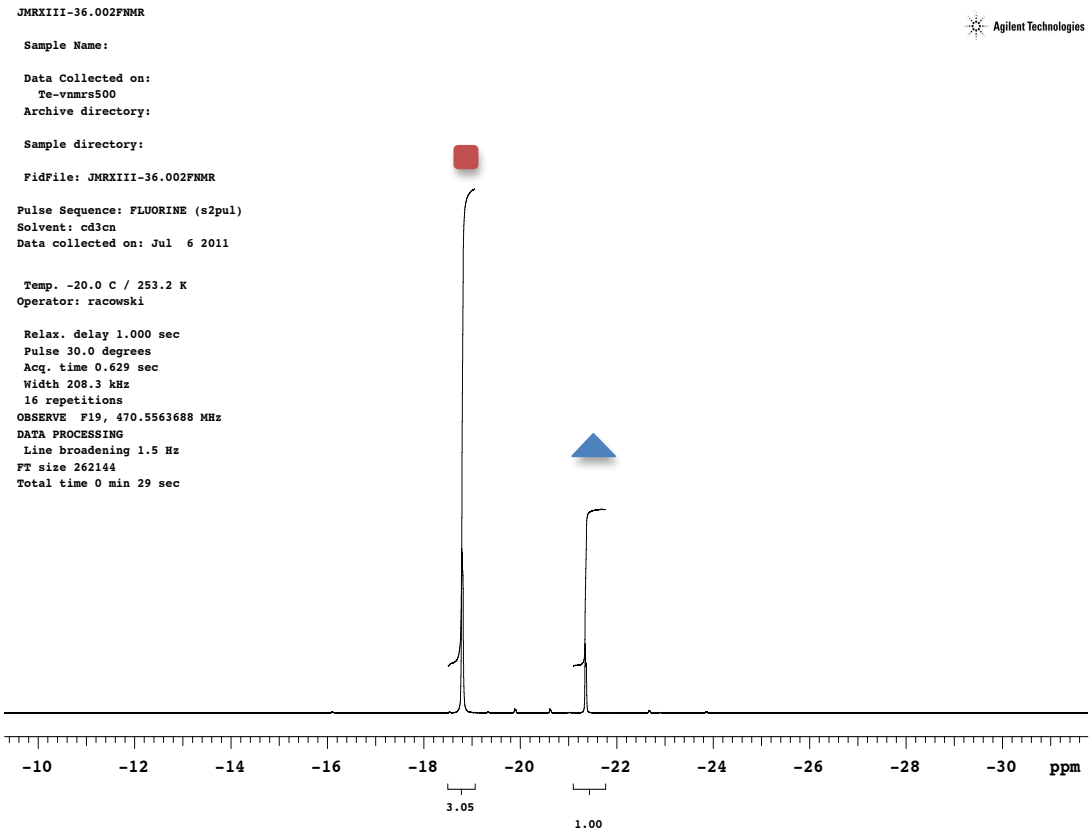

Legend: **Intermediate 8** **Product 5-Cl**

^{1}H NMR spectrum of **8** (CD_3CN, 25 ºC): δ 9.00 (d, *J* = 6 Hz, 1H), 8.66 (d, *J* = 7 Hz, 1H), 8.00 (d, *J* = 9 Hz, 1H), 7.94-7.92 (overlapping peaks with complex **5-Cl**, 2H), 7.67-7.65 (multiple peaks, 2H), 7.11 (t, *J* = 7 Hz, 1H), 7.07-7.01 (overlapping peaks with complex **5-Cl**, 1H), 6.93 (t, *J* = 8 Hz, 1H), 6.56 (multiple peaks, 2H), 6.43 (d, *J* = 8 Hz, 1H), 6.22 (d, *J* = 7 Hz, 1H), 6.14 (d, *J* = 8 Hz, 1H), 1.46 (app s, two overlapping signals, 18H).

Figure 4.4.8.4 ^{1}H NMR spectrum of 8

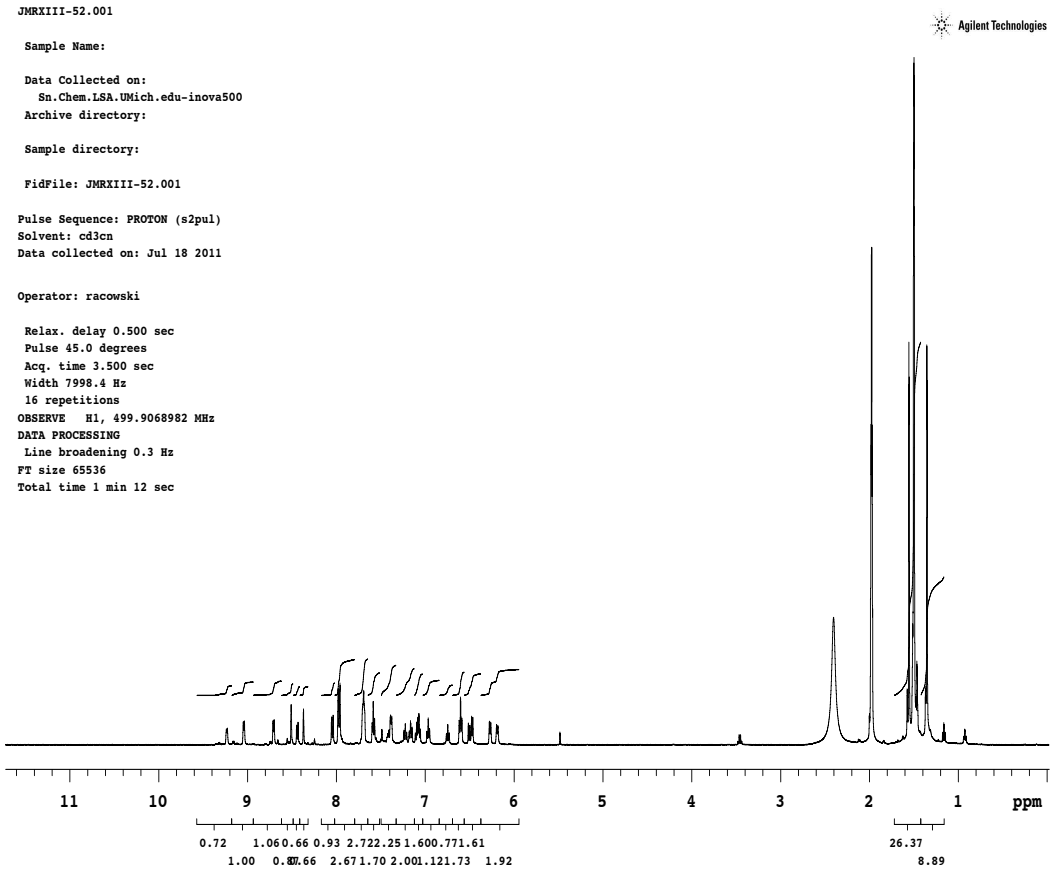

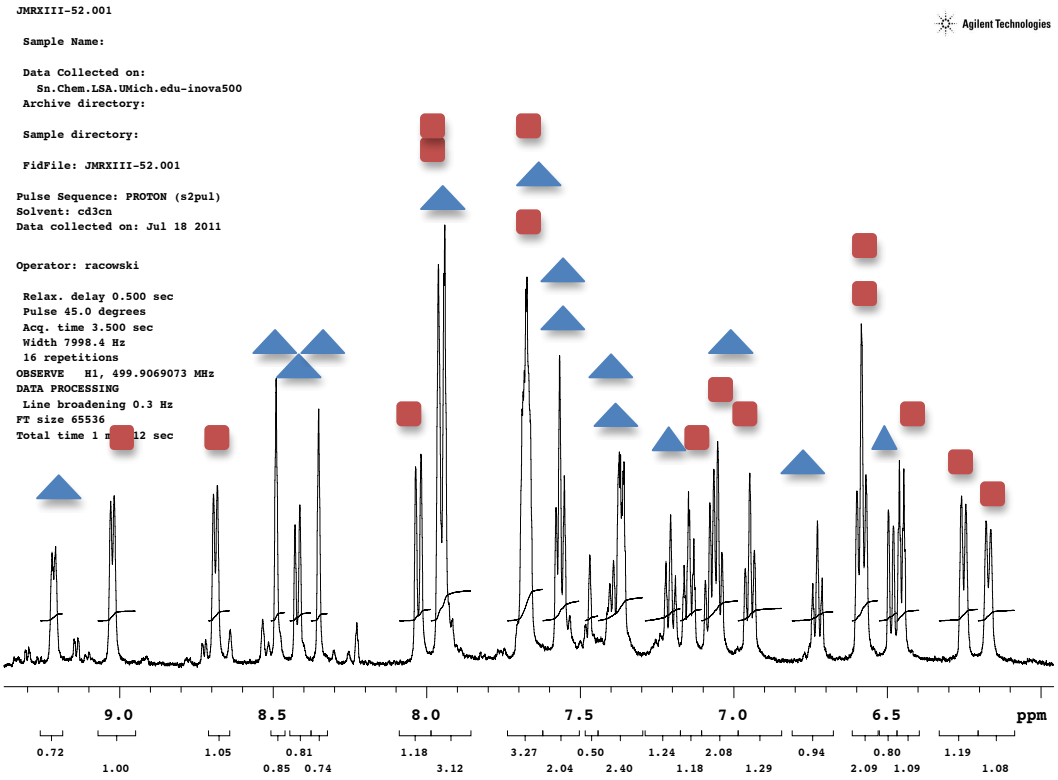

Complex **8-*d*$_5$** was synthesized via an analogous procedure to **8**, but with **4-*d*$_5$** as starting material. *This experiment confirmed the assignment of the intact phenyl ring resonances, since the peaks at 6.14, 6.22, 6.56 (two overlapping peaks) and 6.93 are not observed.*

Scheme 4.4.8.3 Reaction of 4-*d*$_5$ with $C_6D_5ICl_2$

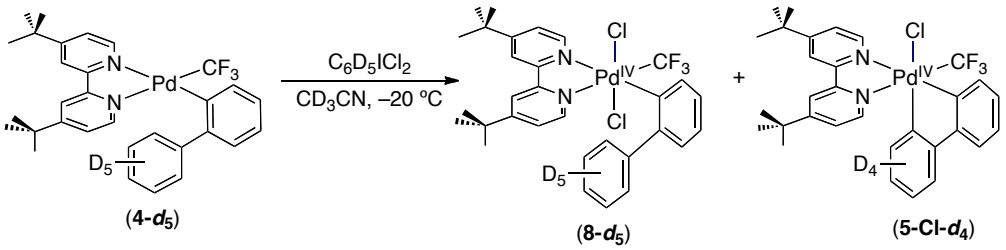

Figure 4.4.8.5 Aromatic Region of ^{1}H NMR with 4 and $C_6D_5ICl_2$

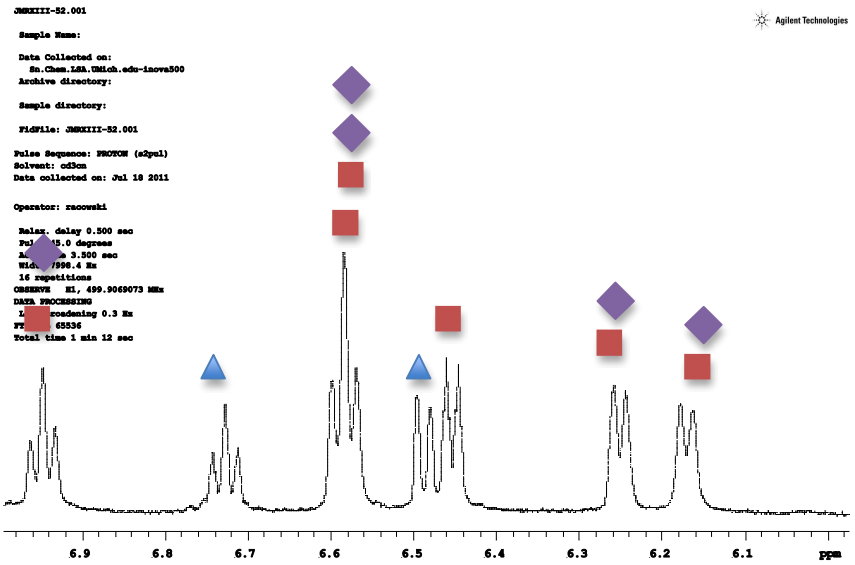

Legend: **Complex 8** **Complex 8 (protons of non-activated aryl ring)**

Complex 5-Cl

Figure 4.4.8.6 Aromatic Region of ^{1}H NMR with 4-d_5 and $C_6D_5ICl_2$

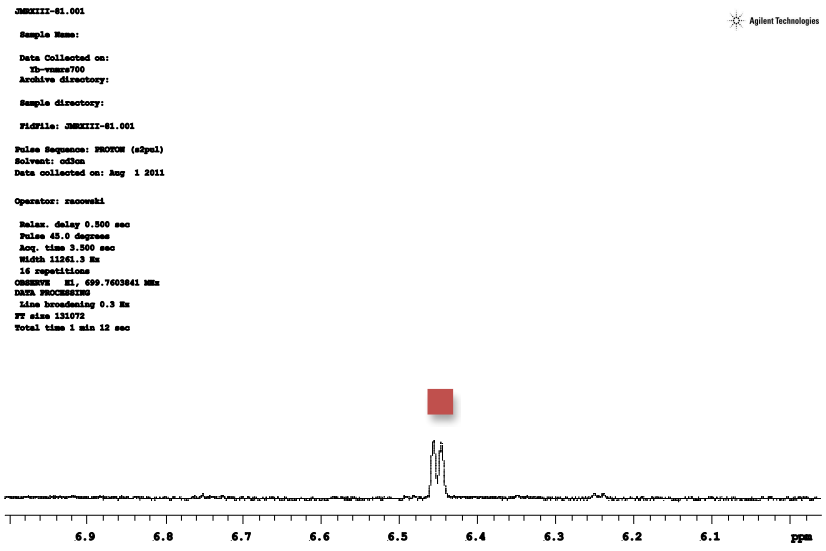

^{1}H-^{1}H COSY (CD_3CN, –15 ºC). *This experiment allows assignment of 5 resonances [at 6.14, 6.22, 6.56 (two overlapping peaks) and 6.93] as belonging to the intact phenyl ring of* ***8***.

Figure 4.4.8.7 ^{1}H-^{1}H COSY of 8 and 5-Cl

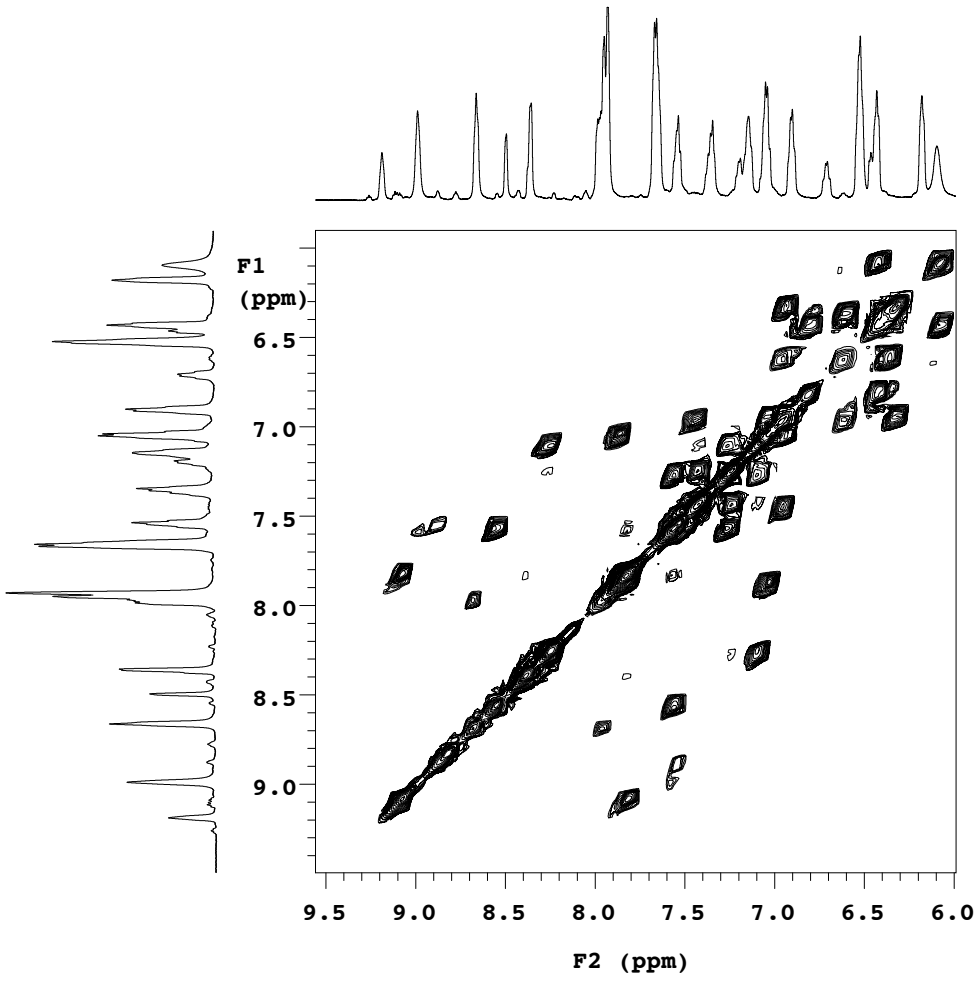

H1, 699.7604179	DATA PROCESSING Sq. sine bell 0.075 sec F1 DATA PROCESSING Sq. sine bell 0.023 sec FT size 4096 x 4096 Total time 43 minutes		JMRXIII-53.COSY Solvent: cd3cn Temp. -15.0 C / 258.1 K Operator: racowski File: JMRXIII-53.COSY GEMINI-400 "Zn.Chem.LSA.UMich.edu"

Diffusion NMR (DOSY gradient compensated stimulated echo with spin lock and convection compensation) (CD_3CN, –15 ºC). Plot below shows chemical shift (ppm) versus diffusion coefficient, D, ($m^2/s \times 10^{-10}$). *All of the aromatic peaks for both **8** and **5-Cl** have very similar diffusion coefficients (D) between 7.0 and 8.0 x 10^{-10} m^2/s. This indicates that **8** and **5-Cl** have similar hydrodynamic radii, which is consistent with formulation of **8** as a monomeric Pd^{IV} species as opposed to a Pd^{III} dimer.*

Figure 4.4.8.8 Diffusion NMR of 8 and 5-Cl

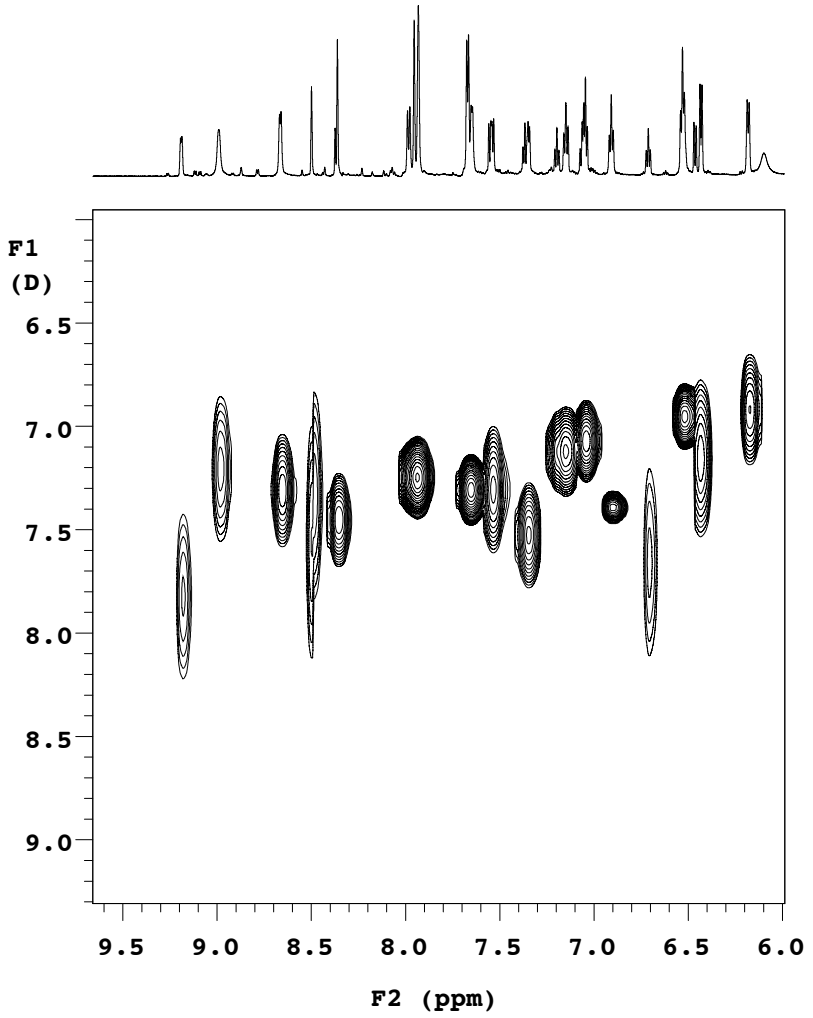

7	DATA PROCESSING Gauss apodization 0.069 sec FT size 4096 Total time 3 minutes		JMRXIII-78.dosytrial Solvent: cd3cn Temp. -15.0 C / 258.1 K Operator: racowski File: JMRXIII-78.dosyaromatic GEMINI-400 "Zn.Chem.LSA.UMich.edu"

^{13}C-^{19}F HMBC (CD_3CN, –30 ºC). *This heteronuclear HMBC shows two cross-peaks for complex **5-Cl**, demonstrating correlations between the fluorines of the CF_3 ligand and the two α-carbons of the cyclometalated ligand. In contrast, the analogous data for **8** show a single cross-peak, indicating that only one C of the σ-aryl ligand is bound to the metal. Additionally, a one bond correlation is seen between fluorine and the carbon of the CF_3* group for both **8** and **5-Cl**.

Figure 4.4.8.9 ^{13}C-^{19}F HMBC of 8 and 5-Cl

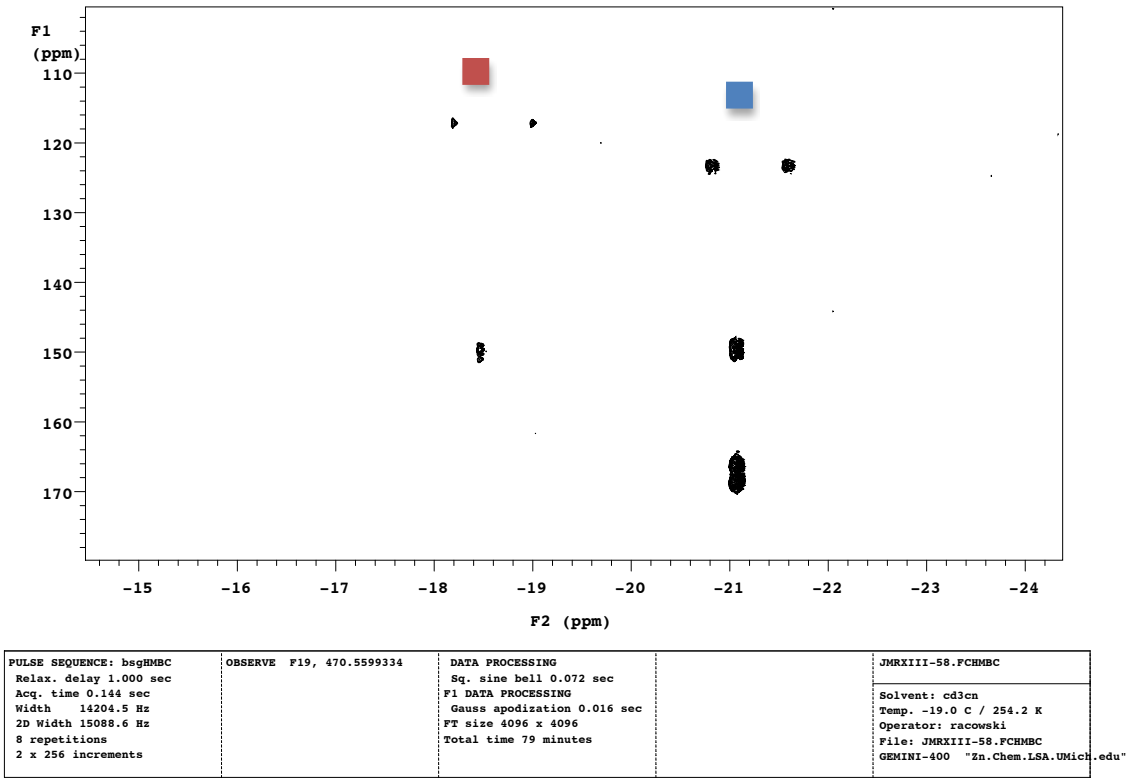

Stereochemistry of 8. Possible isomers of intermediate **8** are shown below. Complexes **8-a**, **8-b**, and **8-c** are stereoisomers, while **8-b/8-b**-*rot* and **8-c/8-c**-*rot* are rotamers. Complexes **8-c**/**8-c**-*rot* are highly unlikely, because they place the strongly donating σ-aryl and CF_3 ligands trans to one another, which is typically strongly disfavored in Pd^{IV} complexes. ^1H-^1H ROESY and NOESY NMR experiments were conducted but did not show strong enough cross-peaks to definitively distinguish between **8-a** and **8-b**.

Scheme 4.4.8.4 Possible Isomers of Intermediate 8

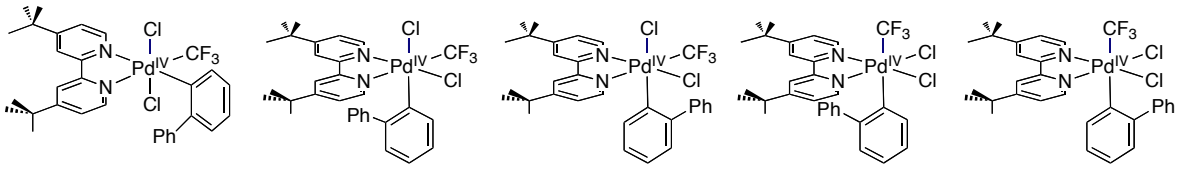

Two pieces of evidence lead me to favor isomer **8-b** over isomer **8-a**. First, the ^1H NMR resonances for the non-cyclometalated ring are significantly shielded [appearing at 6.14, 6.22, 6.56 (two overlapping peaks) and 6.93]. This is consistent with an interaction of the protons on this ring with a pi-system in a structure like **8-b** (see below, the aromatic ring is sitting below the dtbpy ligand). However, NOESY/ROESY NMR experiments did not provide strong enough nOe data to definitively confirm this assignment.

Scheme 4.4.8.5 Depiction of Shielded Protons on Complex 8

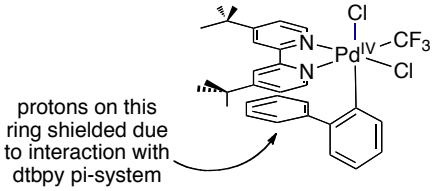

In addition, the stereochemistry of cyclometalation appears consistent with isomer **8-b**. As discussed in detail above, at t=0 (25 ºC), complex **8** was formed as an ~1:1 mixture with **5-Cl**. We believe that the initially formed **5-Cl** is generated by a different pathway – ie, not from **8**. With **4-*d*$_5$** as the starting material, the initially formed **5-Cl-*d*$_4$** was exclusively isomer **I**. Isomer **II** appeared only as **8-*d*$_5$** decayed, suggesting that C–H activation at complex **8-*d*$_5$** produces isomer **II**. The final ratio of **5-Cl-*d*$_4$-I** : **5-Cl-*d*$_4$-II** after 6 h at 25 ºC was ~1 : 1. The result suggests that **8** converts selectively to **5-Cl-*d*$_4$-II**, which is most consistent with isomer **8-b**.

Notably, isomerization of the initially formed **5-Cl-*d*$_4$-I** as the pathway to **5-Cl-*d*$_4$-II** cannot be ruled out; however, I believe that this is unlikely. For example, the related unsymmetrical product **13-OTf** (*vide infra*) *does not* isomerize under analogous conditions.

Scheme 4.4.8.6 Conversion of 8-d_5 to 5-Cl-d_4 (II)

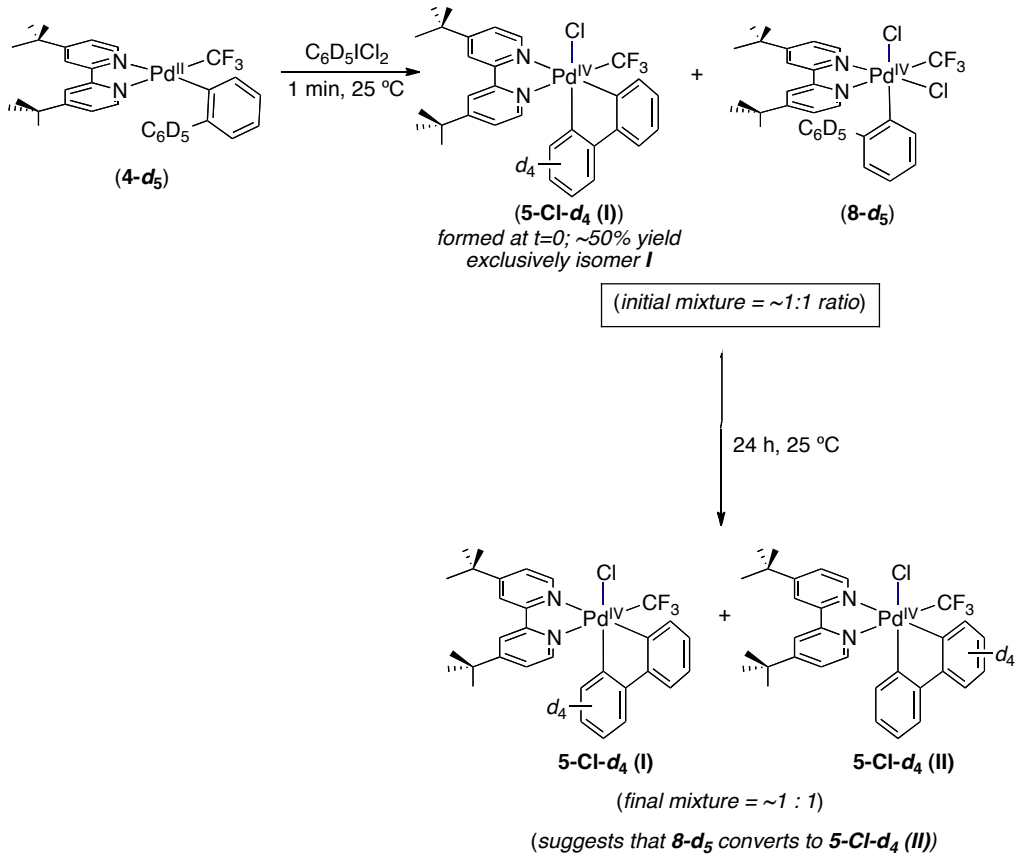

4.4.9 Procedures and Characterization of the Reactions of 4 with Oxidants

Scheme 4.4.9.1 Reaction of 4 with Oxidants

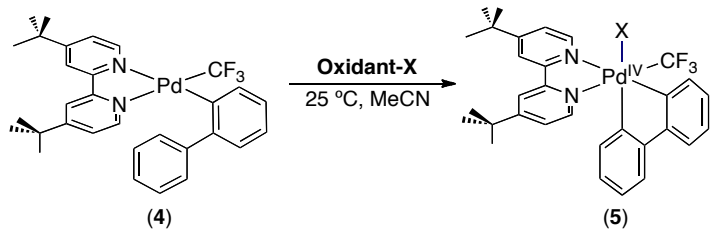

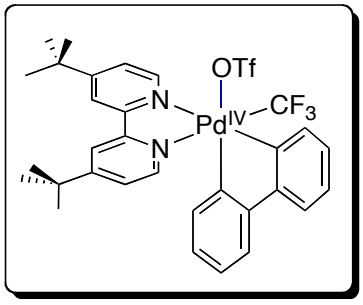

Complex 5-OTf. Complex **4** (137 mg, 0.23 mmol, 1.0 equiv) and NFTPT (66.5 mg, 0.23 mmol, 1.0 equiv) were combined in MeCN (30 mL), and this mixture was stirred for 15 min. The solvent was removed by rotary evaporation, and the resulting yellow solids were dissolved in CH_2Cl_2 (20 mL). This solution was extracted with H_2O (3 x 30 mL). The organic layer was separated and dried over $MgSO_4$. The reaction was concentrated by rotary evaporation, and the remaining solid residue was washed with diethyl ether (2 x 40 mL). The solid material was then dissolved in CH_2Cl_2 (2 mL), and diethyl ether (10 mL) was added to precipitate the product. The precipitate was collected and dried under vacuum to afford **5-OTf** as a light yellow solid (147 mg, 86% yield). ^{1}H NMR (CD_3CN): δ 9.19 (d, *J* = 5 Hz, 1H), 8.55 (s, 1H), 8.41 (s, 1H), 8.03 (d, *J* = 6 Hz, 1H), 7.92 (d, *J* = 8 Hz, 1H), 7.75 (d, *J* = 8 Hz, 1H), 7.59-7.57 (multiple peaks, 2H), 7.51-7.45

(multiple peaks, 2H), 7.30 (t, *J* = 8 Hz, 1H), 7.15 (t, *J* = 6 Hz, 1H), 6.76 (t, *J* = 8 Hz, 1H), 6.38 (d, *J* = 8 Hz, 1H), 1.56 (s, 9H), 1.36 (s, 9H). ^{19}F NMR (CD_3CN): δ –23.37 (s, 3F), –79.34 (s, 3F). ^{13}C NMR (CD_3CN): δ 170.00 (q, *J* = 5 Hz), 167.09, 167.06, 163.01 (q, *J* = 5 Hz), 154.36, 153.59, 150.43 (q, *J* = 5 Hz), 148.58, 148.18, 147.41, 131.52, 129.64, 129.36, 128.82, 128.47, 127.99, 125.60, 124.62, 124.08, 123.86 (q, *J* = 365 Hz), 122.71, 122.43, 121.40 (CF_3 for triflate; identified by ^{19}F-^{13}C HSQC, as resonance was in signal to noise), 36.42, 36.27, 30.07, 29.84. HRMS-electrospray (m/z): $[M–OTf]^+$ $C_{32}H_{32}F_6N_2O_3SPd$, 595.1552; Found, 595.1556.

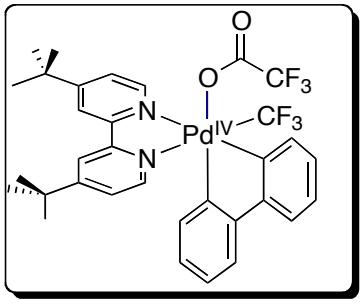

Complex 5-TFA. Complex **4** (60 mg, 0.080 mmol, 1 equiv) and $PhI(O_2CCF_3)_2$ (25 mg, 0.080, 1.0 equiv) were combined in MeCN (15 mL), and this mixture was stirred for 15 min. The reaction mixture was filtered through a plug of Celite, and the Celite was washed with MeCN (5 mL). The solvent was removed by rotary evaporation. The resulting solids were then dissolved in CH_2Cl_2 (3 mL), and pentane (15 mL) was added to precipitate the product. The precipitate was collected and dried under vacuum to afford **5-TFA** as a light yellow solid (41 mg, 73% yield). ^{1}H NMR (CD_3CN): δ 9.32 (d, *J* = 5 Hz, 1H), 8.45 (s, 1H), 8.32 (s, 1H), 7.97-7.92 (multiple peaks, 2H), 7.69 (d, *J* = 8 Hz, 1H), 7.57-7.53 (multiple peaks, 2H), 7.42 (t, *J* = 7 Hz, 1H), 7.37 (d, *J* = 6 Hz, 1H), 7.26 (t, *J* = 8 Hz, 1H), 7.09 (t, *J* = 6 Hz, 1H), 6.71 (t, *J* = 8 Hz, 1H), 6.36 (d, *J* = 8 Hz, 1H), 1.53 (s, 9H), 1.32 (s, 9H). ^{19}F NMR (CD_3CN): δ –26.15 (s, 3F), –75.80 (s, 3F). ^{13}C NMR (CD_2Cl_2): δ 169.96 (q, *J* = 6 Hz), 165.43, 165.36, 162.18 (q, *J* = 6 Hz), 160.91 (q, *J* = 35 Hz), 154.54, 153.95, 151.73 (q, *J* = 6 Hz), 148.81, 148.15, 148.03, 130.85, 129.92,

128.61, 127.74, 127.68, 126.79, 125.07, 124.76, 123.33, 123.25 (q, *J* = 366 Hz), 123.08, 120.01, 119.97, 117.14 (q, *J* = 293 Hz), 36.15, 35.98, 30.67, 30.44. IR (thin film): n 2968.9, 1690.3, 1411.9, 1195.6, 1090.9, 1017.9, 745.7, 606.1 cm^{-1}. HRMS-electrospray (m/z): $[M–O_2CCF_3]^+$ calcd for $C_{33}H_{32}F_6N_2O_2Pd$, 595.1552; Found, 595.1563.

4.4.10 Characterization of 10

Scheme 4.4.10.1 Reaction of 9 with $PhI(Cl)_2$

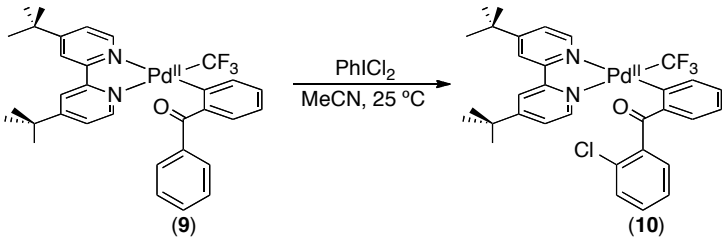

(**9**) (**10**)

Complex 10. Complex **9** (25 mg, 0.4 mmol, 1.0 equiv) and $PhICl_2$ (11 mg, 0.04 mmol, 1.0 equiv) were combined in MeCN (5 mL), and the resulting solution was stirred for 10 min at rt. The solvent was removed under vacuum, the yellow residue was dissolved in CH_2Cl_2 (1 mL), and the product was precipitated with hexanes (10 mL). The precipitate was collected and dried under vacuum to afford **10** as a light yellow solid (25 mg, 95% yield). ^1H NMR (CD_3CN): δ 9.14 (d, *J* = 6 Hz, 1H), 8.62 (s, 1H), 8.53 (s, 1H), 8.32 (d, *J* = 8 Hz, 1H), 8.06-8.00 (multiple peaks, 2H), 7.97 (d, *J* = 6 Hz, 1H), 7.80-7.75 (multiple peaks, 3H), 7.62-7.59 (multiple peaks, 3H), 7.54 (d, *J* = 6 Hz, 1H), 1.55 (s, 9H), 1.42 (s, 9H). ^{19}F NMR (CD_3CN): δ –21.05 (s, 3F). ^{13}C NMR ($CDCl_3$): δ 213.26, 173.84, 167.12, 166.91, 153.64, 153.42, 149.67, 148.18, 142.11, 141.09, 138.91, 136.11, 133.13, 132.57, 130.66, 129.68, 129.48, 128.40, 126.11, 125.03, 125.33 (q, *J* = 371 Hz), 122.33, 122.02, 119.60, 35.99 (2 overlapping C's), 30.23, 30.14. IR (thin film): ν 2963.2, 1666.2, 1612.4, 1484.0, 1413.3, 1336.9, 1058.1, 1013.9, 849.5, 732.1, 604.5 cm^{-}

[1]. HRMS-electrospray (m/z): $[M+H]^+$ $C_{32}H_{32}F_3N_2OClPd$, 659.1263; Found, 659.1273.

4.4.11 Procedures and Characterization data for 12-OTf/13-OTf and 12-Cl/13-Cl

Scheme 4.4.11.1 Oxidation of 11 with NFTPT

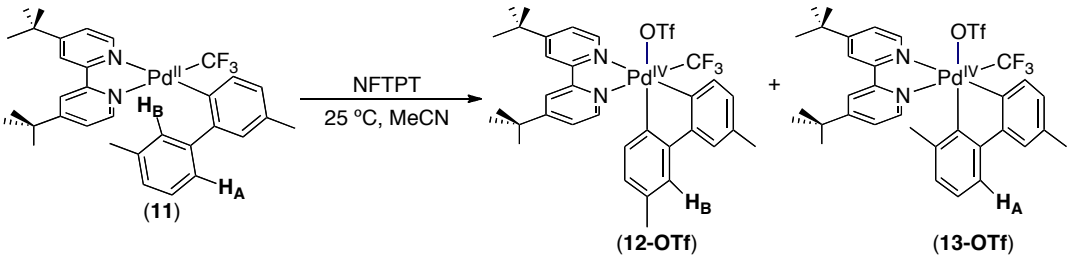

Complexes 12-OTf/13-OTf. Complex **11** (162 mg, 0.29 mmol, 1.0 equiv) and NFTPT (83.8 mg, 0.29 mmol, 1.0 equiv) were combined in MeCN (30 mL), and this mixture was stirred for 15 min at rt. The solvent was removed by rotary evaporation, and the resulting yellow solids were dissolved in CH_2Cl_2 (20 mL). This solution was extracted with H_2O (3 x 30 mL). The organic layer was separated and dried over $MgSO_4$. The reaction was concentrated by rotary evaporation, and the remaining solid residue was washed with diethyl ether (2 x 40 mL). The solid material was then dissolved in CH_2Cl_2 (2 mL), and diethyl ether (10 mL) was added to precipitate the product. A mixture of complexes **12-OTf** and **13-OTf** was obtained in a 1.7 : 1 ratio as a pale yellow solid (135 mg, 64% yield). Complex **12-OTf** was synthesized independently as described below.

Scheme 4.4.11.2 Conversion of 12-OTf/13-OTf to 12-Cl/13-Cl

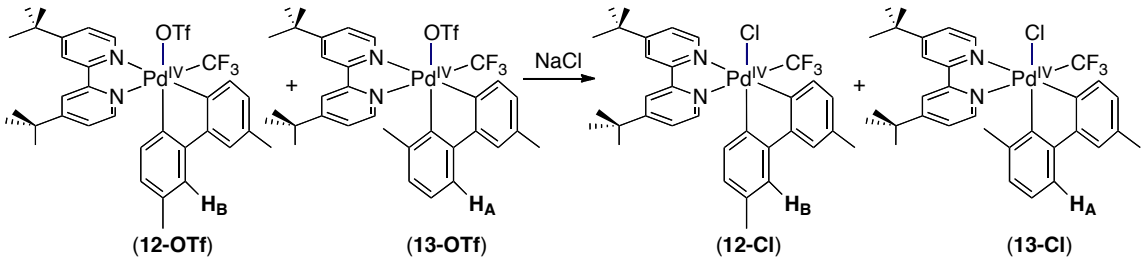

Compounds 12-Cl/13-Cl. The mixture of isomers **12-OTf** and **13-OTf** (20 mg, 0.026 mmol) was dissolved in CH_2Cl_2 (10 mL). This solution was extracted with a saturated aqueous solution of NaCl (10 mL). The organic layer was separated, dried over $MgSO_4$, and concentrated under vacuum to afford an inseparable mixture of **12-Cl** and **13-Cl** as a pale yellow solid (16 mg, 93% yield). Complex **12-Cl** was synthesized independently as described below.

NMR characterization and structural assignment of 12-OTf/13-OTf and 12-Cl/13-Cl. A series of 2D NMR experiments (^{1}H-^{1}H COSY, ^{1}H-^{13}C HSQC, ^{19}F-^{13}C HSQC, ^{1}H-^{13}C HMBC and ^{19}F-^{1}H HOESY were conducted to completely characterize the mixtures of isomers **12/13**. The major isomers **12-OTf** and **12-Cl** were synthesized and analyzed independently (*vide infra*). Complexes **13-OTf** and **13-Cl** (the minor regioisomers) were characterized as part of a mixture with **12-OTf** or **12-Cl**, respectively. The most diagnostic resonances for **13-OTf** and **13-Cl** were those corresponding to H23, H24 and H25. ^{19}F-^{13}C HSQC correlation was used to determine the ^{13}C NMR shift for the CF_3 peak of the minor isomers **13-OTf** and **13-Cl** and for the triflate CF_3 peak for **12-OTf** and **13-OTf**. ^{19}F-^{1}H HOESY was used to establish the geometry about the octahedral Pd center in **12-Cl/13-Cl**. This information was extrapolated to **12-OTf/13-OTf.** This experiment showed a correlation between the fluorines of the CF_3 ligand and H1,

consistent with the geometry shown. Based on the X-ray structure of **12-Cl**, this proton is 3.157 Å from the closest fluorine.

Scheme 4.4.11.3 Depiction of F-H Correlation Observed in ^{19}F-^{1}H HOESY Experiment for 12-Cl/OTf and 13-Cl/OTf

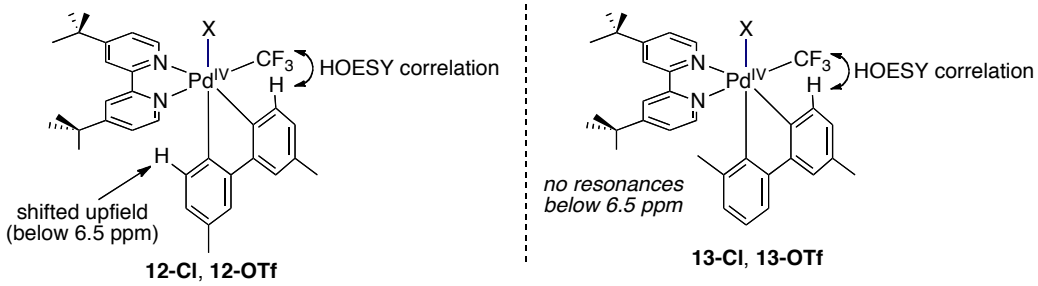

Independent synthesis of 12-Cl. Compound **11** (75 mg, 0.12 mmol, 1.0 equiv) and $PhICl_2$ (33 mg, 0.12, 1.0 equiv) were combined in MeCN (20 mL), and this mixture was stirred for 10 min. The solvent was removed by rotary evaporation. The resulting solids were then dissolved in CH_2Cl_2 (2 mL), and hexanes (10 mL) was added to precipitate the product. The precipitate was collected and dried under vacuum to afford **12-Cl** as a light yellow solid (61 mg, 77% yield, single isomer detected by ^{1}H NMR spectroscopy). ^{1}H NMR (CD_2Cl_2): δ 9.22 (H1, d, *J* = 6 Hz, 1H), 8.24 (H16, d, *J* = 8 Hz, 1H), 8.21 (H6, s, 1H), 8.07 (H9, s, 1H), 7.79 (H2, d, *J* = 6 Hz, 1H), 7.63 (H13, d, *J* = 6 Hz, 1H), 7.39 (H20, s, 1H), 7.30 (H23, s, 1H), 7.23 (H14, d, *J* = 6 Hz, 1H), 6.97 (H17, d, *J* = 9 Hz, 1H), 6.49 (H26, d, *J* = 9 Hz, 1H), 6.32 (H27, d, *J* = 8 Hz, 1H), 2.43 (H25, s, 3H), 2.22 (H19, s, 3H), 1.49 (H12, s, 9H), 1.30 (H5, s, 9H). ^{19}F NMR (CD_2Cl_2): δ –20.97. ^{13}C NMR (CD_2Cl_2): δ 165.40 (C15), 164.50 (C10), 164.40 (C3), 163.48 (C28), 153.39 (C8), 153.11 (C7), 150.73 (C1), 147.58 (C21), 147.63 (C14), 147.38 (C22), 135.30 (C24), 133.77 (C16), 129.20 (C27), 128.81 (C17), 127.94 (C26), 125.52 (C2), 125.07 (C18), 124.65 (C13), 123.56 (C20), 123.45 (C23), 122.78 (CF_3) (q, *J* = 364 Hz), (120.23 (C6), 120.15 (C9), 35.49 (C4), 35.01 (C11), 30.39 (C12), 30.31 (C5),

21.25 (C25), 21.06 (C19). HRMS-electrospray (m/z): $[M–Cl]^+$ calcd for $C_{33}H_{36}ClF_3N_2Pd$, 623.1860; Found, 623.1871.

Scheme 4.4.11.4 Labeling Scheme of Protons and Carbons for 12-Cl

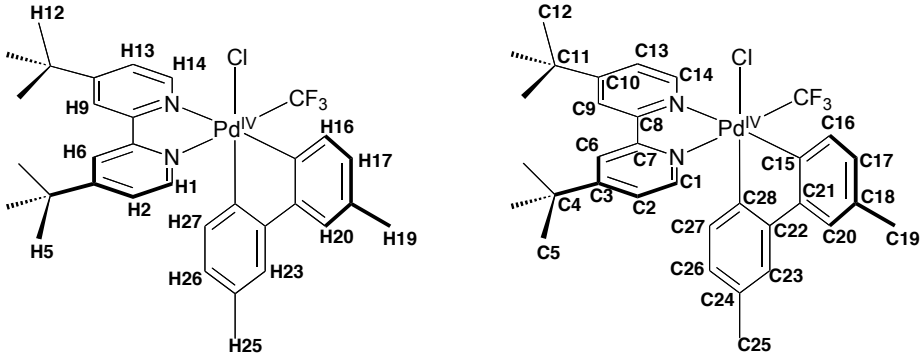

Independent synthesis of 12-OTf. Complex **12-Cl** (30 mg, 0.045 mmol, 1 equiv) and AgOTf (12 mg, 0.047 mmol, 1.05 equiv) were dissolved in MeCN (6 mL), and the resulting suspension was stirred for 15 min at rt. The reaction mixture was filtered through a plug of Celite, and the filtrate was concentrated under vacuum. The resulting yellow residue was dissolved in CH_2Cl_2 (6 mL), and this solution was extracted with water (2 x 20 mL). The organic extracts were separated, dried over $MgSO_4$, and concentrated to ~1 mL. Pentane was added to precipitate the product. The precipitate was collected and dried under vacuum to afford **12-OTf** was obtained as a light yellow solid (32 mg, 92% yield). ^{1}H NMR (CD_3CN): δ 9.15 (H1, d, *J* = 6 Hz, 1H), 8.53 (H6, s, 1H), 8.38 (H6, s, 1H), 8.00 (H2, d, *J* = 6 Hz, 1H), 7.75 (H16, d, *J* = 7 Hz, 1H), 7.59 (H20, s, 1H), 7.57 (H14, d, *J* = 7 Hz, 1H), 7.45 (H13, d, *J* = 6 Hz, 1H), 7.43 (H23, s, 1H), 7.09 (H17, d, *J* = 7 Hz, 1H), 6.54 (H26, d, *J* = 8 Hz, 1H), 6.21 (H27, d, *J* = 8 Hz, 1H), 2.49 (H19, s, 3H), 2.25 (H25, s, 3H), 1.55 (H5, s, 9H), 1.37 (H12, s, 9H). ^{19}F NMR (CD_3CN): δ –23.37 (s, 3F), –79.34 (s, 3F). ^{13}C NMR (CD_3CN): δ 167.04 (C3), 166.94 (C10), 166.88 (C15), 159.83 (C28), 153.46 (C7), 153.18 (C8), 150.53 (C1), 148.19

(C22), 148.13 (C14), 147.02 (C21), 138.38 (C18), 137.86 (C24), 130.99 (C16), 129.62 (C17), 129.28 (C27), 129.19 (C26), 126.47 (C2), 125.41 (C13), 125.40 (C20), 124.65 (C23), 123.68 (CF_3) (q, *J* = 364 Hz), 122.60 (C6), 122.47 (C9), 120.90 (CF_3 for triflate determined by HSQC ($^{19}F/^{13}C$)), 36.42 (C11), 36.30 (C4), 30.11 (C5), 29.87 (C12), 20.80 (C19), 20.34 (C25). HRMS-electrospray (m/z): $[M–OTf]^+$ $C_{32}H_{32}F_6N_2O_3SPd$, 623.1880; Found, 623.1876.

Scheme 4.4.11.5 Labeling Scheme of Protons and Carbons for 12-OTf

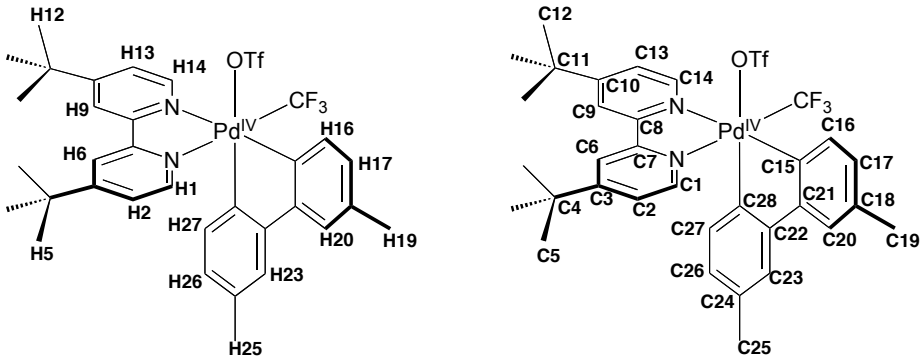

Characterization data for 13-OTf. Full spectral data for compound **13-OTf** were not obtained due to the inability to resolve all of the peaks from **12-OTf**. Importantly, the peaks that were well-resolved correspond to H23-25, which clearly show a triplet for H24 and a COSY relationship. Further characterization was achieved by converting this mixture to a mixture of **12-Cl** and **13-Cl** (for which all of the ^1H and ^{13}C NMR resonances were well-resolved and could be assigned by 2D NMR). ^1H NMR (CD_3CN): δ 9.19 (H1, d, *J* = 6 Hz, 1H), 8.00 (H6, s, 1H), 7.50 (H23, d, *J* = 7 Hz, 1H), 7.22 (H24, t, *J* = 7 Hz, 1H), 6.95 (H25, d, *J* = 7 Hz, 1H), 2.33 (s, 1H). ^{19}F NMR (CD_3CN): δ –22.91 (s, 3F), –79.36 (s, 3F). ^{13}C NMR (CD_3CN): δ 150.58 (C1), 132.18 (C25), 128.27 (C24), 125.20 (C20), 124.20 (C23), 124.01 (CF_3), 122.44 (C3), 121.84 (C9), 120.90 (CF_3 of triflate). HRMS-electrospray (m/z): $[M–OTf]^+$ $C_{32}H_{32}F_6N_2O_3SPd$, 623.1880; Found, 623.1865.

Scheme 4.4.11.6 Labeling Scheme of Protons and Carbons for 13-OTf

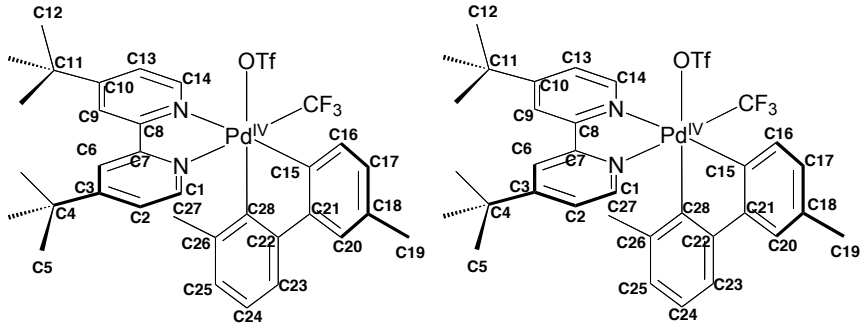

Characterization data for 13-Cl. ^{1}H NMR (CD_2Cl_2): δ 9.28 (H1, d, *J* = 6 Hz, 1H), 8.36 (H16, d, *J* = 8 Hz, 1H), 8.16 (H6, s, 1H), 8.06 (H9, s, 1H), 7.71 (H2, d, *J* = 6 Hz, 1H), 7.66 (H13, d, *J* = 6 Hz, 1H), 7.43 (H20, s, 1H), 7.37 (H23, d, *J* = 6 Hz, 1H), 7.22 (H14, d, *J* = 6 Hz, 1H), 6.95 (H17, t, *J* = 8 Hz, 1H), 6.55 (H25, d, *J* = 8 Hz, 1H), 6.90 (H24, d, *J* = 8 Hz, 1H), 2.42 (H27, s, 3H), 2.22 (H19, s, 3H), 1.50 (H12, s, 9H), 1.30 (H5, s, 9H). ^{19}F NMR (CD_2Cl_2): δ –19.84. ^{13}C NMR (CD_2Cl_2): δ 168.42 (C15), 165.75 (C28), 164.64 (C10), 164.30 (C3), 152.74 (C8), 153.24 (C7), 151.95 (C1), 148.01 (C22), 147.90 (C14), 147.57 (C21), 136.16 (C18), 134.67 (C16), 128.40 (C17), 127.61 (C26), 126.40 (C24), 125.84 (C25), 124.62 (C2), 124.56 (C13), 123.59 (C20), 122.91 (CF_3), 120.15 (C6), 120.03 (C23), 120.01 (C9), 35.56 (C11), 34.84 (C4), 30.37 (C12), 30.40 (C5), 21.26 (C27), 21.06 (C19). HRMS-electrospray (m/z): $[M–Cl]^+$ calcd for $C_{33}H_{36}ClF_3N_2Pd$, 623.1860; Found, 623.1872.

Scheme 4.4.11.6 Labeling Scheme of Protons and Carbons for 13-Cl

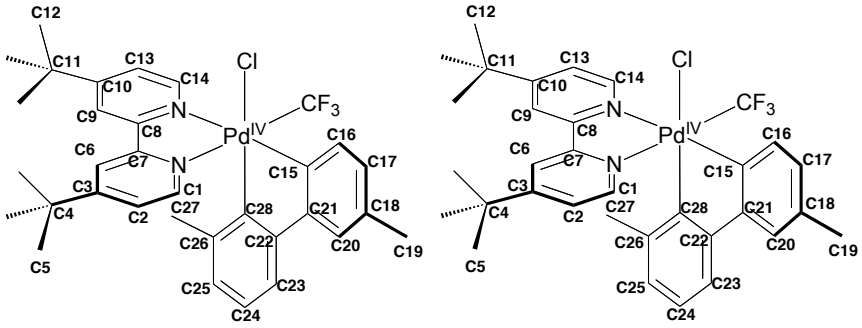

4.4.12 Selectivity of Cyclometalation at 14-F

Scheme 4.4.12.1 Reaction of 14-I with AgF

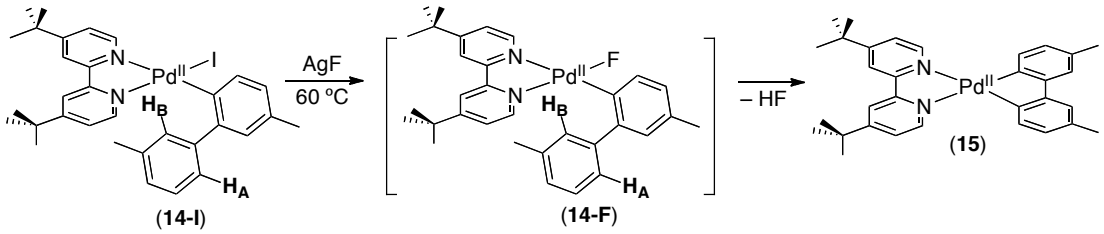

A solution of complex **14-I** (50 mg, 0.063 mmol, 1 equiv) and AgF (5 equiv) in benzene (12 mL) was sonicated for 4 h at 25 °C. The reaction mixture was filtered through a plug of Celite and the plug was washed with CH_2Cl_2 (15 mL). The resulting solution was concentrated by rotary evaporation to ~2 mL, and ether/pentane (15 mL) was added to precipitate the product. The precipitate was collected and dried under vacuum to afford **15** as a yellow solid (31 mg, 89% yield). ^{1}H NMR (CD_2Cl_2): δ 9.12 (d, *J* = 6 Hz, 2H), 8.05 (s, 2H), 7.58 (d, *J* = 6 Hz, 2H), 7.32 (d, *J* = 7 Hz, 2H), 7.12 (s, 2H), 6.71 (d, *J* = 7 Hz, 2H), 2.29 (s, 6H), 1.43

(s, 18H). ^{13}C NMR ($CDCl_3$, 52 ºC): δ 163.67, 157.45, 155.48, 150.49, 136.37, 135.37, 125.92, 122.97, 120.67, 119.31, 117.35, 35.42, 30.23, 21.19. HRMS-electrospray (m/z): $[M+H]^+$ calcd for $C_{32}H_{36}F_3N_2Pd$, 555.1986; Found, 555.1997.

4.4 References and Footnotes

1. (a) Powers, D. C.; Ritter, T. *Top. Organomet. Chem.* **2011**, *35*, 129. (b) Xu, L. M.; Li, B. J.; Yang, Z.; Shi, Z. J. *Chem. Soc. Rev.* **2010**, *39*, 712. (c) Sehnal, P.; Taylor, R. J. K.; Fairlamb, I. J. S. *Chem. Rev.* **2010**, *110*, 824. (d) Deprez, N. R.; Sanford, M. S. *Inorg. Chem.* **2007**, *46*, 1924. (e) Muniz, K. *Angew. Chem. Int. Ed.* **2009**, *48*, 9412. (f) Canty, A. J. *Dalton Trans.* **2009**, *47*, 10409.

2. For recent examples, see: (a) Zhao, X. D.; Dong, V. M. *Angew. Chem. Int. Ed.* **2011**, *50*, 932. (b) Oloo, W.; Zavalij, P. Y.; Zhang, J.; Khasin, E.; Vedernikov, A. N. *J. Am. Chem. Soc.* **2010**, *132*, 14400. (c) Powers, D. C.; Benitez, D.; Tkatchouk, E.; Goddard, W. A. III; Ritter, T. *J. Am. Chem. Soc.* **2010**, *132*, 14092. (d) Khusnutdinova, J. R.; Rath, N. P.; Mirica, L. M. *J. Am. Chem. Soc.* **2010**, *132*, 7303. (e) Shabashov, D.; Daugulis, O. *J. Am. Chem. Soc.* **2010**, *132*, 3965. (f) Furuya, T.; Benitez, D.; Tkatchouk, E.; Strom, A. E.; Tang, P.; Goddard, W. A.; Ritter, T. *J. Am. Chem. Soc.* **2010**, *132*, 3793. (g) Racowski, J. M.; Dick, A. R.; Sanford, M. S. *J. Am. Chem. Soc.* **2009**, *131*, 10974.

3. (a) Wang, X.; Leow, D.; Yu, J.-Q. *J. Am. Chem. Soc.* **2011**, *133*, 13864. (b) Hull, K. L.; Lanni, E. L.; Sanford, M. S. *J. Am. Chem. Soc.* **2006**, *128*, 14047.

4. Sibbald, P. A.; Rosewall, C. F.; Swartz, R. D.; Michael, F. E. *J. Am. Chem. Soc.* **2009**, *131*, 15945.

5. Pilarski, L. T.; Selander, N.; Bose, D.; Szabo, K. J. *Org. Lett.* **2009**, *11*, 5518.

6. Hickman, A. J.; Sanford, M. S. *ACS Catal.* **2011**, *1*, 170.

7. Kawai, H.; Kobayshi, Y.; Oi, S.; Inoue, Y. *Chem. Commun*. **2008**, 1464.

8. For intermolecular C–H activation at Pt^{IV} centers, see: Shul'pin, G. B.; Nizova, G. V.; Nikitaev, A. T. *J. Organomet. Chem.* **1984**, *276*, 115.

9. For intramolecular C–H activation at Pt^{IV} centers, see: Mamtora, J.; Crosby, S. H.; Newman, C. P.; Clarkson, G. J.; Rourke, J. P. *Organometallics* **2008**, *27*, 5559.

10. Whitfield, S. R.; Sanford, M. S. *J. Am. Chem. Soc.* **2007**, *129*, 15142.

11. a) Campora, J.; Lopez, J. A.; Palma, P.; Rio, D.; Carmona, E.; Valerga, P.; Graiff, C.; Tiripicchio, A. *Inorg. Chem.* **2001**, *40*, 4116. b) Campora, J.; Palma, P.; del Rio, D.; Carmona, E.; Graiff, C.; Tiripicchio, A. *Organometallics*, **2003**, *22*, 3345. c) Campora, J; Palma, P.; del Rio, D.; Lopez, J. A.; Alvarez, E.; Connelly, G. N.*Organometallics* **2005**, *24*, 3624.

12. For representative reviews on intramolecular C–H activation see: (a) Albercht, M. *Chem. Rev.* **2010**, *110*, 576. (b) Dupont, J.; Consorti, C. S.; Spencer, J. *Chem. Rev.* **2005**, *105*, 2527. (c) Brune, M. I. *Angew. Chem., Int. Ed. Engl.* **1977**, *16*, 73.

13.Use of bidentate sp^2 N-donor ligands to stabilize Pd^{IV}: Canty, A. J. *Acc. Chem. Res.* **1992**, *25*, 83.

14. Use of chloride ligands to stabilize Pd^{IV}: (a) McCall, A. S.; Wang, H.; Desper, J. M.; Kraft, S. *J. Am. Chem. Soc.* **2011**, *133*, 1832. (b) Vicente, J.; Arcas, A.; Julia-Hernandez, F.; Bautista, D. *Chem. Commun.* **2010**, *46*, 7253. (c) Vicente, J.; Chicote, M. T.; Lagunas, M. C.; Jones, P. G.; Bembenek, E. *Organometallics* **1994**, *13*, 1243. (d) Alsters, P. J.; Engel, P. M.; Hogerheide, M. P.; Copijn, M.; Spek, A. L.; van Koten, G. *Organometallics* **1993**, *12*, 1831. (e) Gray, L. R.; Gulliver, D. J.; Levason, W.; Webster, M. *J. Chem. Soc., Dalton Trans.* **1983**, 133. (f) Kukushkin, Y. N.; Sedova, G. N.; Vlasova, R. A. *Zh. Neorg. Khim.* **1978**, *23*, 1977. (g) Uson, R.; Fornies, J.; Navarro, R. *J. Organomet. Chem.* **1975**, *96*, 307.

15. Use of $PhICl_2$ to oxidize Pd^{II} to Pd^{IV}: (a) Ref. 12a. (b) Pearson, S. L.; Sanford, M. S.; Arnold, P. *J. Am. Chem. Soc.* **2009**, *131*, 13812. (c) Whitfield, S. R.;

Sanford, M. S. *J. Am. Chem. Soc.* **2007**, *129*, 15142. (d) Lagunas, M.-C.; Gossage, R. A.; Spek, A. L.; van Koten, G. *Organometallics* **1998**, *17*, 731.

16. (a) Ball, N. D.; Gary, J. B.; Ye, Y.; Sanford, M. S. *J. Am. Chem. Soc.* **2011**, *133*, 7577. (b) Ye, Y.; Ball, N. D.; Sanford, M. S. *J. Am. Chem. Soc.* **2010**, *132*, 14682. (c) Ball, N. D.; Kampf, J.; Sanford, M. S. *J. Am. Chem. Soc.* **2010**, *132*, 2878.

17. When the reaction was conducted at –30 ºC, the initial NMR spectrum showed the presence of intermediate **8** along with some of the C–H activation product **5-Cl** (ratio **8** : **5-Cl** = 3 : 1). The [**8**] did not change over several hours at –30 ºC, and this ratio remained constant over that time. Conversion of **8** to a mixture of **5-Cl** and **6** only occurred when the mixture was warmed. These data suggest that the **5-Cl** formed initially in the –30 ºC experiment is generated by a different, heretofore undetected intermediate. See Supporting Information for a detailed discussion.

18. ^{1}H NMR spectroscopic studies of the oxidation of **4**-$\boldsymbol{d_5}$ (in which the pendant phenyl ring is deuterated) further confirmed the assignment of the 5 aromatic protons of this ring in intermediate **8**.

19. A key remaining question is the stereochemistry about the octahedral Pd^{IV} center in **8**. We have conducted several experiments to probe this, and they provide tentative support for the structure shown in Scheme 3.3.3. See Section 3.4 for a detailed discussion.

20. An alternative possible route to **10** would involve electrophilic chlorination of the aromatic ring similar to that described in ref. 14a.

21. Notably, similar selectivity was reported in ref. 3, where cyclopalladation at Pd^{IV} is proposed as a key step in catalysis.

22. The oxidation of **11** with $PhICl_2$ under otherwise identical conditions provided **12-Cl** as the major product with >10 : 1 selectivity. This suggests that site selectivity in C–H activation at Pd^{IV} is highly sensitive to the ligand environment

at the metal center. More extensive investigations of ligand effects in this system are ongoing.

23.Under analogous conditions (benzene, 4 h, 60 ºC), the reaction of **11** with NFTPT resulted in the same 1.7 : 1 ratio as observed in Scheme 3.3.5.

24. For examples, see ref. 12 as well as: Kalyani, D.; Sanford, M. S. *Org. Lett.* **2005**, *7*, 4149.

25. Takahashi, Y.; Ito, S. S., Sukai, S.; Ishii, Y. *J. Chem. Soc., Dalton Trans.* **1970**, *17*, 1065.

26. Taylor, R. T.; Stevenson, T. A. *Tetrahedron Lett.* **1988**, *29*, 2033.

27. Remy, M. S. Ph. D. Thesis. “Group 10 Methyl Transfer Reactions Towards Catalyst Development for Oxidative Oligomerization of Methane,” University of Michigan, **2011**.

28. Qin, Z.; Jennings, M. C.; Puddephatt, R. J. *Inorg. Chem.* **2001**, *41*, 3967.

Chapter 5: Conclusions

5.1 Conclusions and Future Directions

Over the last two decades, numerous reagents have been utilized to oxidize Pd^{II} model complexes to Pd^{IV} species. Furthermore, a wide variety of supporting ligands have been shown to support and stabilize observable Pd^{IV} adducts. However, in the past, C–C bond-forming reductive elimination was the primary decomposition pathway of these systems. This has hampered efforts to conduct detailed mechanistic investigations of C–X bond formation at Pd^{IV}. In contrast, the examples discussed in Chapters 2 and 3 describe Pd^{IV} compounds that decompose via carbon-heteroatom bond-forming reductive elimination.

The investigations presented in this thesis along with other recent studies in the field have begun to uncover the molecular mechanisms of carbon-heteroatom bond-forming reductive elimination from Pd^{IV} centers. Together these studies have begun to address fundamental questions about C–X reductive elimination from Pd^{IV}, such as the electronic requirements of C–X coupling, the effects of ancillary ligands, the influence of solvent and additives, and the relative rates of competing transformations. All of these results lend support for the potential feasibility of C–X coupling from Pd^{IV} in the catalytic oxidation reactions presented in Chapter 1.

The future of this field is bright, as there are still many outstanding mechanistic questions to be answered. For instance, now that systems have

been identified to investigate sp^3-C–X bond-formation from Pd^{IV} in high yields (Chapter 3), it would be interesting to explore the stereochemical outcome (retention vs inversion) and stereospecificity of sp^3-C–heteroatom reductive elimination from Pd^{IV}. These questions are crucial for developing well-controlled asymmetric catalytic transformations.

Furthermore, many organometallic Pd^{IV} species that are present during catalytic processes contain different heteroatom X-type ligands. Therefore, designing approaches to understand what controls the relative rates of different C–X reductive elimination reactions is of critical importance to the field. While an initial attempt to address this issue was made in Chapter 3, Scheme 3.4.2, there are still many questions to be addressed about competing C–heteroatom bond-forming processes, such as the effect of solvent, the influence of ligand structure and complex geometry, and the role of additives.

Additionally, studies of C–X reductive elimination from Pd^{IV} mono-organo complexes are important future targets, since such adducts more closely resemble putative catalytic intermediates than most of the complexes discussed herein. Efforts in all of these areas are bound to inform the development and optimization of novel catalytic transformations.

Finally, the results presented in Chapter 4 discuss the first example of C–H activation at a Pd^{IV} center. While the initial observation of intramolecular C–H at Pd^{IV} was very exciting, there are several important questions that arise from this result. For example, what is the mechanism and electronic requirements for C–H activation at Pd^{IV}? We envision that the question of electronic requirements might be addressed by modifying the biphenyl ligand of the Pd^{IV} complex (**1**) (Scheme 5.1.1) with various electronically differentiated substituents to study the rate of C–H activation to form **2**. Also, exploration of the effect of solvent on this transformation would be useful. Eyring analysis as well as determining the intramolecular kinetic isotope effect should also provide insight into the mechanism of C–H activation at Pd^{IV}. Additionally, extending the substrate scope of C–H activation at Pd^{IV} to intermolecular C–H activation, which more closely

mimics catalytic processes, would provide valuable information for the development of new methodology.

Scheme 5.1.1 Proposed Electronic Modification of 1 to Investigate the Rate of C–H Activation at Pd^{IV}

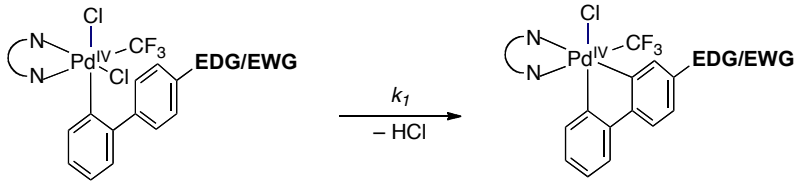

(**1**) (**2**)

Lastly and most excitingly, we believe that Chapter 4 lays the groundwork for debunking the assumption that Pd^{IV} is only relevant in reductive elimination reactions. The work in Chapter 4 represents the first report of an organometallic transformation other than bond-forming reductive elimination at Pd^{IV}. This result serves as motivation to explore other organometallic processes at Pd^{IV}, such as insertion reactions of π substrates or nucleopalladation of alkenes and alkynes. Excitingly, we obtained a very promising preliminary result when we investigated insertion reactions of π substrates. Reacting complex **3** in CH_2Cl_2 with CO for 15 min resulted in the quantitative conversion of complex **3** to organic product **6**. We hypothesize that compound **6** is generated via CO insertion at Pd^{IV} followed by C–C reductive elimination. More specifically, CO first replaces the triflate ligand of complex **3** to form intermediate **4**. Then, insertion of CO into the sp^3-carbon bond of complex **3** takes place (**5**), followed by bond-forming C–C reductive elimination to generate the organic product (**4**). Notably, Pd^{II} complex **7** is unreactive for up to 48 h under the analogous conditions. We are optimistic that monitoring the reaction by react-IR might provide evidence to substantiate our mechanistic hypothesis. Moreover, the result in Scheme 5.1.2 motivates us to pursue further study of new organometallic transformations at Pd^{IV}. It is our hope

that these stoichiometric findings will guide the development of novel, innovative catalytic reactions.

Scheme 5.1.2 CO Insertion at Pd^{IV}

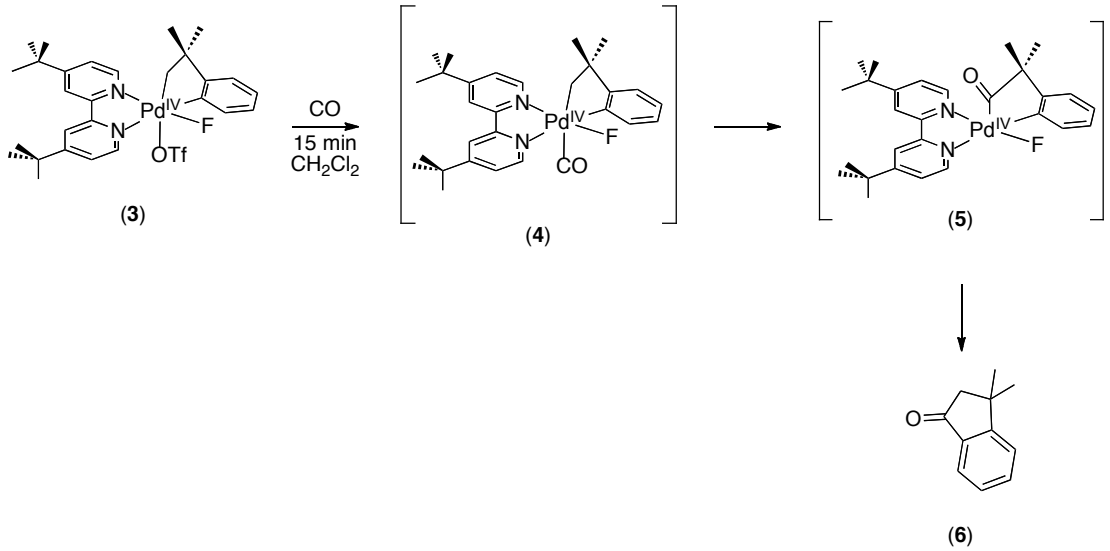

(**3**) (**4**) (**5**) (**6**)

Scheme 5.1.3 Pd^{II} Complex (7) not Reactive with CO

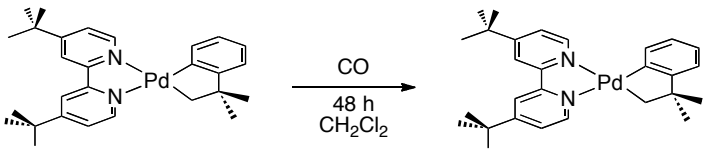

(**7**) (**7**)